SYNTHESIS AND CHARACTERIZATION OF NICKEL, PALLADIUM AND CHROMIUM COMPLEXES AS OLEFIN OLIGOMERIZATION CATALYSTS

Moses Mokgolela Mogorosi

UNIVERSITY OF CAPE TOWN

2009

Synthesis and Characterization of Nickel, Palladium and Chromium Complexes as Olefin Oligomerization Catalysts

Moses Mokgolela Mogorosi

A thesis submitted in fulfilment of the requirement for the degree

Doctor of Philosophy

Department of Chemistry

University of the Cape Town

Supervisor: John R. Moss

Co-supervisor: Gregory S. Smith

2009

DECLARATION

I declare that "**Synthesis and Characterization of Nickel, Palladium and Chromium Complexes as Olefin Oligomerization Catalysts**" is my own work and to the best of my knowledge has never been reported or submitted for any degree or examination in any university. All sources of information used are cited, acknowledged and completely referenced at the end of each chapter.

Signed by candidate

.....

Moses Mokgolela Mogorosi

ACKNOWLEDGMENTS

I wish to express my heartfelt gratitude and appreciation to the following people, without whose contribution this thesis would not be possible:

My supervisor Professor John Moss and co-supervisor Gregory Smith for their patience, enthusiasm, encouragement and support throughout the course of this project.

Professor Roger Hunter, whom I consider my mentor, thank you for all the constructive criticism, constant encouragement and support and most importantly for the invaluable training.

Professor Alan Hutton for his help with conductivity measurements. Professor Michael Claeys for all the discussions with problems relating to catalysis. Professor James Darkwa for invaluable advice and encouragement.

The analytical staff at the University of Cape Town: Mr Pete Roberts and Mr Noel Hendricks for recording NMR spectra, Mr Piero Benincasa for recording the elemental analysis and EI-MS. Dr Hong Su for the X-ray structural determination of some of my complexes.

I wish to express gratitude to SASOL and NRF Thrip for financial support.

Dr Subelia Botha and Dr S. Churms for their help with proofreading my thesis. Emma for the encouragement and advice throughout my thesis.

Last but not least I wish to dedicate this thesis to my family (Morwa, Jeanette, Itumeleng, Mothusi and Milly) for showing me nothing but unconditional support throughout the course of my studies.

ABSTRACT

New *N*-functionalized 2-phosphinobenzaldimino (P^N) ligands (**L**) bearing 3-picolyl (**41**), furfuryl (**42**), thiophene-2-methyl (**43**), thiophene-2-ethyl (**44**), and benzyl (**45**) groups have been prepared in good yield. In addition, 2-iminopyridyl (N^N) (**46**), 2-bromobenzaldimino (**47**), and 2-phenoxyimino (O^N) (**48**) ligands and precursors, bearing furfuryl groups, were prepared in good yield. The amino analogues of **47** and **48** were obtained by reduction of the imine bonds using sodium borohydride. All compounds were fully characterized using spectroscopic and analytical techniques, including melting point, ^{1}H, ^{13}C, and ^{31}P NMR, IR spectroscopy, MS, and elemental analysis.

These ligands (**L**) were reacted with appropriate metal precursors to give the corresponding metal complexes of the type Pd**L**MeCl (**51** – **55**), Pd**L**Cl_2 (**56** – **63**), Ni**L**Br_2 (**75** – **82**), and Cr**L**(THF)Cl_3 (**83** – **88**). Cationic palladium complexes (**64** – **74**) were obtained by the reaction of halide abstracting reagents ($AgBF_4$, $AgPF_6$, and $NaBAr^F{}_4$) with complexes **51** – **55** in the presence of acetonitrile. The palladium complexes were fully characterized using melting point, IR and NMR spectroscopy, MS, and elemental analysis. Owing to the paramagnetic nature of the nickel and chromium complexes, only IR spectroscopy, MS and elemental analysis were used to characterize these complexes. The structures of palladium complexes **53** and **71** and the nickel complex **76** were unambiguously determined using X-ray crystallography. The neutral complexes **56** – **63** and **75** – **82** were evaluated as catalysts for ethylene oligomerization, after activation with co-catalyst (MMAO, $EtAlCl_2$, or Et_2AlCl), while the cationic palladium complexes were used as ethylene oligomerization catalysts without need for a co-catalyst. Upon activation with $EtAlCl_2$, all nickel complexes proved to be highly active catalysts for ethylene oligomerization, producing mainly ethylene dimers. On the other hand, palladium complexes showed low ethylene oligomerization activities, with the cationic complexes giving the lowest activities. Unexpectedly, high catalytic activities were observed in the oligomerization of 1-hexene by neutral palladium dichloride/$EtAlCl_2$ catalyst systems, with mainly 1-hexene dimers and trimers being produced. Chromium complexes showed moderate catalytic activities for ethylene oligomerization/polymerization upon activation with MMAO, producing ethylene dimers, trimers, and polyethylene.

ABBREVIATIONS

Å	angstrom
acac	acetylacetone
Ar	aromatic
atm	atmosphere
br	broad
ca	approximately
calc	calculated
COD	cycloocta-1,5-diene
δ	chemical shift
°	degrees
°C	degrees Celsius
DCM	dichloromethane
DFT	density functional theory
DME	dimethoxyethane
DMSO	dimethyl sulfoxide
DMSO-d_6	deuterated dimethyl sulfoxide
d	doublet
dd	doublet of doublets
ddd	doublet of doublet of doublets
dt	doublet of triplets
EI-MS	electron impact mass spectrometry
ESI-MS	electrospray ionization mass spectrometry
EPR	electron paramagnetic resonance
Eq	equation
Equiv	equivalent(s)
Et	ethyl

Et_2O	diethyl ether
Et_3N	triethylamine
FT-IR	fourier transform infrared spectroscopy
g	gram(s)
GC	gas chromatography
h	hour(s)
HCl	hydrochloric acid
Hz	hertz
^{i}Pr	isopropyl
IR	infrared
J	coupling constant
MHz	megahertz
Me	methyl (CH_3)
m	multiplet
M.p.	melting point
m/z	mass to charge ratio
MAO	methylaluminoxane
MMAO	modified methylaluminoxane
min	minute(s)
mL	millilitres
mmol	millimoles
M_n	number average molecular weight.
NMR	nuclear magnetic resonance
n.d.	not determinded
PDI	polydispersity index
PE	polyethylene

Ph	Phenyl
ppm	parts per million
psig	pound per square inch gauge
q	quartet
RT	room temperature
s	singlet
sept	septet
tlc	thin layer chromatography
t	triplet
tt	triplet of triplets
^{t}Bu	tertiary-butyl
THF	tetrahydrofuran
TOF	turnover frequency
UV-Vis	ultraviolet-visible
wt	weight

TABLE OF CONTENTS

LIST OF FIGURES

LIST OF SCHEMES

LIST OF TABLES

CHAPTER 1
INTRODUCTION AND LITERATURE REVIEW OF NICKEL, PALLADIUM, AND CHROMIUM ETHYLENE OLIGOMERIZATION CATALYSTS

1.1 Scope of this Review

This review outlines the fundamental concepts that render transition metals unique as potential homogeneous catalysts (with particular focus on ethylene oligomerization). The review seeks to illustrate the complexity and diverse roles played by the ligands in catalysis. The history of homogeneous ethylene oligomerization, with particular focus on nickel, palladium and chromium catalyst systems, is described. An example of a commercial process that produces oligomers from ethylene and transforms by-products into value-added products is illustrated. The primary principles of ethylene oligomerization are discussed; these include the main processes involved in the production of oligomers or polymers (i.e. chain propagation and chain transfer), different pathways towards the generation of the cationic active species, as well as the proposed structure of the widely used co-catalyst methylaluminoxane (MAO and MMAO). Emphasis will be placed on some recent advances in ethylene oligomerization, illustrating the contribution of a diverse range of ligand systems to the performance of transition metal oligomerization catalysts. Detailed mechanistic aspects for both major and minor products are discussed. It is noteworthy that catalytic activities and selectivities (units) reported in this chapter are quoted as in the respective references.

1.2 Homogeneous Catalysis

Homogeneous catalysis refers to a system in which the catalyst exists in the same phase as the reactants and products. Catalyzed processes such as ethylene oligomerization and hydroformylation are considered homogeneous systems even though ethylene, carbon monoxide and hydrogen are gases at room temperature. A system, therefore, qualifies to be homogeneous if the catalyst, starting reactants and products can exist in a common solvent.

The focus on homogeneous catalysis followed from the discovery of hydroformylation (oxo synthesis) by Otto Roelen in 1938 [1]. Since then, it has been repeatedly shown that homogeneous catalysts offer significant advantages over their heterogeneous counterparts. Homogeneous catalysts generally show improved catalytic activities and high selectivities and function under milder conditions. Much insight into the mode of catalyst action can be obtained through various studies, and most importantly, electronic and steric properties of the ligands can be tailored to bring about improved catalyst performance [1,2].

1.3 Transition Metals in Catalysis

There are five main reasons that transition metals have dominated the field of catalysis and these include:

1.3.1 Bonding Ability

Transition metals have partially filled *d* and *f* orbitals. The *d*-block metals that are most often employed in catalysis possess nine valence shell orbitals (s, p_x, p_y, p_z, d_z^2, $d_{x^2-y^2}$, d_{xz}, d_{yz}, d_{xy}) that accommodate valence electrons and that can form hybrid molecular orbitals in bonding with other groups. These valence orbitals allow transition metals to form σ- and π- bonds with other moieties and ligands [2].

1.3.2 Wide-Ranging Choice of Ligands

A ligand refers to any element or combination of elements which form(s) chemical bond(s) with a transition metal. The fact that transition metals can form bonds with almost any organic molecule is the fundamental reason why transition elements have such rich coordination chemistry and the reason they are relevant in catalysis. Ligands can be formally ionic, e.g. Cl^-, H^-, OH^-, CN^-, $alkyl^-$, $aryl^-$, $COCH_3^-$, or neutral, e.g. tertiary, secondary, or primary phosphines, phosphites, C_2H_4, H_2O and nitriles, and amines [2].

1.3.3 Ligand Effects

The ability of transition metal catalysts to accommodate both participative ligands (those that take an active part in a catalytic cycle) and non-participative (e.g. PPh_3) within their coordination sphere offers the possibility of directing the course of a reaction. Modification of

electronic and steric properties of the non-participative ligand can influence the processes involving the participative ligand. It is generally accepted that a ligand can influence the steric or electronic environment, or both, at the transition metal active site [2]. There are two main concepts used to „predict' the effect of non-participative ligands (shown in 1.3.3.1 and 1.3.3.2):

1.3.3.1 *Trans*- Effect and Electron Donor-Acceptor Properties

The *trans*-effect refers to the ability of a coordinated ligand to exert a profound influence on the metal-to-ligand bond and lability of a *trans*-positioned ligand within a square planar or octahedral complex. This effect directly influences the rate of substitution of the ligand *trans* to itself. In general, good σ-donor ligands (e.g. H^-, $SnCl_3^-$) have high *trans*-effects due to the contribution of more electron density to the shared orbital between itself and the *trans*-ligand, thereby weakening the bond of the leaving group (i.e. the *trans* ligand). The presence of strong *trans*-effect groups in a catalyst system can have a beneficial effect in improving the activity of the system where ligand or substrate dissociation is the rate-determining step [2-4].

1.3.3.2 Cone angle: steric parameter θ

The concept of cone angle arose from the observation that the competition for coordination of the phosphorus ligand (**L**) on Ni(0) as described by Eq.1 could not be sufficiently explained in terms of electronic character only.

$$\mathbf{NiL_4} + n\mathbf{L'} \rightleftharpoons \mathbf{NiL_{(4-n)}L_n'} + n\mathbf{L} \qquad \text{Eq 1.1}$$

The position of the equilibrium was mainly dictated by the physical bulk of the phosphorus ligand (**L'**), with ligands bearing large cone angles showing poor competitive ability for coordination to Ni(0) [2].

The cone angle concept developed by Tolman has been used as a quantitative measure of steric effects of symmetric trivalent phosphorus ligands (tertiary phosphines and phosphites). This concept has also been used to explain structural and thermodynamic aspects of metal complexes. Tolman's cone angle steric measurements were achieved by placing the ligand **P** atom 2.28 Å from an apex, **M** (metal atom) and enclosing the ligand in a ligand cone generated from the apex. For symmetrical ligands the cone angle was measured from the point which

gave the largest θ on the ligand and all cone angles were measured with a constant **M** – **P** bond distance (Figure 1.1) [2,5].

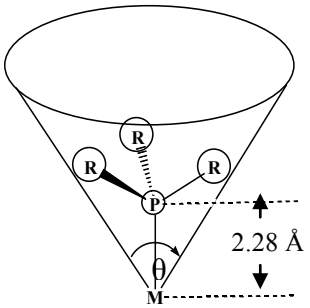

Figure 1.1 *Tolman cone angle for a symmetrical phosphorus ligand (PR_3)*

The above model has also been used to measure cone angles of amines [5a], alkyl groups [5e], and cyclopentadienyl ligands [5d,5f].

1.3.4 Variability of Oxidation States

In principle, a transition metal can have access to as many oxidation states as it has valence *d* and *s* electrons. For example Cr, $3d^5 4s^1$, can have oxidation states 0 to VI. The ability to form stable complexes with transition metals in a variety of oxidation states is common, although not all transition metals form stable complexes for all of their oxidation states. In general π-bonding ligands such as phosphines and amines tend to favour metals in low oxidation states while small ionic σ-bonding ligands such as H^- and F^- favour transition metals in their high oxidation states. More important, however, is the ability for transition metals to interconvert between oxidation states during the course of a chemical/catalytic reaction [2]. A good example is the palladium-catalyzed Heck C-C coupling reaction that makes use of a Pd(0) catalyst precursor such as $Pd(PPh_3)_4$ [2]. The first step in the cycle is the oxidative addition of an aryl halide to form a Pd(II) intermediate. This is followed by coordination of an olefin and its insertion *syn* to the aryl group. The product is released after a β-hydride elimination step. The resultant complex subsequently undergoes reductive elimination of H-X, which regenerates the Pd(0) species (Scheme 1.1).

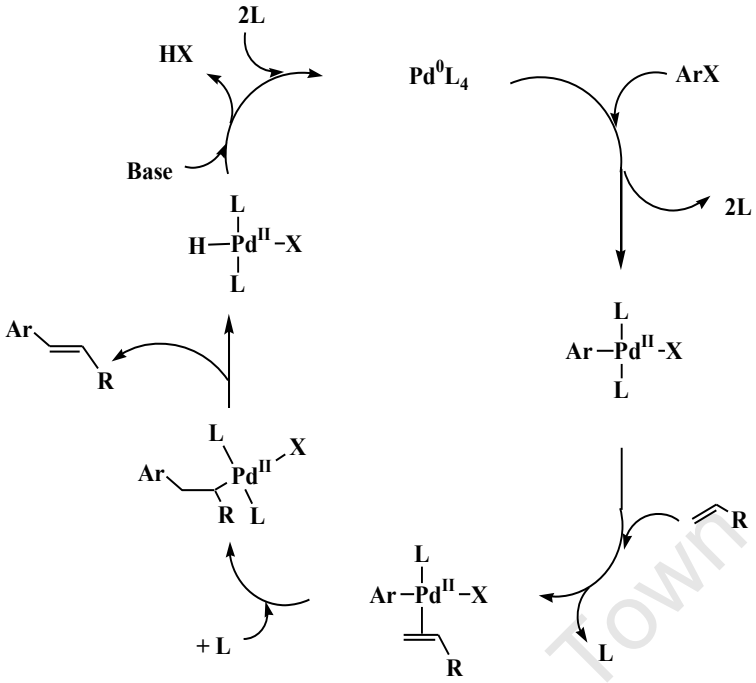

Scheme 1.1 *Catalytic cycle for the palladium catalyzed Heck C–C coupling reaction describing the interconvertion of the oxidation states during the course of a chemical/catalytic reaction [2].*

1.3.5 Variability of Coordination Number

Most transition metals prefer coordination numbers of four or six. However, transition metals with coordination numbers as high as nine have been encountered (e.g. ReH_9^{2-}, $WH_6(PR_3)_3$). A catalytic reaction such as hydroformylation, in which an aldehyde is formed, requires that the metal centre be able to coordinate simultaneously the olefin, carbon monoxide and hydrogen during the course of the reaction, as well as non-participative ligands that may be present. In addition, most transition metals are able to interchange rapidly between different coordination numbers [2].

1.4 Introduction to Ethylene Oligomerization/Polymerization

The interest in olefin oligomerization/polymerization dates back to 1949 when Gellert and Ziegler treated ethylene with lithium aluminium hydride ($LiAlH_4$) in ether at 180 – 200°C and observed a rapid drop in the ethylene pressure [6a]. The products isolated in this experiment were identified as a mixture of α-olefins. However, it was observed that not only had the $LiAlH_4$ catalyzed the oligomerization of ethylene to α-olefins, but that the $LiAlH_4$ itself had

undergone addition with ethylene to yield triethylaluminium ($AlEt_3$) as the major product. It was this latter product that was believed to initiate the chain growth reaction. It was further observed that chain cleavage (elimination) could be curbed by lowering the reaction temperature (chain growth and chain elimination reactions are discussed in detail in the next section). For example, at 100 °C waxy products with molecular weights up to 5000 g/mol were obtained, while efficient ethylene dimerization was achieved at 170 °C [6].

In 1953 during a routine ethylene polymerization experiment ($AlEt_3$-C_2H_4 catalyst system), Ziegler *et al.* obtained butene instead of the anticipated long-chain aluminium alkyls [7]. This ethylene dimerization method proved to be much more effective than that developed by Wilke [8]. This unexpected result was said to be the result of impurities of nickel compounds that remained in the autoclave despite thorough cleaning. This result (the "nickel effect"), unlocked a new chapter in catalysis [6,8]. The discovery of the "nickel effect" spurred the scanning of most transition metals in the periodic table as potential catalysts for olefin conversions. These efforts subsequently resulted in Ziegler and Natta winning Nobel prizes for the discovery of the highly active Ziegler-Natta polymerization catalyst in the 1950's [9].

In 1965, Keim was given a mandate by Shell Oil to design a system that would convert ethylene into value added chemicals (such as α-olefins). He used the model shown below in his catalyst design [10a].

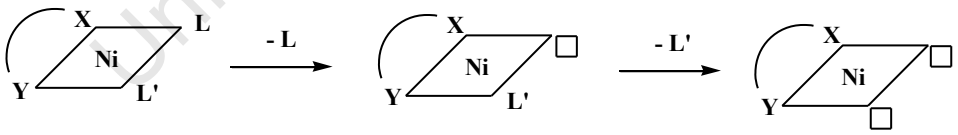

Scheme 1.2 *Proposed model for the formation of vacant coordination sites [10a]*

Chelating ligands (X^Y) were chosen since they favour square planar structure with free coordination sites for the formation of an octahedral system. Atoms X and Y should behave as electron donors and acceptors respectively. Exchange of ligands L and L′ for ethylene should be facile [10a,c]. This rather straightforward concept led to the unearthing of the well-known Shell High Olefin Process (SHOP). This technology makes use of neutral nickel(II) complexes bearing a bidentate mono-anionic (P^O) ligand (Figure 1.2).

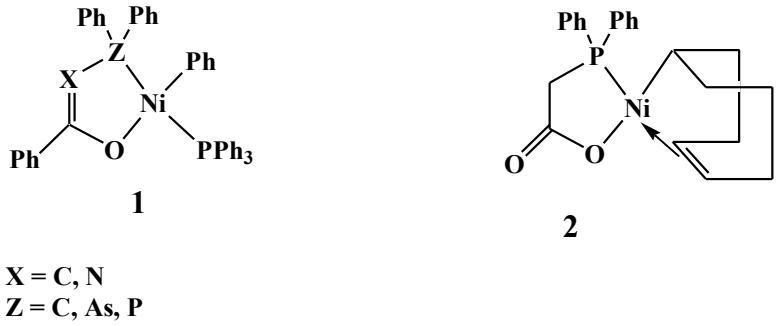

Figure 1.2 *Representation of various SHOP catalysts*

At a temperature of 50 °C and an ethylene pressure of 50 bar, complex **1** (X = Z = C) was found to be an efficient ethylene oligomerization catalyst, affording up to 99% linear olefins consisting of 98% α-olefins. The SHOP process produces an industrially desirable geometric distribution of $C_4 - C_{30}$ olefins [10a,11]. The α-olefins, particularly those in the higher carbon range, have great commercial applications. These olefins are mainly used in fine chemicals, as comonomers ($C_4 - C_8$) in the polymerization of ethylene to give linear low density polyethylene (LLDPE), and as synthetic lubricants (C_{10}), plasticizer alcohols ($C_6 - C_{10}$), and surfactants ($C_{12} - C_{20}$) [11]. In the SHOP process, the remaining unmarketable α-olefins are transformed via double bond isomerization and metathesis catalytic reactions into linear olefins of any carbon chain length. A schematic diagram depicting the products manufactured by Shell via flexible combination of oligomerization, isomerization and metathesis is shown in Scheme 1.3.

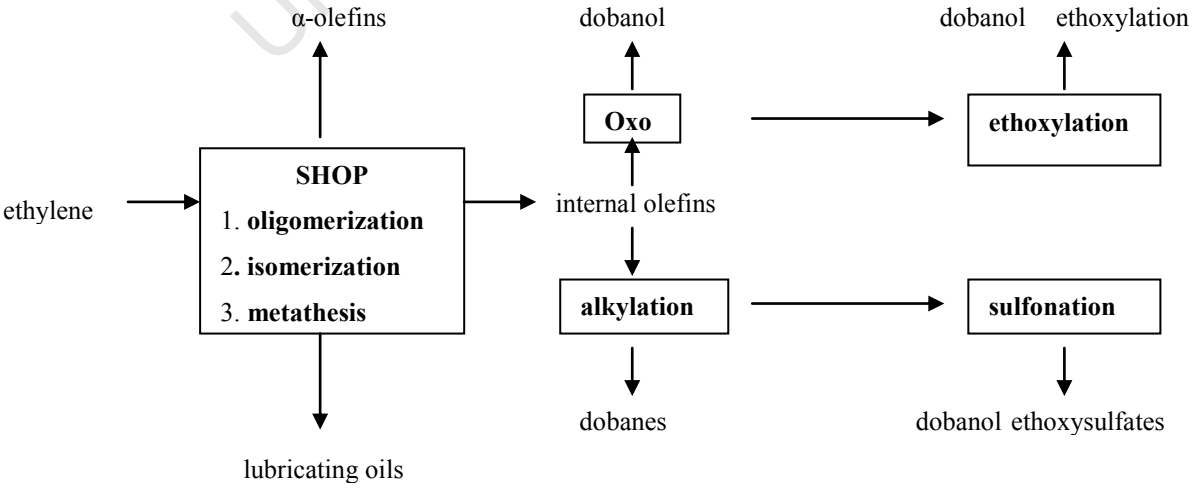

Scheme ***1.3*** *Primary and secondary products of the SHOP process [6a]*

In general, linear alpha olefin (LAO) producers may be grouped into two categories: the "*full range"* process and "*on-purpose"* process. "*Full range"* producers include companies such as Shell, BP Amoco and Chevron Phillips and involves a one-step process in which the chain growth and termination occur simultaneously. The drawback with this reaction is the propensity towards the reaction of the formed α-olefins with aluminium alkyls yielding an increase in the amount of branched olefins. A basic characteristic of the chemistry of these metal-catalyzed ethylene oligomerization processes is that they produce a mathematical distribution (Schulz-Flory or Poisson) of α-olefins which often does not match market demand [12a]. Value-added fractions produced, such as 1-butene, 1-hexene and 1-octene, would then have to be separated into pure forms by fractional distillation.

Consequently, selective ethylene dimerization, trimerization and tetramerization have attracted much interest and attention during the past decade. Over the years, the above-mentioned companies have made efforts to narrow the broad distribution of olefins to high value comonomers (1-hexene and 1-octene). These attempts have involved increased capital expenditure and operational complexities. The "*on-purpose"* route to LAO's involves selective synthesis of short chain α-olefins: i) 1-butene is synthesized by ethylene dimerization in the Middle east, ii) 1-hexene is synthesized by ethylene trimerization by Chevron Phillips and iii) 1-hexene and 1-octene are extracted from synthol by SASOL. The last "*on-purpose"* route to specific LAO's is different from the previously mentioned "*on-purpose"* routes in that it is not based on selective ethylene oligomerization [11b, 12].

Selective ethylene trimerization has received the most attention (compared to ethylene dimerization and the recently discovered ethylene tetramerization). Manyik *et al.* of Union Carbide reported the first selective ethylene trimerization to 1-hexene in 1977 [13]. 1-Hexene was found to be an oligomeric by-product in the ethylene polymerization catalyzed by a homogeneous chromium-based system [chromium(III)*tris*(2-ethylhexanoate)/hydrolyzed triisobutylaluminium]. The investigation of the liquid product was motivated by the observation of a polymer with butyl side chains [12a,12d,13]. Later, Briggs and others developed a catalyst system involving a donor ligand system (selected from dimethoxybenzene, monoglyme, diglyme, triglyme and *o*-dimethoxybenzene) to give a different kind of catalyst system: [chromium(III)*tris*(2-ethylhexanoate)/donor ligand/hydrolyzed triisobutylaluminium] which produced 1-hexene as a major product with

selectivities of up to 74 % as well as by a small amount of polyethylene [14,12d]. These results prompted companies including Phillips Petroleum Corporation, Mitsubishi Chemical Corporation and Sumitomo Chemical Company to investigate this system further, using pyrrole or 2,5-dipyrrole donor ligands. In particular, the four-component catalyst incorporating halide promoters were investigated, e.g. [chromium(III) *tris*(2-ethylhexanoate)/2,5-dimethylpyrrole/$AlEt_3$/CCl_4]. Chromium(III) complexes containing tridentate ligands have also recently been shown to be highly active and selective catalysts for ethylene trimerization to 1-hexene when activated with MAO [12b,15].

1.5 Principle Steps In Ethylene Oligomerization

1.5.1 Chain Growth and β-Hydride Elimination

The type of oligomer/polyolefin obtained during the ethylene oligomerization/polymerization reaction depends mainly on the number (n) of reacting molecules of ethylene. Dimerization is achieved when n = 2; oligomerization when 2 < n < 100; and polymerization when n > 100. In general, the catalytic process involves three main steps:

1) activation of a neutral catalyst precursor to generate the cationic active catalyst (section 1.5.2).

2) chain growth (propagation) step

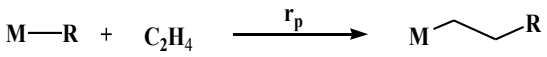

where **R** = alkyl or hydrogen; $\mathbf{r_p}$ = propagation rate and M–R is the active catalyst.

3) β-hydride elimination step

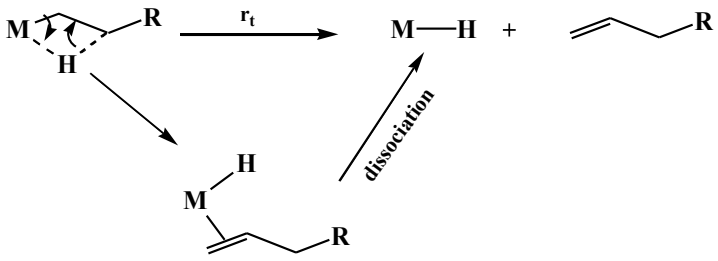

where $\mathbf{r_t}$ = chain-transfer rate.

The β-hydride elimination in the third step occurs in order to restore the very reactive metal hydride species which catalyzes subsequent ethylene reactions. Reaction rates $\mathbf{r_p}$ and $\mathbf{r_t}$, determine the product's molecular weight. In the case where $\mathbf{r_p} > \mathbf{r_t}$ chain propagation occurs preferentially over β-hydride elimination resulting in formation of high molecular weight polyethylene. On the other hand, when $\mathbf{r_t} > \mathbf{r_p}$, the β-hydride elimination step is much faster than chain propagation and dimers can be obtained. When $\mathbf{r_t} \approx \mathbf{r_p}$, oligomers are obtained.

To a large extent these rates are affected by the ligand backbone. For example, complexes **3** primarily produced 1-C_4 when only two *ortho*-alkyl substituents were present around the aryl ring (e.g. **3a-d**). When the size of the *ortho*-alkyl substituents (e.g. **3e**) or the number of substituents around the aryl ring was increased, only waxes and polyethylene were produced. The catalyst formed by replacing one imine group with a carbonyl **(4)** only produced waxes and polyethylene, indicating that electronic effects also played a significant role in determining the product distribution [17b].

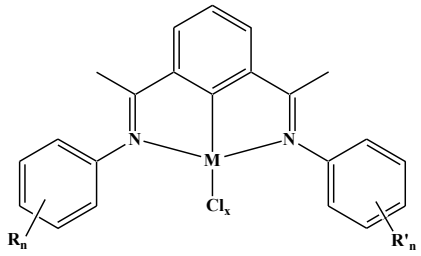

M = Cr(II); X = 1
M = Cr(III); X = 2

3

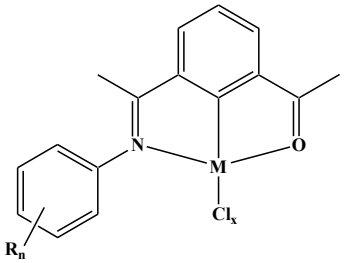

M = Cr(II); X = 1
M = Cr(III); X = 2

4

	a	b	c	d	e	f	g	h	i	j	k	l	m	n
Rn	-	2-Me	2-Et	2-^{i}Pr	2-^{t}Bu	2,6-Me$_2$	2,5-^{t}Bu$_2$	2,6-Me$_2$	2,6-^{i}Pr$_2$	2-^{t}Bu	2,4,6-Me$_3$	2,4,6-Me$_3$	2,4,6-Me$_3$	2,6-^{i}Pr$_2$
R'n	-	2-Me	2-Et	2-^{i}Pr	2-^{t}Bu	2,6-Me$_2$	2,5-^{t}Bu$_2$	-	-	-	4-^{t}Bu	2-Me	2-Et	2,6-^{i}Pr$_2$

Figure 1.3 *Molecular structures of some chromium(II) and chromium(III) complexes employed as catalysts in ethylene oligomerization/polymerization reactions*

In addition properties such as oxidation state, electronic and steric properties of the ligand, as well as parameters such as reaction temperature, ethylene pressure, and solvent were found to have a significant effect on the type of olefin product distribution produced [16]. For example, di- and trivalent chromium complexes **3** and **4** employed in ethylene oligomerization/polymerization gave similar product distributions (Figure 1.3). This indicates that the more stable Cr(III) complex could be a precursor to the less stable Cr(II) species, in view of the fact that it would be difficult for Cr(II) to be oxidized to Cr(III) in the presence of a reducing medium (MAO), whereas it would be plausible for Cr(III) to be reduced to Cr(II) under similar conditions [17a].

1.5.2 Generation of the Cationic Active Species

It is generally accepted that the catalytically active species in ethylene oligomerization is a coordinatively unsaturated cationic species. This alkyl species can be generated in three ways as shown in Scheme 1.4 below. **Path A** involves the abstraction of a halide (X = halide, anionic ligand) using halide abstracting reagents such as $NaBAr^{F}_{4}$ (Ar^{F} = 3,5-$(CF_3)_2C_6H_3$) [18c], $AgBF_4$, $AgPF_6$, or $AgOSO_2CF_3$ (AgOTf), in the presence of a weakly coordinating group (e.g. CH_3CN, PPh_3, etc.) [18d,18e]. This route is particularly important with late transition metal catalysts. Cationic alkyl, aryl and allyl complexes of the kind mentioned above have been isolated and fully characterized. These cationic complexes can be used in ethylene

oligomerization reactions without use of a co-catalyst and are therefore referred to as as "single component" catalysts [18c]. Similarly, **Path B** involves abstraction of one or two alkyl groups depending on the mole ratio of the alkyl abstracting reagent. Some reagents used for this purpose include $[Ph_3C][B(C_6F_5)_4]$, $B(C_6F_5)_3$, or $[H(OEt_2)_2][BAr^F{}_4]$ [18c]. The role of the reagents $[Ph_3C][B(C_6F_5)_4]$ and $[H(OEt_2)_2][BAr^F{}_4]$ [18d] is to effect substitution of the alkyl group (**R**) with a weakly coordinating group as is the case with halide substitution. On the other hand, with $B(C_6F_5)_3$ the alkyl group is only partially abstracted giving a "cationic-like" species [18a].

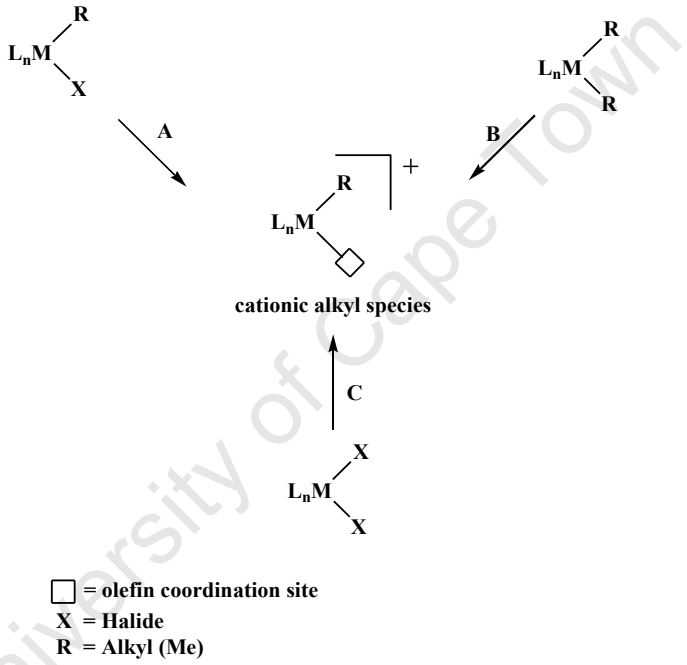

Scheme 1.4 *Routes to the catalytically active species [18a]*

Path C can be achieved in two ways: 1) the dihalide complex can be treated with an alkylating reagent (e.g. MeLi) to yield a dialkyl complex which can then be activated following **Path B**. 2) alternatively, alkylaluminium halides, especially aluminoxanes (e.g. MAO), that can perform both steps can be employed. The exact structure of MAO is not known, but it is believed to consist of oligomeric $[Al(Me)O]_n$ units in a linear and/or cyclic form [19a]. The multiple equilibria present in a solution of MAO and participation of residual trimethylaluminium (TMA) in the interconversion of various MAO oligomers have made it difficult to determine the structure of MAO [19b]. The structure of $[^tBuAlO]_x$ was characterized and reported over a decade ago. Spectral analysis of this compound showed that

the structure was neither linear nor cyclic but a cage-structure [19c, 19d]. In addition, from theoretical studies conducted by Zurek and Ziegler [19e], it was concluded that MAO models consisting of three-coordinate oxygen and four-coordinate aluminium in a three-dimensional cage structure are significantly more stable than linear, ring or fused ring structures, in agreement with experimental findings by Barron and others [19f,19g,19l,19h–19j]. The originally proposed structures for MAO are shown below in Figure 1.4.

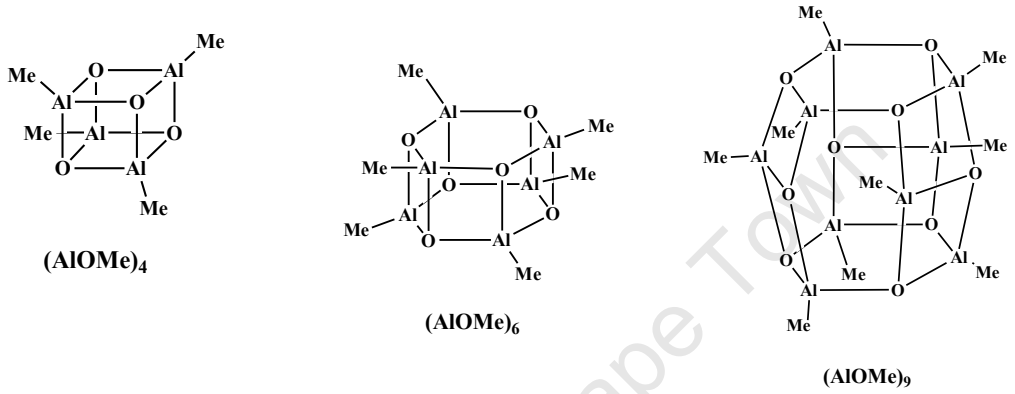

Figure 1.4 *Proposed cage structures of MAO, (AlOMe)n, n = 4, 6, 9 [19b]*

However, the structures shown above show MAO, $(AlOMe)_n$, as containing only four-coordinate aluminium centers, which cannot be regarded as being significantly Lewis acidic. The residual TMA present in MAO serves to enhance the activity of MAO [19b, 19d, 19k). This, therefore, indicates that the Al:O:Me ratio is not 1:1:1. NMR studies conducted by Imhoff *et al.* showed that the Al, O, Me, composition was $(AlO_{0.80-0.75}Me_{1.4-1.5})_m$ [19m]. Zhakharov *el al.* then constructed a model for the "true" MAO using DFT studies which included the interaction of the original MAO with TMA [19n]. Figure 1.5 shows the incorporation of TMA into the original structure of MAO $(AlOMe)_9$.

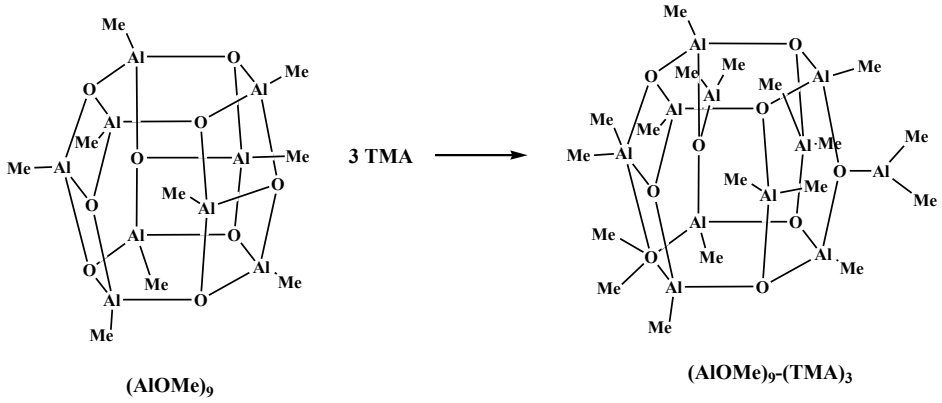

Figure 1.5 *Proposed structure of "true" MAO after incorporation of TMA [19b]*

In general, it is assumed that the function of MAO is 1) to abstract the halide and alkylate the catalyst precursor, 2) to stabilize the cationic alkyl species by acting as a counter-ion and 3) to prevent bimolecular reduction of the catalyst. These functions, therefore, account for the large quantities of MAO required for good oligomerization/polymerization activity. MAO is also believed to scavenge impurities such as water and oxygen from the reaction medium. However, the major function of MAO is the generation of the active species [19j]. Even though MAO is highly reactive, it has the drawback of being highly unstable. This drawback was the main motivation for the preparation of modified MAO (MMAO). MMAO has improved stability as well as better solubility in aliphatic solvents. This compound is prepared by the controlled hydrolysis of a mixture of trimethylaluminium (TMA) and triisobutylaluminium (i.e. MMAO = MAO containing 25 % isobutyl groups) [18b].

1.6 Some Developments in Catalytic Ethylene Oligomerization

1.6.1 Late Transition Metal Ethylene Oligomerization Catalysts (Ni and Pd)

As described earlier, the discovery of the "nickel effect" emphasized the oligomerization potential of nickel catalysts (section 1.4, p 7). Nickel catalysts favour ethylene oligomerization over polymerization due to the highly competitive chain transfer reaction relative to chain propagation [6c]. In the 1990's, interest in late transition-metal complexes as catalysts for ethylene reactivity was renewed by the discovery of highly active α-diimine-based complexes by Brookhart [20a] and Gibson [21]. An important observation made by Brookhart and co-workers was the marked effect that ligand manipulation has on the product formed (Figure 1.6). It was observed that by eliminating the steric bulk of the *ortho*-substituent on the aryl-

substituted α–(diimine)Pd and Ni complexes, only ethylene oligomers were formed as opposed to high molecular weight polyethylene produced when bulky ortho-substituents were present [20a, 22].

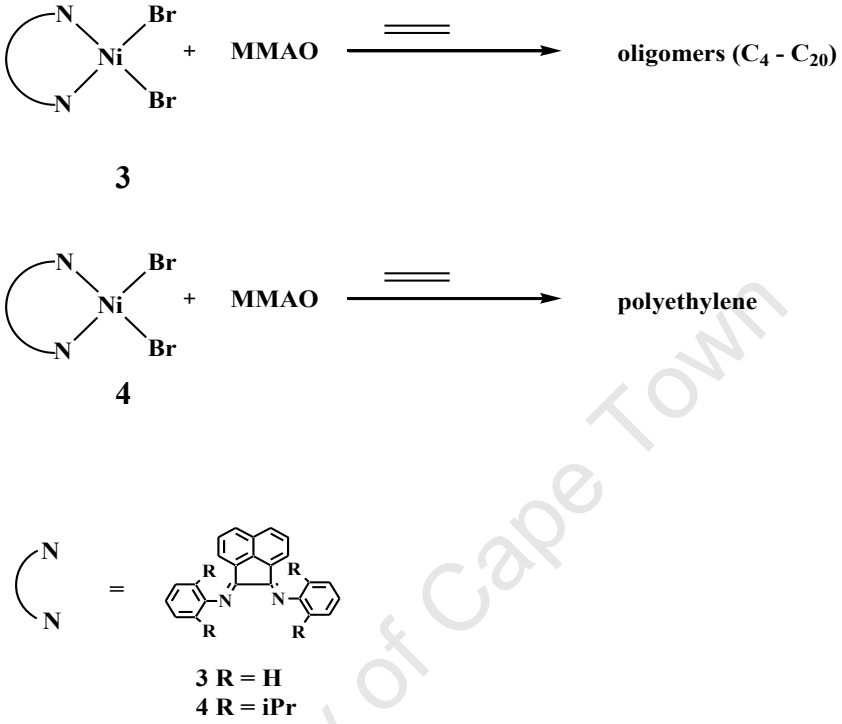

Figure 1.6 *Brookhart's ethylene oligomerization and polymerization catalyst systems*

These discoveries resulted in many research groups making efforts to design new ligand systems, in an effort to find highly active and selective catalyst systems, particularly those containing late transition metals. This resulted in the preparation of numerous Ni and Pd complexes bearing a range of ligand systems with coordination modes such as bidentate N^N [23], N^O [24], P^N [25], P^P [26], P^O [27] and tridentate, N^N^N [28], N^N^O [29], N^P^N, P^N^P [25o], P^N^N [30].

As described in Scheme 1.4, nickel and palladium active ethylene oligomerization catalysts can be generated from neutral catalyst precursors or cationic catalyst precursors. Many of these catalyst precursors make use of ligand systems prepared from Schiff base condensation reactions. Some examples of these imine-based ligands and their complexes have been reviewed in the literature [31].

An example depicting the preparation of an imine-based ligand system (**A**) is shown below in Scheme 1.5.

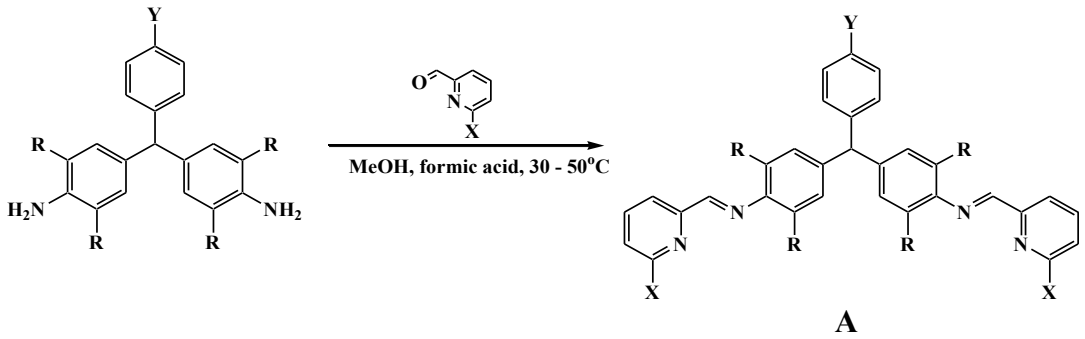

	a	b	c	d	e	f	g	h	i	j	k
Y:	H	H	H	NO_2	NO_2	NO_2	NO_2	NO_2	OCH_3	OCH_3	OCH_3
R:	Me	Et	iPr	Me	Et	iPr	iPr	iPr	Me	Et	iPr
X:	H	H	H	H	H	H	Me	Ph	H	H	H

Scheme 1.5 *Example of a Schiff base ligand synthesis [23c]*

The condensation of substituted amines with substituted aldehydes or ketones has found wide application in the design of ligands. This is largely due to the ease of preparation of the ligands, as well as the simplicity with which the ligands can be tailored. The example depicted in Scheme 1.5 describes the condensation of two primary amines (in one molecule) with a substituted 2-pyridinecarboxaldehyde, to give a dimeric iminopyridyl ligand. The scheme illustrates how a library of ligands can be generated via one reaction sequence [23c].

1.6.2 Neutral Ni and Pd Complexes in Ethylene Oligomerization

1.6.2.1 Nickel complexes bearing [N^N], [N^N^N] and [N^O] ligand systems

The majority of ethylene oligomerization catalyst systems reported to date consist of [N^N] and [N^N^N] ligand systems [23,28]. This is not surprising considering the exceptional success these catalyst systems have had since their recognition as ethylene oligomerization/polymerization catalysts [20,21].

The effects of parameters such as ligand environment, co-catalyst concentration and temperature were demonstrated using a series of complexes **5a-l** (Figure 1.7). Diethylaluminium chloride (Et_2AlCl) was found to give the most active catalyst system and

was thus used as a co-catalyst in subsequent investigations. Variation of the electron-donating capacity of $\mathbf{R^2}$ proved to have a significant effect on the catalyst performance, increasing the catalyst activity in the order Ph < Me < H (10.7, 21.4, and 41.2 x 10^5 g product.mol^{-1}Ni.h^{-1} respectively). It was observed that increasing the steric bulk of $\mathbf{R^1}$ and $\mathbf{R^3}$ significantly decreased the catalytic activity (i.e. from $\mathbf{R^1 = R^3 = H}$ to $\mathbf{R^1 = R^3}$ = Me**)** from 20.3 to 7.7 x 10^5 g product.mol^{-1}Ni.h^{-1} for the dichloride complexes. On the other hand, for complexes with $\mathbf{R^1 \neq R^3}$ it was observed that increasing the steric bulk of $\mathbf{R^1}$ (^{i}Pr, Cy ^{t}Bu,) while keeping $\mathbf{R^2}$ = Me resulted in a gradual increase in activity, 7.7, 20.1, 33.9 x 10^5 g product.mol^{-1}Ni.h^{-1} respectively for the dichloride complexes [28f].

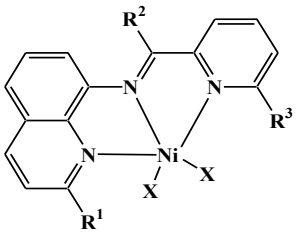

5

	a	b	c	d	e	f	g	h	i	j	k	l
R1:	H	Me	Me	H	^{i}Pr	^{i}Pr	^{t}Bu	^{t}Bu	Cy	Cy	H	H
R2:	H	H	H	H	H	H	H	H	H	H	Me	Ph
R3:	H	H	Me	Me	H	Me	H	Me	H	Me	H	H

X : Cl or Br

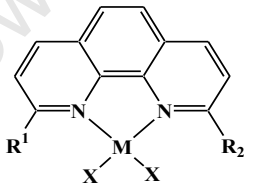

6

	a	b
R^1:	Ph	Naphthyl
R^2:	Ph	Naphthyl

X : Cl or Br

Figure 1.7 *Symmetrical and unsymmetrical diimine complexes [23a, 28f]*

For complexes **6,** a similar trend of improved catalytic activity with increasing steric bulk of $\mathbf{R^1}$ and $\mathbf{R^2}$ was observed, with catalytic activities following the order $\mathbf{R^1 = R^2}$ = Ph < $\mathbf{R^1}$ = Ph; $\mathbf{R^2}$ = Naphthyl < $\mathbf{R^1 = R^2}$ = Naphthyl after activation with MAO. Nickel dibromide complexes gave activities of 72, 90, 136 x 10^3 g.mol^{-1}Ni.h^{-1} respectively [23a].

The role played by the ligands in ethylene oligomerization, and indeed in almost all kinds of catalytic reactions, is particularly important. For example, in the case of N-heterocyclic ligands, the electron-donating capacity of the coordinating nitrogen can be modified by the introduction of the second heteroatom in the ring [23w]. A few recent examples are given below in Figure 1.8.

Complexes **7** and **8** are similar in many respects, differing mainly in the presence of a benzimidazolyl group rather than benzoxazolyl group in **8**. For both complexes **7** and **8** co-catalysts MAO, MMAO and Et_2AlCl were used, with best activities and selectivities observed with Et_2AlCl. Complexes **7** were found to be mainly ethylene dimerization catalysts, yielding up to 98 % C_4 and 3 % C_6. The ligand architecture was found to have a great influence on the catalyst performance. Increasing the steric bulk of $\mathbf{R^1}$ resulted in decreased catalytic activity in the order $\mathbf{R^1}$ = iPr < Et < Me (12.0, 8.95 and 6.29 x 10^5 g prod.mol^{-1}Ni.h^{-1} respectively) but improved α-olefin selectivity (75, 83 and 87 % respectively). Having $\mathbf{R^1}$ = Cl resulted in lower activity (3.08 x 10^5 g.mol^{-1}Ni.h^{-1}). Similarly, having $\mathbf{R^2}$ = Br resulted in lower activity of 7.31 x 10^5 g prod. mol^{-1}Ni.h^{-1}. Complex **7** bearing $\mathbf{R^1}$ = $\mathbf{R^2}$ = Me gave the best activity (52.0 x 10^5 g prod. mol^{-1}Ni.h^{-1}) but showed reduced α-olefin selectivity (21 %). Addition of an auxiliary ligand to the system (20 equiv. PPh_3) led to higher activity and longer catalyst lifetime [28b].

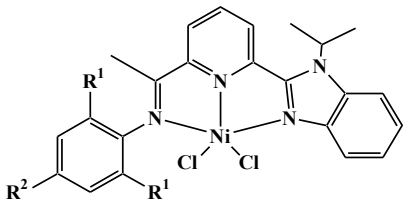

7

	a	b	c	d	e	f
$\mathbf{R^1}$:	H	Et	iPr	Cl	Me	Me
$\mathbf{R^2}$:	H	H	H	H	Me	Br

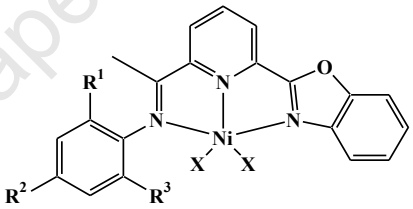

8

	a	b	c	d	e	f	g
$\mathbf{R^1}$:	Me	Et	iPr	Cl	Br	Me	Me
$\mathbf{R^2}$:	H	H	H	H	H	Me	Br
X:	Cl or Br						

Figure 1.8 *Examples of benzimidozolylpyridine (**7**) and benzoxazazolylpyridine (**8**) derivatives [28b, 28c]*

Upon activation with Et_2AlCl, complexes **8** produced predominantly C_4 olefins (up to 100% C_4). Contrary to what was found for catalyst **7**, bulkier substituents gave improved activities in the order $\mathbf{R^1}$ = Me < Et < ^{i}Pr (1.74, 3.48 and 8.31 x 10^5 g prod.mol^{-1}Ni.h^{-1} respectively) but slightly lower selectivity for α-olefin (91.5, 90.6 and 82 % respectively). Increasing the temperature to 50 °C led to an improvement in activity (1.45 x 10^6 g prod.mol^{-1}Ni.h^{-1}). Further increasing the temperature was found to decrease activity (3.87 x 10^5 g prod.mol^{-1}Ni.h^{-1}). Addition of an auxiliary ligand (20 equiv. PPh_3) was also found to improve activity (7.19 x 10^6 g.mol^{-1}Ni.h^{-1}) significantly at the expense of α-olefin selectivity (8 %) [28c].

N-heterocyclic-containing ligands such as pyrroleimines have also been coordinated to nickel (**9** and **10**) and used in nickel-catalyzed ethylene oligomerization **(**Figure 1.9). It is noteworthy that even though the σ-donor properties of these ligands are similar to those of α-diimines or pyridines they do not have sufficient steric bulk to impede the axial phase in the coordination plane [23b, 28o].

Complex **9** was activated with MAO, and produced oligomers in the range C_4 – C_8, with minute quantities of C_{10} – C_{14}. When $\mathbf{R^1}$ was sterically bulky ($\mathbf{R^1}$ = ^{i}Pr) the catalytic activity was relatively low (0.82 x 10^5 g.mol^{-1}Ni.h^{-1}) and a greater proportion of higher olefins was produced (C_6 = 23 % and C_8 = 50 %). On the other hand, with $\mathbf{R^1}$ = H and $\mathbf{R^2}$ = NO_2 the catalytic activity improved (3.17 x 10^5 g.mol^{-1}Ni.h^{-1}) and the major products were C_4 (32 %) and C_6 (50%). An increase in reaction temperature (0 – 40 °C) led to an increase in activity (0.72, 3.17 and 3.60 x 10^5 g prod.mol^{-1}Ni.h^{-1} at 0, 20 and 40 °C respectively) for **9b**. A further increase to 60 °C led to a decrease in activity (1.83 x 10^5 g prod.mol^{-1}Ni.h^{-1}), probably due to decomposition of the active species or low solubility of ethylene at those high temperatures [23b].

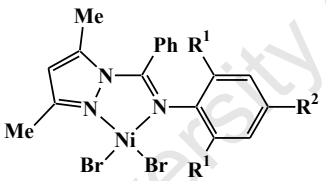

9

	a	b
$\mathbf{R^1}$:	^{i}Pr	H
$\mathbf{R^2}$:	H	NO_2

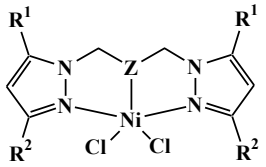

10

	a	b	c	d	e
$\mathbf{R^1}$:	Me	Me	Cl	H	Me
$\mathbf{R^2}$:	Me	Me	H	Ph	Me
Z =	NBz	NBu	S	S	S

Figure 1.9 *Some examples of pyrazolylimine ligands **9** and **10** [23b, 28o]*

Complex **10** on the other hand produced mainly dimerization products (up to 100 % C_4) upon activation with MAO or Et_2AlCl, with the latter co-catalyst giving higher activities (up to 9.10 x 10^4 mol C_2H_4.mol^{-1}Ni.h^{-1} compared to 1.89 x 10^4 mol C_2H_4.mol^{-1}Ni.h^{-1} for MAO) but lower α-olefin selectivities (72.0 – 81.3 % C_4 as opposed to 71.9 – 93.7 % for MAO). The catalytic performance was greatly affected by the ligand environment. The catalyst with **Z** = N-benzyl

(**10a**) was approximately 3 times more active than the one bearing **Z** = N-butyl (**10b**) i.e. 1.13 x 10^4 mol C_2H_4.mol^{-1}Ni.h^{-1} for **10b** and 3.90 x 10^4 mol C_2H_4.mol^{-1}Ni.h^{-1} for **10a**. The presence of a bulky phenyl on the pyrazolyl group (**10d**) resulted in a decrease in activity (1.05 x 10^5 mol C_2H_4.mol^{-1}Ni.h^{-1}) compared to **10e** bearing a methyl group (1.89 x 10^4 mol C_2H_4. mol^{-1}Ni.h^{-1}) [28o].

Complexes containing both a *hard* oxygen and *soft* nitrogen (Figure 1.10) can also offer interesting and unique bonding properties that may have a direct influence on catalytic reactions. The coordinating groups (oxygen and nitrogen) in the examples given below all have different σ-donor properties and this would affect the catalysis in various ways [24].

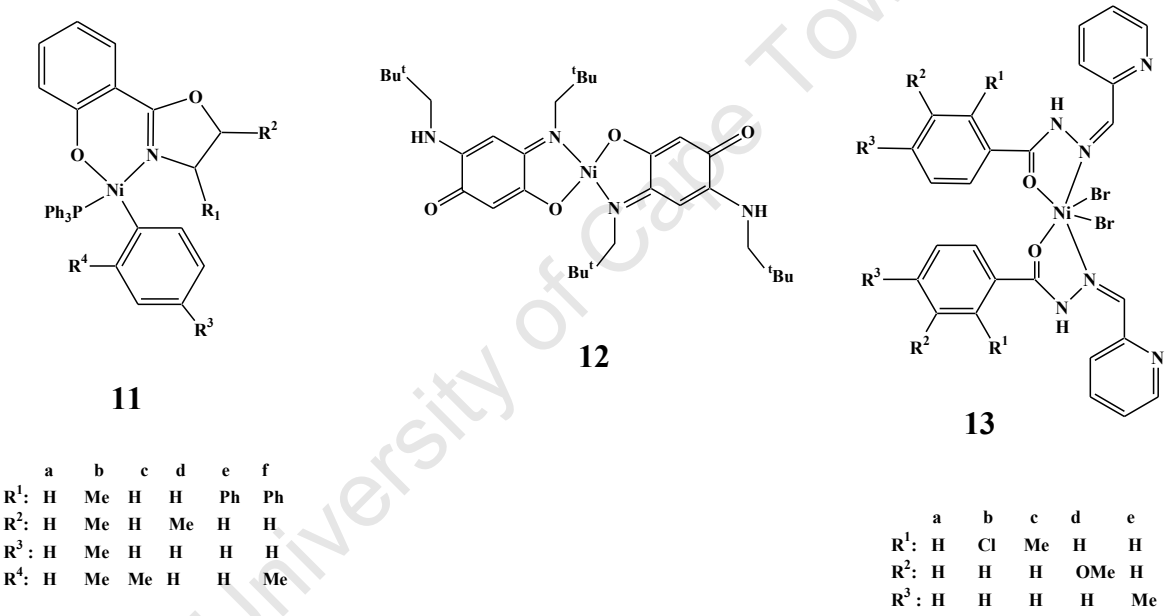

Figure 1.10 *Examples of complexes bearing N^O ligands [24c,24f,24g]*

Upon activation with MAO, DIBAL-H (diisobutylaluminium hydride) or $AlEt_3$, complex **11** showed high activities (up to 5.51 x 10^5 g prod.mol^{-1}Ni.h^{-1}) and selectivity for $C_4 - C_8$ olefins. The best activity (5.51 x 10^5 g prod.mol^{-1}Ni.h^{-1}) was observed for the catalyst bearing no substituents on the oxazoline and aryl rings i.e. $R^1 = R^2 = R^3 = R^4 = H$, while the lowest activity was observed for the catalyst with R^4 = Me (3.65 x 10^5 g prod.mol^{-1}Ni.h^{-1}). The major product when MAO was employed as co-catalyst was C_6 (up to 85 %), however of the C_4 olefins produced only 1-C_4 was detected. Selectivity when DIBAL-H was employed as a co-

catalyst resulted in C_4 being produced as the major product (up to 56 %) with a decrease in 1-C_4 (54 %). Better selectivities for C_4 were observed when $AlEt_3$ was used as a co-catalyst (up to 80 %) with only 1-C_4 detected. Overall, catalytic systems activated with MAO showed the highest catalytic activities [24f].

Complex **12** was found to be completely inactive when less than 6 equiv. of $EtAlCl_2$ were used. However, good catalytic activities of 2.85 x 10^5 mol C_2H_4.mol^{-1}Ni.h^{-1} and 4.50 mol C_2H_4.mol^{-1} Ni.h^{-1} at 6 and 10 equiv. $EtAlCl_2$ respectively were observed. The main products obtained were C_4 and C_6 olefins (approximately 50:50) with minute quantities of C_8 [24g].

Upon activation with MAO (Ni/Al ratio 50 – 1000) complex **13** showed good catalytic activity and selectivity for C_4 up to 100 % with 1-C_4 as high as 99 %. Complex **13e** gave the best catalytic activity (1.17 x 10^5 mol C_2H_4.mol^{-1}Ni.h^{-1}) at 300 equiv. MAO, with selectivities up to 100 % for the C_4 olefins (of which 99 % was 1-C_4). Lower activities (3.34 x 10^4 mol C_2H_4. mol^{-1}Ni.h^{-1} for **13b** and 3.80 x 10^4 mol C_2H_4.mol^{-1}Ni.h^{-1} for **13c**) were observed when $\mathbf{R^1}$ = Cl and Me respectively [24c].

1.6.2.2 Ni complexes bearing [P^N], [P^O] and [P^N^P] ligand systems

In much the same way as a coordinating nitrogen ligand can be modified (sterically or electronically) the σ-donor properties of a phosphine can be tailored by the introduction or modification of different groups on the phosphorus, as shown in some of the examples in Figure 1.11.

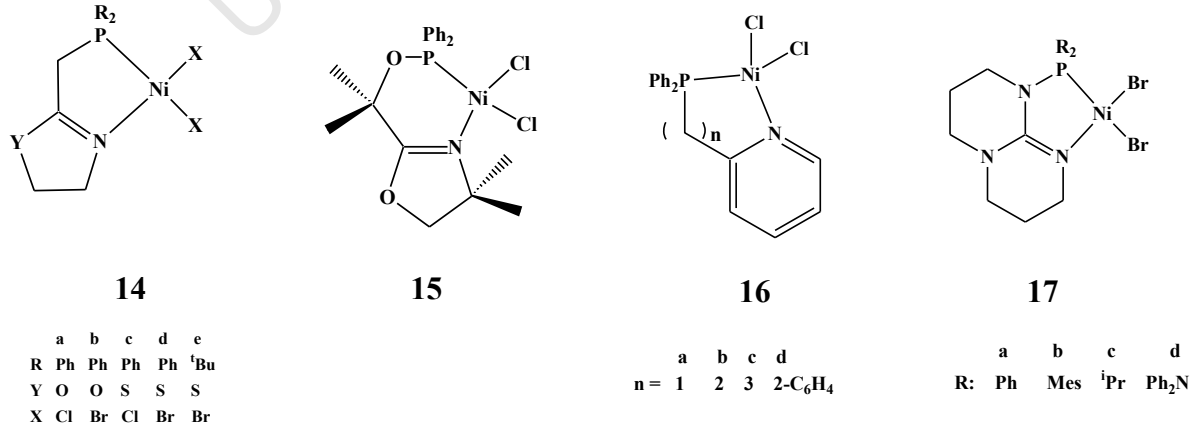

14

	a	b	c	d	e
R	Ph	Ph	Ph	Ph	^{t}Bu
Y	O	O	S	S	S
X	Cl	Br	Cl	Br	Br

15

16

	a	b	c	d
n =	1	2	3	2-C_6H_4

17

	a	b	c	d
R:	Ph	Mes	^{i}Pr	Ph_2N

Figure 1.11 *Examples of some nickel complexes bearing P^N ligands [25a, 25b, 25q]*

The electronic properties of a phosphine such as $–PPh_2$ can be modified by inclusion of heteroatoms such as oxygen (**15**) or nitrogen (**16**) directly bonded to the phosphorus atom. In addition, the basicity of a phosphine can be altered by substituting aryl groups in $–PPh_2$ for alkyl groups. These modifications will consequently have direct influence on the catalyst performance [25b, 25q].

Complexes **14** were activated with $EtAlCl_2$ (2 – 6 equiv.) at 45 bar and 25 – 30 °C. All these catalyst precursors produced mainly C_4 and C_6 olefins as well as minute quantities of $C_8 – C_{10}$ olefins. Dichloride and dibromide catalyst precursors were found to yield comparable activities. Replacing oxygen with sulfur in the azoline ring resulted in a significant decrease in activity (4.65 – 1.06 x 10^4 mol $C_2H_4.mol^{-1}Ni.h^{-1}$) at lower co-catalyst molar ratio (2 equiv.) while at higher co-catalyst ratio (6 equiv.) the activities were found to be 7.88 – 7.19 x 10^4 mol $C_2H_4.mol^{-1}Ni.h^{-1}$. Activation with MAO at 2000 equiv. was also conducted, with catalyst-precursors showing improved activities (up to 23 x 10^4 mol $C_2H_4.mol^{-1}Ni.h^{-1}$) and production of short-chain olefins in the $C_4 – C_{10}$ range. A decrease in activity was observed on substituting oxygen with sulfur in the azoline ring (10.8 – 5.92 x 10^4 mol $C_2H_4.mol^{-1}Ni.h^{-1}$ respectively); however, selectivity for C_4 was improved (75.3 – 89.1 %) [25a].

Complex **15** bearing a phosphinite group ($-OPPh_2$) was found to show good activity upon activation with $EtAlCl_2$. Complex **15** showed a gradual increase in activity (4.44 – 4.99 x 10^4 mol $C_2H_4.mol^{-1}Ni.h^{-1}$ respectively) with increase in co-catalyst concentration (2 – 6 equiv.) at the expense of C_4 selectivity (81 % at 2 equiv. and 64 % at 6 equiv.) [25a]. Compared to complex **15** bearing a phosphinite group, complexes **14a** and **14b** (bearing a phosphine group) showed significant improvements in activities on increasing the co-catalyst concentration from 2 to 6 equiv. (4.65 – 7.88 x 10^4 mol $C_2H_4.mol^{-1}Ni.h^{-1}$ for **14a** and 4.42 – 6.39 x 10^4 mol $C_2H_4.mol^{-1}Ni.h^{-1}$ for **14b**). However, as with **15,** selectivities for **14a** and **14b** declined on increasing the co-catalyst concentration (80 % at 2 equiv. and 53 % at 6 equiv. for **14a** and 71 % at 2 equiv. and 62 % at 6 equiv. for **14b**) [25a].

Pyridyl-phosphine complexes (**16**) were activated with MAO (230 equiv.) at 10 bar and 30°C producing up to 96 % C_4 and minute quantities of $C_6 – C_{10}$ olefins. The effect of the bite angle formed by the ligand was investigated. The bite angles (β_n) were found to be **16a**: 87.2°, **16b**: 94.7, **16c**: 101.8° and **16d**: 90.8°. A good correlation between bite angle and activity for **16a** –

16c (30, 70 and 85 x 10^3 mol C_2H_4.mol^{-1}Ni.h^{-1} respectively) was observed with only **16d** deviating from the trend (78 x 10^3 mol C_2H_4.mol^{-1}Ni.h^{-1}) [25q].

Complex **17** bearing a rigid *N*-phosphino guanidine ligand showed moderate activity (6.34 x 10^3 mol C_2H_4.mol^{-1}Ni.h^{-1}) after activation with $EtAlCl_2$ at 1 bar. The reaction was highly exothermic, reaching 80°C. These catalysts produced mainly C_4 and C_6 olefins as well as small quantities of C_8. Complex **17d**, having the weakest σ-donor phosphorus, showed the lowest activity (1.58 x 10^3 mol C_2H_4 .mol^{-1}Ni.h^{-1}) and selectivity for C_4 olefins (54.5 %), while complex **17c** bearing the strongest σ-donor phosphorus displayed the best activity (6.34 x 10^3 mol C_2H_4.mol^{-1}Ni.h^{-1}) as well as C_4 selectivity (85.4 %) [25a].

An interesting feature with the **17a**/$EtAlCl_2$/C_2H_4 catalyst system was a reaction between the reaction solvent (toluene) and ethylene which resulted in formation of < 1 % C_4 and C_6 products. GC analysis revealed the presence of C_4-, C_6-, C_8-, and C_{10}-alkyl substituted toluenes (Scheme 1.6 below).

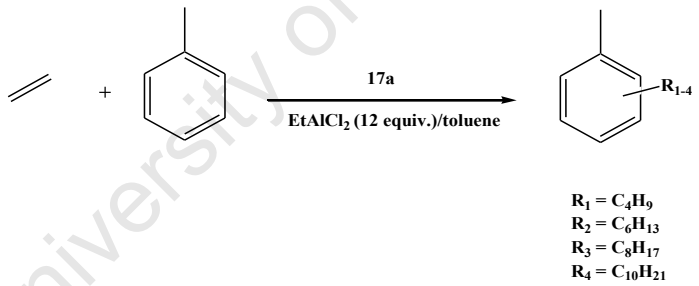

Scheme 1.6 *Formation of alkyl-substituted toluenes [25b]*

A plausible explanation for the formation of alkyl-substituted toluenes was that the active species, formed by **17a** and the alkyl aluminium co-catalyst was extremely active, but had a very short lifetime. A significant amount of short-chain olefins generated before loss of catalyst activity subsequently underwent the slower Friedel-Crafts alkylation reaction with toluene [25b]. Recently, Darkwa *et al*. observed a similar alkylation of the solvent with the preformed olefins, using their pyrazolyl-pyridineNi(II)-$EtAlCl_2$ catalyst system [23c'].

Tridentate (P^N^P) complex **18** (Figure 1.12) showed good catalytic activity upon activation with MAO and $EtAlCl_2$ (up to 1.14 x 10^5 g prod.mol^{-1}Ni.h^{-1}and 3.74 x 10^5 g prod.mol^{-1}Ni.h^{-1}

respectively). The major products were found to be C_4 (up to 92.1 % for MAO and 79.6 % for $EtAlCl_2$) and small quantities of C_6 and C_8 olefins. For both systems, selectivities for 1-C_4 within the C_4 fraction were high, up to 99 %. There was a good correlation between the steric bulk of **R[1]** and catalytic activity, following the order H < Me < OMe < Et < ^{i}Pr (3.16, 3.94, 5.58, 7.72 and 9.33 x 10^4 g prod. $mol^{-1}Ni.h^{-1}$ respectively for MAO-activated catalysts and 1.04, 2.78, 3.33, 3.24, 3.74 x 10^5 g $prod.mol^{-1}Ni.h^{-1}$ respectively for $EtAlCl_2$-activated catalysts). Higher activities were observed at lower concentrations of MAO, i.e. 1.02 and 1.14 x 10^5 g $prod.mol^{-1}Ni.h^{-1}$ at 250 equiv. and 500 equiv. respectively, compared to 9.33 x 10^4 g $prod.mol^{-1}Ni.h^{-1}$ obtained at 1000 equiv [26a].

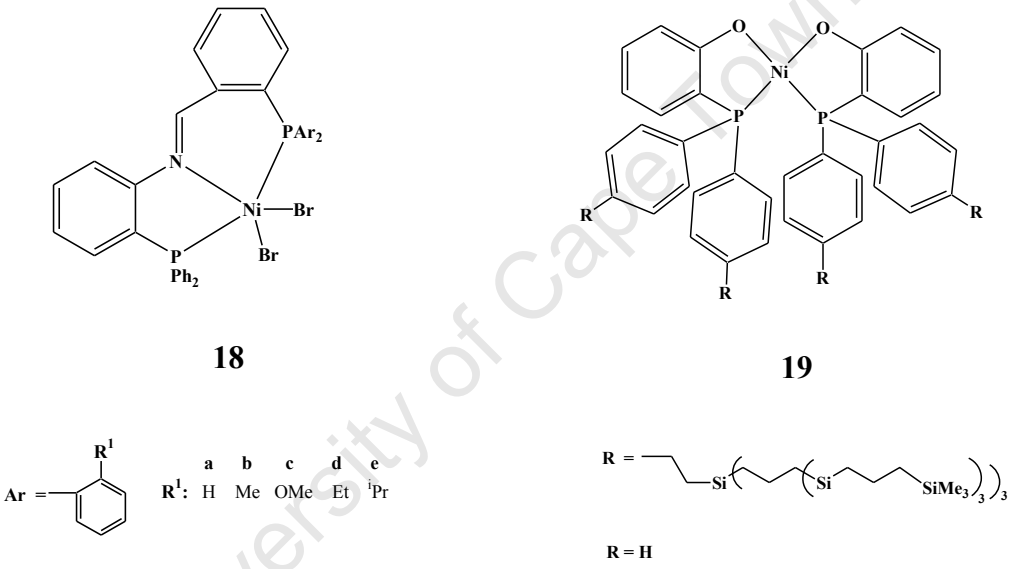

Figure 1.12 *Examples of some nickel complexes bearing P^N^P and P^O ligands [26a, 27d]*

Dendrimer **19** was used without an activator for catalytic ethylene oligomerization in polar (methanol) and non-polar (toluene) solvents, and was found to give moderate activity of 7.70 x 10^3 mol C_2H_4. $mol^{-1}Ni.h^{-1}$. Higher activities were observed when reactions were carried out in toluene (7.70 x 10^3 mol $C_2H_4.mol^{-1}Ni.h^{-1}$) compared to methanol (3.24 x 10^3 mol $C_2H_4.mol^{-1}$ $Ni.h^{-1}$) and H_2O (3.50 x 10^3 mol C_2H_4. $mol^{-1}Ni.h^{-1}$). The lower activities in methanol are thought to be due to either the presence of larger quantities of inactive species in methanol than in toluene, or to competition between methanol and ethylene for coordination. Reactions conducted in methanol gave 30 wt % of a Schulz-Flory distribution of low molecular weight olefins (C_4 – C_{30}) and insoluble higher molecular weight olefins (70 wt %) with 0.05 wt %

internal olefins. However, addition of PPh_3 in the methanol experiment resulted in mainly lower molecular weight olefins being formed (80 wt %) [27d].

1.6.2.3 Pd complexes bearing [N^N] and [P^N] ligand systems

Compared to neutral nickel complexes, there are a very small number of reports in the literature describing ethylene oligomerization catalyzed by neutral palladium catalyst precursors. The main reason is presumably the very low activity (or inactivity) observed with these catalyst systems. Nevertheless, there have been a few reports in which ethylene oligomerization has been catalyzed by neutral palladium catalyst precursors.

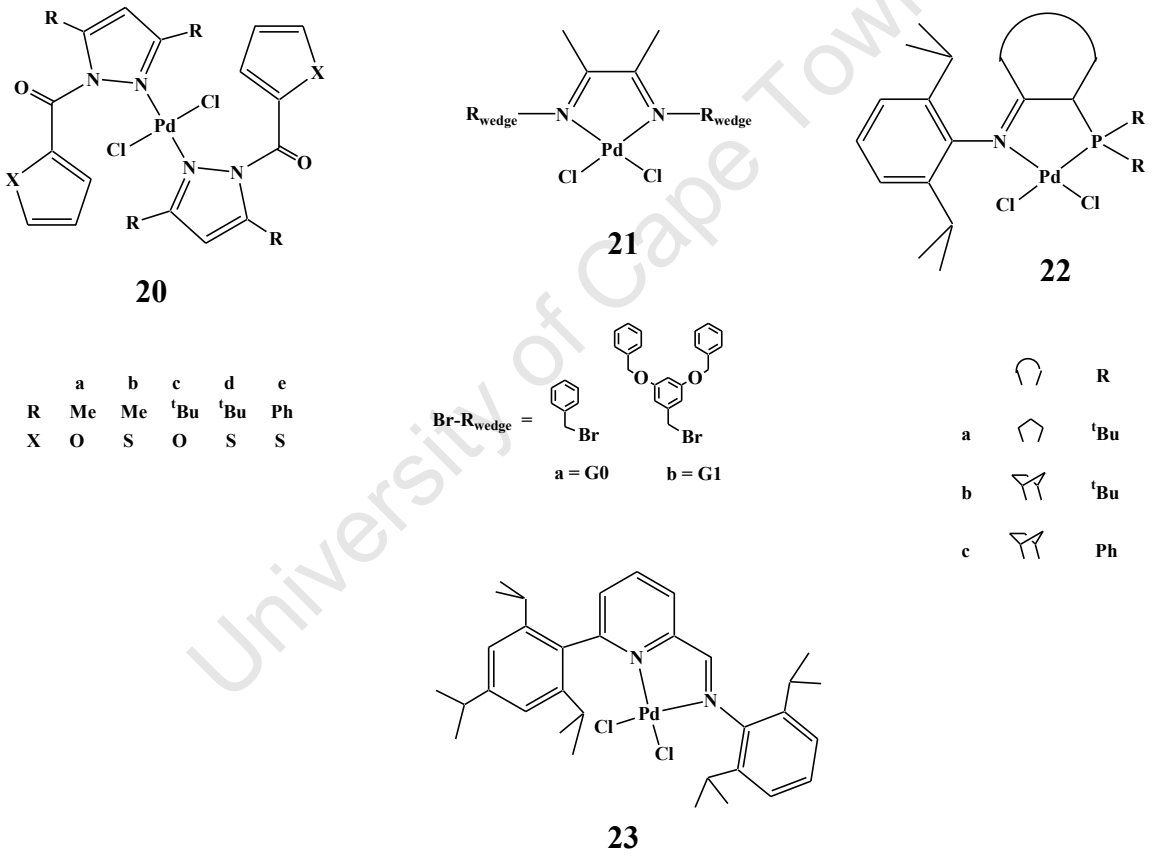

Figure 1.13 *Examples of some neutral palladium complexes bearing N^N and N^P ligands [23d',23h,25t,23e']*

Complexes **20a-e** were found to be highly active, giving activities up to 1.1 x 10^6 $g.mol^{-1}Pd.h^{-1}$ when activated with $EtAlCl_2$, and selectivities for higher carbon oligomers (up to 77 % C_{10}, 64 % C_{12} and C_{14} <11 %). Catalytic activity and oligomer selectivity were found to be affected by parameters such as co-catalyst molar ratio, ethylene pressure, reaction temperature and time. The effect of co-catalyst molar ratio was investigated using catalyst precursor **20a**, which

showed the optimum co-catalyst molar ratio to be 1000 equiv., yielding an activity of 1.1 x 10^5 g.mol^{-1}Pd.h^{-1} and selectivities of 50 % C_{10} and 45 % C_{12}. Increasing the ethylene pressure (5, 10, 20, 35) at 500 equiv. of $EtAlCl_2$ was found to gradually increase activity (1.8, 2.2, 2.8 and 5.4 x 10^5 g.mol^{-1}Pd.h^{-1} respectively), but decreased selectivity for C_{10} (77, 61, 51, and 48 % respectively). An increase in temperature from 25 °C to 60 °C led to an increase in the catalytic activity from 1.8 x 10^5 g.mol^{-1}Pd.h^{-1} at 25 °C to 1.1 x 10^6 g.mol^{-1}Pd.h^{-1} at 60 °C, with selectivity for C_{10} decreasing from 77 % to 32 %, while that of C_{12} increased from 25 % to 61 % [23d'].

α-Diimine palladium complexes **21** containing dendritic wedges were investigated for ethylene oligomerization and were found to show activity upon activation with MAO (400 equiv.). Owing to the reaction work-up employed, only higher carbon oligomers were detected (C_{10}, C_{12}, C_{14}+). More oligomeric products were obtained with the first generation dendritic wedge **21a** (112 mg), while 66 mg oligomer was obtained with **21b** [23h].

The sterically encumbered palladium complexes **22** were found to be inactive when activated with MAO, while the nickel counterparts were found to polymerize ethylene with activities up to 4.7 x 10^4 mol C_2H_4.mol^{-1}Ni^{-1} and polymer molecular weight up to 2000 g.mol^{-1}. On the other hand, the sterically encumbered palladium complexes **23** showed good activity towards ethylene polymerization (up to 2.0 x 10^4 g.mol^{-1}Pd.h^{-1}.bar^{-1}) when activated with MAO and MMAO. Higher activities and product distribution were observed for the nickel analogues. Activities of up to 1.6 x 10^5 g.mol^{-1}Ni.h^{-1}.bar^{-1} were observed, with oligomers (up to 1.86 g, of which 1.27 g were butenes) and polymer (up to 0.06 g) [25t,23e'].

1.6.3 Cationic Pd and Ni Complexes in Ethylene Oligomerization

1.6.3.1 Pd and Ni complexes bearing [N^N], [N^P], [N^O] and [P^O] ligand systems

It is generally accepted that the catalytically active species in ethylene oligomerization reactions is the cationic hydride complex, typically generated *in situ* as in the examples described before. It is, however, possible to synthesize and isolate cationic complexes (Ni and Pd) bearing a weak coordinating group (e.g. NCMe) that can be displaced by ethylene during the catalytic reaction. Owing to their cationic nature, the metal centers in these complexes are

electrophilic enough to coordinate ethylene and thus propagate to form oligomers/polymers without the use of a co-catalyst.

Selected examples of cationic nickel and palladium complexes and their catalytic performances are discussed below.

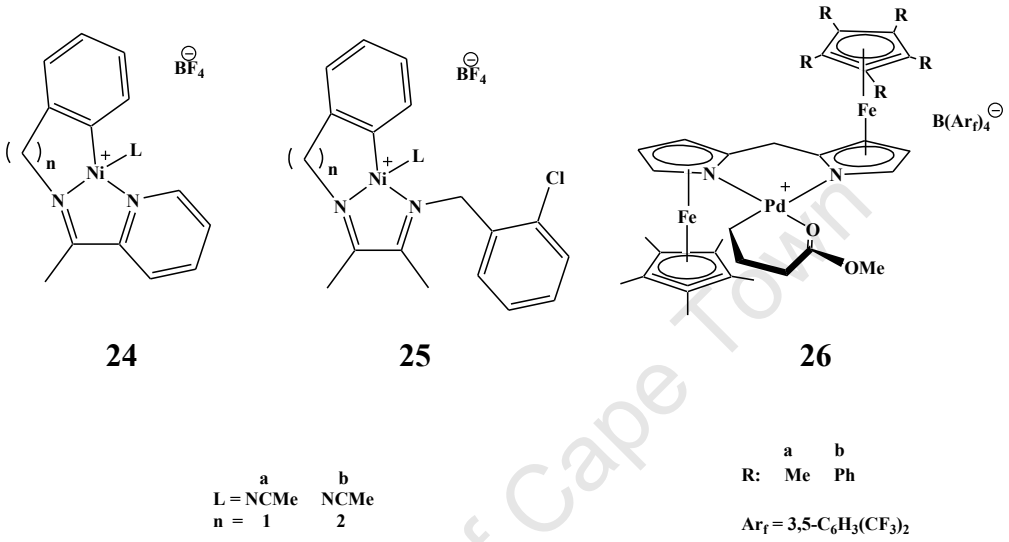

Figure 1.*14 Examples of some cationic nickel and palladium complexes bearing N^N ligands [23n, 23h]*

Complexes **24** and **25** were found to give low oligomerization activities and a Schulz-Flory distribution of oligomers ranging from C_4 to C_{18} in all cases. For **24** a better activity (1.63 x 10^3 mol C_2H_4.mol^{-1}Ni.h^{-1}) was observed for a five-membered metallacycle **24a** compared to that for the six-membered metallacycle **24b** (0.390 x 10^3 mol C_2H_4.mol^{-1}Ni.h^{-1}). The opposite effect was observed for **25**, with the six-membered metallacyclic complex **25b** showing activity (0.165 x 10^3 mol C_2H_4.mol^{-1}Ni.h^{-1}) superior to that of a five-membered metallacycle **25a,** which only afforded 0.050 x 10^3 mol C_2H_4.mol^{-1}Ni.h^{-1} [23n].

Complex **26a** was found to show low (0.060 x 10^3 mol C_2H_4.mol^{-1}Ni.h^{-1}) to moderate (2.08 x 10^3 mol C_2H_4.mol^{-1}Ni.h^{-1}) activities at 20 °C and 80 °C, yielding high molecular weight oligomers (200 - 600 g.mol^{-1}) with moderate branching (20 – 60 branches /1000C). The catalyst activity was found to improve with increasing temperature from 20 °C to 80 °C (2.08 x 10^3 mol C_2H_4.mol^{-1}Ni.h^{-1}), with a further increase in temperature (120 °C) resulting in a significant drop in activity (0.992 x 10^3 mol C_2H_4.mol^{-1}Ni.h^{-1}). However, at high temperatures

the average molecular weight of the oligomer decreased, probably due to increased rate of chain transfers at these temperatures. Increasing the pressure (from 100 to 500 psig) also caused an improvement in activity (from 2.08 to 3.11 x 10^3 mol C_2H_4.mol^{-1}Ni.h^{-1}).
The unsymmetrical complex **26b** was found to exhibit activities as low as 0.0540 x 10^3 mol C_2H_4.mol^{-1}Ni.h^{-1} at 40 °C. Increasing the temperature to 80 °C proved detrimental to the catalyst's activity which dropped to 0.00250 x 10^3 mol C_2H_4.mol^{-1}Ni.h^{-1}. The diminished activity for **26b** was proposed to be due to the difference in relative rates of the migratory insertion step (Figure 1.15).

In simple terms, migratory insertion can be thought of as attack of the nucleophilic $\mathbf{R_2}$ on the electrophilic ethylene. The $\mathbf{R_2}$ *trans* to the cyclopentadienyl azaferrocene (δ^-) in **26b** is less nucleophilic compared to the one in **26a** (δ^{--}), thus faster rates are observed for **26a**.

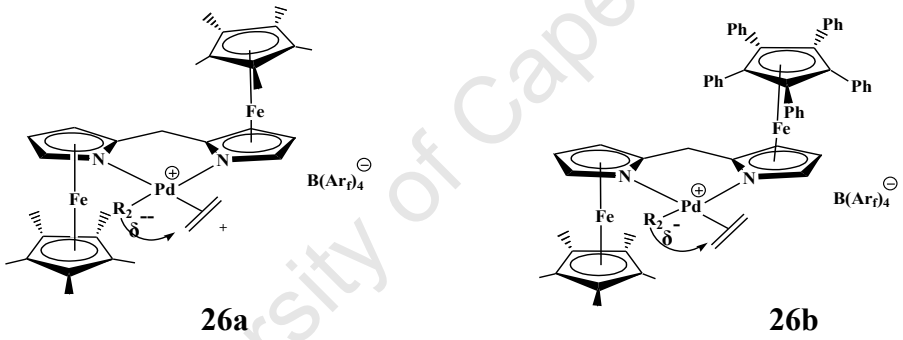

26a **26b**

Figure 1.15 *Structures showing nucleophilic attack of* $\boldsymbol{R_2}$ *on ethylene [23h]*

Oligomerization with complexes **27a** and **27b** (Figure 1.16) was found to commence at room temperature without any observed induction period. These catalysts showed moderate activities, up to 5.05 x 10^3 mol C_2H_4.mol^{-1}Ni.h^{-1} and selectivities for C_4 and C_6 with small quantities of C_8. Complex **27b** bearing **R** = Cy showed an increase in formation of the C_6 product (C_4 = 44.8 % and C_6 = 38.8 %) compared to its phenyl-substituted counterpart (C_4 = 68.0% and C_6 = 27.8 %). The palladium analogues **27c** and **27d** were found to show moderate catalytic activity, reaching a maximum of 4.29 x 10^3 mol C_2H_4.mol^{-1}Ni.h^{-1}. Heating was necessary to initiate the catalytic reaction [27c].

Complexes **28** on the other hand gave very low catalytic activities (up to 16 mol C_2H_4.mol Ni.h^{-1}) at 30°C and was selective for short-chain oligomers (C_4 – C_{10}) with C_4 being the major olefin. An inverse relationship was observed between the size of the catalyst metallacycle (i.e. n = 1 – 3) and activity. Activity dropped from 8.00 mol C_2H_4.mol^{-1}Ni.h^{-1} (n = 1) to 2.70 mol C_2H_4.mol^{-1}Ni.h^{-1} (n = 3). Complexes **28d** bearing an aryl phosphine gave higher activity of 16 mol C_2H_4.mol^{-1}Ni.h^{-1} at the expense of C_4 selectivity. Due to the very low activities observed for **28**, odd-numbered olefins (C_5, C_7, C_9) resulting from insertion of ethylene molecules into the Pd-CH_3 bond of the starting parent catalyst, could also be detected [25o].

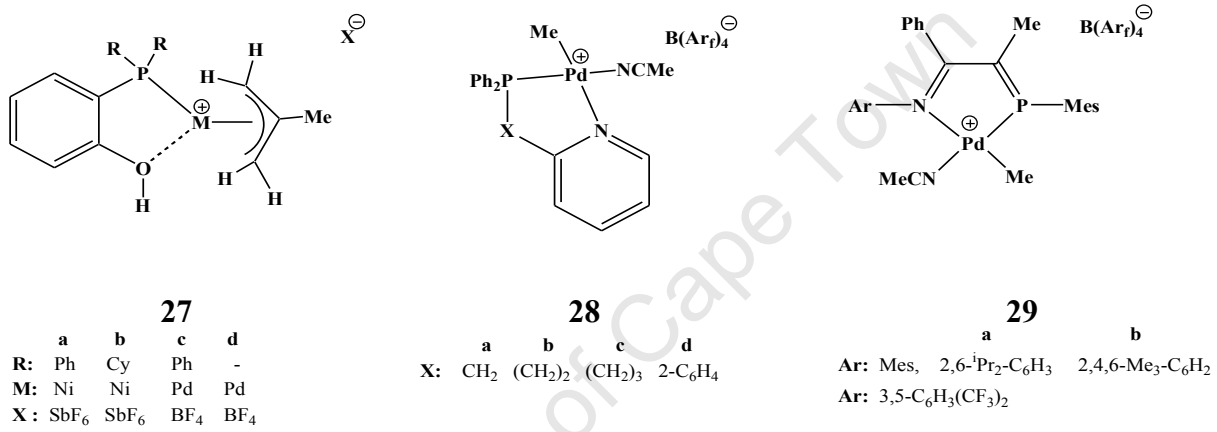

Figure 1.16 *Examples of cationic nickel and palladium complexes bearing N^N, P^N and P^O ligands [27c,25m,25o]*

Complexes **29** also showed low catalytic activities and produced mainly high molecular weight oligomers (230 – 670 g.mol^{-1}). A higher catalytic activity of 94 mol C_2H_4.mol^{-1}Ni.h^{-1} was observed for **29b** bearing a less sterically hindered active site, compared to the more hindered **29a** (23 mol C_2H_4.mol^{-1}Ni.h^{-1}). Ethylene insertion barriers calculated for **29a** were found to be high, which could explain the low activities observed.

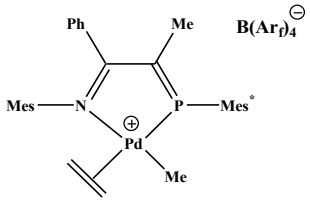

Mes = 2,6-di-^{i}Pr$_2$ C_6H_3
Mes* = 2,4,6-^{t}Bu$_3$ C_6H_2

29c

Figure 1.17 *Ethylene coordinated complex generated from* ***29b*** *[25m]*

Complex **29c** (Figure 1.17) was generated at -78 °C under excess of ethylene (20 equiv.). Migratory insertion of ethylene into the Pd-CH_3 bond was observed at -23 °C, with k = 7.9 x 10^{-5} s^{-1} corresponding to $\Delta G^{\ddagger}$ = 19.2 kcal.mol^{-1}. The insertion of ethylene into the Pd-alkyl bond was measured giving k = 2.4 x 10^{-5} s^{-1} and $\Delta G^{\ddagger}$ = 18.7 kcal.mol^{-1}. This value was higher when compared to migratory insertion barriers for the corresponding cationic (diimine)Pd(Me)(C_2H_4) complexes which were found to be approximately $\Delta G^{\ddagger}$ = 17 kcal.mol^{-1}. This difference in the insertion barriers (2 kcal. mol^{-1}) could account for the low activities observed in complexes **29a–c** compared to their diimine Pd analogues (i.e 4.5 x 10^3 mol C_2H_4.mol^{-1}Pd.h^{-1} for the (diimine)Pd and 94 mol C_2H_4.mol^{-1}Pd.h^{-1} for **29b**) [25m].

The nickel complexes **30a** and **30c** were found to be very active and selective for C_4 olefins at 25°C and high pressures (200 psig). Catalytic activities as high as 1.3 x 10^6 mol C_2H_4.mol^{-1} Ni.h^{-1} were observed with **30a**, with selectivities for C_4 ranging from 84 % (**30a**) to 98 % (**30c**). Complex **30b** on the other hand gave polyethylene at high temperatures (100 °C). A plausible reason for the contrasting results observed for **30a, 30b** and **30c** could be presence of the steric bulk on the aryl groups positioned both above and below the axial sites of the molecule (**30b**), which retards the rate of chain transfer to yield high molecular weight polyethylene (up to 1130 g.mol^{-1}Ni.h^{-1}) [25r].

Palladium complexes (**27a–c**) were found to be less active, with activities as high as 1.30 x 10^3 mol C_2H_4.mol^{-1}Pd.h^{-1}, with **31a** and **31c** giving exclusively C_4 olefins and **31b** giving a mixture of C_4 and C_6 olefins. In all cases selectivity for α–olefins was observed to be > 90 % [25s].

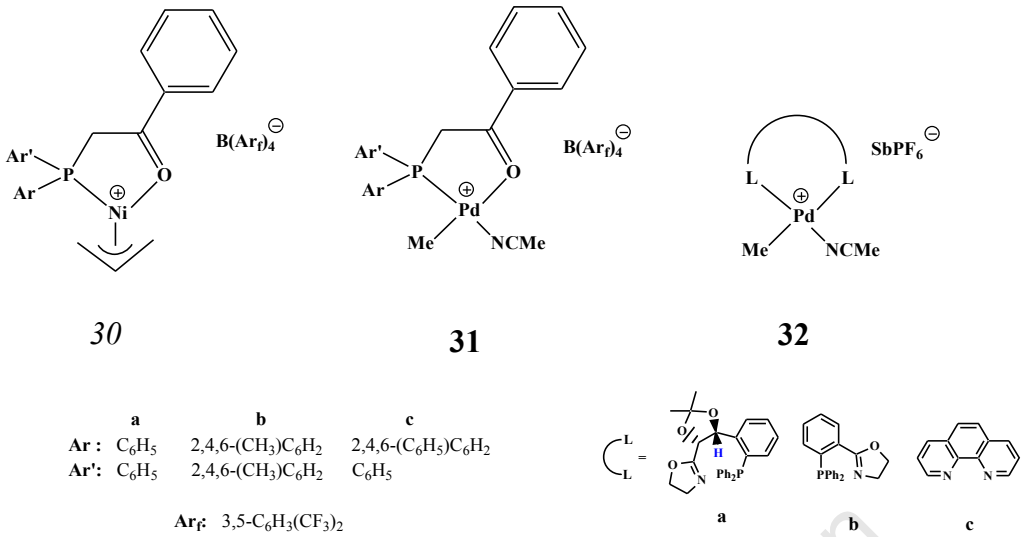

Figure 1.18 *Cationic nickel and palladium complexes bearing N^N, P^N and P^O ligands [25r, 25s]*

The related complexes **32a-c** were all found to show moderate activities of up to 1.57 x 10^4 mol C_2H_4.mol^{-1}Pd.h^{-1}, with **32a** yielding a statistical (Schulz-Flory) distribution of olefins and **32b** and **32c** producing only C_4 olefins. This result illustrated the effect of the axial C_{sp3}**H**···Pd interaction which promoted chain propagation, leading to production of α-olefins up to C_{24}. Complexes **32a-c** produced up to 75 % linear α-olefins, with branched products not observed. Increasing pressure was found to improve the catalyst's activity, (0.790 x 10^4 mol C_2H_4.mol.Pd.h^{-1} at 200 psig and 2.56 x 10^4 mol C_2H_4.mol^{-1}Pd.h^{-1} at 700 psig), while an increase of temperature from 25 °C to 50 °C resulted in a 10-fold improvement in activity to 1.57 x 10^4 mol C_2H_4.mol^{-1}Pd.h^{-1} [25r].

1.6.4 Mechanism of Ethylene Oligomerization Catalyzed by Nickel or Palladium Complexes

It is apparent that most of the catalysts described in this chapter favour chain transfer over chain propagation, thus showing a preference for oligomer formation over polymer formation. Brookhart *et.al.* determined that reduction of steric bulk of the *ortho*-substituents in Ni(II) and Pd(II) aryl-substituted α-diimine catalysts resulted in an increase in the rate of associative chain transfer. This led to a Schulz-Flory distribution of linear α-olefins (C_4 – C_{24}) with small quantities of internal olefins and no formation of branched olefins [23a']. However, a substantial number of nickel and palladium ethylene oligomerization catalysts show high

activities but very poor selectivities for linear α-olefins. Scheme 1.7 and Scheme 1.8 below outline the accepted mechanisms for the generation of α-olefins and their isomerized linear and branched products [23b',27c, 24f,25i].

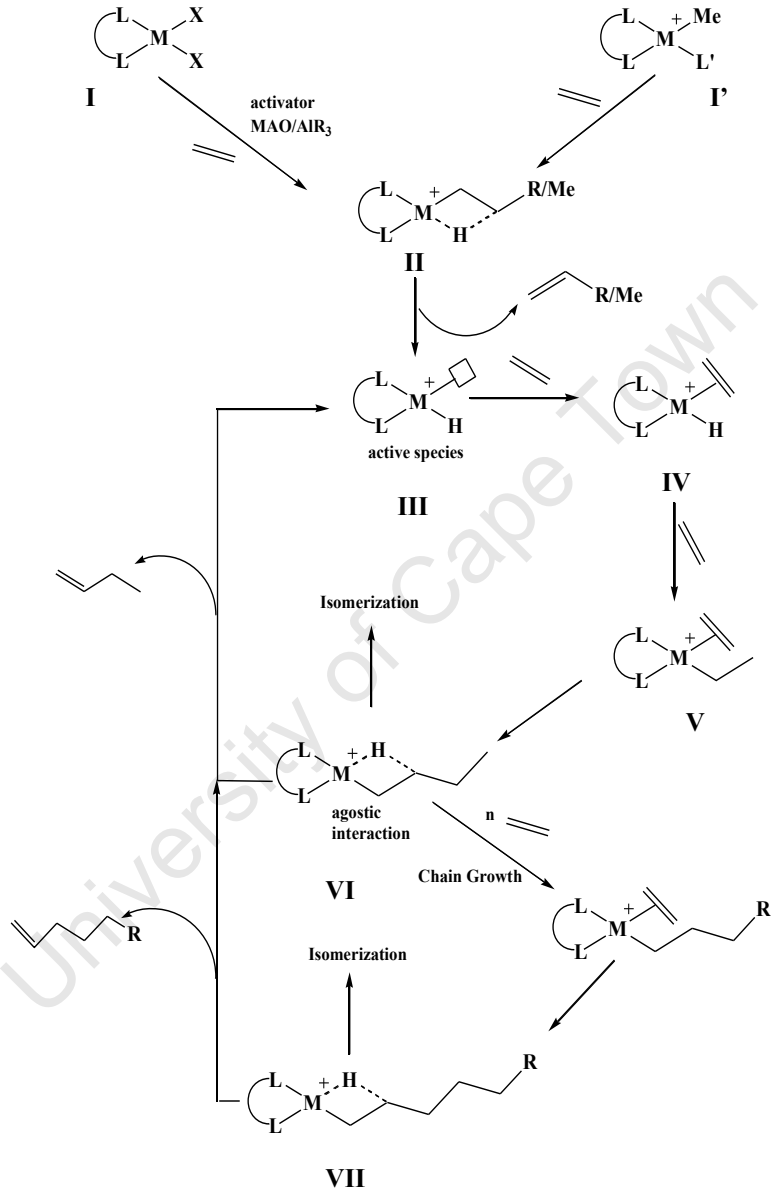

Scheme 1.7 *Proposed ethylene oligomerization mechanism for α-olefins [23b',27c, 24f,25i]*

The cationic active species **III** can be generated from the dihalide complex **I** (Ni(II) or Pd(II)) activated with an alkylaluminium compound (e.g. MAO) or by means of single-component system (**I'**), in which a weakly coordinated ligand (**L**', e.g. NCMe) is displaced by ethylene.
The reactive cationic hydride **III** then coordinates ethylene (**IV**) which inserts into the M–H bond giving species **V**. This undergoes a second insertion of ethylene to yield a C_4 alkyl

complex **VI**. The C_4 alkyl complex can undergo β-hydride elimination to give 1-C_4 followed by regeneration of the active hydride intermediate (**III**). Alternatively species **VI** can coordinate and insert a number of ethylene molecules to give intermediate **VII**. Chain termination by intermediates of different carbon chain lengths furnishes a Schulz-Flory distribution of α-olefins. For both intermediates **VI** and **VII**, β-hydride elimination can lead to the production of α-olefins, internal olefins (isomerization) and branched products. Most nickel and palladium complexes are selective for C_4 and C_6 products, however selectivity for linear products and α-olefins is usually very low. The mechanism for isomerization is shown in Scheme 1.8 [23b', 27c, 24f, 25i].

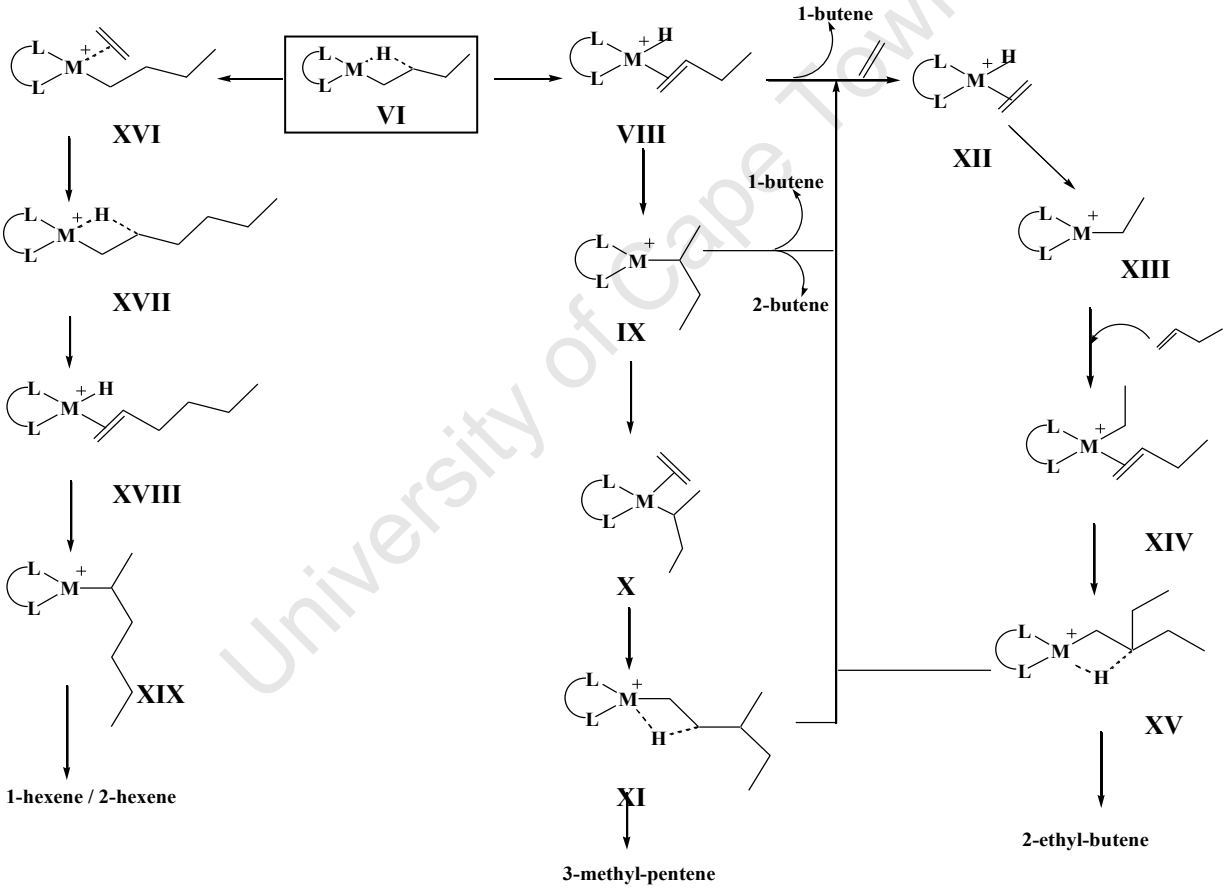

Scheme 1.8 *Proposed mechanism for double-bond isomerization and formation of branched olefins [23b', 27c, 24f, 25i]*

The scheme above shows the formation of C_4 (i.e. 1-C_4, 2-C_4) as well as C_6 secondary products. For the formation of linear C_6 olefins (i.e. 1-C_6 and 2-C_6), intermediate **VI** undergoes coordination of another molecule of ethylene (**XVI**) and insertion to give **XVII** followed by β-

hydride abstraction to give **XVIII** which can undergo reinsertion at the terminal or β-carbon to yield 1-C_6 and cis/trans 2-C_6 respectively. Similarly, **VI** can undergo β-hydride abstraction to give **VIII** which can reinsert into the M-H bond at the β-carbon to give **IX**. This intermediate can undergo β-hydride elimination at the terminal or β-carbon to yield 1-C_4 and cis/trans 2-C_4 respectively. Intermediate **IX** can also undergo coordination and insertion of a molecule of ethylene giving **X** and **XI** respectively, followed by β-hydride elimination and dissociation of the olefin to give 3-methyl-pentene. On the other hand intermediate **VIII** can dissociate 1-C_4 and coordinate and insert a molecule of ethylene to give **XII** and **XIII** respectively. Intermediate **XIII** can then coordinate and insert a molecule of 1-C_4 to give intermediate **XIV** and **XV** respectively followed by β-hydride elimination and dissociation to yield 2-ethyl-butene.

1.7 Chromium Complexes in Ethylene Oligomerization

For many years, chromium catalyst systems, especially those bearing cyclopentadienyl and its substituted analogues, had been widely used to polymerize ethylene to polyethylene [32]. However, the discovery of ethylene trimerization using a chromium catalyst system by Manyik inspired interest among the research community to employ chromium complexes as potential oligomerization catalysts [13,32–42].

In the past few years, ligand systems for highly active and selective homogeneous chromium-catalyzed ethylene trimerization catalysts have been developed [32–42]. Ligand systems such as the S^N^S and P^N^P shown below have revealed good catalytic performance toward the selective production of 1-C_6 [12a,33].

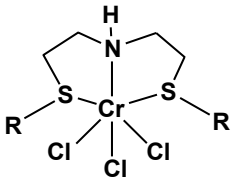

33

	a	b	c	d
R:	Me	Et	^{n}Bu	^{n}decyl

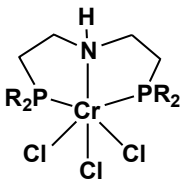

34

	a	b	c
R:	Et	Ph	Cy

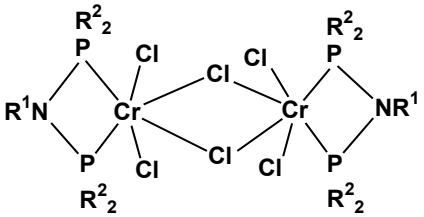

35

	a	b	c	d	e
R^1:	Me	^{i}Pr	Cy	Ph	pentyl
R^2:	Ph	Ph	Ph	Ph	Ph

Figure 1.19 *Examples of S^N^S and P^N^P catalyst precursors [12a,33]*

Upon activation with MAO, complexes **33** showed good catalytic activities (up to 2.98 x 10^5 mol C_2H_4.mol^{-1}Cr.h^{-1}), producing C_6 with selectivities up to 98.4 wt % (of which 99.7 % was 1-C_6) and a small amount of polyethylene (0.10 wt %). Similarly, complexes **34** furnished good catalytic activities (up to 3.74 x 10^4 mol C_2H_4.mol^{-1}Cr.h^{-1}) and C_6 selectivities of up to 99.1 % of which 1-C_6 was 93.2 %. A small amount of polyethylene (2.1 %) was also produced [12a].

The P^N^P chromium catalyst precursors **35**, employed for ethylene tetramerization, gave 1-C_8 with selectivities of up to 68.3 %. The discovery of this catalyst precursor was a breakthrough given that the reaction has been proposed to proceed via an extension of the ethylene trimerization mechanism. Budzelaar *et al.* had earlier argued that the proposal was unlikely [34]. Overett *et al.* then undertook deuterium-labeling investigations using a mixture of C_2H_4 and C_2D_4 to verify the mechanistic pathway for ethylene tetramerization and found that it indeed proceeds via metallacyclic intermediates as shown for ethylene trimerization [35]. A catalytic cycle depicting the selective production of 1-C_4, 1-C_6 and 1-C_8 is shown in Scheme 1.9.

Different product distributions using chromium catalysts have also been reported (i.e. catalysts not selective for C_6 and C_8). For example, complex **36** was activated with a number of alkylaluminium co-catalysts (Et_3Al, Et_2AlCl, MAO and MMAO), with MMAO giving the best catalytic activity (1.76 x 10^5 g.mol^{-1}Cr.h^{-1}) at 25 °C, 10 bar, and 1000 equiv. MMAO. Reaction

temperature was found to have a marked effect on the catalytic activity and product distribution. For example, the activity for oligomeric components increased gradually with an increase in temperature from 0 to 40 °C (1.63 x 10^3 g.mol^{-1}Cr.h^{-1} and 3.12 x 10^3 g.mol^{-1}Cr.h^{-1} respectively), while a further increase in temperature to 60 °C resulted in a decline in oligomerization activity (2.28 x 10^3 g.mol^{-1}Cr.h^{-1}). The activity for polymeric components was also observed to decrease with increasing reaction temperature. The catalyst showed declining polymerization acivities of 2.73 x 10^4 g.mol^{-1}Cr.h^{-1}, 5.10 x 10^3 g.mol^{-1}Cr.h^{-1}, and 1.40 x 10^3 g.mol^{-1}Cr.h^{-1} at 0, 40, and 60 °C respectively [36].

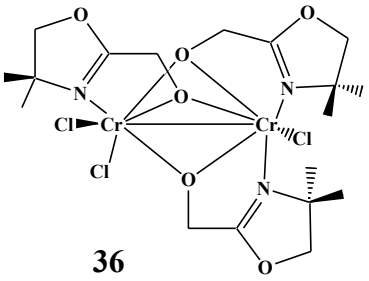

36

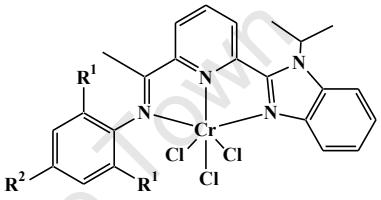

37

	a	b	c	d	e	f
R^1:	Me	Et	^{i}Pr	F	Cl	Me
R^2:	H	H	H	H	H	Me

Figure 1.20: *Examples of oxazoline alcoholate **36** and α-diimine **37** chromium complexes*

Complex **37** on the other hand produced a statistical distribution of oligomers ($C_4 - C_{36}$) upon activation with MMAO. This catalyst system gave moderate to high activities, up to 1.31 x 10^5 g.mol^{-1}Cr.h^{-1} at 1 atm and 3000 equiv. MMAO and 3.95 x 10^6 g.mol^{-1}Cr.h^{-1} at 10 atm and 1500 equivalents MMAO [37].

Owing to the high selectivities for α-olefins observed in ethylene oligomerization with chromium catalysts, the mechanistic pathway for these systems is believed to proceed via metallacycloalkane intermediates. The catalytic cycle (Scheme 1.9 below) begins with coordination of two molecules of ethylene to chromium (**I**) followed by oxidative coupling of the two ethylene molecules into the chromium centre to form a chromacyclopentane (**II**). This intermediate can then undergo intramolecular β-hydride elimination and dissociation of the olefin to yield selectively the ethylene dimerization product 1-C_4. Alternatively a third molecule of ethylene can coordinate and insert to form a chromacycloheptane (**III**), which can then decompose via intramolecular β-hydride elimination and dissociation of the olefin to yield

1-C_6 [12a,13,38]. A further molecule of ethylene can also coordinate and insert into the chromocycloheptane intermediate to form a chromacyclononane (**IV**) intermediate which can decompose to give 1-C_8 [35]. Jolly *et al.* isolated metallacyclic intermediates (chromacyclopentane and chromacycloheptane) and characterized them by single crystal X-ray crystallography [39].

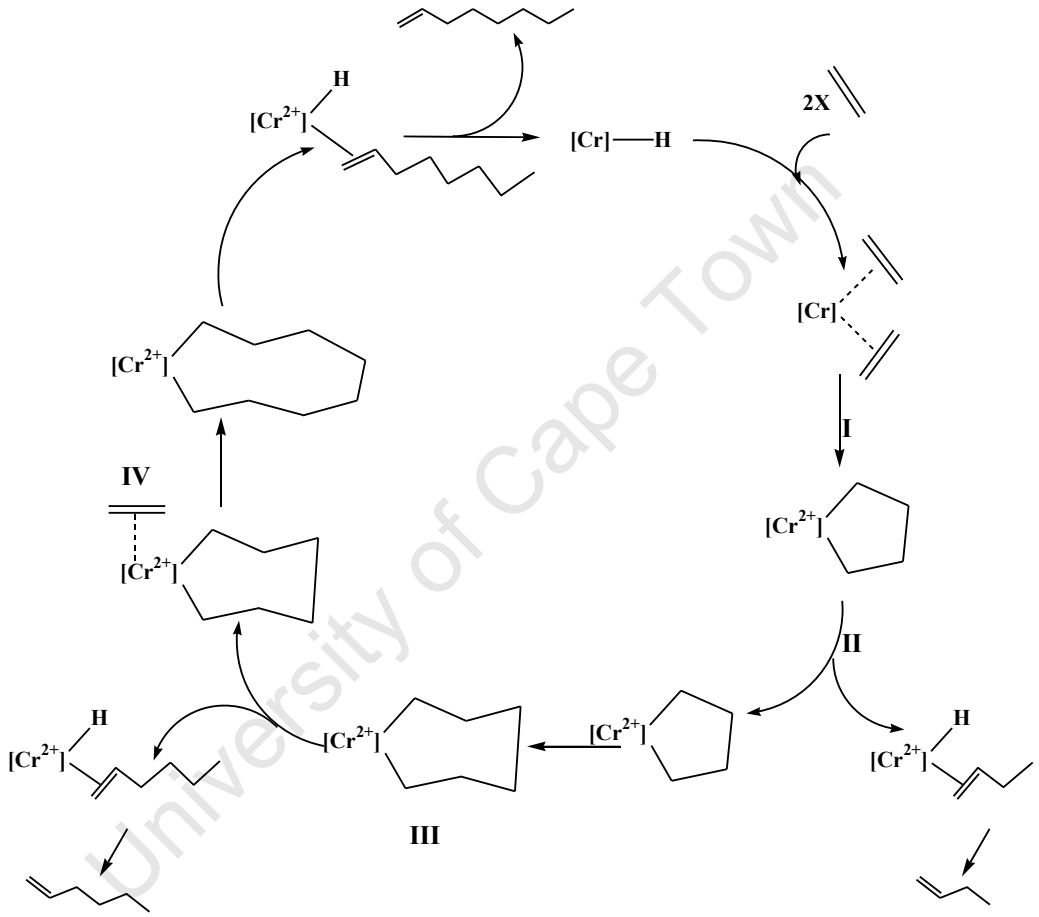

Scheme 1.9 *Catalytic cycle for ethylene trimerization and tetramerization via metallacyclic intermediates [35]*

The ethylene tetramerization catalytic cycle described above allows for the production of by-products such as methylcyclopentane and methylenecyclopentane as the third major products after 1-C_6 and 1-C_8 [35]. Scheme 1.10 below describes the proposed formation of these by-products.

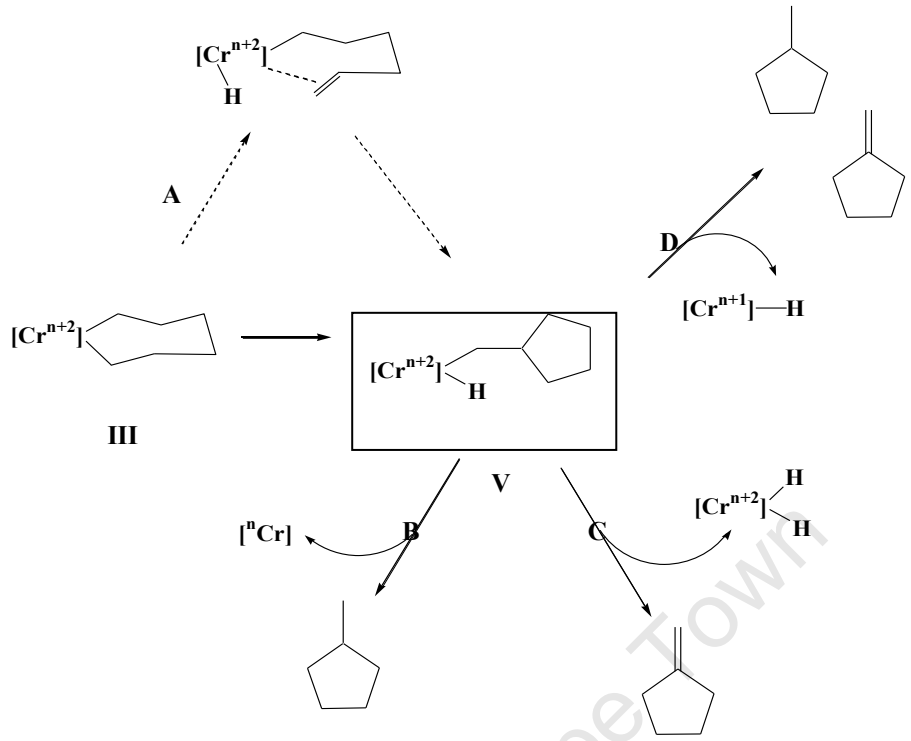

Scheme 1.10 *Proposed mechanism for the formation of methylcyclopentane and methylenecyclopentane [35].*

In the catalytic tetramerization reaction above, methylcyclopentane and methylenecyclopentane are typically formed in 1:1 ratio. These products are proposed to form by rearrangement of the chromacycloheptane (**III**) to give the Cr cyclopentylmethyl hydride intermediate **V** (via path **A**) that competes with chain transfer to yield 1-C_6. Intermediates can undergo two competitive pathways with similar rates. These are reductive elimination (**B**) to yield methylcyclopentane and β-hydride elimination (**C**) to give methylenecyclopentane. Alternatively, a disproportionation process (**D)** of intermediate **V** can yield the two products [35,34].

Gibson *et. al.*, using their N^N^N catalyst system (Figure 1.21), were able to demonstrate that much larger oligomers could be formed via the described metallacyclic pathway and involving larger chromacycles [40].

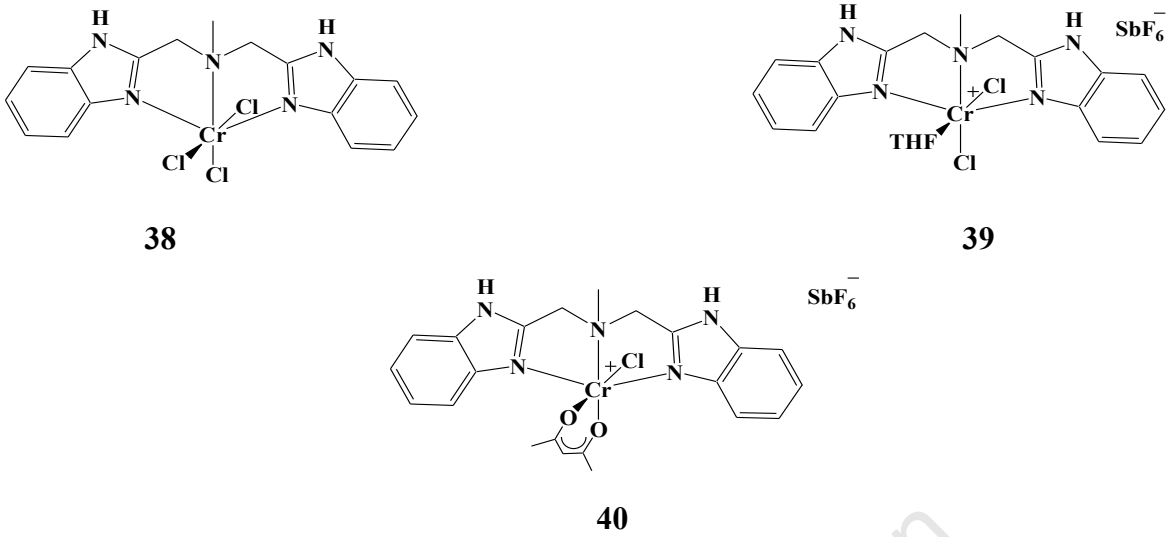

38 **39**

40

Figure 1.21 *Bis(benzimidazolyl)methylamine chromium complexes [40b]*

All complexes **38** – **40** showed good catalytic activities with complex **38** giving activities of 1.02 x 10^5 g.mol^{-1}Cr.h^{-1}.bar^{-1} at 4 bar ethylene pressure, while complexes **39** and **40** afforded lower catalytic activities of 1.56 x 10^4 g.mol^{-1}Cr.h^{-1}.bar^{-1} and 2.11 x 10^4 g. mol^{-1}Cr.h^{-1}.bar^{-1} respectively at the same pressure. The lower activities for **39** and **40** were attributed to the presence of the oxygen donor groups from THF and acac ligands respectively. All complexes gave 99 wt % α-olefins ranging from C_4 – C_{38}. When a 50:50 mixture of C_2H_4 and C_2D_4 was used, even-numbered α-olefins with H/D isotopomers of both the major (C_{4n}) and minor (C_{4n+2}) products were obtained. This product distribution (predominantly affording α-olefins) suggested a metallacyclic pathway [40].

Efforts to better understand the mechanistic pathway for the highly selective Cr-catalyzed ethylene trimerization and tretramerization reactions are ongoing. Much effort has been put into the determination of the oxidation state of the active chromium intermediate. EPR and UV-Vis spectroscopic studies have been important in the investigation of the paramagnetic chromium complexes. A plausible active species in ethylene oligomerization is a Cr(II) species, generated from a reaction of a reducing alkylaluminium (e.g. MAO) and a Cr(III) complex. Gambarotta *et. al.* prepared Cr(II) and Cr(III) complexes and showed that the Cr(II) complex performed better in ethylene oligomerization (3.81 x 10^3 g.g^{-1}Cr.h^{-1}) compared to its Cr(III) counterpart (2.32 x 10^4 g.g^{-1}Cr.h^{-1}), indicating that the Cr(III) complex could be a precursor to the active Cr(II) species. Since the d^3 and d^4 electronic configurations of the

Cr(III) and Cr(II) complexes provide distinct EPR spectral features, EPR studies have proved important in determining the oxidation states of the abovementioned chromium species [42b]. For example, Evans *et. al.* observed a significant reduction of the strong isotropic d^3 EPR signal upon addition of three molar equivalents of Me_3Al to a solution of the Cr(III) parent complex to give an EPR silent species. This corresponds to the proposed change in the oxidation state from the Cr(III) to the Cr(II) species. Addition of an excess of the Me_3Al resulted in complete loss of the EPR resonance. In their UV-visible studies, the solution of the Cr(III) catalyst precursor immediately changed colour from purple to yellow-green on addition of Me_3Al. The UV-visible spectrum showed a change from two bands to one. It was proposed that the blue shift could be due to the substitution of the chlorides for methyl groups in the Cr(III) species. This transition was proposed to be accompanied by a change in oxidation state from Cr(III) to Cr(II) [42a,41,40].

1.8 Summary

The oligomerization of ethylene into valuable higher olefins (1-C_4, 1-C_6, and 1-C_8) has been a subject of great interest both academically and commercially. Transition metal complexes have shown significant potential as homogeneous catalysts for ethylene oligomerization.

This review chapter describes the important aspects and factors affecting catalyst performance, with particular focus on chromium, nickel, and palladium catalysts for ethylene oligomerization. Undoubtedly, the ligand is the most important component in homogeneous catalysis. Minor modifications to the ligand backbone can result in major changes in the catalyst performance. In addition, the metal center has been shown to have a great influence on the oligomerization/polymerization activity and product distribution. Effects of varying reaction parameters such as co-catalyst molar ratio, reaction temperature and time, and ethylene pressure have been found to influence the catalytic activity and product distribution. Literature examples have been discussed to highlight these points. Ethylene oligomerization mechanistic pathways were also discussed.

1.9 Aims and Objectives of the Thesis

1.9.1 Aims

It is clear that there is widespread interest in the use of Ni-, Cr- and Pd-based catalyst systems for ethylene oligomerization. Numerous examples of highly active complexes bearing bidentate or tridentate ligands have been reported. Bidentate N^N and tridentate N^N^N ligand systems appear to be more prevalent, with relatively fewer examples of P^N ligands in ethylene oligomerization having been reported. Therefore the aims of this project are:

- The design and synthesis of new bidentate P^N ligands (**L**)
- Coordination of the ligands (**L**) to Ni, Pd, and Cr centers to produce metal complexes
- Testing of the resultant complexes for ethylene oligomerization activity

1.9.2 Specific goals

A series of new iminophosphine ligands (**L**) of the type (**A**) with the general structure shown below has been prepared.

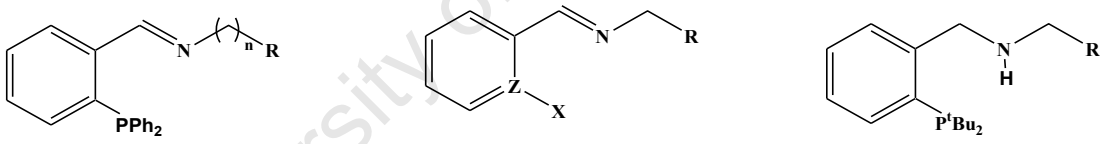

A

R = furyl or thiophene

B

Z = C, **X** = OH
Z = N
R = furyl

C

R = furyl

For comparison, the coordinating properties of the groups (X, Z, and N) as well as the length of the spacer ($_n$) (compounds **A** and **B**) have been varied to probe the effect of these groups on catalysis. For the preparation of the more basic P^{t}Bu$_2$ substituted ligand (**C**), 2-bromobenzaldamino precursor was used. Group **R** represent potential weakly coordinating groups as well as non-coordinating aromatic rings.

The abovementioned ligands have been used for the preparation of neutral Ni, Pd, and Cr complexes of the type Ni**L**Br$_2$, Pd**L**Cl$_2$, Pd**L**MeCl, and Cr**L**Cl$_3$.THF. Analogous cationic Pd complexes have also been prepared from the neutral Pd**L**MeCl complexes by abstraction of the chloride using ($AgBF_4$, $AgPF_6$, $NaBAr^F{}_4$).

The neutral metal complexes mentioned above have been activated with a series of alkylalumimium co-catalysts in order to determine which co-catalyst would be most efficient. Cationic Pd complexes on the other hand, were employed in ethylene oligomerization without a co-catalyst. For both the neutral and cationic catalysts, reaction conditions such as co-catalyst molar ratio (Al/Metal), reaction time, temperature, and ethylene pressure have been investigated to determine optimum catalytic conditions.

1.10 References

1. Cornils, B.; Herrmann, W. A. *Applied Homogeneous Catalysis With Organometallic Compounds, Wiley-VCH*, **Vol 1**, p245 – 256; p3 – 5; p719.
2. Masters, C. *Homogeneous Transition-metal Catalysis – a gentle art*, London New York: Chapman and Hall, **1981**, p5 – 23.
3. Schrauzer, G. N. *Transition Metals in Homogeneous Catalysis*, New York: Marcel Dekker, **1971**, p10 – 11.
4. a) Coe, B. J.; Glenwright, S. J. *Coord. Chem. Rev.*, **2000**, *203*, 5. b) Hughes, R. P.; Meyer, M. A.; Tawa, M. D.; Ward, A. J.; Williamson, A.; Rheingold, A. L.; Zakharov, L. N. *Inorg. Chem*., **2004**, *43*, 747. c) Kuznik, N.; Wendt, O. F.; *J. Chem. Soc., Dalton Trans.,* **2002**, 3074. d) Yamashita, M.,; Cuevas Vicario, J. V.; Hartwig, J. F. *J. Am. Chem. Soc.*, **2003**, *125*, 16347. e) Tolman, C. A. *J. Am. Chem. Soc.*, **1970**, 92, 2009. e) Pombeiro, A. J. L. *J. Organomet. Chem.*, **2005**, 690, 6021.
5. a) Seligson, A. L.; Trogler, W. C. *J. Am. Chem. Soc.*, **1991**, *113*, 2527. b) Smith, J. M.; Taverner B. C.; Coville, N. J. *J. Organomet. Chem.*, **1997**, *530*, 131. c) Smith, J. M.; Coville, N. J. *Organometallics*, **2001**, *20*, 1215. d) Coville, N. J.; Loonat, M. S.; White, D.; Carlton, L. *Organometallics*, **1992**, *11*, 1082. e) Datta, D.; Majumdar, D. *J. Phys. Org. Chem.*, **1991**, *4*, 611. f) Nomura, M.; Takayama, C.; Sugiyama, T.; Yokoyama, Y.; Kajitani, M. *Organometallics*, **2004**, *23*, 1305.
6. a) Ziegler, K.; Gellert, H.; Kühlhorn, H.; Martin, H.; Meyer, K.; Nagel, K.; Sauer, H.; Zoser, K. *Angew. Chem*, **1952**, *64*, 323. b) Ziegler, K.; *Angew. Chem*, **1955**, *67*, 541. c) Wilke, G. *Angew. Chem. Int. Ed.*, **2003**, *42*, 5000.
7. Ziegler, K.; Holzkamp, E.; Breil, H.; Martin, H. *Angew. Chem*, **1953**, *67*, 541.
8. a) Wilke, G. *Angew. Chem. Int. Ed.*, **1988**, *100*, 190. b) Wilke, G. *Angew. Chem. Int. Ed. Engl*, **1988**, *27*, 185.
9. a) Long, P. *J. Am. Chem. Soc.*, **1959**, *81*, 5312. b) Gavens, P. D.; Bottril, M.; Kelland, J. W.; McMeeking, J. *Comprehensive Organometallic Chemistry,* Eds, Wilkinson, G.; Stone, F. G. A.; Abel, E. W. Pergamon, Oxford, 1982, **vol 3**, p. 475. c) Ziegler, K.; Hopzkamp, E.; Breil, H.; Martin, H. *Angew. Chem.* **1955**, *67,* 541. d) Fischer, K.; Jonas, K.; Misbach, P.; Stabba, R.; Wilke, G. *Angew. Chem.* **1973**, *85*, 1002; *Angew. Chem.* **1973**, 12, 943. d) Natta, G. *Angew. Chem.* **1956**, *68*, 393.

10. a) Keim, W. *Angew. Chem. Int. Ed. Engl.*, **1990**, *29*, 235. b) Peuckert, M.; Keim, W. *Organometallics*, **1983**, *2*, 594. c) Keim, W.; Hoffmann, B.; Lodewick, R.; Peuckert, M.; Schmidt, G.; Fleischhauer, J.; Meier, U. *J. Mol. Catal.*, **1979**, *6*, 79.
11. a) Keim, W.; Kowaldt, F. H.; Goddard, R.; Krüger, C. *Angew. Chem. Int. Ed. Engl.*, **1978**, *17*, 466. b) Keim, W.; Behr, A.; Limbacker, B.; Krüger, C. *Angew. Chem. Int. Ed. Engl.*, **1983**, *22*, 503.
12. a) Dixon, J. T.; Green, M. J.; Hess, F. M.; Morgan, D. H. *J. Organomet. Chem.*, **2004**, *689*, 3641. b) Carter, A.; Cohen, S. A.; Cooley, N. A.; Murphy, A.; Scutt, J.; Wass, D. F. *Chem. Comm.*, **2002**, 858. c) Reagan, W. K. EP 0417477 (Phillips Petroleum Company), March 20, **1991**. d) Luo, H.; Li, D.; Li, S. *J. Mol. Catal. A*: *Chem.*, **2004**, *221*, 9.
13. a) Manyik, R. M.; Walker, W. E.; Wilson, T.P. *J. Catal.*, **1977**, *47*, 197. b) (Union Carbide Corporation) US 3300458, 1967.
14. Briggs, J. R. *J. Chem. Soc. Chem. Comm,* **1989**, *11*, 674.
15. a) McGuinness, D.S.; Wasserscheid, P.; Keim, W.; Morgan, D.; Dixon, J. T.; Bollmann, A; Maumela, H.; Hess, F.; Englert, U. *J. Am. Chem. Soc*., **2003**, *125*, 5272. b) Köhn, R.D.; Haufe, M.; Kociok-köhn, G.; Grimm, S.; Wasserscheid, P.; Keim, W. *Angew. Chem. Int. Ed*., **2000**, *39*, 4337. c) Agapie, T.; Schofer, S. J.; Labinger, J. A.; Bercaw, J. E. *J. Am. Chem. Soc.*, **2004**, *126*, 1304.
16. Skupińska, J. *Chem. Rev.*, **1991**, *91*, 613.
17. a) Crewdon, P.; Gambarotta, S.; Djoman, M.; Korobkov, I.; Duchateau, R. *Organometallics*, **2005**, *24*, 5214. b) Small, B. L.; Carney, M. J.; Holman, D. M.; O'Rourke, C. E.; Halfen, J. A. *Macromolecules*, **2004**, *37*, 4375.
18. a) Britovsek, G. P. J.; Gibson, V. C.; Wass, D. F. *Angew. Chem. Int. Ed.*, **1999**, *38*, 428. b) Gibson, V. C.; Spitzmesser, S. K. *Chem. Rev.*, **2003**, *103*, 283c) Brookhart, M.; Grant, B.; Volpe, A. P. *Organometallics*, **1992**, *11*, 3920. d) Yang, X.; Stern, C. L.; Marks, T. J. *J. Am. Chem. Soc.*, **1991**, *113*, 3623; *J. Am. Chem. Soc.*, **1994**, *116*, 10015. d) Strauss, S. H. *Chem. Rev.*, **1993**, *93*, 927. e) Beck, W.; Sunkel, K. *Chem. Rev.*, **1988**, *88*, 1405.

19. a) Resconi, L.; Bossi, S.; Abis, L. *Macromolecules*, **1990**, *23*, 4489. b) van Rensburg, W. J.; van der Berg, J.; Steynberg, P. J. *Organometallics*, **2007**, *26*, 1000.c) Sinn, H.; Kiminsky, W. *Adv. Organomet. Chem.,* **1984**, *18*, 99. d) Sinn, H. *Macromol. Symp.*, **1995**, *97*, 27. e) Zurek, E.; Ziegler, T. *Inorg. Chem.*, **2001**, *40*, 3279. f) Mason, M. R.; Smith, J. M.; Bott, S. G.; Barron, A. R. *J. Am. Chem. Soc.*, **1993**, *115*, 4971. g) Harlan, C. J.; Mason, M. R.; Barron, A. R. *Organometallics*, **1994**, *13*, 2957. h) Kaminsky, W. *Macromol. Chem. Phys.*, **1996**, *197*, 3907. i) Kaminsky, W. *J. Chem. Soc., Dalton Trans*., **1998**, 1413. j) Pasynkiewicz, S. *Polyhedron*, **1990**, *9*, 429. k) Möhring, P. C.; Coville, N. J. *J. Organomet. Chem.*, **1994**, *479*, 1. l) Watanabi, M.; McMahon, N.; Harlan, C. J.; Barron, A. R. *Organometallics*, **2001**, *20*, 460. m) Imhoff, D. W.; Simeral, L. S.; Sangokoya, S. A.; Peel, J. H. *Organometallics*, **1998**, *82*, 93. n) Zakharov, I. I.; Zhakharov, V. A. *Macromol. Theory Simul.*, **2001**, *10*, 108.

20. a) Johnson, L. K.; Killian, C. M.; Brookhart, M. *J. Am. Chem. Soc.*, **1995**, *117*, 6414. b) Svododa, M.; tom Dieck, H. *J. Organomet. Chem.*, **1980**, *191*, 321.

21. Britovsek, G. J. P.; Gibson, V. C.; Kimberly, B. S.; Maddox, P. J.; McTavish, S. J.; Solan, G. A. White, A. J. P.; Williams, D. J. *J. Chem. Commun.*, **1998**, 849.

22. a) Killian, C. M.; Tempel, D. J.; Johnson, L. K.; Brookhart, M. *J. Am. Chem. Soc.*, **1996**, *118*, 11664. b) Killian, C. M.; Johnson, L. K.; Brookhart, M. *Organometallics*, **1997**, *16*, 2005.

23. a) Yang, P.; Yang, Y.; Zhang, C.; Yang, X.; Hu, H-M.; Gao, Y.; Wu, B.; *Inorg. Chim. Acta*, **2009**, *362*, 89. b) Wang, Y-Y.; Lin, S-A.; Zhu, F.; Gao, H-Y.; Wu, Q.; *Inorg. Chim. Acta*, **2009**, *362*, 166. c) Bahuleyan, B. K.; Lee, U.; Ha. C.; Kim, I. *Appl. Catal. A: Gen.*, **2008**, *351*, 36. d) Matthew, P. C.; Burns, C. T.; Jordan, R. F. *Organometallics*, **2008**, *26*, 6750. e) Meinhard, D.; Wegner, M.; Kipiani, G.; Hearly, A.; Reuter, P.; Fischer, S.; Marti, O.; Rieger, B. *J. Am. Chem. Soc.*, **2007**, *129*, 9182. f) Zhang, S.; Sun, W-H, Kuang, X.; Vystorop, I.; Yi, J. *J. Organomet. Chem.*, **2007**, *692*, 5307. g) Champouret, Y. D. M.; Fawcett, J.; Nodes, W. J.; Singh, K.; Solan, G. A. *Inorg. Chem.* **2006**, *45*, 9890. h) Blom, B.; Overett, M. J.; Meijboom, R.; Moss, J. R. *Inorg. Chim. Acta*, **2005**, *358*, 3491. i) Nelkenbaum, E.; Kapon, M.; Eisen, M. S. *Organometallics*, **2005**, *24*, 2645. j) Jie, S.; Zhang, D.; Zhang, T.; Sun, W-H; Chen, J.; Ren, Q. R.; Liu, D.; Zheng, G.; Chen, W. *J. Organomet. Chem.*, **2005**, *690*, 1739. k) Tang, X.; Sun, W-H.; Gao, T.; Hou, J.; Chen, J.; Chen, W. *J. Organomet. Chem.*, **2005**, *690*, 1570. l**)** Gao, H.; Guo, W.; Bao, F.; Gui, G.;

Zhang, J.; Zhu, F.; Wu, Q. *Organometallics*, **2004**, *23*, 6273. m) Helldörfer, M.; Backhaus, H. G.; Alt, H. G. *Inorg. Chem.* **2003**, *351*, 34. n) Ceder, R. M.; Muller, G.; Ordinas, M.; Font-Bardia, M.; Solans, X., *J. Chem. Soc., Dalton Trans.*, **2003**, 3052. o) Helldörfer, M.; Backhaus, J.; Milius, W.; Alt, H. G. *J. Mol. Catal. A: Chem.*, **2003**, *193*, 59. p) Spencer, L. P.; Altwer, R.; Wei, P.; Gelmini, L.; Gauld, J.; Stephan, D. W. *Organometallics*, **2003**, *22*, 3841. q) Spencer, L. P.; Altwer, R.; Wei, P.; Gelmini, L.; Gauld, J.; Stephan, D. W. *Organometallics*, **2003**, *22*, 3841. r**)** Bernardo-Gusmão, K.; Queiros, L. F. T.; de Souza, R. F.; Leca, F.; Loup, C.; Réau, R. *J. Catal.*, **2003**, *219*, 59. s) Beaufort, L.; Benvenuti, F.; Delaude, L.; Noels, A. F. *J. Mol. Catal. A: Chem.*, **2008**, *283*, 77. t) Gibson, V. C.; Halliwell, G. M.; Long, N. J.; Oxford, J. P.; Smith, A. M.; White, A. J. P.; Williams, D. J. *J. Chem. Soc., Dalton Trans.*, **2003**, 918. u) Salo, E.; Guan, Z. *Organometallics*, **2003**, *22*, 5033. v) Blum, M. E.; Folli, C.; Walter, O.; Döring, M. *J. Mol. Catal. A: Chem.*, **2005**, *229*, 177. w) Gao, R.; Xiang, L.; Hao, X.; Sun, W-H.; Wang, F.; *J. Chem. Soc., Dalton Trans.*, **2008**, 5645. x) Kunrath, F.; de Souza, R. F.; Casagrande, Jr., O. L.; Brooks, N. R.; Young, Jr., V. G. *Organometallics*, **2003**, *22*, 4739. y) Meneghetti, S, P.; Lutz, P. J.; Kress, J. *Organometallics.*, **1999**, *19*, 2734. z) Ceder, R. M.; Muller. G.; Ordinas, M.; Maestro, M. A.; Mahía, J.; Bardia, M. F.; Solans, X.; *J. Chem. Soc., Dalton Trans.*, **2001**, 977. 23a') Killian, C. M.; Johnson, L. K.; Brookhart, M. *Organometallics.*, **1997**, *16*, 2005. b') Svejda, S. A.; Brookhart, M. *Organometallics.*, **1999**, *18*, 65. c') Ojwach, S. O; Guzei, I. A.; Benade, L. L.; Mapolie, S. F.; Darkwa, J. *Organometallics.*, **2009**, *28*, 2127. d') Ojwach, S.; Tshivhase, M. G.; Guzei, I. A.; Darkwa, J. Mapolie, S. F. *Can. J. Chem.*, **2005**, *83*, 843. e') Irrgang, T.; Keller, S.; Maisel, H.; Kretschmer, W.; Kempel, R. *Eur. J. Inorg. Chem.* **2007**, 4221.

24. a) Kermagoret, A.; Braunstein, P. *J. Chem. Soc., Dalton Trans.*, **2008**, 1564. b) Taquet, J-P.; Siri, O.; Braunstein, P.; *Inorg. Chem.*, **2006**, *45*, 4668. c) Hou, J.; Sun, W-H.; Zhang, D.; Chen, L.; Li, W.; Zhao, D.; Song, H. *J. Mol. Catal. A: Chem.*, **2005**, *231*, 221. d) Zhang, Y-M.; Lin, Q.; Wei, T-B.; Zhang, D-H.; Jie, S-Y. *Inorg. Chim. Acta*, **2005**, *358*, 4423. e) Sun, W-H., Zhang, W.; Gao, T.; Tang, X.; Chen, L.; Li, Y.; Jin, X. *J. Organomet. Chem.*, **2004**, *689*, 917. f) Zhao, W.; Huang, Y. Q. J.; Duan, J. *J. Organomet. Chem.*, **2004**, *689*, 2614. g) Taquet, J-P,; Siri, O.; Braunstein, P.; Welter, R. *Inorg. Chem.*, **2004**, *43*, 6944. h) Hou, L. C. J.; Sun, W-H.; *Appl. Catal. A: Gen.*, **2003**, *246*, 11. i) Carlini, C.; Isola, M. Luizzo, V. Galletti, A. M. R.; Sbrana, G. *Appl. Catal. A: Gen.*, **2002**, *231*, 307. j) Carlini, C.; Marchionna, M.; Galletti, A. M. R.; Sbrana, G. *J. Organomet.*

Chem., **2001**, *169*, 79. k) Wang, C.; Friedrich, S.; Younkin, T. R.; Li, R. T.; Grubbs, R. H.; Bansleben, D. A.; Day, M. W. *Organometallics*, **1998**, *17*, 3149.

25. a) Chaven, P.; Rios, I. G.; Kermagoret, A.; Pattacini, R.; Meli, A.; Bianchini, C.; Giambastiani, G.; Braunstein, P. *Organometallics*, **2009**, *28*, 1776. b) Dyer, P. W.; Fawcett, J.; Hanton, M. J. *Organometallics*, **2008**, *27*, 5082. c) Weng, Z.; Teo, S.; Liu, Z-P.; Hor, T. S. A. *Organometallics*, **2007**, *26*, 2950. d) Jie, S.; Agostinho, M.; Kermagoret, A.; Cazin, C. S. J.; Braunstein, P. *J. Chem. Soc., Dalton Trans.*, **2007**, 4472. e) Anderson, C. E.; Batsanov, A. S.; Dyer, P. W.; Fawcett, J.; Howard, J. A. K.; *J. Chem. Soc., Dalton Trans.*, **2006**, 5362. f) Sirbu, D.; Consiglio, G.; Gischig, S. *J. Organomet. Chem.*, **2006**, *691*, 1143. g) Tang, X.; Zhang, D.; Jie, S.; Sun, W-H.; Chen, J. *J. Organomet. Chem.*, **2005**, *690*, 3918. h) Weng, Z.; Teo, S.; Hor, T. S. A. *Organometallics*, **2006**, *25*, 4878. i) Speiser, F.; Braunstein, P.; Saussine, L. *Acc. Chem. Res.*, **2005**, *38*, 784. j) Speiser, F.; Braunstein, P. *Organometallics*, **2004**, *23*, 2633. k) Chen, H-P.; Liu, Y-H.; Peng, S-M.; Liu, S-T. *Organometallics*, **2003**, *22*, 4893. l) Keim, W.; Killat, S.; Nobile, C. F.; Suranna, g. P.; Englert, U.; Wang, R.; Mecking, S.; Schröder, D. L. *J. Organomet. Chem.*, **2002**, *662*, 150. m) Daugulis, O.; Brookhart, M. *Organometallics*, **2002**, *21*, 5926. n) Sun, W-H.; Li, Z.; Hu, H.; Wu, B.; Yang, H.; Zhu, N.; Leng, X.; Wang, H. *New. J. Chem.*, **2002**, *26*, 1474. o) Speiser, F.; Braunstein, P.; Saussine, L. *J. Chem. Soc., Dalton Trans.*, **2004**, 1539. p) Shi, P-Y.; Liu, Y-H.; Peng, S-M, Liu, S-T. *Organometallics*, **2002**, *21*, 3207. q) Flapper, J.; Kooijman, H.; Lutz, M.; Spek, A. L.; van Leeuwen, P. W. N. M.; Elsevier, C. J.; Kamer, P. C. J. *Organometallics*, **2009**, *28*, 1180. r) Doherty, M. D.; Trudeau, S.; White, P. S.; Morken, J. P.; Brookhart, M. . *Organometallics*, **2007**, *26*, 1269. s) Malinoski, J. M.; Brookhart, M. . *Organometallics*, **2003**, 22, 5324. t) Guan, Z.; Marshall, W. J. *Organometallics*, **2002**, *21*. 3580.

26. a) Hou, J.; Sun, W-H.; Zhang, S.; Ma, H.; Deng, Cooley, N. A.; Green, S. M.; Wass, D. F.; Heslop, Y; Lu, X. *Organometallics*, **2006**, *25*, 236. b) K.; Orpen, A. G.; Pringle, P. G. *Organometallics*, **2001**, *20*, 4769. c) Guan, Z.; Marshall, W. J. *Organometallics*, **2002**, *20*, 3580.

27. a) Kermagoret, A.; Braunstein, P. *J. Chem. Soc., Dalton Trans.*, **2008**, 822. b) Kuhn, P.; Sémeril, D.; Matt, D.; Chetcuti, M. J.; Lutz, P. *J. Chem. Soc., Dalton Trans.*, **2007**, 515. c) Heinicke, J.; Köhler, M.; Peulecke, N.; Kindermann, M. K.; Keim, W.; Köckerling, M. *Organometallics*, **2005**, *24*, 344. d) Müller, C.; Ackerman, L. J.; Reek, J. N.H., Karmer, P. C. J.; van Leeuwen, P. W. N. M. *J. Am. Chem. Soc.*, **2004**, *126*, 14960. e) Heinicke, J.;

Köhler, M.; Peulecke, N.; Keim, W.; *J. Catal.*, **2004**, *225*, 16. f) Wasserscheid, P.; Hilgers, C.; Keim, W. *J. Mol. Catal. A: Chem.*, **2004**, *214*, 83. g) Speiser, F.; Braunstein, P. *Inorg. Chem.*, **2004**, *43*, 4234.

28. a) Shen, M.; Hao, P.; Sun, W-H, *J. Organomet. Chem.*, **2008**, *693*, 1683. b) Chen, Y.; Hao, P.; Zuo, W.; Gao, K.; Sun, W-H. *J. Organomet. Chem.*, **2008**, *693*, 1829. c) Gao, R.; Zhang, M.; Liang, T.; Wang, F.; Sun, W-H. *Organometallics*, **2008**, *27*, 5641. d) Yang, Y.; Yang. P.; Zhang, C.; Li, G.; Yang, X-J.; Wu, B.; Janiak, C.; *J. Mol. Catal. A: Chem.*, **2008**, *296*, 9. e) Zhang, M.; Gao, R.; Hao, X.; Sun, W-H. *J. Organomet. Chem.*, **2008**, *693*, 3867. f) Sun, W-H.; Wang, K.; Wedeking, K.; Zhang, D.; Zhang, S.; Cai, J.; Li, Y. *Organometallics*, **2007**, *26*, 4781. g) Adewuyi, S.; Li, S.; Zhang, S.; Wang, W.; Hao, P.; Sun, W-H.; Tang, N.; Yi, J. *J. Organomet. Chem.*, **2007**, *692*, 3532. h) Hao, P.; Zhang, S.; Sun, W-H.; Shi, Q.; Adewuyi, S.; Lu, X.; Li, P. *Organometallics*, **2007**, *26*, 2439. i) Zhang, S.; Sun, W-H.; Kuang, X.; Vystorop, I.; Yi, J. *J. Organomet. Chem.*, **2007**, *692*, 5307. j) Champouret, Y. D. M. Maréchal, J-D, Chaggar, R. K.; Fawcett, J.; Singh, K.; Maseras, F.; Solan, G. A. *New J. Chem.*, **2007**, *31*, 75. k) Sun, W-H.; Zhang, S.; Jie, S.; Zhang, W.; Li, Y.; Ma, H.; Chen, J.; Wedeking, K.; Fröhlich, R. *J. Organomet. Chem.*, **2006**, *691*, 4196. l) Bahuleyan, B. K.; Park, D-W, Ha, C-S.; *Catal. Surv.*, **2006**, *10*, 65. m) Ajella, N.; Kuhn, M. C. A.; Boff, A. D. G.; Hörner, M.; Thomas, C. M.; Carpentier, J-F.; Casagrande, Jr., O. L. *Organometallics*, **2006**, *25*, 1213. n) Wang, L.; Sun, W-H.; Han, L.; Yang, H.; Hu, Y.; Jin, X. *J. Organomet. Chem.*, **2002**, *658*, 62. o) de Oliviera, L. L.; Campedelli, R. R.; Kuhn, M. C. A.; Capentier, J-F.; Casagrande, Jr., O. L., *J. Mol. Catal. A: Chem.*, **2008**, *288*, 58.

29. Yang, Q-Z.; Kermagoret, A.; Agostinho, M.; Siri, O.; Braunstein, P.; *Organometallics*, **2006**, *25*, 5518.

30. a) Hou, J.; Sun, W-H.; Zhang, S.; Ma, H.; Deng, Y.; Lu, X. *Organometallics*, **2006**, *26*, 236. b) Zhang, C.; Sun, W-H.; Wang, Z-X, *Eur. J. Inorg. Chem.*, **2006**, *23*, 4895.

31. a) Gibson, V. C.; Redshaw, C.; Solan, G. A. *Chem. Rev.*, **2007**, *107*, 1745. b) Brookhart, M.; Ittel, S. D.; Johnson, L. K. *Chem. Rev.*, **2000**, *100*, 1169. c) Gibson, V. C.; Spitzmesser, S. K. C*hem. Rev.*, **2003**, *103*, 283.

32. a) Theopold, K. W. *Eur. J. Inorg. Chem.*, **1998**, *15*, 158. b) Britovsek, G. J. P.; Gibson, V. C.; Wass, D. F. *Angew. Chem. Int. Ed.*, **1999**, *38*, 428. c) Döhring, A.; Göhre, J.; Jolly, P. W.; Kruger, B.; Rust, J.; Verhovnik, G. P. J *Organometallics*, **2000**, *19*, 388. d) Bazan, G. C.; Rogers, J. S.; Fang, C. C. *Organometallics*, **2001**, *20*, 2059.

33. a) McGuinness, D. S.; Wasserscheid, P.; Keim, W.; Morgan, D.; Dixon, J. T. Bollmann, A.; Maumela, H.; Hess, F.; Englert, U. *J. Am. Chem. Soc.*, **2003**, *125*, 5272. b) Bollmann, A.; Blann, K.; Dixon, J. T.; Hess, F.; Killian, E.; Maumela, H.; McGuinness, D. S.; Morgan, D. H.; Neveling, A.; Otto, S.; Overett, M.; Slawin, A. M. Z.; Wasserscheid, P.; Kuhlmann, S. *J. Am. Chem. Soc.*, **2004**, *126***,** 14712.
34. Blok, A. N. J.; Budzelaar, P. H. M. Gal, A. W. *Organometallics*, **2003**, *22*, 2564.
35. Overett, M. J.; Blann, K.; Bollmann, A.; Dixon, J. T.; Haasbroek, D.; Killian, E.; Maumela, H.; McGuinness, D. S.; Morgan, D. H. *J. Am. Chem. Soc.*, **2005**, *127***,** 10723.
36. Jie, S.; Pattacini, R.; Rogez, G.; Loose, C.; Kortus, J.; Braunstein, P. *J. Chem. Soc., Dalton Trans.*, **2009**, 97.
37. Chen, Y.; Zuo, W.; Hao, P.; Zhang, S.; Gao, K.; Sun, W-H. *J. Organomet. Chem.*, **2008**, *693*, 750.
38. Briggs, J. R. *J. Chem. Soc. Chem.*, **1989**, *11*, 674. b) Mahomed, H.; Bollmann, A.; Dixon, J. T.; Griesel, V. G. L.; Grove, G.; Hess, F.; Maumela, H. Pepler, L. *App. Catal. A*: *Gen*., **2003**, *255*, 355.
39. Emrich, R.; Heinemmann, O.; Jolly, P. W.; Krüger, C.; Verhovnik, G. P. J. *Organometallics*, **1997**, *16*, 1511.
40. a) Tomov, A. K.; Chirinos, J. J.; Jones, D. J.; Long, R. J.; Gibson; *J. Am. Chem. Soc.*, **2005**, *127*, 10166. b) Tomov, A. K.; Chirinos, J. J.; Long, R. J.; Gibson; Elsegood, M. R. J. *J. Am. Chem. Soc.*, **2006**, *128***, 77**04.
41. Wass, D. F. *J. Chem. Soc., Dalton Trans.*, **2007**, 816.
42. a) Moulin, J. O.; Evans, J.; McGuinness, D. S.; Reid, G.; Rucklidge, A. J.; Tooze, R. P.; Tromp, M. *J. Chem. Soc., Dalton Trans.*, **2008**, 1177. b) Temple, A. J. C.; Crewdson, P.; Gambarotta, S.; Korobkov, I.; Duchateau, *J. Am. Chem. Soc.*, **2006**, *128*, 9238.

CHAPTER 2
SYNTHESIS AND CHARACTERIZATION OF IMINOPHOSPHINE, PHENOXYIMINE, AND IMINOPYRIDYL LIGANDS AND THE CORRESPONDING COMPLEXES

2.1 Introduction

There is an ongoing interest in the design of new ligands that can induce improved catalytic activities and selectivities of metal-catalyzed reactions. Since the introduction of the concept of hemilability by Rauchfuss and others [1,2], heteroditopic ligands containing soft phosphorus and hard nitrogen donor atoms, (P^N) ligands have elicited growing interest in the coordination chemistry of transition metals as well as in homogeneous catalysis. This concept describes ligands that bind well enough to the transition metal (particularly soft metals, e.g. Pd) to allow isolation of the complex but would readily dissociate at the weakly bound hard end of the ligand (e.g. N or O), thereby generating a vacant site. The soft end of the ligand (P-) in this system should remain strongly attached to the metal center, thus ensuring the integrity of the metal-ligand association [1b,2c,2d].

Heteroditopic ligands of the type mentioned above can display coordination modes that are different from those of their P^P and N^N counterparts, in that the π-acceptor character of the phosphorus ligand can stabilize metal centers in low oxidation states, while the nitrogen σ-donor ability makes the metal in low oxidation states more prone to oxidative addition reactions. This can improve the stability of intermediate oxidation states or geometries during a catalytic cycle. In addition, the steric and electronic properties of these ligands can be fine-tuned by altering the ligand backbone, or the P- or N-bound substituents [1b].

Owing to the properties described above, a fair number of reports employing P^N ligands have been published, encompassing a wide range of catalytic reactions. Among the most studied bidentate P^N ligands are the pyridylphosphines and iminophosphines [3]. Tridentate

iminophosphinopyridines (P^N^N) [4] as well as iminophosphinophenol and iminophosphinothiol (P^N^X, X = OH, SH) [5,2c] ligands have been reported.

This chapter describes the synthesis and characterization of some iminophosphine, iminopyridyl, and iminophenol ligands as well as the respective neutral Pd(II) , Ni(II), Cr(III) and cationic Pd(II) complexes. These compounds have been characterized using a range of analytical and spectroscopic techniques, including ^{1}H-NMR, ^{13}C-NMR, ^{31}P-NMR, FTIR spectroscopy, mass spectrometry, elemental analysis, and conductometry for the cationic complexes. Single crystal X-ray structure determinations of selected palladium and nickel complexes were also conducted.

2.2 Results and Discussion

2.2.1 Synthesis and Characterization of Ligands

The ligands were prepared by a Schiff-base condensation reaction of an aldehyde (2-(diphenylphosphino)benzaldehyde, salicylaldehyde, or 2-bromobenzaldehyde) and the appropriate amine (Scheme 2.1) following modified literature methodologies [3d,3h,4b,6].

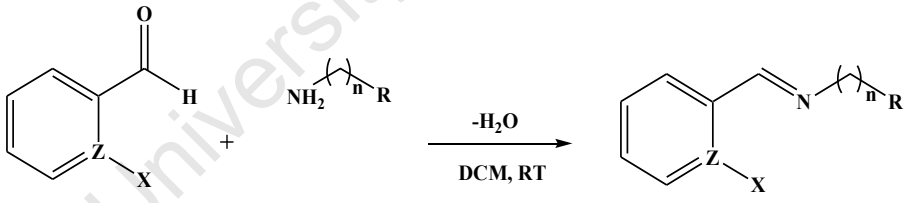

	Z	X	n	R
41	C	PPh_2	1	3-pyridyl
42	C	PPh_2	1	2-furyl
43	C	PPh_2	1	2-thiophenyl
44	C	PPh_2	2	2-thiophenyl
45	C	PPh_2	1	Ph
46	N	-	1	2-furyl
47	C	Br	1	2-furyl
48	C	OH	1	2-furyl

Scheme 2.1 *Synthesis of imino- ligands* ***41 – 48***

The reactions were carried out in DCM in the presence of excess Na_2SO_4, to remove H_2O formed as a by-product and left to stir at room temperature for ~ 16h. Following filtration and removal of the solvent, the crude products were obtained as pale yellow oils. The crude oily products of **41** – **46** were successfully solidified by dissolving the oils in hot hexane followed by hot filtration of the resultant solution. The solution was then cooled overnight to give air-stable off-white powders, while **47** and **48** were obtained as yellow-orange oils. Ligands **41** – **48** were obtained in good yields of 63 – 95 %. Ligands **41** – **45** were found to be stable towards phosphine oxidation in the solid state. Spectroscopic (^{1}H-NMR, ^{13}C-NMR, ^{31}P-NMR spectroscopy, FTIR spectroscopy, and mass spectroscopy) and analytical data (elemental analysis) confirmed the proposed structures.

2.2.1.1 IR and Mass Spectroscopy for Ligands 41 – 48

IR spectroscopy was used to confirm the functional groups indicative of a successful reaction. The disappearance of the carbonyl stretching vibration in the region 1700 – 1800 cm^{-1} suggested successful condensation of the carbonyl and the amine. Strong bands in the region 1619 – 1635 cm^{-1} in the IR spectra of ligands **41** – **48** indicated successful formation of the imine functionality. The imine stretch vibration bands were observed in the range 1500 – 1700 cm^{-1} (Table 2.1), in agreement with the literature values for related compounds [2a,4,7].

For ligand **48**, a broad band in the region 2800 – 3000 cm^{-1} indicated the presence of an O-H functionality [8]. The absence of both a carbonyl band and an N-H band in the IR spectrum of **48** suggested that tautomerism did not occur (Figure 2.1).

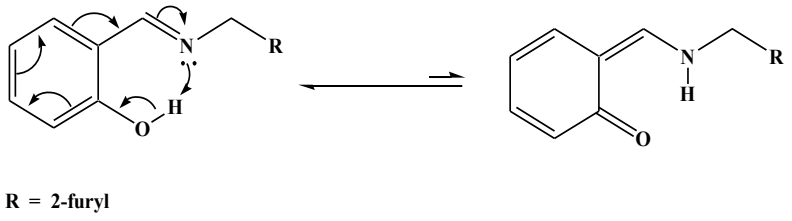

R = 2-furyl

Figure 2.1 *Tautomerism of the phenoxyimine to a keto-amine*

Satisfactory elemental analytical data as well as the positive ion mass spectral data were obtained for ligands **41** – **48** and agreed well with the proposed structures (Scheme 2.1). In all

cases, the parent ion ($[M]^+$) was obtained as the highest molecular weight fragment, with the exception of ligand **42**, which gave $[M+H]^+$ as the highest molecular weight fragment (Table 2.1).

2.2.1.2 ^{1}H-NMR, ^{13}C-NMR, and ^{31}P-NMR Spectroscopy for Ligands 41 – 48

The ^{1}H-NMR spectra of the ligands depicted in Scheme 2.1 were consistent with their structures and were in agreement with ^{1}H-NMR data of related compounds reported in the literature [3–6]. The disappearance of the aldehyde proton signal at δ 10.5 ppm and appearance of the imine signals (**H**C=N) at δ 8.39 – 9.02 ppm confirmed condensation of the aldehydes and the respective amines. In the case of iminophosphine ligands (**41** – **45**) the imine proton signals appeared as doublets, with coupling constants of $J_{P\text{-}H}$ = 4.9 – 5.8 Hz. This phosphorus coupling is presumed to be due to a through-space coupling, arising from the ligand's conformation in which the imine proton points towards the phosphorus lone pair (Figure 2.2). This observation is consistent with that reported by Rauchfuss and others for related ligands [7,4b].

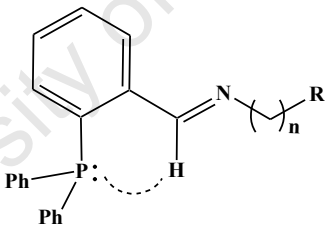

Figure 2.2 *Structure of a ligand depicting a through-space coupling of the imine proton with phosphorus*

Appearance of the imine proton signal as a doublet for the iminophosphine ligands (**41** – **45**) was not observed for the 2-pyridyl (**46**), 2-bromo (**47**) and 2-hydroxyl (**48**) analogues, which further confirmed that the coupling observed for ligands **41** – **45** was due to P–H coupling (Table 2.1). The signals for the methylene protons were observed as sharp singlets in the region δ 3.02 – 4.86 ppm in the ^{1}H NMR spectra of the ligands [4a]. The chemical shifts due to the aromatic protons of the phenyl groups, benzaldimino group and pyridyl group were observed in the region δ 6.24 – 8.45 ppm.

^{13}C NMR spectra of ligands **41** – **48** gave the expected number of carbon peaks for each compound, indicative of formation of only one product in each case. The signals for the imine carbons were also observed as doublets for the iminophosphine ligands **41** – **45** with large coupling constants of $J_{P\text{-}C}$ = 21.0 – 22.7 Hz in the region δ 160.6 – 169.4 ppm. The signal for the imine carbons for **46** – **48** appeared as singlets at δ 162.1 – 166.3 ppm. Methylene signals of ligands **41** – **48** also appeared as singlets in the region δ 55.2 – 65.1 ppm. For ligand **44** bearing an ethyl spacer, the methylene signals appeared as two triplets in the region δ 31.4 – 62.5 ppm. Zotto and Vrieze reported similar chemical shifts for the methylene signals for the methylene spacer (-CH_2-) at δ 51.6ppm [4a] and the ethylene analogue (-CH_2-CH_2-) at δ 40.1 and 61.6 ppm [4b]. For ligands **41** – **45**, the benzaldimino and the phenyl carbon signals were observed as doublets, indicating coupling of these carbons with the phosphorus, while those for **46** – **48** appeared as singlets. The alkenyl and aromatic signals (benzaldimino, phenyl, furyl, thiophenyl and pyridyl) were observed in the expected regions δ 107.4 – 161.1 ppm [4].

The ^{31}P-NMR spectra of the iminophosphine ligands **41** – **45** each only showed one singlet in the region δ -13.2 – -13.9 ppm. This signal was shifted slightly downfield compared to the starting 2-diphenylphosphinobenzaldehyde signal at δ -11.7 ppm. This downfield shift could be attributed to the absence of the more electron-withdrawing carbonyl group. The appearance of one singlet in the ^{31}P-NMR spectra suggests the formation of only one product. This observed downfield shift has been documented in the literature for related iminophosphine compounds [1,2,4].

2.2.2 Imine-Bond Reduction of Ligands 47 and 48

The imine bonds of ligands **47** and **48** were successfully reduced using $NaBH_4$ in anhydrous methanol following literature procedures (Scheme 2.2) [2a,4a], to afford **49** and **50** in good yield (63 – 77%). Ligand **49** was isolated as a stable yellow oil, while ligand **50** was also isolated as a yellow oil but that slowly decomposed after 30 – 60 min. The decomposition could be due to the slow rearrangement of **50**. The compound still decomposed under an atmosphere of argon. This could imply that **50** could sensitive towards light or temperature. The resultant product/products could not be identified owing to the complex NMR spectra after 30 – 60 min of **50**.

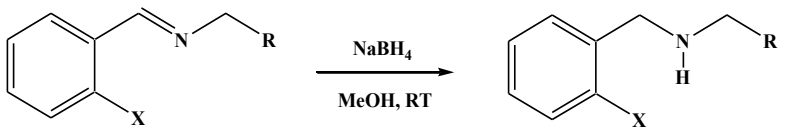

	X	R
47	Br	2-furyl
48	OH	2-furyl

	X	R
49	Br	2-furyl
50	OH	2-furyl

Scheme 2.2 *Reductions of the imine bond with $NaBH_4$*

2.2.2.1 IR and Mass Spectroscopy of Ligands 49 and 50

Successful reduction of the imine functionalities of **47** and **48** was verified by the disappearance of the imine stretching vibration bands at 1635 and 1631 cm^{-1} respectively in the IR spectrum and appearance of a new broad band at 3450 and 3442 cm^{-1} respectively due to the N-H stretching vibration (Table 2.1). The elemental analysis and mass spectroscopic data of ligand **49** were in agreement with the proposed structures shown in Scheme 2.2, while ligand **50** gave unsatisfactory microanalytical data, which may be due to its rapid decomposition.

2.2.2.2 ^{1}H-NMR and ^{13}C-NMR Studies of Ligands 49 and 50

The disappearance of the imine signals at δ 8.75 ppm and δ 8.39 ppm in the ^{1}H-NMR spectra of ligands **47** and **48** respectively accompanied by the appearance of new methylene singlets at δ 3.90 ppm and δ 3.97 ppm respectively indicated successful reduction of the imine bond (Table 2.1). The new amine proton signal for **49** was observed as a sharp singlet at δ 1.90 ppm, while that for **50** appeared as a broad signal at δ 1.81 ppm. Zotto et al. have observed similar results for related compounds [4a].

In the ^{13}C-NMR spectra of ligands **49** and **50**, the reduction of the imine bond was verified by the disappearance of the imine signals at δ 162.1 and 166.3 ppm respectively with formation of the new methylene signal at δ 45.4 ppm for **49** and δ 44.3 ppm for **50**. The benzaldiminic and furyl signals appeared in the region δ 107.0 – 157.9 ppm. Zotto et al. also observed similar chemical shifts for related ligands [4a].

The preparation of a di-*tert*-butylphosphine (-P^{t}Bu$_2$) substituted analogue of **49** was attempted. The synthesis involved preparation of the Grignard reagent by reacting **49** with Mg in THF. A catalytic amount of I_2 was necessary to initiate the reaction. After stirring at room temperature for 16 h, the Grignard reagent was slowly added to a deoxygenated THF solution of ClP^{t}Bu$_2$ at -78 °C. The reaction mixture was allowed to warm to room temperature and left to stir for another 16 h. The work-up involved addition of distilled H_2O, previously deoxygenated with argon for 30 min, followed by quick extraction with deoxygenated Et_2O and removal of the solvent *in vacuo*. The ^{31}P-NMR spectrum of the ligand revealed the major product to be the phosphine oxide, even after efforts to minimize contact of the product with oxygen. It was then decided that the palladium and nickel complexes of this ligand would be generated *in situ* as will be discussed later.

Table 2. 1 Selected spectroscopic (^{1}H, ^{13}C, and ^{31}P NMR, IR, MS) and microanalytical data of **41** – **50**

Ligand	Formula	^{1}H-NMR (HC=N) (ppm)	^{13}C-NMR (HC=N) (ppm)	^{31}P-NMR (ppm)	IR (cm^{-1}) ν(C=N)	[d] [M]$^+$ (calc.) m/z
41	$C_{25}H_{21}N_2P$	9.02 (d)	161.4 (d)	-13.2	[a]1635	379.92 (380.42)
42	$C_{24}H_{20}NOP$	8.99 (d)	161.5 (d)	-13.9	[a] 1634	[c]369.81 (369.40)
43	$C_{24}H_{20}NPS$	9.02 (d)	160.8 (d)	-13.8	[a] 1625	385.56 (385.46)
44	$C_{25}H_{22}NPS$	8.91 (d)	160.6 (d)	-13.6	[a] 1636	400.04 (399.49)
45	$C_{26}H_{22}NP$	9.03 (d)	160.7 (d)	-13.6	[a] 1636	379.42 (379.43)
46	$C_{11}H_{10}N_2O$	8.43 (s)	163.6 (s)	-	[a] 1649	[c]186.99 (186.21)
47	$C_{12}H_{10}BrNO$	8.75 (s)	162.1 (s)	-	[b] 1635	264.45 (264.12)
48	$C_{12}H_{11}NO_2$	7.93 (s)	166.3 (s)	-	[b] 1631	200.34 (200.22)
49	$C_{12}H_{12}BrNO$	-	-	-	-	266.33 (266.13)
50	$C_{12}H_{13}NO_2$	-	-	-	-	202.96 (203.20)

[a] Recorded as KBr pellets

[b]Recorded as a solution in DCM

[c][M+H]$^+$

[d]EI-MS

2.2.3 Synthesis and Characterization of Neutral Pd, Ni and Cr Complexes

2.2.3.1 Neutral Palladium Complexes

Palladium methylchloride complexes **51** – **55** were obtained from the reactions of ligands **41** – **45** and Pd(COD)MeCl in DCM at room temperature for 6 hr. Upon completion of the reaction, the solvent was removed and the resultant crude solid was recrystallized from DCM and Et_2O to give complexes **51** – **55** as pale yellow microcrystals in 63 – 86 % yield. Spectroscopic and analytical data for these complexes were in agreement with the proposed structures (Scheme 2.3).

Palladium dichloride complexes **56** – **63** were obtained from the reaction of ligands **41** – **46**, **48**, **49** with $Pd(COD)Cl_2$ (Scheme 2.3) in DCM for 6 h at room temperature. At the end of the reaction, the crude yellow precipitate of complexes **56** – **61** was filtered and washed with ice-cold DCM and dried *in vacuo* to give complexes **56** – **61** as yellow powders in 63 – 83 % yield. For complexes **62** and **63** the solvent was removed and resultant crude solid recrystallized from DCM and Et_2O to give complexes **62** and **63** as orange microcrystals in 62 – 82 % yield.

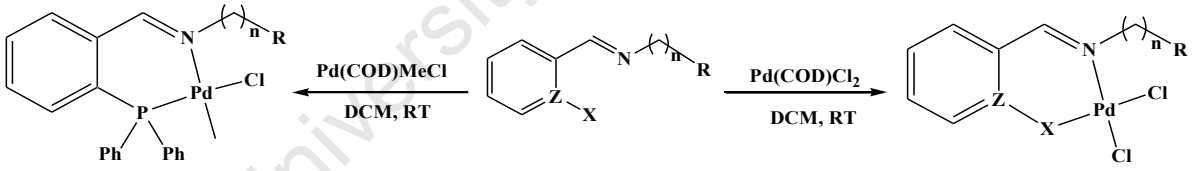

	Z	X	n	R
51	C	PPh_2	1	3-pyridyl
52	C	PPh_2	1	2-furyl
53	C	PPh_2	1	2-thiophenyl
54	C	PPh_2	2	2-thiophenyl
55	C	PPh_2	1	Ph

	Z	X	n	R
56	C	PPh_2	1	3-pyridyl
57	C	PPh_2	1	2-furyl
58	C	PPh_2	1	2-thiophenyl
59	C	PPh_2	2	2-thiophenyl
60	C	PPh_2	1	Ph
61	N	-	1	2-furyl
62	C	P^tBu_2	1	2-furyl
63	O	-	1	2-furyl

Scheme 2.3 *Synthesis of palladium methylchloride and palladium dichloride complexes*

2.2.3.2 IR and Mass Spectroscopy for complexes 51 – 55

The IR spectroscopic data of complexes **51** – **55** revealed a bathochromic (red) shift of about 3 – 8 cm^{-1}, with $\nu_{C=N}$ stretching vibration bands appearing in the region 1628 – 1637 cm^{-1} (Table 2.3). This shift suggested coordination of the imine nitrogen to the palladium metal center. Similar shifts for related complexes have been reported in the literature [2a,5c,11]. Excellent elemental analytical data and positive ion mass spectral data were consistent with the proposed structures (Scheme 2.3). The mass spectral data revealed $[M\text{-}Cl]^+$ as the highest molecular weight fragment for all the complexes (Table 2.3).

2.2.3.3 ^{1}H-NMR, ^{13}C-NMR, and ^{31}P-NMR studies of complexes 51 and 55

The ^{1}H-NMR spectra of complexes **51** – **55**, showed imine protons in the region δ 8.91 – 9.03 ppm. The observed upfield shifts of 0.7 – 1.1 ppm with respect to the free ligands further confirmed coordination of the imine nitrogen to the metal center (Table 2.3). This upfield shift could be attributed to back-bonding from palladium to the imine bond. In addition, Liu *et al.* proposed that this unexpected upfield shift of the imine signal in the ^{1}H HMR spectra could be due to the change in the conformation of the ligand (Figure 2.1) in order to facilitate coordination of the imine nitrogen to the metal center [10a]. A downfield shift of δ 0.72 – 0.81 ppm was also observed for the methylene signals, presumably due to the coordination of the adjacent imine nitrogen and consequent deshielding of these protons. No significant changes in chemical shifts were observed for the olefinic signals of the furyl and the thiophenyl with respect to those of the free ligands, suggesting that these groups did not participate in bonding with the metal center. The ^{1}H NMR spectra of **51** – **55** revealed the Pd–Me proton signals as doublets with coupling constants of $J_{P\text{-}H}$ = 3.1 – 3.3 Hz, indicative of the *cis* configuration of the methyl group with respect to the phosphine group. This observation is in accord with reported data for bidentate κ^2–P^N complexes [1c,10a,11].

Confirmation of coordination of the imine nitrogen in the ^{13}C NMR spectra of **51** – **55** was verified by the downfield shifts of the imine signal by δ 2.1 – 4.0 ppm with respect to the free ligands. Similar trends have been noted in the literature for related compounds [1c,2a,4a,5c,10a,11d].

The ^{31}P-NMR spectra of complexes **51** – **55** showed the expected downfield shift to δ 36.6 – 38.5 ppm with respect to the free ligands which appeared at δ -13.20 – -13.99 ppm, due to coordination of the phosphine moiety to the palladium center. The appearance of one signal in the ^{31}P-NMR spectra suggested formation of one species.

The *cis* geometry of the methyl group and the phosphine in these κ^2–P^N coordinated palladium methylchloride complexes **51** – **55** was unambiguously confirmed by the X-ray structural determination of complex **53** shown in Figure 2.3.

2.2.3.4 Single crystal X-ray structure determination of the Pd(II) complex (53)

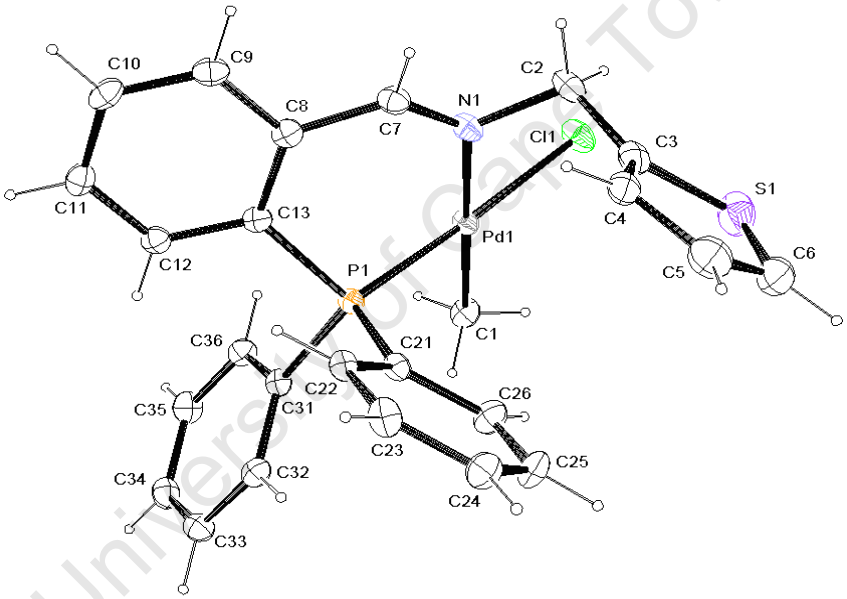

Figure 2.3 *The ORTEP plot of the molecular structure of* ***53*** *showing the atomic numbering*

The slow evaporation of a DCM solution of **53** at room temperature afforded pale yellow single crystals suitable for X-ray diffraction (Figure 2.3). The atomic labels of **53** are given in the ORTEP picture in Figure 2.3. Selected bond lengths and bond angles are given in Table 2.2.

Table 2.2 Selected bond distances and angles for the palladium complex **53**

Bond Distances (Å)		Bond Angles (°)	
Pd(1) – C(1)	2.040(2)	P(1) – Pd(1) – N(1)	86.38(5)
Pd(1) – N(1)	2.160(2)	P(1) – Pd(1) – C(1)	90.67(7)
Pd(1) – P(1)	2.1874(6)	N(1) – Pd(1) – Cl(1)	93.68(5)
Pd(1) – Cl (1)	2.3980(6)	C(1) – Pd(1) – Cl(1)	89.55(7)
P(1) – C(13)	1.825(2)	P(1) – Pd(1) – Cl(1)	177.08(2)
N(1) – C(7)	1.281(3)	N(1) – Pd(1) – C(1)	175.31(9)

The molecular structure above revealed a slightly distorted square-planar geometry around the palladium metal center. The ligand **43** was shown to bind in the expected κ^2–P^N fashion with a bite angle P(1)–Pd(1)–N(1) of 86.38(5)°. The angle deviated slightly from the expected angle of 90°, presumably due to the strain imposed by the six membered chelate ring P(1)–C(13)–C(8)–C(7)–N(1)–Pd(1). However, this reduction in the bite angle was compensated for by an increase in the N(1)–Pd(1)–C(1) angle of 93.68(5)°. This deviation of the bite angle from 90° has been observed for similar complexes; for instance, Zotto *et al.* and Liu *et al.* reported bite angles of 85.05(12)° and 85.34(6)° respectively for related complexes [4a,4b,4e,10a]. The remaining two angles around the metal center (i.e. P(1)–Pd(1)–C(1) and C(1)–Pd(1)–Cl(1)) were close to the expected value of 90° (90.67(7)° and 89.55(7)° respectively). The Pd(1)–Cl(1) was observed to be slightly longer (2.3980(6)Å) compared to that of related (diimine)palladium methylchloride complex (2.300(4)Å) [13]. This bond lengthening could be due to the *trans*-effect imposed by the diphenylphosphine group, while the Pd(1)–C(1) bond length (2.040(2)Å) *trans* to the imine nitrogen was in accord with similar κ^2–P^N complexes 2.040(4)Å [4b]. This bond length (Pd(1)–C(1)) was also in close agreement with that of a related diimine complex, measured at 2.020(11)Å [13]. The Pd(1)–N(1) (2.160(2)Å) and Pd(1)–P(1) (2.1874(6)Å) bond lengths agreed well with those found in related structures [4,10a].

2.2.3.5 Neutral palladium dichloride complexes 56 – 63

Due to the insolubility of complexes **56** – **61** in common organic solvents, with the exception of **61,** which could only be dissolved in DMSO, only ^{1}H-NMR and ^{31}P-NMR analyses were conducted as a suspension in DMSO-d_6. ^{13}C-NMR analyses for these palladium dichloride complexes proved to be unsuccessful.

2.2.3.6 IR and Mass spectroscopy for ligands 56 – 63

Coordination of the imine nitrogen to the palladium metal center was confirmed by a bathochromic shift (5 – 20 cm^{-1}) of the imine stretching vibration bands in the region $\nu_{C=N}$ 1621 – 1635 cm^{-1} with respect to the free ligands (Table 2.3). For complex **63**, the disappearance of a band at 2884 cm^{-1} (due to the OH) confirmed the deprotonation of the hydroxyl proton and formation of a σ-bond to the metal center. Excellent elemental analytical data and positive ion mass spectral data were consistent with the proposed structures for complexes **56** – **63** (Scheme 2.3). The mass spectral data for these complexes also showed $[M\text{-}Cl]^{+}$ as the highest molecular weight fragment with the exception of complex **63** which gave $[M\text{-}Cl\text{-}PPh_3]$ as the highest molecular weight fragment (Table 2.3).

2.2.3.7 ^{1}H-NMR, ^{13}C-NMR, and ^{31}P-NMR studies of complexes 56 and 63

As with palladium methylchloride complexes, coordination of the imine nitrogen to the palladium center was confirmed by an upfield shift of the imine signal by 0.2 – 0.7 ppm in the region δ 8.34 – 8.72 ppm of the ^{1}H NMR spectrum. Conversely, a 0.2 ppm downfield shift was observed for **61**. In addition, all the imine protons appeared as singlets as opposed to the doublets observed for the free ligands. This could be due to the ligand's conformational change in which the imine carbon now points away from the phosphorus group in order to enable κ^2–P^N coordination to occur. A downfield shift of 0.27 – 0.81 ppm was observed for the methylene signals [12b].

A more significant downfield shift to δ 31.7 – 37.3 ppm was observed in the ^{31}P-NMR spectra of complexes **56** – **59** with respect to δ -13.20 – -13.99 ppm for the free ligands.

Increasing the basicity of the phosphine was achieved by replacing the phenyl substituents of the diphenylphosphino group with *tert*-butyl groups. The palladium complex bearing a di-*tert*-butylphosphinoamine ligand was prepared as shown in Scheme 2.4 below.

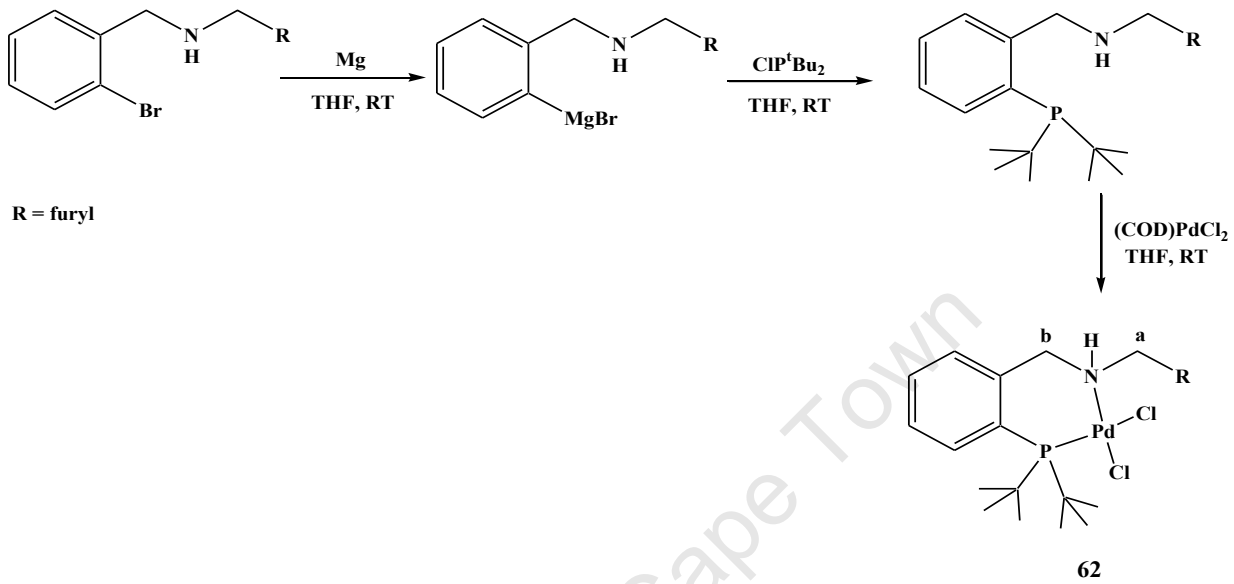

Scheme 2.4 *Preparation of the di-tert-butylphosphinoamine palladium dichloride complex* ***62***

Preparation of the ligand was carried out as described before (p 54), however, after the reaction of the Grignard reagent with ClP^tBu_2, the resultant product was not isolated directly. Instead the reaction solution containing the ligand was slowly added to a THF solution of $Pd(COD)Cl_2$ at 0 °C, yielding a dark orange solution. The reaction mixture was then allowed to warm to room temperature and left to stir for 16 h. The solvent was subsequently removed, resulting in a dark orange solid, which was recrystallized, from DCM and Et_2O to give **62** as a dark orange microcrystaline solid in moderate yield (66 %).

Coordination of the –NH bond in the ^{1}H-NMR spectrum was confirmed by a downfield shift of the –NH signal to δ 4.52 ppm. The ^{1}H-NMR spectrum of complex **62** proved interesting due to the presence of a chiral –NH group, formed as a consequence of coordination to the palladium metal center. The presence of this chiral amine center resulted in both sets of the methylene signals (H_a and H_b, Scheme 2.4) in the complex being diastereotopic (Figure 2.4). These two sets of methylene protons were thus observed as multiplets, due to a combination of geminal

and possibly long-range coupling with the furyl and benzaldaminic protons. The multiplet at δ 3.81 ppm was assigned to H_a, while the one at δ 4.21 – 4.44 ppm was assigned to H_b (Scheme 2.4).

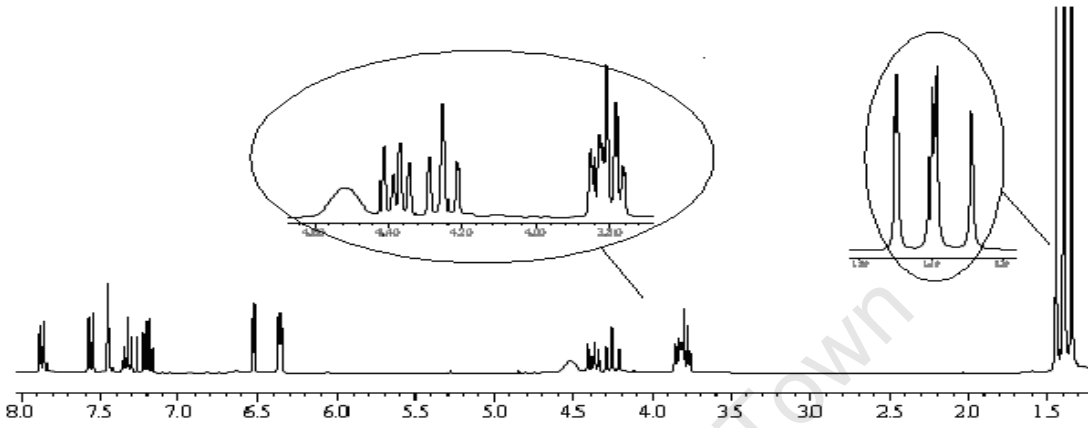

Figure 2.4 *The ^{1}H-NMR spectrum of complex* ***62.***

The methyl signals of the *tert*-butylphosphine groups appeared as two doublets at δ 1.37 and 1.42 ppm with coupling constants of $J_{P\text{-}H}$ = 14.9 Hz each, because of their diastereotopic nature since the phosphorus group is a prochiral center in the chiral **62**. Figure 2.5 depicts a proposed pseudo-chair conformation for **62** in which the *tert*-butyl groups lie in the equatorial and axial positions, showing the different chemical environments in which the two *tert*-butyl groups exist.

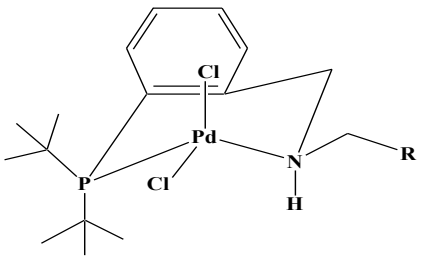

R = furyl

Figure 2.5 *Structure showing the different chemical environments in which the two tert-butyl groups exist*

The ^{13}C-NMR spectrum for **62** showed the expected number of signals for the proposed structure. The methyl signals of the *tert*-butylphosphine group also appeared as two doublets at

δ 28.9 and 29.0 ppm, with coupling constants of $J_{P\text{-}C}$ = 5.2 Hz each. The quaternary carbon of the *tert*-butyl groups was observed as a doublet at δ 43.3 ppm with a coupling constant of $J_{P\text{-}C}$ = 4.9 Hz. The methylene carbon signals were also observed as doublets at δ 47.3 ppm (H_a) and δ 54.1 ppm (H_b) with coupling constants of $J_{P\text{-}C}$ = 3.1 Hz and $J_{P\text{-}C}$ = 2.7 Hz respectively. An unexpected observation in the ^{13}C-NMR of **62** was the appearance of the aryl signals as singlets, implying that these signals may not be coupling with the phosphorus.

Coordination of the phosphine to the palladium was confirmed in the ^{31}P-NMR by the appearance of a signal at δ 158.6 ppm. Appearance of only one singlet also verified that only one product had formed.

The phenoxyimine palladium complex (**63**) was prepared from a reaction of ligand **48** with $Pd(COD)Cl_2$ as shown in Scheme 2.5.

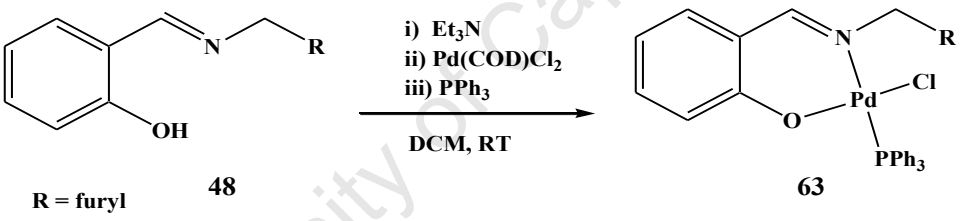

Scheme 2.5 *Preparation of the phenoxyimine palladium complex* ***63***

Deprotonation of the phenolic proton was achieved by treatment of the ligand with an equimolar amount of Et_3N. The reaction was left to stir at room temperature for 15 min, after which time an equimolar amounts of $Pd(COD)Cl_2$ and PPh_3 were added to the reaction mixture. This resulted in an immediate colour change from yellow to dark orange. After stirring the reaction for 14 hr the solvent was removed and the resultant orange solid recrystallized from DCM and Et_2O to give **63** as an orange crystalline solid in good yield (82 %).

In the ^{1}H-NMR spectrum, coordination of the imine nitrogen to the palladium metal center was verified by an upfield shift of the imine vinyl signal from δ 8.39 ppm for the free ligand to δ 7.93 ppm (Table 2.3). The upfield shift could be due to the more electron-donating character

of PPh_3 *trans* to the imine group. Confirmation of the *trans* geometry of PPh_3 to the imine group was verified by the appearance of the imine signal as a doublet with a large coupling constant of $J_{P\text{-}H}$ = 16.8 Hz. This *trans* disposition of the imino group and PPh_3 has been observed in the literature for related compounds [4a,2a]. The disappearance of the phenolic proton at δ 13.17 ppm suggested successful deprotonation and formation of a phenoxy σ–bond with the metal center. An increase in the relative integration of the aromatic protons also indicated coordination of PPh_3. The methylene group was also observed as a doublet ($J_{P\text{-}H}$ = 2.4 Hz) indicating the coupling of these protons with the phosphorus (PPh_3).

The presence of a single peak at δ 23.10 ppm in the ^{31}P-NMR spectrum of **63** confirmed coordination of PPh_3 and formation of only one isomer.

Table 2.3 Selected spectroscopic (^{1}H, ^{13}C, and ^{31}P NMR, IR, MS) and microanalytical data for complexes **51 – 63**

Complex	Formula	^{1}H-NMR (HC=N (Ligand)	^{13}C-NMR (HC=N) (Ligand)	^{31}P-NMR (Ligand)	[a]IR (Ligand) cm^{-1} ν(C=N)	[d]$[M]^{+}$ (calc.) m/z
51	$C_{26}H_{24}ClN_2PPd$	8.33 (9.02)	163.6 (161.4)	37.3 (-13.2)	1633 (1636)	[b] 501.51 (501.83)
52	$C_{25}H_{23}ClNOPPd$	8.21 (8.99)	163.7 (161.5)	37.7 (-13.9)	1637 (1645)	[b] 490.34 (490.42)
53	$C_{25}H_{23}ClNPPdS$	8.23 (9.02)	162.9 (160.8)	36.6 (-13.8)	1630 (1636)	[b] 506.02 (505.87)
54	$C_{26}H_{25}ClNPPdS$	7.86 (8.91)	163.2 (160.7)	36.6 (-13.6)	1632 (1636)	[b] 520.72 (520.90)
55	$C_{27}H_{25}ClNOPPd$	8.09 (9.03)	164.6 (160.7)	38.5 (-13.6)	1628 (1636)	[b] 501.08 (500.84)
56	$C_{25}H_{21}Cl_2N_2PPd$	8.34 (9.02)	n.d.	37.3 (-13.2)	1635 (1645)	[b] 522.25 (522.25)
57	$C_{24}H_{20}Cl_2NOPPd$	8.72 (9.02)	n.d.	32.1 (-13.9)	1626 (1635)	[b] 522.11 (522.25)
58	$C_{24}H_{20}Cl_2NPPdS$	8.72 (8.99)	n.d.	31.8 (-14.0)	1629 (1634)	[b] 526.87 (527.29)
59	$C_{25}H_{22}Cl_2NPPdS$	8.80 (9.02)	n.d.	31.6 (-13.6)	1621 (1636)	[b] 541.33 (541.31)
60	$C_{26}H_{22}Cl_2NPPd$	8.52 (8.91)	n.d.	n.d.	1629 (1636)	[b] 520.93 (521.26)
61	$C_{11}H_{10}Cl_2N_2OPd$	8.58 (8.40)	172.0 (163.6)	-	1627 (1636)	[b] 328.12 (328.04)
62	$C_{20}H_{30}Cl_2NOPd$	-	-	158.6	-	[b]473.51 (473.26)
63	$C_{30}H_{25}ClNO_2PPd$	7.93 (8.39)	163.9 (157.9)	23.1	1625 (1631)	[c,d]306.51 (306.61)

[a]Recorded as KBr pellets
[b]Represents m/z for the fragment $[M - Cl]^{+}$
[c]Represents m/z for the fragment $[M - Cl - PPh_3]^{+}$
[d]EI-MS

2.2.3.8 Synthesis and characterization of cationic palladium complexes

Cationic palladium complexes **64** – **74** were obtained from palladium methylchloride complexes **51** – **55** using halide abstracting reagents ($AgBF_4$, $AgPF_6$, or $NaBAr^F_4$) in the presence of acetonitrile to give cationic solvento ($NCCH_3$) palladium complexes (Scheme 2.6).

To a DCM solution of the palladium methylchloride complex was added the acetonitrile solution of the halide abstracting reagent. A white precipitate (AgCl/NaCl) immediately formed. The reaction mixture was left to stir at room temperature for 1 h, and filtered through Celite to remove the AgCl/NaCl precipitate. The solvent was then removed and the resultant solid re-dissolved in DCM, to ensure complete removal of AgCl/NaCl. Where some AgCl/NaCl was present, the solid was filtered through Celite once again. After filtration of AgCl/NaCl, the solvent was reduced and Et_2O added to precipitate the product. The mixture was then left to crystallize slowly at -16 °C, followed by filtration and drying to give stable pale yellow microcrystalline solids of **64** – **74** in good yield (65 – 90 %).

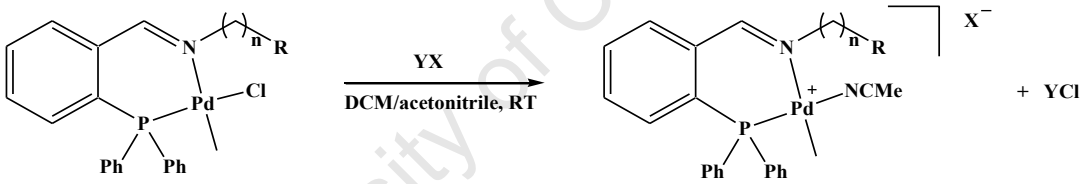

	Y	X	n	R
64	Ag	BF_4	1	2-furyl
65	Ag	PF_6	1	2-furyl
66	Na	BAr^F_4	1	2-furyl
67	Ag	BF_4	1	2-thiophenyl
68	Ag	PF_6	1	2-thiophenyl
69	Na	BAr^F_4	1	2-thiophenyl
70	Ag	BF_4	2	2-thiophenyl
71	Ag	PF_6	2	2-thiophenyl
72	Ag	BF_4	2	Ph
73	Ag	PF_6	2	Ph
74	Na	BAr^F_4	2	Ph

Scheme 2.6 *Preparation of cationic palladium complexes* ***64*** *–* ***74***

2.2.3.9 IR, mass spectroscopy and conductivity studies on complexes 64 – 74

The IR spectra of the cationic complexes revealed a slight hypsochromic (blue) shift to $\nu_{(C=N)}$ 1634 – 1643 cm^{-1} for the cationic palladium complexes **64** – **74** with respect to the neutral palladium methylchloride complexes (**51** – **55**) observed at 1632 – 1637 cm^{-1} (Table 2.5). The *end-on* coordination of acetonitrile to the palladium metal center was confirmed by the appearance of two medium stretching vibration bands at $\nu_{(N\equiv C)}$ 2289 and 2318 cm^{-1}. These values correspond to the *end-on* coordination of acetonitrile and are in line with the literature values [3j,3k,10a].

To confirm the cationic character of these complexes, conductance measurements were carried out on standard solutions of complexes **64** – **74** (5 x 10^{-3} M) in nitrobenzene. The molar conductivity of these cationic complexes at the abovementioned concentration were observed to be in the range of 130 - 144 $\Omega^{-1}.cm^2.mol^{-1}$, as expected for 1:1 electrolytes (Table 2.5) [10b]. The conductance values obtained were consistent with the values obtained for similar cationic palladium complexes [2c,2d,10b].

Elemental analysis and mass spectroscopy confirmed the proposed structures for complexes **64** – **74** (Scheme 2.6). The mass spectral data for these complexes gave $[M\text{-}NCCH_3]^+$ as the highest molecular weight fragment for all the complexes, except for complexes **65** and **69**. The latter complexes gave the highest molecular weight fragment of $[M\text{-}NCCH_3\text{-}PF_6]^+$ and $[M\text{-}NCCH_3\text{-}BAr^F{}_4]^+$ respectively (Table 2.5).

2.2.3.10 ^{1}H-NMR, ^{13}C-NMR, and ^{31}P-NMR studies on complexes 64 – 74

In the ^{1}H-NMR spectra of complexes **64** – **74**, coordination of acetonitrile was confirmed by the appearance of a singlet at δ 2.0 – 2.5 ppm, corresponding to the methyl group of acetonitrile [3k]. The retention of the *cis* configuration of the Pd-Me group with respect to the phosphine was confirmed by appearance of the methyl signal as a doublet with a small coupling constant of $J_{P\text{-}C}$ = 1.8 – 2.2 Hz [3k,3j].

The ^{13}C-NMR spectra of **64** – **74** gave the expected number of signals. The appearance of the Pd-**Me** as a doublet in the ^{13}C-NMR spectra of these complexes further verified retention of the *cis* configuration of the methyl and the phosphine groups. *End-on* coordination of acetonitrile

to the metal center was confirmed by the presence of signals at *ca.* 2.7 ppm (assigned to N≡C**C**H_3) and *ca.* 120.6 ppm (assigned to N≡**C**CH_3) [3j]. In general, there was a downfield shift of the signals in the ^{1}H, ^{13}C and ^{31}P-NMR spectra of the complexes **64** – **74** relative to the neutral methylchloride complexes, presumably due to the formation of the electron deficient cationic palladium metal center [10a].

Appearance of only one signal in the ^{31}P-NMR spectra of complexes **64** – **74** proved formation of only one isomer in all cases, with the exception of the complexes bearing PF_6 counterion in which the expected septet for PF_6 was observed around -143.9 ppm.

2.2.3.11 Single crystal X-ray structure determination of the cationic Pd(II) complex (71)

The structure of **71** was unambiguously confirmed in the solid state by X-ray diffraction (Figure 2.6).

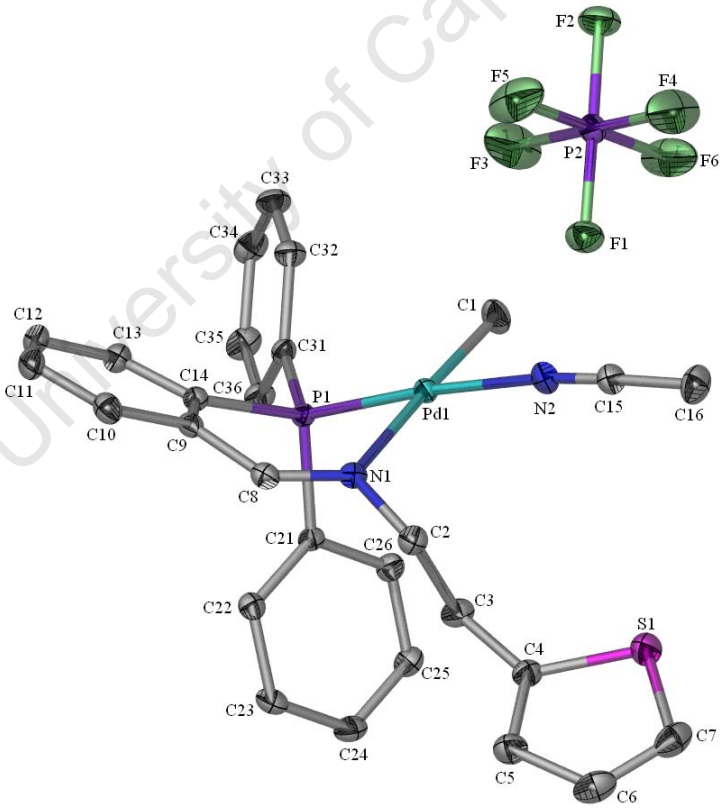

Figure 2.6 *The ORTEP plot of the molecular structure of **71** showing the atomic numbering*

Pale yellow single crystals suitable for single crystal X-ray diffraction were obtained by slow diffusion of diethyl ether into a DCM solution of **71** at room temperature. The molecular structure of **71** showing the atomic labelling scheme is depicted in Figure 2.6. All hydrogen atoms are omitted for clarity. Selected bond lengths and bond angles are given in Table 2.4.

Table 2.4 Selected bond distances and angles for the palladium complex **71**

Bond Distances (Å)		Bond Angles (°)	
Pd(1) – C(1)	2.040(2)	P(1) – Pd(1) – N(1)	86.32(4)
Pd(1) – N(1)	2.1588(16)	P(1) – Pd(1) – C(1)	93.18(7)
Pd(1) – N(2)	2.0977(17)	N(1) – Pd(1) – N2(1)	92.21(6)
Pd(1) – P(1)	2.2054(6)	C(1) – Pd(1) – N2(1)	88.09(8)
P(1) – C(14)	1.8222(19)	P(1) – Pd(1) – N(2)	175.68(5)
N(1) – C(8)	1.277(3)	N(1) – Pd(1) – C(1)	177.21(8)
		Pd(1) – N(2) – C(15)	174.03(18)

The molecular structure revealed a slightly distorted square-planar geometry around the palladium, consistent with the neutral palladium methylchloride complex **53**. The bite angle P(1)–Pd(1)–N(1) was observed to be 86.32(5)°. The molecular structure (Figure 2.6) confirmed coordination of an acetonitrile molecule and the preservation of the *cis*-arrangement of the methyl and the phosphine groups. No significant differences were observed between the bond lengths Pd(1)–C(1) = 2.040(2), Pd(1)–N(1) = 2.160(2) for the palladium methylchloride **53** and the cationic palladium complex **71** (2.040(2) and 2.1588(16) respectively). As observed for complex **53** the angles around the palladium center deviated slightly from the expected 90°, probably due to the strain imposed by the six-membered chelating ring P(1)–C(14)–C(9)–C(8)–N(1)–Pd(1). Angles P(1)–Pd(1)–C(1) and N(1)–Pd(1)–N(2) were observed to be slightly more than 90° (93.18°(7) and 92.21°(6) respectively). However, these increased bond angles were compensated for by angles P(1)–Pd(1)–N(1) and C(1)–Pd(1)–N(2) which were observed to be 86.32(4)° and 88.09°(8) respectively. This deviation of the bond angles from a perfect 90° has been noted in the literature for related complexes [4a,4b,4d]. For example, Liu *et al.* reported angles of P(1)–Pd(1)–C(1) (90.38(13)°, N(1)–Pd(1)–N(2) 99.05(11)°, C(1)–Pd(1)–N(2) 87.3(2)°, and P(1)–Pd(1)–N(1) 83.28(7)° for the related cationic complexes [4d]. The Pd(1)–N(2) also was observed to be slightly longer (2.0977(17)Å) compared to the Pd(1)–N(2) bond length of a related cationic (diimine)palladium complex (1.971(7)Å) but somewhat

shorter than that observed by Liu *et al.* for a related P^N complex (2.112(3) Å) [14,4d]. This significant bond lengthening observed between the P^N and the N^N systems could be due to the *trans*-effect imposed by the diphenylphosphino group, while the Pd(1)–C(1) bond length (2.040(2)Å) *trans* to the imine nitrogen gave a bond length that was in accord with similar κ^2–P^N complexes 2.040(4)Å [4b]. The bond length (Pd(1)–C(1)) was in close agreement with that of the diimine counterpart, measured at 2.020(11)Å [13]. The Pd(1)–N(1) (2.160(2)Å) and Pd(1)–(1) (2.1874(6)Å) bond lengths agreed well with those found in related structures [4].

Table 2.5 Selected spectroscopic (IR, MS) and microanalytical data for complexes **64** – **74**

Complex	Formula	[a]IR cm^{-1} (Ligand)		Λ_M	[e][M]$^+$ (calc.)
		ν(C=N)	ν(C≡N)	Ω^{-1}.cm^2.mol^{-1}	m/z
64	$C_{27}H_{26}BF_4N_2OPPd$	1637	2289, 2318	141	[b]577.72 (577.65)
65	$C_{27}H_{26}F_6N_2OP_2Pd$	1637	2286, 2317	132	[c]490.97 (490.85)
66	$C_{59}H_{38}BF_{24}N_2PPd$	1640	2286, 2317	131	[d]490.88 (490.85)
67	$C_{27}H_{26}BF_4N_2PPdS$	1639	2283, 2318	131	[b]593.54 (593.72)
68	$C_{27}H_{26}F_6N_2P_2PdS$	1637	2289, 2318	140	[b]652.01 (651.88)
69	$C_{59}H_{38}BF_{24}N_2PPdS$	1643	2290, 2318	135	[d]506.89 (506.92)
70	$C_{28}H_{28}BF_4N_2PPdS$	1634	2278, 2313	133	[b]607.91 (607.75)
71	$C_{28}H_{28}F_6N_2P_2PdS$	1637	2278, 2306	144	[b]665.63 (665.91)
72	$C_{29}H_{28}BF_4N_2PPd$	1634	2278, 2312	134	[b]587.83 (587.69)
73	$C_{29}H_{28}F_6NP_2Pd$	1638	2287,2317	130	[b]646.03 (645.85)
74	$C_{61}H_{40}BF_{24}N_2PPd$	1640	2289, 2318	142	[b]1364.43 (1364.14)

[a] Recorded as KBr pellets
[b] Represents m/z for the fragment $[M - NCCH_3]^+$
[c] Represents m/z for the fragment $[M - NCCH_3 - PF_6]^+$
[d] Represents m/z for the fragment $[M - NCCH_3 - BAr^F{}_4]^+$
[e]ESI-MS

2.2.3.12 Synthesis and characterization of nickel and chromium complexes

Nickel complexes **75 – 82** were obtained from a reaction of ligands **41 – 46** with Ni(DME)Br_2 in anhydrous DCM (Scheme 2.7). The salmon pink reaction mixture was left to stir at room temperature for 16 h. In most instances, the colour changed after 15 min to give a green, dark brown, or dark purple solution/precipitate. The solvent was then reduced and the product precipitated with a small amount of Et_2O. Filtration of the product and drying *in vacuo* gave complexes **75** – **82** in good yield (69 – 92 %). The di-*tert*-butylphosphine substituted complex

was prepared from ligand **49** in a similar manner to the palladium complex **62** discussed previously.

2.2.3.13 IR and mass spectroscopy for complexes 75 – 82

As in the case with the palladium complexes, the nickel complexes **75** – **80**, **82** showed bathochromic IR shifts of 6 – 27 cm^{-1} for the imine stretching vibrations, demonstrating coordination of the imine nitrogen to the nickel metal center (Table 2.7). The elemental analysis and mass spectroscopic data of complexes **75** – **82** confirmed the proposed molecular structures (Scheme 2.7). The mass spectral data for the nickel complexes **75** – **81** also gave $[M\text{-}Br]^+$ as the highest molecular weight fragment, with the exception of complex **82** which gave $[M\text{-}PPh_3]^+$ (Table 2.7). Attempts to obtain NMR spectroscopic data of these complexes were not successful due to peak broadening, indicating the presence of paramagnetic species in solution.

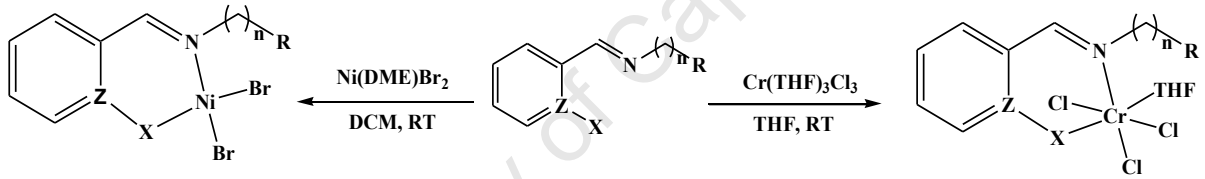

	Z	X	n	R
75	C	PPh_2	1	3-pyridyl
76	C	PPh_2	1	2-furyl
77	C	PPh_2	1	2-thiophenyl
78	C	PPh_2	2	2-thiophenyl
79	C	PPh_2	1	Ph
80	N	-	1	2-furyl
81	C	P^tBu_2	1	2-furyl
82	C	O	1	2-furyl

	Z	X	n	R
83	C	PPh_2	1	3-pyridyl
84	C	PPh_2	1	2-furyl
85	C	PPh_2	1	2-thiophenyl
86	C	PPh_2	2	2-thiophenyl
87	C	PPh_2	1	Ph
88	N	-	1	2-furyl

Scheme 2.7 *Preparation of nickel and chromium complexes*

Chromium complexes **83 – 88** were obtained from the reaction of ligands **41 – 46** with $Cr(THF)_3Cl_3$ in anhydrous THF (Scheme 2.7). The purple reaction mixture changed colour to dark green within 10 min of stirring at room temperature. The reaction was then left to stir for 16 h. The solvent was reduced and the product precipitated with Et_2O and dried *in vacuo*. As with the nickel complexes, attempts to obtain NMR spectroscopic data of these complexes were not successful due to the paramagnetic nature of these complexes.

2.2.3.14 IR and mass spectroscopy for complexes 83 – 88

Chromium complexes **83** – **88** also showed bathochromic shifts of 7 – 21 cm^{-1}, confirming coordination of the imine nitrogen to the chromium metal centre (Table 2.7). The elemental analysis and mass spectroscopic data of complexes **83** – **88** confirmed the proposed molecular structures (Scheme 2.7). The elemental analytical and mass spectral data revealed that the complexes were monomeric six coordinate complexes with a molecule of the solvent (THF). On the other hand, the mass spectral data gave $[M\text{-}THF]^+$ as the highest molecular weight fragment, with the exception of complexes **83** which gave $[M]^+$ as the highest molecular weight fragment.

2.2.3.15 Single crystal X-ray structural determination of the Ni(II) complex (76)

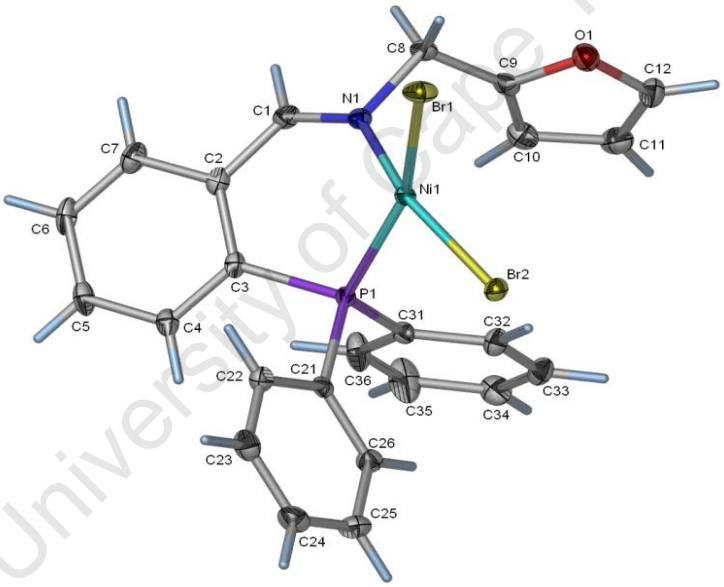

Figure 2.7 *The ORTEP plot of the molecular structure of* ***76*** *showing the atomic numbering*

The solid state structure of **76** was determined by X-ray diffraction (Figure 2.7). Dark purple single crystals suitable for single crystal X-ray diffraction were obtained by slow evaporation of a DCM solution of **76**. The atomic labels of the asymmetric molecule are given in the ORTEP picture in Figure 2.7 above. The non-hydrogen atoms were refined anisotropically and the hydrogens are placed geometrically with idealized riding models. Selected bond lengths and angles are listed in Table 2.6.

Table 2.6 Selected bond distances and angles for the nickel complex **76**

Bond Distances (Å)		Bond Angles (°)	
Br(1) – Ni(1)	2.3875(4)	N(1) – Ni(1) – P(1)	90.82(6)
Br(2) – Ni(1)	2.3031(4)	P(1) – Ni(1) – Br(2)	89.38(2)
Ni(1) – N(1)	1.8912(19)	N(1) – Ni(1) – Br(1)	92.51(6)
Ni(1) – P(1)	2.1497(6)	Br(2) – Ni(1) – Br(1)	93.708(13)
P(1) – C(3)	1.820(2)	P(1) – Ni(1) – Br(1)	157.72(2)
N(1) – C(1)	1.284(3)	N(1) – Ni(1) – Br(2)	163.05(6)

The molecular structure revealed a somewhat distorted square-planar geometry around the nickel metal center, as evidenced by the N(1)–Ni(1)–Br(2) and P(1)–Ni(1)–Br(1) bond angles that deviated from the expected 180° plane by 17.0° and 22.2° respectively. In view of the fact that square-planar nickel complexes are generally diamagnetic, dark purple crystals were analyzed by ^{1}H NMR spectroscopy which proved inconclusive due to broad peaks. The peak broadening indicated that a paramagnetic species was present in solution. This could be due a rapid change in the coordination geometry around the metal center in solution. Furthermore, an interesting observation was an orange coloured solution that was obtained when the dark purple crystals were dissolved in DCM. This change in colour could be a result of a structural change in solution. Hayter *et al.* conducted experiments (using $[NiX_2(PR(C_6H_5)_2)_2]$, X = Cl, Br, I; R = alkyl) that suggested that the energy difference between the square planar and tetrahedral isomers was small [15a]. The authors also observed colour changes of solution, attributed to the different coordination geometric forms (square planar and tetrahedral). In some instances the differently coloured crystals were structurally characterized, proving that the formation of differently coloured crystals for an individual complex was due to formation of two coordination geometries (square planar and tetrahedral) [15]. Recently, Dyer *et al*. isolated and structurally characterized some nickel complexes with square planar coordination geometries. The NMR spectra of some crystals revealed that the complexes were paramagnetic. The magnetic moments measured were found to be lower than the predicted spin-only magnetic moments for tetrahedral d^8 species. These lower magnetic moments were thus presumed to be due to moderate distortions from planarity around the metal center, caused by geometric and steric constraints imposed by the ligands [9].

The ligand **42** was observed to bind in the expected κ^2-P^N fashion with a P(1)–Ni(1)–N(1) bite angle of 90.8°. This bite angle is comparable to related six-membered P–Ni–N bite angles (88.41(9)° [4a] and 89.32(10) [16]). The chelating ring (P(1)–C3(1)–C2(1)–C(1)–N(1)– Ni(1)) adopts a boat conformation. The expected lengthening (0.08 Å) of the Ni–Br bond *trans* to the phosphine group could be due to the *trans*-effect imposed by the diphenylphosphino group. Sun *et al*. reported a Ni–Br bond length slightly longer by 0.05 Å for their related κ^2-P^N nickel dibromide complex [15]. The Ni(1)–N(1) and Ni(1)–P(1) bond lengths were found to be 1.891 and 2.150 Å, which were consistent with previously reported values [9,16,17].

Table 2.7 Selected spectroscopic (IR, MS) for complexes **75** – **87**

Complex	Formula	[a]IR (Ligand) ν(C=N)	Mass spec. (calc.) m/z
75	$C_{25}H_{21}Br_2N_2NiP$	1625 (1635)	[c,f]518.88 (519.02)
76	$C_{24}H_{20}Br_2NNiOP$	1628 (1634)	[c,f]508.36 (507.99)
77	$C_{24}H_{20}Br_2NNiPS$	1626 (1636)	[c,f]524.19 (534.06)
78	$C_{25}H_{22}Br_2NNiPS$	1632 (1636)	[c,f]538.24 (538.09)
79	$C_{26}H_{22}Br_2NNiP$	1618 (1636)	[c,f]517.79 (518.03)
80	$C_{11}H_{10}Br_2N_2Ni$	1622 (1645)	[c,f]324.85 (324.81)
81	$C_{20}H_{30}Br_2NNiOP$	-	[c,f]468.33 (468.02)
82	$C_{30}H_{25}Br_2NNiO_2P$	1619 (1631)	[d,f]338.59 (338.81)
83	$C_{26}H_{22}Cl_3CrN_2P$	1628 (1635)	[b,g]611.08 (610.88)
84	$C_{24}H_{20}Cl_3CrNOP$	1627 (1634)	[e,g]527.66 (527.75)
85	$C_{24}H_{20}Cl_3CrNPS$	1628 (1636)	[e,g]543.16 (543.41)
86	$C_{25}H_{23}Cl_3CrNPS$	1627 (1636)	[e,g]557.67 (557.84)
87	$C_{26}H_{22}Cl_3CrNP$	1629 (1636)	[e,g]537.76 (537.93)
88	$C_{11}H_{10}Cl_3CrN_2O$	1624 (1645)	[e,g]344.73 (344.76)

[a]Recorded as KBr pellets
[b] Represents m/z for $[M]^+$
[c] Represents m/z for the fragment [M – Br]
[d]Represents m/z for the fragment $[M - PPh_3]^+$
[e]Represents m/z for the fragment $[M - THF]^+$
[f]EI-MS
[g]ESI-MS

2.3 Summary

A series of bidentate ligands (**L**) and precursors of the following types: 2-phosphinobenzaldimino (**41** – **45**), iminopyridyl (**46**), and 2-phenoxyimino (**48**) and 2-bromobenzaldimino (**47**) have been prepared in good yields. The imine-bond reduction of compounds **47** and **48** was successfully achieved by the reaction with $NaBH_4$ to give the corresponding 2-bromobenzaldamino ligand (**49**) as a stable oil and a less stable 2-phenoxyamino ligand (**50**) respectively in moderate yield. Compound **47** was used in the preparation of the more basic di-*tert*-butylphosphinoamino ligand *in situ*. All ligands have been characterized by spectroscopic and analytical methods.

The corresponding metal complexes of the type Pd**L**MeCl, Pd**L**Cl_2, Ni**L**Br_2, and Cr**L**(THF)Cl_3 were prepared and characterized using spectroscopic and analytical methods. Cationic palladium complexes were prepared from the reaction of the Pd**L**MeCl and a halide abstracting reagent ($AgBF_4$, $AgPF_6$, and $NaBAr^F{}_4$) in the presence of a weakly coordinating solvent ($NCCH_3$). In addition to spectroscopic and analytical methods, conductometry was also used to verify 1:1 electrolytes for the cationic complexes. The molecular structures of complexes **56**, **71**, and **76** were unambiguously confirmed in the solid state by X-ray crystal structural analysis.

2.4 References

1. a) Jeffrey, J. C.; Rauchfuss, T. B. *Inorg. Chem.*, **1979**, *18*, 2658. b) Espinet, P.; Soulantica, K. *Coord. Chem. Rev.*, **1999**, 499. c) Flapper, J.; Kooijman, H.; Lutz, M.; Spek, A. L.; van Leeuwen, P. W. N. M.; Elsevier, C. J.; Kamer, P. C. J. *Organometallics*, **2009**, *28*. 1180. d) Shaffer, A. R.; Schmidt, A.R. *Organometallics*, **2009**, 28, 2494.
2. a) Crochet, P.; Gimeno, J.; Borge, J.; García-Granda, S. *New J. Chem.*, **2003**, *27*, 414. b) Best, J.; Wilson, J. M.; Adams, H.; Gonsalvi, L.; Peruzzini, M.; Haynes, A. *Organometallics*, **2007**, *26*, 1960. c) Sánchez, G.; Momblona, F.; Serrano, J. L.; García, L.; Pérez, E.; Pérez, J.; López, G. *J. Coord. Chem.*, **2002**, *55*, 917. d) Sánchez, G. ; Momblona, F. ; Pérez, J. ; López, G. *Trans. Met. Chem.*, **2001**, *26*, 100.
3. a) Brunner, H. ; Füsrt, J. *Inorg. Chem.*, **1994**, *220*, 63. b) Wehman, P.; van Donge, H. M. A.; Hagos, A.; Kamer, P. C. J.; van Leeuven, P. W. N. M. *J. Organomet. Chem.*, **1997**, *535*, 183. c) Bacchi, A. ; Carcelli, M. ; Costa, M. ; Leporati, A. ; Leporati, E. ; Pelagatti, P. ; Pelizzi, C. ; Pelizzi, G. *J. Organomet. Chem.*, **1997**, *535*, 107. d) Gao, J-X.; Ikayira, T.; Noyori, R. *Organometallics*, **1996**, *15*, 1087. e) Antonaroli, S.; Crociani, B. *J. Organomet. Chem.*, **1998**, *560*, 137. f) Xu, L. ; Zhu, D. ; Wu, F. ; Wang, R. ; Wan, B. *J. Mol. Catal. A : Chem.*, **2005**, *237*, 210. g) Catsoulacos, D. P. ; Steele, B. R. ; Heropoulos, G. A. ; Micha-Screttas, M. ; Screttas, C. G. *Tet. Lett.*, **2003**, *44*, 4575. h) Shirakawa, E.; Nakao, Y.; Murota, Y.; Hiyama, T. *J. Organomet. Chem.*, **2003**, *670*, 132. i) Lavery, A.; Nelson, S. M. *J. Chem. Soc. Dalton Trans.*, **1984**, 615. j) Keim, W. ; Killat, S. ; Nobile, C. F. ; Suranna, G. P. ; Englert, U. ; Wang, R. ; Mecking, S. ; Schröder, D. L. *J. Organomet. Chem*, **2002**, *662*, 150. k) Shi, P-Y.; Liu, Y-H.; Peng, S-M.; Liu, S-T. *Organometallics*, **2002**, *21*, 3203.
4. a) Zotto, A. D.; Baratta, W.; Ballico, M.; Herdtweck, E.; Rigo, P. *Organometallics*, **2007**, *26*, 5636. b) Rülke, R. E.; Kaasjager, V. E.; Wehman, P.; Elsevier, C. J.; van Leeuwen, P. W. N. M.; Vrieze, K. *Organometallics*, **1996**, *15*, 3031. c) Masson, J-P.; Bahsoun, A. A.; Youinou, M-T, Osborn, J. A. *C. R. Chimie*, **2002**, *5*, 303. d) Reddy K. R., Surekha K.; Lee G-H; Peng S-M.; J-T. Chen, S-T. Liu *Organometallics*, **2001**, *20*, 1292. e) del Campo, O.; Carbayo, A.; Cuevas, J. V.; García-Herbosa, G.; Munoz, A. *Eur. J. Inorg. Chem*. **2009**, 2254.

5. a) Bayly, S. R.; Cowley, A. R.; Dilworth, J. R.; Ward, C. V. *J. Chem. Soc. Dalton.*, *Trans.*, **2008**, 2190. b) Kim, I.; Kwak, C. H.; Kim, J. S.; Ha, C-S. *Appl. Catal. A*: *Gen.*, **2005**, *287*, 98. c) Bhattacharyya, P.; Loza, M. L.; Parr, J.; Slawin, M. Z. *J. Chem. Soc. Dalton.*, *Trans.*, **1999**, 2917.

6. a) Wang, C.; Friedrich, S.; Youkin, T. R.; Li, R. T.; Grubbs, R. H.; Bansleben,D. A.; Day, M. W. *Organometallics*, **1998**, *17*, 3149. b) Lavery, A.; Nelson, S. M. *J. Chem. Soc. Dalton.*, *Trans.*, **1984**, 615.

7. a) Rauchfuss, T. B. *J. Organomet. Chem*, **1978**, *162*, C19. b) Jeffrey, J. C.; Rauchfuss, T. B.; Tucker, P. A. *Inorg. Chem.*, **1980**, *19*, 3306.

8. Freedman, H. H. *J. Am. Chem. Soc*. **1961**, *83*, 2900.

9. Dyer, P. W.; Fawcett, J.; Hanton, M. J. *Organometallics*, **2008**, *27*, 5087. b) Chaven, P.; Rios, I. G.; Kermagoret, A.; Pattacini, R.; Meli, A.; Bianchini, C.; Giambastiani, G.; Braunstein, P. *Organometallics*, **2009**, *28*, 1776.

10. Reddy, K. R.; Tsai, W-W.; Surekha, K.; Lee, G-H.; Peng, S-M. Chen, J-T.; Liu, S-M. *J. Chem. Soc. Dalton.*, *Trans.*, **2002**, 1776. b) Geary, W. J. *Coord. Chem. Rev.*, **1971**, *7*, 81.

11. a) Sirbu, D.; Cossiglio, G.; Gischig, S. *J. Organomet. Chem*, **2006**, *691*, 1143. b) Chen, H-P.; Liu, Y-H.; Peng, S-M.; Liu, S-T. *Organometallics*, **2003**, *22*, 4893. c) Shaffer, A. R.; Schmidt, J. A. R. *Organometallics*, **2009**, *28*, 2494. d) Daugulis, O.; Brookhart, M. *Organometallics*, **2003**, *21*, 5926.

12. a) Blom. B.; Overett, M. J.; Meijboom, R.; Moss, J. R. *Inorg. Chim. Acta*, **2005**, *358*, 3491. b) Ojwach, S. O.; Tshivhase, M. G.; Guzei, I. A.; Darkwa, J. Mapolie, S. F. *Can. J. Chem.*, **2005**, *83*, 843.

13. Tempel, D. J.; Johnson, L. K.; Huff, R. L.; White, P. S.; Brookhart, M. *J. Am. Chem. Soc.*, **2000**, *122*, 6686.

14. Maneghetti, S. P.; Lutz, P. J.; Kress, J *Organometallics*, **1999**, *15*, 2735.

15. a) Hayter, R. G.; Humiec, F. S. *Inorg. Chem.*, **1965**, *12*, 1701. b) Sacconi, L.; Ciampolini, M.; Nardi, N. *J. Am. Chem. Soc.*, **1964**, *86*, 819.

16. Tang, X.; Zhang, D.; Jie, S.; Sun, W-H.; Chen, J. *J. Organomet. Chem*, **2005**, *690*, 3918.

17. a) Speiser, F.; Braunstein, P.; Saussine, L. *Organometallics*, **2004**, *23*, 2625. b) Lloyd-Jones, G. C.; Butts, C. P. *Tetrahedron*, **1998**, *54*, 901.

CHAPTER 3
CATALYTIC OLIGOMERIZATION OF ETHYLENE

3.1 Introduction

The transformation of readily available ethylene into valuable polymers or oligomers has been an area of great interest since the 1950's. Since then, efforts to design selective and efficient catalyst systems have been intensified.

This chapter describes investigations of ethylene oligomerization using neutral catalyst precursors (nickel, palladium, and chromium) activated by co-catalysts such as MMAO, $EtAlCl_2$ and Et_2AlCl. Single component cationic palladium catalysts bearing P^N and related ligands are also described (Figure 3.1).

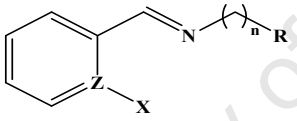

	Z	X	n	R
41	C	PPh_2	1	3-pyridyl
42	C	PPh_2	1	2-furyl
43	C	PPh_2	1	2-thiophenyl
44	C	PPh_2	2	2-thiophenyl
45	C	PPh_2	1	Ph
46	N	-	1	2-furyl
47	C	Br	1	2-furyl
48	C	OH	1	2-furyl

Figure 3.1 *Bidentate ligand systems employed in the preparation of Pd, Ni, and Cr complexes*

The choice of the P^N coordinating ligand system was based on their ability to improve thermal stability [1] of the corresponding catalysts, presumably due to the presence of the strong phosphorus-metal bond [2], thereby curbing rapid catalyst deactivation/decomposition at high temperature. The stability of the catalysts at high temperatures is particularly important since ethylene oligomerization reactions can be highly exothermic [1a]. In addition P^N ligands offer unique trans-effects due to the different electron donor and acceptor capabilities of phosphorus and nitrogen that may improve the catalyst's performance [1].

In general the iminophosphine ligands described in this section contain the diphenylphosphinobenzaldimino group. The bidentate ligand system was important in our

ligand design since palladium and nickel have a preference for a coordination number of four (even though five coordinate Ni(II) complexes are known). As mentioned above, the use of iminophosphine ligands could offer unique trans-effects and possibly promote good ethylene oligomerization. In order for the olefin oligomerization reaction to proceed, at least one vacant site is required for the coordination of the olefin and a metal-carbon bond for the growing chain. This process may not be as facile for a tridentate system (in a four coordinate catalyst system) in which only one coordination site is readily available. For the reaction to proceed, one of the coordinating tridentate groups must dissociate to allow insertion of the coordinated olefin and for subsequent coordination of ethylene. Depending on the strength of coordination of this group to the metal center, this ligand system might have a negative effect on the activities of the catalyst since this group might compete with ethylene for coordination.

In our model below (Figure 3.2), the side groups (furyl and thiophenyl) were chosen as the active catalyst stabilizing groups.

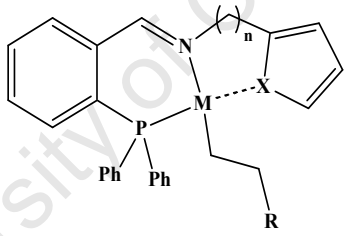

X = O (furyl), S (thiophene)
R = growing chain
M = palladium, nickel

Figure 3.2 *Structure of a stabilized coordinatively unsaturated catalyst species.*

In polymerization reactions, the active catalysts are commonly stabilized by the metal-hydrogen agostic interactions. We suggest that in our catalyst system, the active catalyst may be better stabilized by the presence of the furyl or thiophenyl groups (Figure 3.2). The furyl or thiophene group in our design does not form strong coordinate bonds as would be the case with the pyridyl analogue. The rationale rests in the position of the lone pairs on oxygen and sulfur of the furyl and thiophenyl groups respectively (Figure 3.3). These are nearly perpendicular to the ring, in contrast to the lone pair on the pyridyl nitrogen which is coplanar

to the pyridyl ring. The coplanarity of the pyridyl lone pair renders them available for coordination.

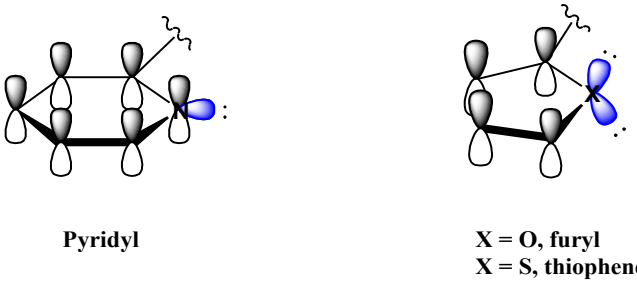

Pyridyl **X = O, furyl**
X = S, thiophene

Figure 3.3 *Molecular representations of the pyridyl, furyl and thiophenyl coordinating lone pairs [3]*

On the other hand, furyl and thiophenyl lone pairs are more aromatic and thus not readily available for coordination. The proposed metal-oxygen or metal-sulfur interaction in Figure 3.2 should thus be strong enough to stabilize the catalyst's vacant site but weak enough to be displaced by the incoming ethylene.

The effects of varying the coordination groups were also investigated. These include the effect of increasing the basicity of the phosphorus group by replacement of the phenyl groups with tertiary butyl groups, replacing the phosphine group with a hydroxyl, and replacing the diphenylphosphinobenzaldimino group with the pyridylimino group.

3.2 Catalytic Oligomerization of Ethylene

In this project, nickel, palladium and chromium complexes have been evaluated as catalyst precursors in ethylene oligomerization in an effort to determine the effect of the ligands on the catalytic performance of the complexes. Different reaction conditions were investigated, including the selection of the co-catalyst (MMAO, Et_2AlCl, $EtAlCl_2$), co-catalyst concentration (Al/Ni or Al/Pd molar ratio), reaction temperature (0 – 10, 40 – 50, 80 – 110 °C), ethylene pressure (10, 30, 50 bar) and reaction time (1, 5, 10, 15, 30, 60 min).

3.2.1 General

All nickel (**75 – 82**) and palladium catalysts (**56 – 74**) were found to be active towards ethylene oligomerization, producing mainly butenes (C_4, sum of all butenes) and hexenes (C_6, sum of all hexenes) with no polymer detected. Chromium complexes on the other hand, produced C_4 and C_6 as well as a significant amount of polyethylene. Identification and quantification of the oligomeric products were carried out using GC. The internal standard method (equation 1) was used for the quantification of the oligomeric products [4]:

$$\text{Relative Response Factor} = (A_c \times C_{is}) / (A_{is} \times C_c) \qquad \textbf{Eq. 1}$$

A_c = Peak area of the target analyte
A_{is} =Peak area of the internal standard
C_{is} = Concentration (mass) of the internal standard
C_c = Concentration (mass) of the target analyte

At the end of the reaction, the ethylene inlet valve was closed and the autoclave rapidly cooled to -27 – -35 °C, at which temperature the residual ethylene was vented and an internal standard (nonane) added. A sample for GC was collected in a cooled screw cap vial.

Owing to the fact that the major product in our catalytic oligomerization system was C_4 (a gas at room temperature), it was decided that the reaction volume would be used to quantify the total C_4 produced. Use of Eq. 1 above allowed for the accurate quantification of the C_6 fraction by relating the individual GC peak areas of the C_6 isomers to the respective volumes together with the known volume and GC peak area of the internal standard. The GC response factor was determined to be unity. Thus, the total volume of the C_6 isomers produced in the catalytic reaction was obtained by adding together these individual volumes. The volumes of the C_6 fraction and the solvent were subtracted from the reaction total volume, to give the volume of the C_4 product produced. To obtain the relative percentages of the C_4 isomers (i.e. 1-C_4 and 2-C_4) it was assumed that the C_4 components would evaporate at the same rate and therefore the relative amounts of the different C_4 (1-C_4 and 2-C_4) isomers in the reaction mixture stays constant.

3.2.2 Nickel-Catalyzed Ethylene Oligomerization

A series of iminophosphine, pyridylimine, and phenoxyimine nickel catalyst precursors (**75** – **82**, Figure 3.4) were investigated for ethylene oligomerization under various reaction conditions. The effect of changing parameters such as co-catalyst concentration (Al/Ni molar ratio), reaction time, and reaction temperature and ethylene pressure were investigated.

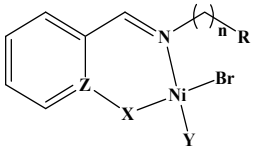

	Z	X	Y	n	R
75	C	PPh_2	Br	1	3-pyridyl
76	C	PPh_2	Br	1	2-furyl
77	C	PPh_2	Br	1	2-thiophenyl
78	C	PPh_2	Br	2	2-thiophenyl
79	C	PPh_2	Br	1	Ph
80	N	-	Br	1	2-furyl
81	C	P^tBu_2	Br	1	2-furyl
82	C	O	PPh_3	1	2-furyl

Figure 3.4 *Nickel catalyst precursors employed in the investigations of ethylene oligomerization*

3.2.2.1 Selection of a Co-Catalyst

This study was aimed at investigating the effect of three co-catalysts, i.e. MMAO, Et_2AlCl, and $EtAlCl_2$ which were used to activate the representative nickel catalyst precursors **76**, **80**, **81**, **82**, in an effort to establish the most efficient co-catalyst for subsequent investigations. This involved the variation of the co-catalyst molar ratio (Al/Ni) at 10 bar for 15 min. It was observed that higher Al/Ni ratios were required for MMAO and Et_2AlCl catalyst systems (100 – 500 and 50 – 300 respectively), compared to $EtAlCl_2$ which only required 2, 4, 10 equiv (Figure 3.5). The large Al/Ni molar ratios required for MMAO and Et_2AlCl could be due to the presence of $^tBu_3Al$ and Et_3Al in the solutions of MMAO and Et_2AlCl respectively. These impurities have been reported to interfere in the activation of catalyst precursors [5]. The low Al/Ni ratios required with $EtAlCl_2$ could be attributed to its strong Lewis acidity. Hata and Miyake observed that $EtAlCl_2$ was effective at low molar ratios, with higher molar ratios resulting in the decomposition of the catalyst during the catalytic reaction [5c].

The catalytic activities of the reactions were calculated and represented as g(oligomeric product).$mol^{-1}Ni.h^{-1}$ ($g.mol^{-1}Ni.h^{-1}$), while the selectivities of the oligomeric products are represented as weight percentages (wt %).

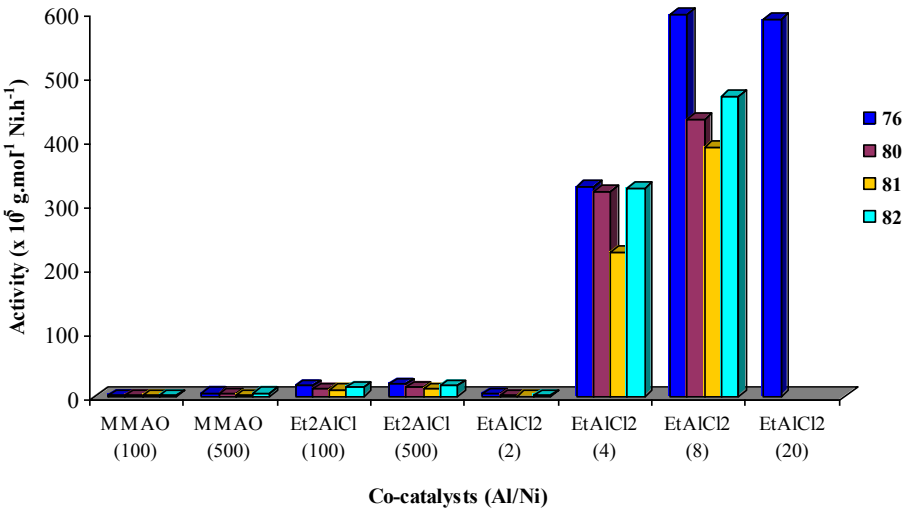

Figure 3.5 *The effect of using different co-catalysts at different Al/Ni molar ratios on the catalytic activities of complexes **76**, **80**, **81**, **82** for ethylene oligomerization*

In general, the catalyst bearing the phosphinoimine (**76**) proved to be the most active when activated with all the co-catalysts investigated (Figure 3.5), while its *tert*-butyl analogue (**81**) showed the lowest catalytic activity (Table 3.1, entries 16 – 22), presumably as a result of the lowered electrophilicity of the active center due to the presence of the highly electron-donating di-*tert*-butylphosphine group. The catalysts bearing the pyridylimine and the phenoxyimine ligands gave comparable catalytic activities (Figure 3.5).

In all cases, the most Lewis acidic co-catalyst ($EtAlCl_2$) gave the best catalytic activities (Figure 3.5). For example, catalyst **76**/$EtAlCl_2$ only required 2 molar equivalents $EtAlCl_2$ to give 4.0 x 10^3 $g.mol^{-1}Ni.h^{-1}$ (Table 3.1, entry 5). Moderate catalytic activities with only 2 molar equivalents of $EtAlCl_2$ have been reported by Braunstein *et al.* for related nickel complexes [6]. High catalytic activity of 596.9 x 10^3 $g.mol^{-1}Ni.h^{-1}$ was achieved with an Al/Ni ratio of only 8 with catalyst **76**/$EtAlCl_2$ (Table 3.1, entry 7). Further increasing the $EtAlCl_2$ ratio to 20 resulted in no significant increase in the catalytic activity (589.8 x 10^3 $g.mol^{-1}Ni.h^{-1}$, entry 8). Low catalytic activities were observed with MMAO and Et_2AlCl as co-catalysts. This could be due to the interference by trialkylaluminium impurities in MMAO and Et_2AlCl or to their relatively lower Lewis acidity [5]. Slight improvements in catalytic activities were observed when the co-catalyst molar ratios were increased. For example, catalytic activities of 2.3 and 5.2 x 10^3 $g.mol^{-1}Ni.h^{-1}$ were observed when **76** was activated with 100 and 500 molar equivalents of MMAO respectively (entries 1 and 2).

Similarly, activities of 6.7 and 9.3 x 10^3 g.mol^{-1}Ni.h^{-1} were observed when **76** was activated with 100 and 300 molar equivalents of Et_2AlCl respectively (entries 3 and 4). With nitrogen-based tridentate nickel systems Sun *et al*. also observed that the catalyst precursors activated with the more Lewis acidic Et_2AlCl, gave better catalytic activities compared to the less acidic MAO and MMAO counterparts [7]. In addition, Braunstein *et al.* observed that molar ratios of $EtAlCl_2$ of only 2 and 6 gave more active catalysts compared to those obtained when 400 to 800 molar equivalents of MAO were employed, further demonstrating the important role played by the co-catalyst Lewis acidity [6a]. Catalyst systems using **80**, **81**, and **82** followed similar trends to those observed with **76**. As a result of these findings, $EtAlCl_2$ was selected as the co-catalyst for subsequent investigations.

All catalysts investigated in this study proved to be highly selective for ethylene dimerization (up to 99.4 %, Table 3.1 entry 2) with low ethylene trimerization products (up to 4 %, entry 19) being observed. The ligand backbone of catalyst precursors **76** – **82** proved to have no significant influence on the product distribution (i.e. on the proportion of C_4 produced). However, the type and ratio of co-catalyst had a marked effect on the amount of the 1-C_4 produced, (see Figure 3.6).

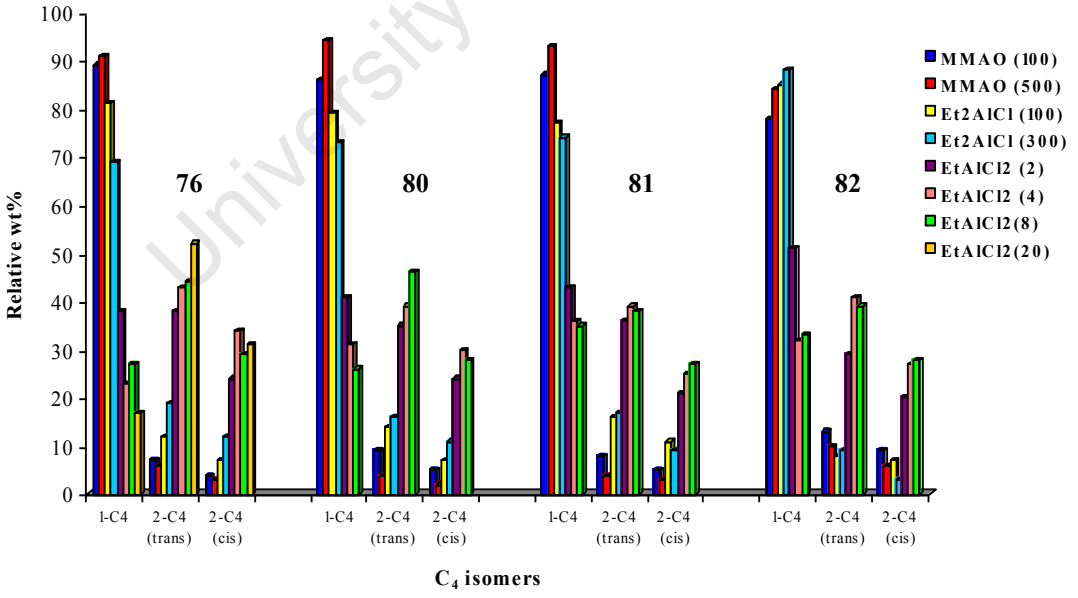

Figure 3.6 *The C_4 product distribution for catalyst precursors **76, 80 – 82** with different co-catalysts*

Improved 1-C_4 selectivities were observed when MMAO was used as a co-catalyst. For example catalyst **80**/MMAO gave up to 94 % 1-C_4 within 99 % C_4 fraction (Table 3.1, entry

10). On the other hand, catalyst precursors activated with $EtAlCl_2$ revealed the worst selectivities for 1-C_4. For example, catalyst **80**/MMAO gave 41 % 1-C_4 within the 98 % C_4 fraction (Table 3.1, entry 13). The same behaviour was observed with the other representative catalysts investigated. Braunstein *et al.* observed the same behaviour for related nickel compounds [6].

Table 3.1 Influence of co-catalyst and co-catalyst concentration on catalytic activity and product distribution for complexes **76**, **80**, **81**, **82** [a]

Entry	Complex	Co-catalyst	Al/Ni	Activity[b]	Oligomers (wt %)		
					C_4	C_6	1-C_4
1	**76**	MMAO	100	2.3	98.7	1.3	89
2		MMAO	500	5.2	99.4	0.6	91
3		Et_2AlCl	100	6.7	98.3	1.7	81
4		Et_2AlCl	300	9.3	98.8	1.2	69
5		$EtAlCl_2$	2	4.0	98.9	2.1	38
6		$EtAlCl_2$	4	328.2	97.2	1.8	23
7		$EtAlCl_2$	8	596.9	96.8	3.2	27
8		$EtAlCl_2$	20	589.8	94.2	5.8	17
9	**80**	MMAO	100	2.3	98.7	1.3	86
10		MMAO	500	4.7	99.1	0.9	94
11		Et_2AlCl	100	12.1	97.6	2.4	79
12		Et_2AlCl	300	14.3	98.1	1.9	73
13		$EtAlCl_2$	2	2.3	98.3	1.7	41
14		$EtAlCl_2$	4	320.2	97.3	2.5	31
15		$EtAlCl_2$	8	432.6	97.0	3.0	26
16	**81**	MMAO	100	1.1	98.7	1.3	87
17		MMAO	500	1.8	98.6	1.4	93
18		Et_2AlCl	100	10.2	97.3	2.7	77
19		Et_2AlCl	300	11.5	96.0	4.0	74
20		$EtAlCl_2$	2	0.3	97.9	2.1	43
21		$EtAlCl_2$	4	225.6	97.3	2.7	36
22		$EtAlCl_2$	8	389.4	95.2	4.8	35
23	**82**	MMAO	100	2.4	98.7	1.3	78
24		MMAO	500	5.1	98.6	1.4	84
25		Et_2AlCl	100	5.2	97.3	2.7	85
26		Et_2AlCl	300	6.5	96.0	4.0	88
27		$EtAlCl_2$	2	2.3	98.9	1.1	51
28		$EtAlCl_2$	4	325.6	97.1	2.9	32
29		$EtAlCl_2$	8	569.4	95.2	4.8	33

[a]General conditions: 5 μmol of catalyst precursor; 50 ml toluene; 30 min. 10 bar, error estimate = ± 0.1, 1-C_4 component is the proportion within the C_4 fraction. [b]Activity = $x10^3$ g(product).mol^{-1}Ni.h^{-1}.

3.2.2.2 The Influence of Reaction Temperature

The effect of temperature on ethylene oligomerization activity was investigated with catalyst systems **75** – **82**/$EtAlCl_2$ (Al/Ni = 8, 10 bar (ethylene pressure), 15 min). The details of this study are given in Table 3.2 and shown graphically in Figure 3.7.

Three temperature ranges, 0 – 10 °C, 40 – 50 °C, and 70 – 80 °C, were investigated. Ethylene oligomerization reactions with the nickel catalysts gave spontaneous exotherms (up to 110°C) as soon as ethylene was introduced, with no induction period observed. Lower temperature ranges (0 – 10 °C and 40 – 50 °C) were achieved and maintained by cooling the autoclave with ice-water, thus the reaction temperatures are recorded as ranges. The reactions carried out at higher temperatures (70 – 80 °C) were achieved by heating the autoclave prior to introducing ethylene.

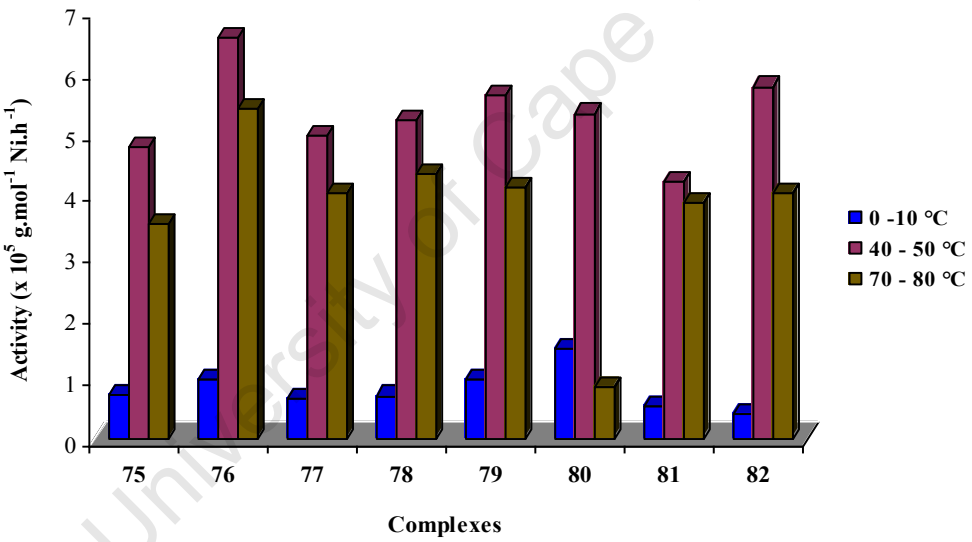

Figure 3.7 *The effect of temperature on ethylene oligomerization activity with* ***75*** *–* ***82****/*$EtAlCl_2$

Table 3.2 Influence of temperature on ethylene oligomerization with complexes **75** – **82**[a]

Entry	Complex	Temp. (°C)	Activity[b]	Oligomerization (wt %)		
				C_4	C_6	1-C_4
1	**75**	0 – 10	0.7	99.7	0.3	51
2		40 – 50	4.8	99.0	1.0	48
3		70 – 80	3.5	97.2	2.8	26
4	**76**	0 – 10	0.9	99.3	0.7	47
5		40 – 50	6.6	98.1	1.9	44
6		70 – 80	5.4	97.6	2.4	22
7	**77**	0 – 10	0.7	98.7	1.3	52
8		40 – 50	4.9	97.1	2.9	43
9		70 – 80	4.0	97.2	2.8	17
10	**78**	0 – 10	0.7	99.3	0.7	48
11		40 – 50	5.2	97.8	2.2	39
12		70 – 80	4.3	96.8	3.2	23
13	**79**	0 – 10	0.9	98.2	1.8	43
14		40 – 50	5.6	98.0	2.0	37
15		70 – 80	4.1	97.6	2.4	15
16	**80**	0 – 10	0.5	98.6	1.4	33
17		40 – 50	5.3	98.3	1.7	25
18		70 – 80	0.9	97.2	2.8	9
19	**81**	0 – 10	0.5	99.1	0.9	54
20		40 – 50	4.2	98.7	1.3	48
21		70 – 80	3.8	98.1	1.9	36
22	**82**	0 – 10	0.4	98.8	1.2	44
23		40 – 50	5.8	97.7	2.3	37
24		70 – 80	4.0	97.5	2.5	31

[a]General Conditions: Time = 15 min; 5 μmol of catalyst precursor; 50 ml toluene; Al/Ni = 8; 10 bar, error estimate = ± 0.1, 1-C_4 component is the proportion within the C_4 fraction. [b]Activity = x 10^5 g(product). mol^{-1}Ni. h^{-1}.

The optimum temperature range was found to be 40 – 50 °C, giving activities up to 6.6 x 10^5 $g.mol^{-1}Ni.h^{-1}$ (Table 3.2, entry 5) with **76** at 10 bar. Lower catalytic activities of 0.9 x 10^5 $g.mol^{-1}Ni.h^{-1}$ and 5.4 x 10^5 $g.mol^{-1}Ni.h^{-1}$ (Table 3.2, entries 4 and 6 respectively) were observed with the same catalyst system at lower temperatures (0 – 10 °C) and higher temperatures (80 – 110 °C) respectively. The same trend was observed for all catalysts investigated, with a significant decrease in catalytic activity observed for catalyst system **80**/$EtAlCl_2$ bearing a pyridylimine ligand at high temperature (0.9 x 10^5 $g.mol^{-1}Ni.h^{-1}$ at 70 – 80 °C (Table 3.2, entry 18)). These observations are consistent with those reported by

Brookhart *et al.* for some Pd(II) and Ni(II)-α-bis(imine) catalysts that rapidly decomposed around 50 °C [9]. The lower catalytic activities observed at 0 – 10 °C could be due to incomplete activation or low solubility of the catalyst at these temperatures. On the other hand, when the reactions were carried out at room temperature (i.e. without cooling or heating the autoclave), the introduction of ethylene was accompanied by a spontaneous exotherm (up to 110 °C) and rapid consumption of ethylene. In general, the temperature gradually dropped from 80 to 60 °C but remained at these temperatures as long as the ethylene pressure was kept constant. However, lower catalytic activities were observed when the reactions were heated at a constant temperature of 70 – 80 °C. This could be attributed to the lower ethylene solubility in toluene at these temperatures (e.g. 0.12 mol. $kg^{-1}bar^{-1}$ at 40 °C and 0.080 mol. $kg^{-1}bar^{-1}$ at 70 °C) [7, 10]. For example, Janiak *et al.* observed decreases in activity of up to 50 % of substituted (phenanthroline)Ni(II)/MAO catalyst system when the temperature was increased from 40 to 80 °C [10d]. The nickel catalyst in our catalyst system proved to be highly stable, given that the catalysts continued to consume ethylene at such high temperatures (up to 60 – 110 °C).

As mentioned earlier, only ethylene dimerization (C_4) and trimerization (C_6) products were formed with the nickel catalysts studied. These showed exceptional selectivity for ethylene dimerization (up to 99.7 %), in which all C_4 products (1-C_4 and *cis* and *trans* 2-C_4) within the C_4 fraction were observed. In all the cases investigated, nine products (3-methyl-1-pentene, 1-hexene, 2-ethylbutene, *trans*-3-hexene, *cis*-3-hexene, *trans*-2-hexene, *cis*-2-hexene, *trans*-3-methyl-2-pentene, *cis*-3-methyl-2-pentene) were observed in the C_6 fraction. Similar product distributions have been reported in the literature for related catalysts [11]. Table 3.3 below shows the relative weight percentages (wt %) of the products formed within each fraction (i.e. C_4 and C_6) for catalysts **75** – **82**/$EtAlCl_2$ at 40 – 50 °C.

Table 3.3 Relative wt % of C_4 and C_6-isomers produced by catalysts **75** – **82**/$EtAlCl_2$ at 40 – 50 °C

Products (wt %)	**75**	**76**	**77**	**78**	**79**	**80**	**81**	**82**
C_4-Isomers								
1-butene	10.4	31.1	27.7	10.6	25.6	18.8	28.9	30.0
trans-2-butene	57.7	46.3	52.6	60.9	56.1	54.4	47.7	45.7
cis-2-butene	31.9	22.6	19.7	28.5	18.3	26.8	23.4	24.3
C_6-Isomers								
3-methyl-1-pentene	1.2	2.4	0.6	1.1	0.5	1.9	0.4	0.9
1-hexene	3.8	6.3	3.4	3.2	2.9	4.1	3.0	3.1
2-ethylbutene	2.7	5.5	4.1	5.2	8.8	1.8	7.4	9.5
trans-2-hexene	10.9	14.0	6.6	7.4	9.3	9.0	8.7	8.4
cis-2-hexene	18.7	17.8	18.4	18.8	21.0	16.9	19.9	17.3
trans-3-hexene	32.2	28.4	29.4	31.3	31.4	29.1	31.2	31.0
trans-3-methyl-2-pentene	6.6	7.3	9.2	8.8	5.0	8.9	6.0	6.3
cis-3-hexene	11.2	10.7	9.9	11.6	11.3	10.7	11.0	10.5
cis-3-methyl-2-pentene	12.7	7.6	18.4	12.6	9.8	17.6	12.4	13.0

Nickel catalysts are widely known to isomerize α-olefins into mixtures of internal olefins [6]. This behaviour is demonstrated in the product distribution shown in Table 3.3. It was observed that within the C_4 fraction (itself accounting for 98.0 – 99.7 % of the total product) there was selectivity of only 10.4 – 31 % for 1-C_4. The bulk of the C_4 fraction was made up of 2-C_4 (67 – 89 %) with the *trans* isomer being the predominant component (up to 60.9% within the 2-C_4 component, Table 3.3). The ability of the nickel catalyst to insert 1-C_4 into a metal-hydride in a 1-2 (**A**) or 2-1 (**B**) fashion is the main reason for the formation of linear and branched C_6 products (Table 3.3). The mechanistic pathway detailing the formation of the product distribution in Table 3.3 was discussed in Chapter 1, section 1.6.4.

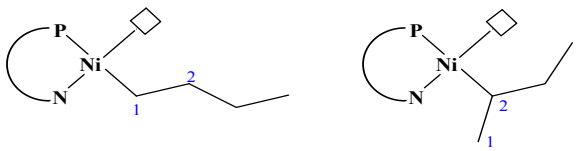

A **B**

A graphical representation of the C_4 isomer distribution at different reaction temperatures is shown in Figure 3.8 below for the representative catalysts **76**, **80** – **82**/$EtAlCl_2$.

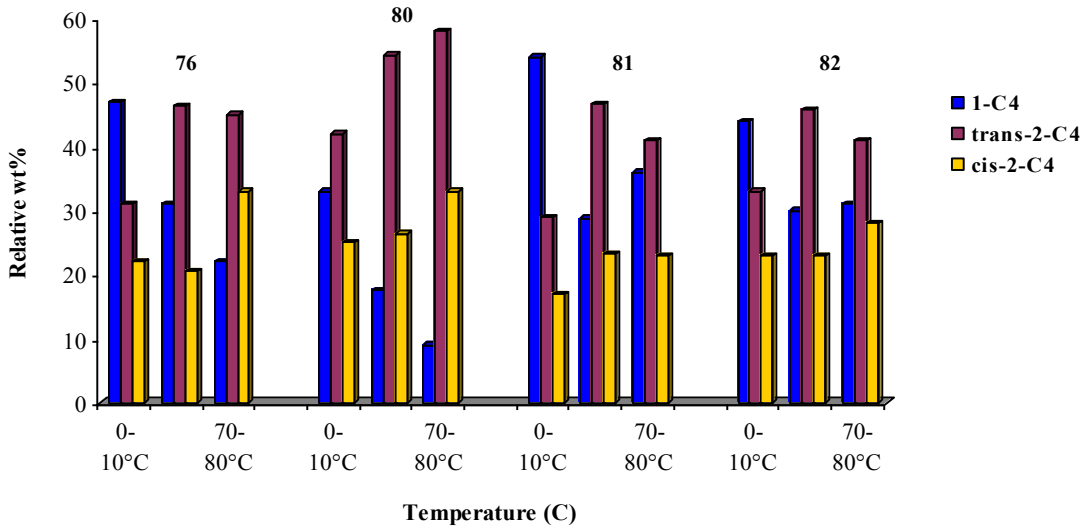

Figure 3.8 *The C_4 isomer distribution at different temperatures with representative catalysts **76**, **80**, **81**, and **82**/$EtAlCl_2$.*

3.2.2.3 The Influence of Reaction Time

In this study, the effect of the reaction time on catalytic activity and product distribution was investigated. Four reaction times (1, 5, 15, 30 min) were explored at a working ethylene pressure of 10 bar and an $EtAlCl_2$ molar ratio of Al/Ni = 8. As mentioned before, the introduction of ethylene resulted in an immediate increase in temperature, along with rapid consumption of ethylene. The start time was measured when the autoclave was filled with the appropriate pressure of ethylene. The pressure was maintained for the duration of the reaction. After the required reaction time the reaction was stopped by the discontinuation of ethylene pressure, followed by rapid cooling of the autoclave to -25 – -35 °C and venting of residual ethylene.

In general, all the catalysts were observed to be very active, giving catalytic activities of 6.3 – 58.4 x 10^4 $g.mol^{-1}Ni.h^{-1}$ with catalyst **76**/$EtAlCl_2$ when the reaction was carried out for 1 and 15 min respectively (Table 3.4, entries 5 and 7). Figure 3.9 illustrates the trends followed by the catalysts **75** – **82**/$EtAlCl_2$.

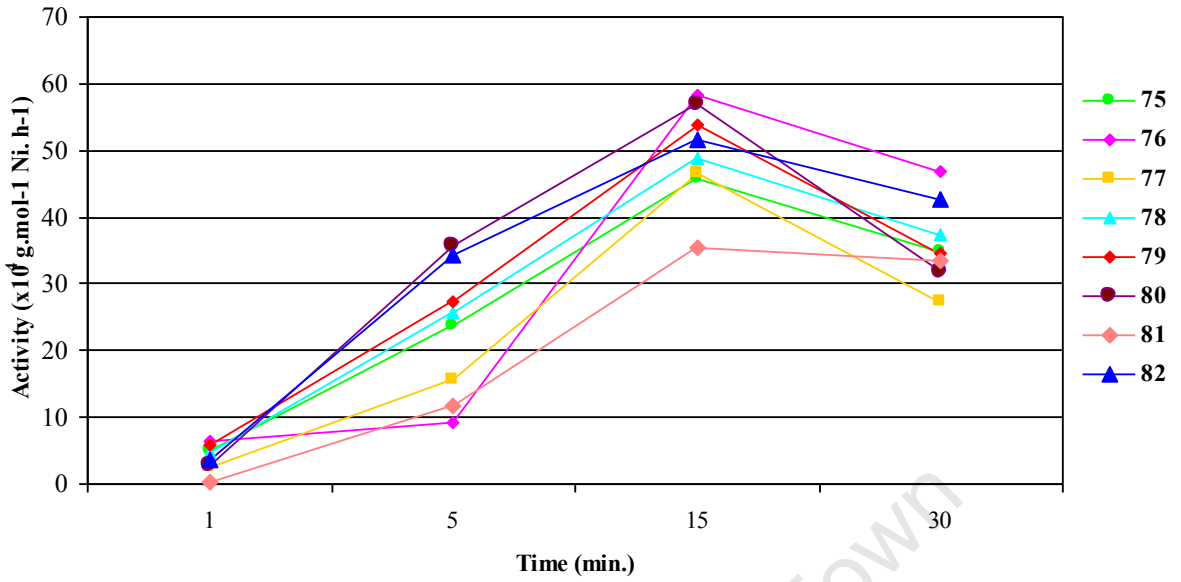

Figure 3.9 *The effect of reaction time on catalytic activity with* ***75*** *–* ***82****/EtAlCl$_2$ catalyst systems*

The details of the catalyst activity and product distribution described above are given in Table 3.4 below. Good catalytic activities of up to 6.3 x 10^4 g.mol^{-1}Ni.h^{-1} with catalyst **76**/EtAlCl$_2$ (Table 3.4, entry 5) were observed even when the reaction was stopped after one minute. All catalysts studied revealed a similar trend between the reaction time and the catalytic activity. The catalytic activities gradually increased, peaking at 15 min (Figure 3.9). For instance, catalyst **76**/EtAlCl$_2$ gave activities of 6.3, 9.1, and 58.4 x 10^4 g.mol^{-1}Ni.h^{-1} when the reactions were carried out for 1, 5, 15 min respectively (Table 3.4 entries 5, 6, and 7). When the reactions were conducted for more than 15 min, catalyst activity either remained relatively constant (**81**, Figure 3.9) or declined (**75** – **80**, **82**, Fig 3.9). Braunstein *et al*. also observed a similar trend for related nickel complexes [11c]. The decrease in the catalytic activity beyond 15 min could be due to the reduced mass transfer of ethylene as a result of the large amounts of product produced in the first 15 min of the catalytic reaction.

Table 3.4 Influence of reaction time on ethylene oligomerization with complexes **75** – **82**[a]

Entry	Complex	Time (min)	Al/Ni	Activity[b]	Oligomerization (wt %)		
					C_4	C_6	1-C_4
1	**75**	1	8	4.9	98.2	1.8	50
2		5	8	23.8	99.5	0.5	42
3		15	8	45.8	98.7	1.3	34
4		30	8	34.8	97.2	2.8	35
5	**76**	1	8	6.3	97.7	2.3	52
6		5	8	9.1	99.0	1.0	42
7		15	8	58.4	97.7	2.3	32
8		30	8	46.8	96.9	3.1	26
9	**77**	1	8	2.4	98.3	1.7	47
10		5	8	15.7	99.2	0.8	49
11		15	8	46.6	97.3	2.7	39
12		30	8	27.3	96.1	3.9	33
13	**78**	1	8	4.7	96.6	3.4	49
14		5	8	25.7	96.8	3.2	44
15		15	8	48.7	99.4	0.6	40
16		30	8	37.3	94.7	5.3	34
17	**79**	1	8	5.9	97.7	2.3	45
18		5	8	27.2	96.0	4.0	45
19		15	8	53.8	96.0	4.0	41
20		30	8	34.5	96.9	3.1	43
21	**80**	1	8	2.8	98.7	1.3	51
22		5	8	35.7	99.4	0.6	47
23		15	8	56.8	97.5	2.5	43
24		30	8	31.9	97.0	3.0	33
25	**81**	1	8	0.2	99.3	0.7	53
26		5	8	11.8	99.5	0.5	48
27		15	8	35.3	98.6	1.4	49
28		30	8	33.4	98.2	1.8	34
29	**82**	1	8	3.6	96.4	3.6	42
30		5	8	34.2	97.4	2.6	38
31		15	8	51.5	97.0	3.0	32
32		30	8	42.7	96.6	3.4	28

[a] General Conditions: Temp = 40 – 50 °C; 5 µmol of catalyst precursor; 50 ml toluene; 10 bar, error estimate = ± 0.1, 1-C_4 component is the proportion within the C_4 fraction. [b]Activity = x 10^4 g.mol^{-1}Ni.h^{-1}.

In general, a gradual decrease in the selectivity for 1-C_4 was observed with longer reaction times (Figure 3.10). For example, when the catalytic reaction was carried out for 1 min up to 51 % of 1-C_4 was produced with catalyst **76**/$EtAlCl_2$ (Figure 3.10), whereas when the reaction was carried out for 30 min the selectivity for 1-C_4 declined to 25 % for the same catalyst. This could be due to the isomerization of 1-C_4 to the 2-C_4 components with longer reaction times. Figure 3.10 below shows the C_4 isomer distribution obtained with the representative catalyst systems **76**, **81**, **82**/$EtAlCl_2$.

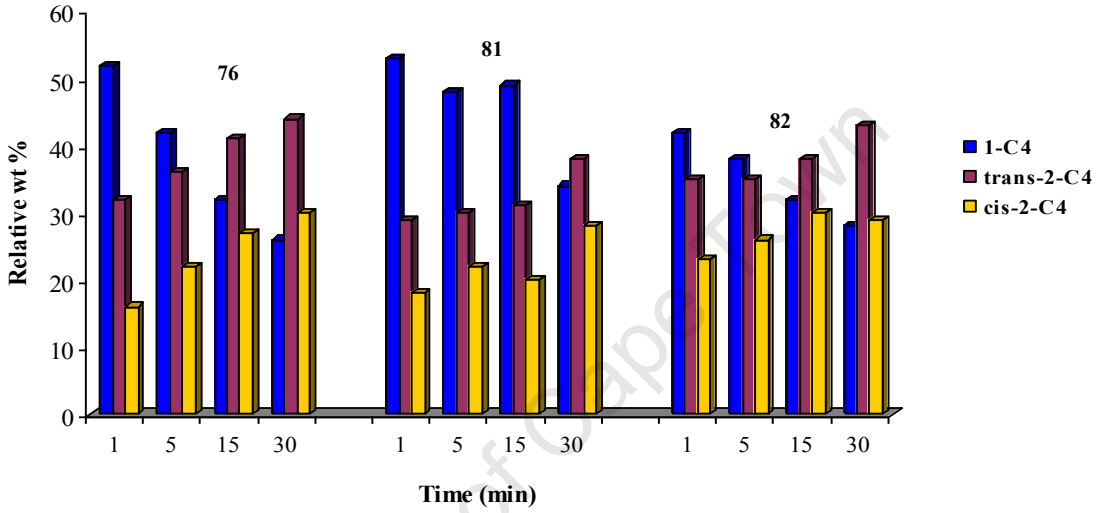

Figure 3.10 *Relative wt % of the C_4-isomers after 1, 5, 15, 30 min for **76**, **81**, and **82**/$EtAlCl_2$*

3.2.2.4 The Influence of Ethylene Pressure

This study was aimed at investigating the effect of ethylene pressure (10, 30, 50 bar) on the catalytic activity and product distribution with catalyst systems **75** – **82**/$EtAlCl_2$. In addition, the effect of varying the ethylene pressure at different co-catalyst molar ratios (Al/Ni = 4, 8 for **75**, **77** – **82**/$EtAlCl_2$ and Al/Ni = 2, 4, 8, 20 for **76**/$EtAlCl_2$) was explored. The details of this study are provided in Table 3.5.

As mentioned before, relatively small quantities of the $EtAlCl_2$ were required to yield good catalytic activities. Increasing the co-catalyst ratio (Al/Ni = 2, 4, 8, 20) with the complex **76** revealed a gradual increase in the catalytic activity (0.1, 11.0, 13.2, 13.8 x 10^5 $g.mol^{-1}Ni.h^{-1}$) respectively at 50 bar (Table 3.5, entries 6, 9, 12, 15 respectively).

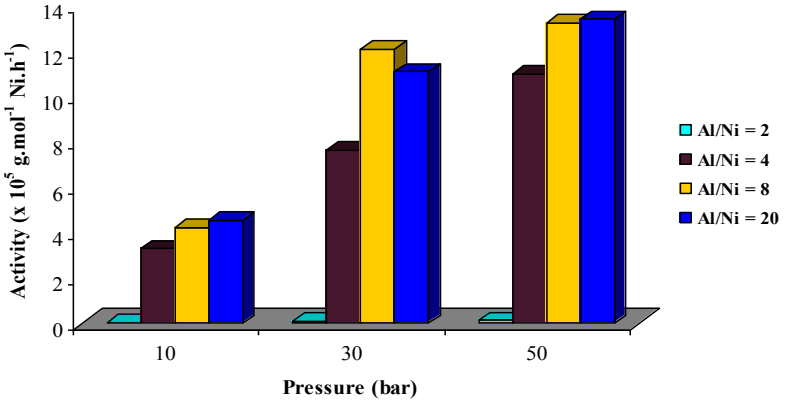

Figure 3.11 *The effect of ethylene pressures at different co-catalyst molar ratios with catalyst system* ***76****/EtAlCl$_2$*

Figure 3.11 above demonstrates that increasing the co-catalyst molar ratio beyond Al/Ni = 8 (i.e. Al/Ni = 20) had no significant effect on the catalytic activity (13.2 g.mol^{-1}Ni.h^{-1} and 13.8 x 10^5 g.mol^{-1}Ni.h^{-1} respectively, Table 3.5, entries 12 and 15) as shown by catalyst **76**/EtAlCl$_2$. The relatively poor catalytic activity observed when Al/Ni = 2 was employed, could be a result of incomplete or slow activation of the catalyst precursor at these molar ratios. The molar ratios of Al/Ni = 4 and 8 were found to be sufficient to give high catalytic activities with catalyst precursors **75**, **77** – **82**.

Table 3.5 Influence of pressure and catalyst molar ratio on ethylene oligomerization with complexes **75** – **82**[a]

Entry	Complex	Pressure	Al/Ni	Activity[b]	Oligomerization (wt %)			
					C_4	C_6	C_8	1-C_4
1	**75**	10	8	4.2	96.7	3.3	-	32
2		30	8	6.8	97.5	2.5	-	39
3		50	8	9.3	98.2	1.6	0.2	43
4	**76**	10	2	0.03	99.8	0.2	-	40
5		30	2	0.08	99.4	0.6	-	41
6		50	2	0.1	99.5	05	-	45
7		10	4	3.3	98.9	1.1	-	32
8		30	4	7.7	97.9	2.1	-	33
9		50	4	11.0	99.3	0.7	-	45
10		10	8	4.2	97.0	3.0	-	29
11		30	8	12.1	97.7	2.3	-	30
12		50	8	13.2	97.4	2.5	0.1	49
13		10	20	4.6	96.4	3.6	-	35
14		30	20	11.1	96.1	3.9	-	42
15		50	20	13.8	97.2	2.8	-	48
16	**77**	10	8	5.3	96.4	3.6	-	19
17		30	8	8.9	96.1	3.9	-	37
18		50	8	10.7	97.0	3.0	0.06	41
19	**78**	10	8	4.9	97.6	1.4	-	23
20		30	8	11.0	98.3	1.6	0.08	36
21		50	8	12.5	98.5	1.3	0.2	38
22	**79**	10	8	5.3	95.3	4.7	-	20
23		30	8	10.8	96.6	3.4	-	37
24		50	8	12.3	97.6	2.3	0.1	42
25	**80**	10	8	4.7	97.6	2.4	-	24
26		30	8	6.8	97.9	2.1	-	49
27		50	8	10.0	98.4	1.5	0.1	56
28	**81**	10	8	3.7	98.2	1.8	-	59
29		30	8	4.3	98.7	1.2	0.06	58
30		50	8	6.9	99.1	0.7	0.2	64
31	**82**	10	8	5.2	97.9	2.1	-	29
32		30	8	7.9	98.3	1.7	-	32
33		50	8	8.2	98.7	1.3	-	37

[a]General Conditions: Temp = 26°C; 5 μmol of catalyst precursor; 50 ml toluene, error estimate = ± 0.1, 1-C_4 component is the proportion within the C_4 fraction. [b]Activity = x 10^5 g(product).mol^{-1}Ni.h^{-1}.

As mentioned before, all catalyst systems (**75** – **82**/$EtAlCl_2$) produced mainly ethylene dimers (up to 99.8 %) and trimers (up to 4.7 %). Minute quantities of the ethylene tetramers (up to 0.2 %) were observed at high ethylene pressures (30 and 50 bar). All ethylene dimerization isomers (1-C_4, *trans*-2-C_4, *cis*-2-C_4) were produced. Figure 3.11 below shows the ethylene dimerization product distribution (C_4-isomers).

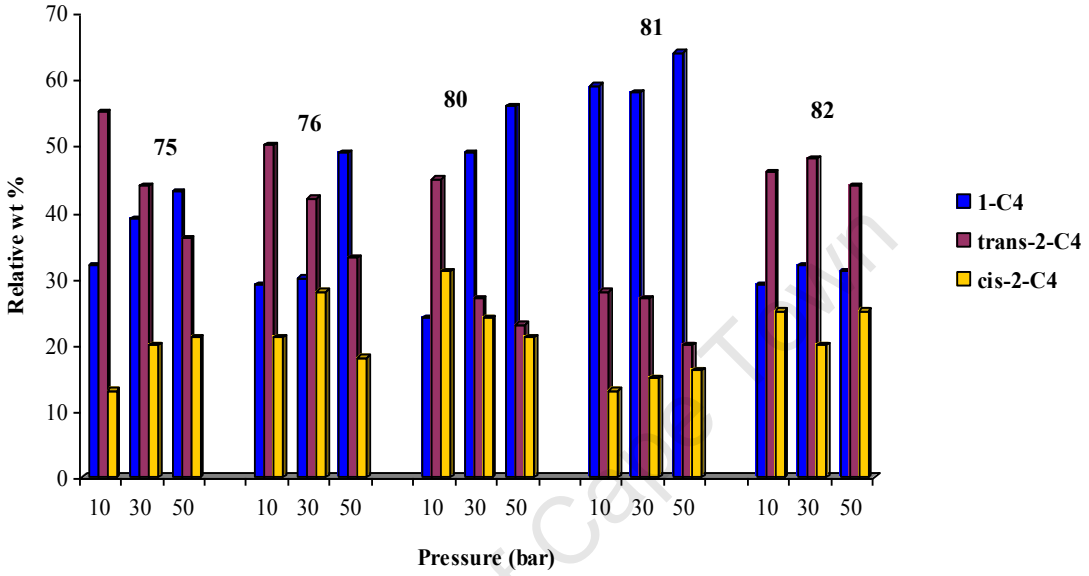

Figure 3.12 *Effect of pressure on relative wt % of the C_4-isomers at 10, 30, 50 bar for **75**, **76**, **80**, **81**, **82**/$EtAlCl_2$ (Al/Ni = 8)*

In general, increasing the pressure from 10 to 50 bar with the iminophosphine catalyst systems **75** – **79**/$EtAlCl_2$ (Table 3.5) resulted in an increase in the selectivity for 1-C_4 (e.g. 29 and 49 % at 10 and 50 bar respectively with **76**/$EtAlCl_2$ at Al/Ni = 8, entries 10 and 12). The effect was marked with the catalyst bearing the pyridylimine ligand **80**/$EtAlCl_2$ which showed an improvement in the selectivity for 1-C_4 from 24 % to 56 % at 10 and 50 bar respectively with Al/Ni = 8 (Table 3.5, entries 25 and 27). On the other hand, catalyst system **81**/$EtAlCl_2$ bearing the more basic and bulky di-*tert*-butylphosphine, gave 1-C_4 as a major product even at lower ethylene pressures (59 and 64 % at 10 and 50 bar respectively at Al/Ni = 8, Table 3.5, entries 28 and 30). This could be attributed to the bulky *tert*-butylphosphine groups retarding secondary coordination of 1-C_4 and consequently its isomerization.

In general, increasing the ethylene pressure had no significant effect on the product distribution (i.e. C_4 and C_6). Catalyst systems **81**/$EtAlCl_2$ and **82**/$EtAlCl_2$ bearing the di-*tert*-

butylphosphine and phenoxyimine respectively showed no appreciable improvement in 1-C_4 selectivity upon increasing the pressure.

Increasing the ethylene pressure at different co-catalyst molar ratios with catalyst **76**/$EtAlCl_2$, revealed a slight decrease in the overall product distribution (i.e. C_4 and C_6). The results could imply that higher co-catalyst molar ratios promote chain propagation and reinsertion of 1-C_4 (thus higher C_6 product at higher co-catalyst molar ratios).

3.2.3 Palladium-Catalyzed Ethylene Oligomerization

A number of neutral iminophosphine, pyridylimine, and phenoxyimine palladium catalyst precursors (**56** – **63**, Figure 3.13) were investigated for ethylene oligomerization under various reaction conditions. Parameters such as co-catalyst concentration (Al/Pd molar ratio), reaction time, reaction temperature, and ethylene pressure, were varied to determine optimal conditions.

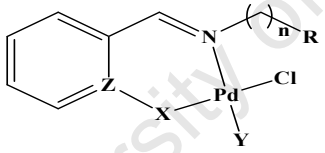

	Z	X	Y	n	R
56	C	PPh_2	Cl	1	3-pyridyl
57	C	PPh_2	Cl	1	2-furyl
58	C	PPh_2	Cl	1	2-thiophenyl
59	C	PPh_2	Cl	2	2-thiophenyl
60	C	PPh_2	Cl	1	Ph
61	N	-	Cl	1	2-furyl
62	C	P^tBu_2	Cl	1	2-furyl
63	C	O	PPh_3	1	2-furyl

Figure 3.13 *Palladium catalyst precursors employed in the investigations of ethylene oligomerization*

3.2.3.1 The Selection of a Co-Catalyst

To establish the most efficient co-catalyst, various co-catalysts (MMAO, Et_2AlCl and $EtAlCl_2$) were used to activate the representative palladium catalyst precursors (**56**, **61**, **62**, **63**) in the oligomerization of ethylene. The co-catalyst molar ratios (Al/Pd) were also varied for each co-catalyst to determine optimum molar ratios (i.e. Al/Pd = 100 and 1000 for MMAO, Al/Pd = 100, 300, 500 for Et_2AlCl, Al/Pd = 4, 10, 50, 100 for $EtAlCl_2$).

Compared to the nickel catalysts discussed in the preceding sections, the palladium catalysts displayed only low catalytic activities. This type of behaviour was also observed by Guan, Rieger and co-workers in their ethylene polymerization studies [1a,12]. In fact, no catalytic

activity was observed when MMAO was used to activate the catalyst precursors **57**, **61**, **62**, **63** (Figure 3.14). This could be due to the lower Lewis acidity of MMAO or deactivation of the active catalyst by the $^{t}Bu_3Al$ impurities in MMAO [5]. Only low catalytic activity of up to 1.9 x 10^2 g.mol^{-1}Pd.h^{-1} was observed with the catalyst system **63**/MMAO with Al/Pd = 1000 (Table 3.6, entry 29).

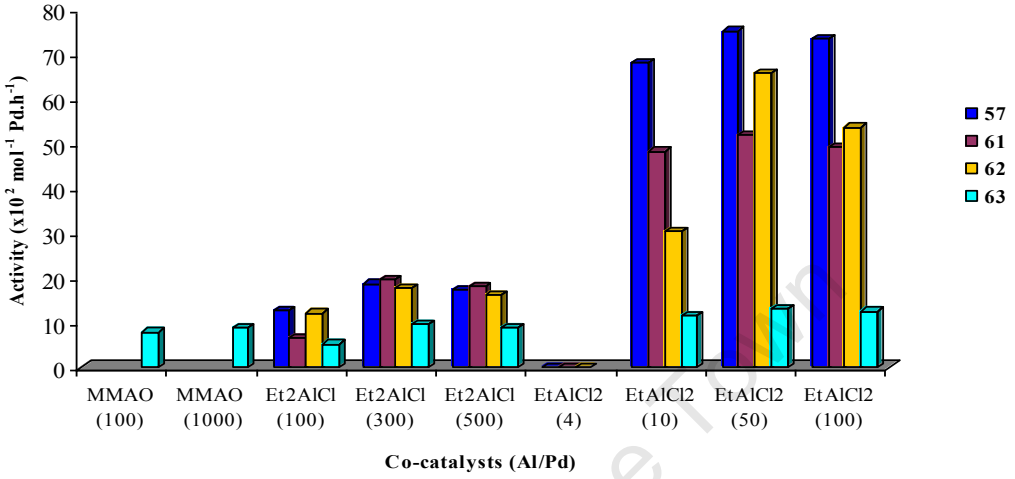

Figure 3.14 *Effect of different co-catalysts on the catalytic activity of complexes **57**, **61**, **62**, **63** for ethylene oligomerization.*

Modest catalytic activities of up to 19.7 x 10^2 g.mol^{-1}Pd.h^{-1} (Table 3.6, entry 13) were observed when Et_2AlCl was employed as a co-catalyst. Increasing the Al/Pd ratio from 100 to 300 led to a significant improvement in the catalytic activity (e.g. 6.7 to 19.7 x 10^2 g. mol^{-1}Pd.h^{-1} with **61**/Et_2AlCl, Table 3.6, entries 12 and 13). Further increasing the Al/Pd ratio to 500 resulted in a decrease in the catalytic activity (16.1 x 10^2 g.mol^{-1}Pd.h^{-1} with **61**/Et_2AlCl, Table 3.6, entry 14). This trend was observed for all catalysts (**57**, **61** – **63**/Et_2AlCl) investigated. The decrease in the catalytic activity at high co-catalyst molar ratios could be ascribed to the increased amount of trialkylaluminium impurities present in the solutions of MMAO and Et_2AlCl [5a,b]. In addition, the fact that our catalyst system is not very hindered at the active site, could encourage interaction with the more bulky trialkylaluminium impurities in the activators resulting in a less active catalyst.

In addition, increasing the co-catalyst molar ratio could facilitate dialkylation of the Pd center, consequently deactivating the catalyst by rapid reductive elimination to give the inactive Pd(0) [5f]. The same behaviour was observed when $EtAlCl_2$ was used as a co-catalyst, with catalytic activities increasing appreciably when the Al/Pd molar ratio was increased from 10 to 50 (Figure 3.14). No catalytic activity was observed at low co-catalyst

molar ratio (Al/Pd = 4), presumably due to insufficient activation of the catalyst precursors. When larger molar ratios (Al/Pd = 10 and 50) were employed, only low catalytic activities were observed (e.g. 68.0 and 75.1 x 10^2 g.mol^{-1}Pd.h^{-1} respectively with **57**/$EtAlCl_2$, Table 3.6, entries 7 and 8), while further increasing the Al/Pd ratio to 100 led to a decline in the catalytic activity (73.5 g. mol^{-1}Pd.h^{-1}, Table 3.6, entry 9). Of the three co-catalysts investigated, $EtAlCl_2$ gave the best catalytic activities and was thus used for subsequent investigations. The higher catalytic activities observed with $EtAlCl_2$ could be attributed to its stronger Lewis acidity compared to MMAO and Et_2AlCl. Lower catalytic activities were observed for the more basic di-*tert*-butylphosphinoamine **62**/$EtAlCl_2$ analogue (62.6 x 10^2 g.mol^{-1}Pd.h^{-1} vs 75.1 x 10^2 g.mol^{-1} Pd.h^{-1} for **62**/$EtAlCl_2$ and **57**/$EtAlCl_2$ respectively at Al/Pd = 50, Table 3.6 entries 26 and 8 respectively). A lower catalytic activity of 13.2 x 10^2 g.mol^{-1}Pd.h^{-1} at Al/Pd = 50 (Table 3.6 entry 35) was displayed by catalyst **63**/$EtAlCl_2$ bearing the phenoxyimine ligand.

Table 3.6 Influence of the co-catalyst and the co-catalyst/catalyst precursor ratio on catalytic activity and product distribution with complexes **57, 61 – 63**[a]

Entry	Complex	Co-catalyst	Al/Pd	Activity[b]	Oligomers		
					C_4	C_6	1-C_4
1	**57**	MMAO	100	-	-	-	-
2		MMAO	1000	-	-	-	-
3		Et_2AlCl	100	12.7	99.1	0.9	84
4		Et_2AlCl	300	18.7	99.8	0.2	81
5		Et_2AlCl	500	17.5	98.1	1.9	67
6		$EtAlCl_2$	4	-	-	-	-
7		$EtAlCl_2$	10	68.0	99.0	1.0	32
8		$EtAlCl_2$	50	75.1	99.5	0.5	21
9		$EtAlCl_2$	100	73.5	96.1	2.9	12
10	**61**	MMAO	100	-	-	-	-
11		MMAO	1000	-	-	-	-
12		Et_2AlCl	100	6.7	99.0	0.0	89
13		Et_2AlCl	300	19.7	99.3	0.7	76
14		Et_2AlCl	500	16.1	98.6	0.4	68
15		$EtAlCl_2$	4	-	-	-	-
16		$EtAlCl_2$	10	48.2	99.8	0.8	31
17		$EtAlCl_2$	50	56.9	99.1	0.2	22
18		$EtAlCl_2$	100	49.1	98.4	1.6	19
19	**62**	MMAO	100	-	-	-	-
20		MMAO	1000	-	-	-	-
21		Et_2AlCl	100	12.1	99.6	0.4	86
22		Et_2AlCl	500	17.8	99.9	0.1	62
23		Et_2AlCl	1000	16.3	98.3	1.7	63
24		$EtAlCl_2$	4	-	-	-	-
25		$EtAlCl_2$	10	30.3	99.5	0.5	39
26		$EtAlCl_2$	50	62.6	99.9	0.1	33
27		$EtAlCl_2$	100	53.1	99.1	0.9	14
28	**63**	MMAO	100	0.6	100	-	82
29		MMAO	1000	1.9	100	-	81
30		Et_2AlCl	100	5.2	99.8	0.2	78
31		Et_2AlCl	500	9.8	99.0	0.0	74
32		Et_2AlCl	1000	8.9	98.5	0.5	62
33		$EtAlCl_2$	4	-	-	-	-
34		$EtAlCl_2$	10	11.6	99.3	0.7	31
35		$EtAlCl_2$	50	13.2	99.2	0.8	33
36		$EtAlCl_2$	100	12.9	98.6	1.4	11

[a]General conditions: 10 μmol of catalyst precursor; 50 ml toluene; 15 min. 10 bar, error estimate = ± 0.1, 1-C_4 component is the proportion within the C_4 fraction.. [b]Activity = $x10^2$ g(product). mol^{-1}Pd. h^{-1}

In all the cases investigated, the oligomerization product distribution (C_4 and C_6) was not affected by the Al/Pd molar ratios at lower concentrations (i.e Al/Pd = 100 – 300 for Et_2AlCl and Al/Pd = 10 – 50 for $EtAlCl_2$). For example, a slight increase in the C_4 fraction (99.1 and 99.8 % at Al/Pd = 10 and 50) was observed with catalyst **57**/Et_2AlCl (Table 3.6, entries 3 and 4). At higher co-catalyst concentrations (Al/Pd = 500) the selectivity for C_4 decreased slightly to 98.1 %, (Table 3.6 entry 5) with the same catalyst.

As mentioned above, all catalysts predominantly produced ethylene dimers and small quantities of ethylene trimers (<1 %). Consistent with the product distribution obtained with the nickel catalysts, the palladium catalysts also yielded 2-C_4 as the major component (upon activation with $EtAlCl_2$) within the C_4 fraction (Figure 3.15). This suggested that the palladium catalysts also had a dual function of oligomerizing ethylene to 1-C_4 as well as isomerizing the formed product (1-C_4) to the corresponding 2-C_4 isomers (*cis* and *trans*) when $EtAlCl_2$ was used. In addition, this suggests that palladium catalysts follow the same pathway as nickel catalysts (Chapter 1, section 1.6.4). This behaviour has been observed before with related systems [11].

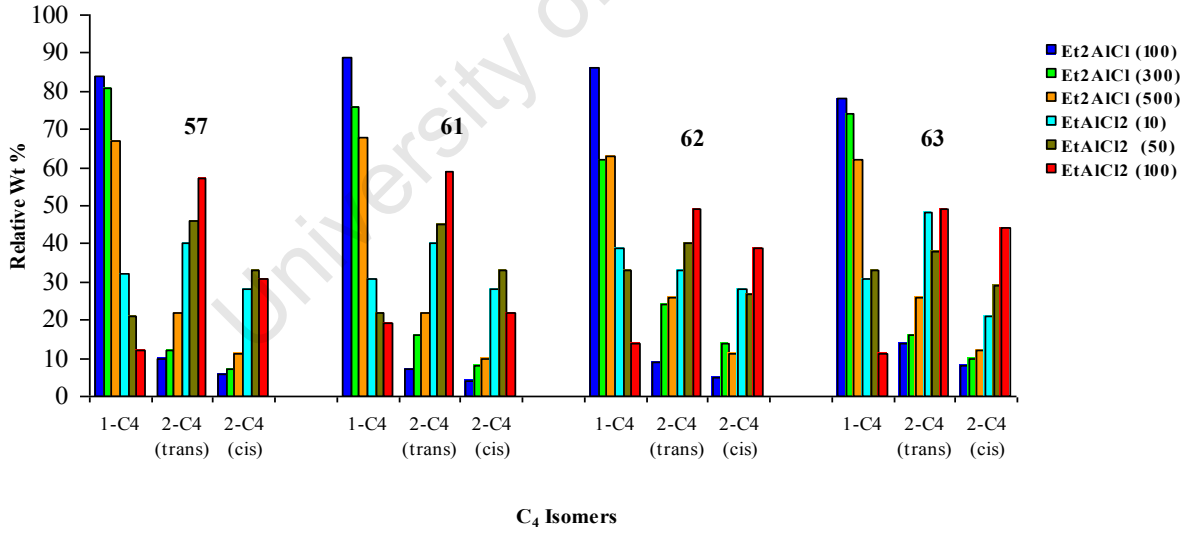

Figure 3.15 *Effect of the co-catalyst concentration on the relative wt % of the C_4-isomers*

The selectivity for 1-C_4 decreased when the co-catalyst concentration was increased (Table 3.6, entries 7 – 9, 16 – 18, 25 – 27, and 34 – 36). Better selectivities for 1-C_4 were observed when MMAO (entries 28 and 29) and Et_2AlCl (entries 3 – 5, 12 – 14, 21 – 23, 30 – 32) were employed as co-catalysts. As was the case with the nickel catalysts, the minor C_6 components

comprised of 3-methyl-1-pentene, *trans*-3-methyl-2-pentene, *cis*-3-methyl-2-pentene, and 2-ethylbutene, as well as 1-hexene, *trans*-2-hexene, and *cis*-2-hexene [10,11].

3.2.3.2 The Influence of Temperature

The effect of temperature on ethylene oligomerization was explored with catalysts **56** – **63**/$EtAlCl_2$ (Al/Pd = 50, at 30 bar ethylene for 15 min). The details of this study are given in Table 3.7 and represented graphically in Figure 3.16. Three reaction temperature ranges (0 – 10, 40 – 50, 70 – 80 °C) were investigated.

Increasing the temperature proved to have an effect on the catalytic activity but very little influence on the product distribution (i.e. relative amounts of C_4 and C_6). In all the cases investigated, increasing the reaction temperature from 0 – 10 to 40 – 50 °C resulted in a significant improvement in the catalytic activity (e.g. 3.3 – 6.1 x 10^3 g.mol^{-1}Pd.h^{-1} with **61**/$EtAlCl_2$, Table 3.7 entries 16 and 17). Further increasing the temperature from 40 – 50 to 70 – 80 °C led to a decrease in the catalytic activity. For example, catalyst **61**/$EtAlCl_2$ gave 0.6 x 10^3 g.mol^{-1}Pd.h^{-1} at 70 – 80 °C (Table 3.7 entry 18). The diminished catalytic activity in the case of **61**/$EtAlCl_2$ bearing a pyridylimine ligand could be due to catalyst instability at high temperatures (Figure 3.16) as observed with the nickel counterpart. This behaviour is consistent with that of Brookhart's Pd(II)-α-bis(imine) catalysts [9]. Another reason for the drop in the catalytic activity could be the lower ethylene solubility in toluene at 70 – 80 °C (i.e. 0.12 mol. kg^{-1}bar^{-1} at 40 °C and 0.080 mol. kg^{-1}bar^{-1} at 70 °C) [7, 10].

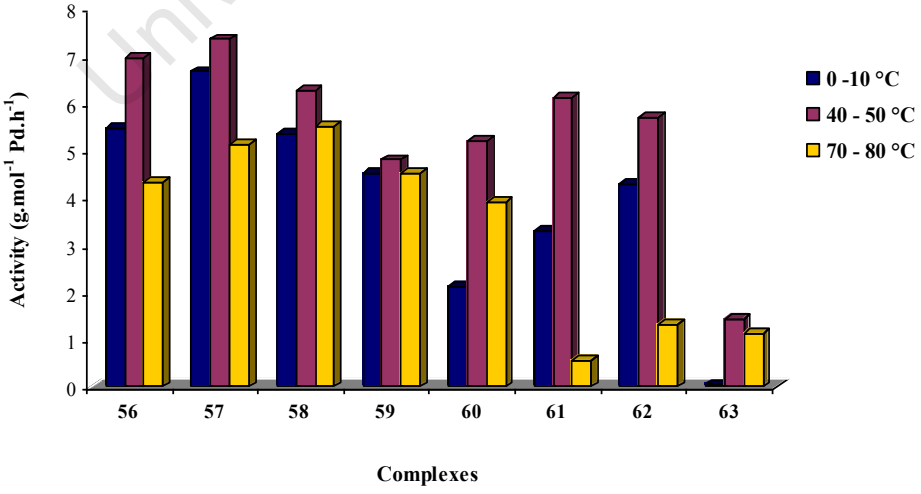

Figure 3.16 *The effect of temperature on ethylene oligomerization reactivity with* ***56*** *–* ***63****/EtAlCl$_2$*

Table 3.7 Influence of temperature on ethylene oligomerization with complexes **56** – **63**[a]

Entry	Complex	Temp. (°C)	Activity[b]	Oligomerization (wt %)		
				C_4	C_6	1-C_4
1	**56**	0 – 10	5.5	99.3	0.7	48
2		40 – 50	6.9	99.5	0.5	25
3		70 – 80	4.3	98.6	1.4	12
4	**57**	0 – 10	6.7	99.7	0.3	39
5		40 – 50	7.4	99.0	1.0	19
6		70 – 80	5.1	99.6	0.4	11
7	**58**	0 – 10	5.4	99.4	0.6	41
8		40 – 50	6.3	99.2	0.8	33
9		70 – 80	5.5	98.9	1.1	13
10	**59**	0 – 10	4.5	99.4	0.6	46
11		40 – 50	4.8	99.8	0.2	29
12		70 – 80	4.5	99.1	0.9	16
13	**60**	0 – 10	2.2	100	-	50
14		40 – 50	5.2	99.3	0.7	23
15		70 – 80	3.9	99.8	0.2	17
16	**61**	0 – 10	3.3	98.9	1.1	37
17		40 – 50	6.1	98.5	1.5	31
18		70 – 80	0.6	99.5	0.5	23
19	**62**	0 – 10	4.4	100	-	53
20		40 – 50	5.7	100	-	41
21		70 – 80	1.3	98.8	1.2	24
22	**63**	0 – 10	0.04	99.3	0.7	55
23		40 – 50	1.4	98.8	1.2	40
24		70 – 80	1.1	98.3	1.7	43

[a]General Conditions: Time = 15 min; 10 µmol of catalyst precursor; 50 ml toluene; co-catalyst: $EtAlCl_2$; Al/Pd = 50; pressure = 30 bar, error estimate = ± 0.1, 1-C_4 component is the proportion within the C_4 fraction.. [b]Activity = x 10^2 g(product).mol^{-1}Pd. h^{-1}.

All of the catalysts investigated showed mainly ethylene dimerization (up to 100 % C_4 with **60**/$EtAlCl_2$, Table 3.7 entry 13) and trimerization (up to 1.7 % C_6 with **63**/$EtAlCl_2$, entry 24). Figure 3.17 shows C_4 isomer distribution for the representative catalysts **57**, **61** – **63**/$EtAlCl_2$.

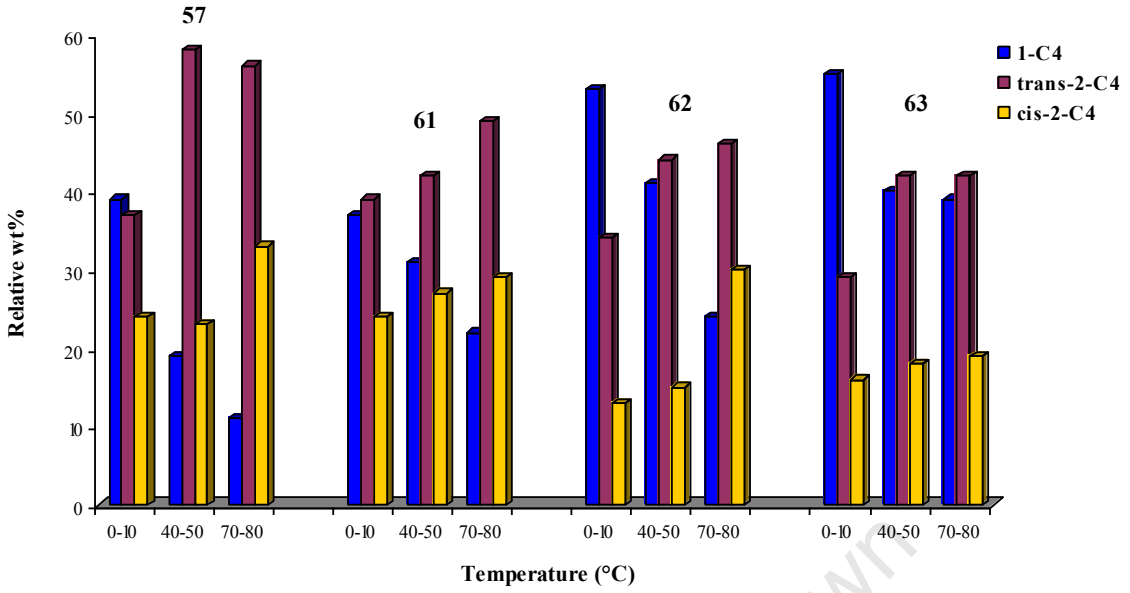

Figure 3.17 *Effect of temperature on C_4 product distribution*

In all cases, high temperatures favoured 1-C_4 double bond isomerization since the selectivity for 1-C_4 gradually decreased with increasing temperature. For instance, at 0 – 10, 40 – 50, and 70 – 80 °C selectivities for 1-C_4 were 39, 19, and 11 % respectively, for catalyst **57**/$EtAlCl_2$ (Table 3.7, entries 4, 5, and 6). Significant decreases in the selectivity for 1-C_4 were observed with the iminophosphine catalysts **57** and **62**/$EtAlCl_2$, (Figure 3.17) and the pyridylimine catalyst **61**/ $EtAlCl_2$, while the selectivity for 1-C_4 with catalyst system **63**/$EtAlCl_2$ remained largely the same at 40 – 50 and 70 - 80°C.

3.2.3.3 The Influence of Reaction Time

This study was aimed at investigating the effect of varying the reaction time on catalytic activity and product distribution. Four reaction times (1, 5, 15, 30 min) were investigated. As was the case with the nickel catalyst systems, the start time was measured when the autoclave was filled with the appropriate pressure of ethylene (working pressure). Ethylene pressure was discontinued at the end of a catalytic run and the autoclave rapidly cooled to -25 – -35 °C before the residual ethylene was vented. Catalysts **56** – **63**/$EtAlCl_2$ proved to have rather short lifetimes as the best catalytic activities, in all cases investigated, were observed when the catalytic reactions were carried out for 1 min. Reactions carried out beyond 1 min showed a gradual decrease in the catalytic activities (Figure 3.18). Increasing the reaction time from 1, 5, 15, to 30 min gave 7.6, 7.1, 6.2, and 4.2 x 10^2 $g.mol^{-1}Pd.h^{-1}$ respectively with catalyst

57/$EtAlCl_2$ (Table 3.8 entries 5, 6, 7, 8). The mode of catalyst deactivation is not clear at this stage since no palladium black was observed in any of the cases investigated.

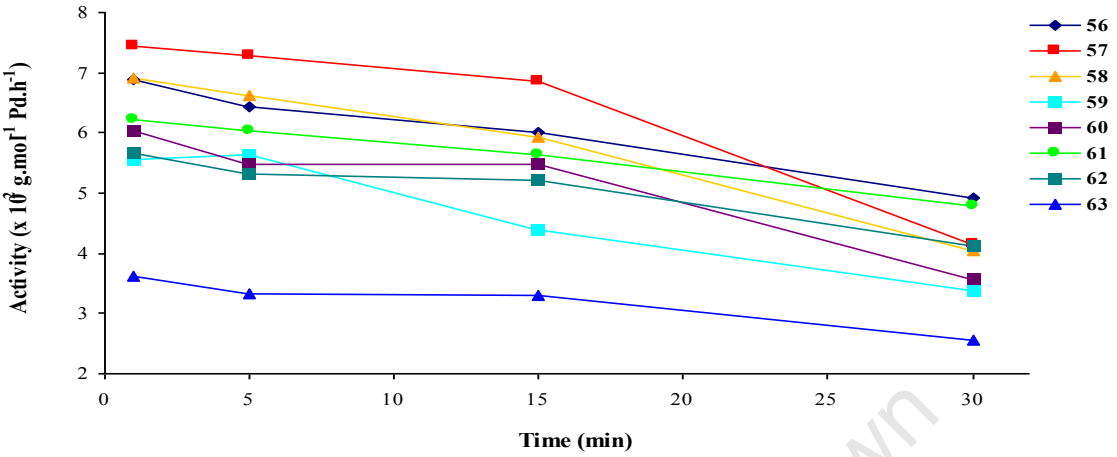

Figure 3.18 *The effect of reaction time on catalytic activity with* ***56*** *–* ***63****/$EtAlCl_2$ catalyst systems*

Selectivities for C_4 up to 99 % were observed with catalyst **62**/$EtAlCl_2$. Increasing the reaction time from 1 to 30 min led to a slight reduction in the amount of C_4 (99.3 and 98.0 at 1 and 30 min respectively with catalyst **56**/$EtAlCl_2$, Table 3.8 entries 1 and 4). All the catalysts investigated followed this trend.

Table 3.8 Influence of reaction time on the catalytic activity with **56** – **63**/$EtAlCl_2$[a]

Entry	Complex	Time (min)	Al/Pd	Activity	Oligomerization (wt %)		
					C_4	C_6	1- C_4
1	**56**	1	50	6. 9	99.3	0.7	45
2		5	50	6.4	99.3	0.7	33
3		15	50	6.0	99.1	1.9	20
4		30	50	4.9	98.0	1.8	19
5	**57**	1	50	7.6	99.5	0.5	36
6		5	50	7.1	99.3	0.7	29
7		15	50	6.2	98.7	1.3	22
8		30	50	4.2	98.5	1.5	15
9	**58**	1	50	6.9	99.3	0.7	43
10		5	50	6.6	98.9	1.1	38
11		15	50	5.9	98.7	1.3	29
12		30	50	4.0	98.1	1.9	21
13	**59**	1	50	5.6	99.0	1.0	33
14		5	50	5.3	99.2	0.8	27
15		15	50	4.3	98.6	1.4	23
16		30	50	3.4	98.4	1.6	20
17	**60**	1	50	6.0	99.2	0.8	37
18		5	50	5.4	99.1	0.9	32
19		15	50	4.1	99.2	0.8	25
20		30	50	3.6	98.8	1.2	16
21	**61**	1	50	6.2	98.1	1.9	37
22		5	50	6.0	98.1	1.9	33
23		15	50	5.7	97.8	2.2	31
24		30	50	4.8	97.5	2.5	23
25	**62**	1	50	5.7	99.5	0.5	44
26		5	50	5.3	99.3	0.7	38
27		15	50	5.2	99.3	0.7	37
28		30	50	4.1	99.1	0.9	29
29	**63**	1	50	1.6	99.0	1.0	47
30		5	50	1.3	98.8	1.2	40
31		15	50	0.8	98.4	1.6	37
32		30	50	0.5	98.1	1.9	23

[a] General Conditions: Temp = 40 – 50 °C; 10 µmol catalyst precursor; 50 ml toluene; 30 bar, error estimate = ± 0.1, 1-C_4 component is the proportion within the C_4 fraction. [b]Activity = x 10^2 g(product).mol^{-1}Pd.h^{-1}.

The selectivity for 1-C_4 within the C_4 fraction also decreased gradually as the reaction time was increased. For example, the selectivity for 1-C_4 decreased from 43 to 21 % (within 99.3 and 98.1 % C_4 fraction respectively) when the reaction was carried out for 1 and 30 min respectively with catalyst **58**/$EtAlCl_2$ (Table 3.8, entries 9 and 12). As in the previous studies the major components within the C_4 fraction were the 2-C_4 isomers. To illustrate the C_4 isomer distribution with respect to time, representative catalysts **57**, **61**, **62**/$EtAlCl_2$ are shown graphically in Figure. 3.19.

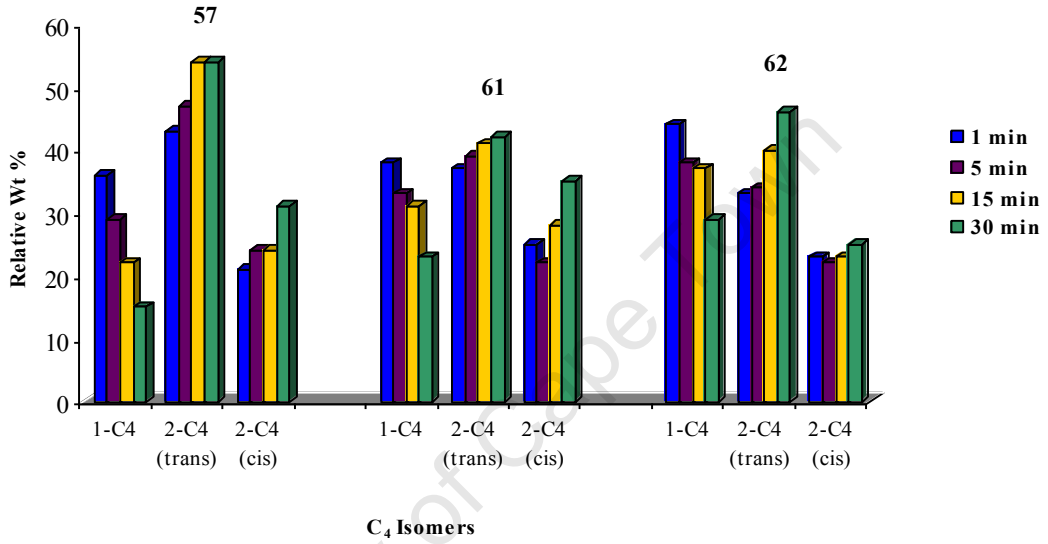

Figure 3.19 *Graphical representation of the effect of time on the C_4 isomer distribution*

3.2.3.4 The Influence of Ethylene Pressure

This study was aimed at investigating the effect of ethylene pressure on catalytic activity and product distribution. It was observed that increasing the ethylene pressure resulted in the improvement of both the catalytic activity and the selectivity (for C_4) for all the catalysts investigated (results in Table 3.9). For example, catalytic activities of 2.5, 6.8, and 7.1 x 10^2 $g.mol^{-1}Pd.h^{-1}$ (Table 3.9, entries 4, 5, 6) were observed when the reactions were carried out at 10, 30, and 50 bar respectively for catalyst **57**/$EtAlCl_2$ (Figure 3.20). The selectivity for the C_4 fraction improved slightly (98.3, 99.1, to 99.7 %) when the ethylene pressure was increased (10, 30, and 50 bar respectively, Table 3.9 entries 4, 5, 6) with catalyst **57**/$EtAlCl_2$. The increase in the catalytic activity at high ethylene pressures could be a result of higher ethylene concentrations in solution (and thus more availability). Consequently, the amount of C_4 would increase by virtue of the catalysts being ethylene dimerization catalysts.

The catalysts bearing diphenylphosphinoimine ligands (**56** – **60**/$EtAlCl_2$) displayed the best catalytic activities (2.5 – 7.7 x 10^2 $g.mol^{-1}Pd.h^{-1}$), while the di-*tert*-butylphosphinoamine analogue (**62**/$EtAlCl_2$) exhibited lower catalytic activities of 1.8 and 4.8 x 10^2 $g.mol^{-1}Pd.h^{-1}$ at 10 and 50 bar respectively (Table 3.9, entries 19 and 21). This could be a result of the reduced electrophilicity of the active center caused by the more electron donating di-*tert*-butylphosphine group in catalyst **62**/$EtAlCl_2$. Even lower catalytic activities were observed with **63**/$EtAlCl_2$ bearing the phenoxyimine ligand (0.8 and 2.1 x 10^2 $g.mol^{-1}Pd.h^{-1}$ at 10 and 50 bar respectively, Figure 3.20 and Table 3.9 entries 22 and 24) presumably due to the presence of the PPh_3 group which might be strongly bound to the active center, thereby limiting coordination of ethylene.

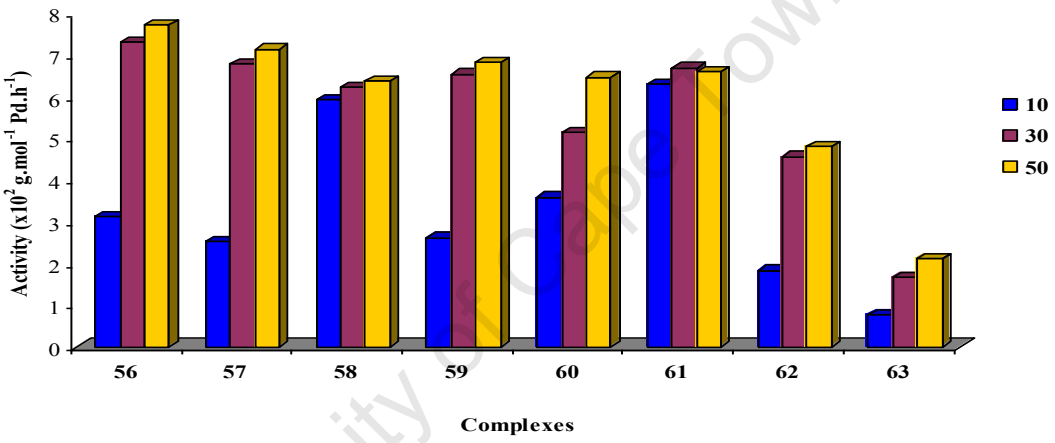

Figure 3.20 *Effect of ethylene pressure on catalytic activity with catalysts* ***56*** *–* ***63****/*$EtAlCl_2$

Table 3.9 Influence of pressure and catalyst concentration on ethylene oligomerization with complexes **56** – **63**[a]

Entry	Complex	Pressure	Al/Pd	Activity[b]	Oligomerization (wt %)		
					C_4	C_6	1-C_4
1	**56**	10	50	3.1	98.1	1.9	33
2		30	50	7.3	98.9	1.1	39
3		50	50	7.7	99.6	2.3	44
4	**57**	10	50	2.5	98.6	1.4	28
5		30	50	6.8	99.1	0.9	33
6		50	50	7.1	99.7	0.3	37
7	**58**	10	50	5.9	98.9	1.1	36
8		30	50	6.2	99.4	0.6	42
9		50	50	6.4	99.3	0.5	43
10	**59**	10	50	2.6	98.3	1.7	26
11		30	50	6.5	98.8	1.2	36
12		50	50	6.8	99.6	0.4	42
13	**60**	10	50	3.6	99.0	1.0	31
14		30	50	5.1	99.3	0.7	39
15		50	50	6.5	100	-	45
16	**61**	10	50	6.3	98.4	1.6	34
17		30	50	6.7	98.4	1.6	36
18		50	50	6.6	99.3	0.7	41
19	**62**	10	50	1.8	98.1	1.9	38
20		30	50	4.6	99.2	0.8	45
21		50	50	4.8	99.5	0.5	45
22	**63**	10	50	0.8	100	-	41
23		30	50	1.6	100	-	44
24		50	50	2.1	100	-	48

[a]General Conditions: Temp = 40 – 50 °C, time = 5 min, 5 µmol of catalyst precursor, 50ml toluene, error estimate = ± 0.1, 1-C_4 component is the proportion within the C_4 fraction. Activity[b] = x 10^3 g(product).mol^{-1}Pd.h^{-1}.

The graphical representation below (Figure 3.21) illustrates the effect of ethylene pressure on the C_4 isomer distribution with the representative catalysts **57**, **61**, **62**/$EtAlCl_2$. The 1-C_4 component within the C_4 fraction was observed to increase gradually as the ethylene pressure was increased from 10 to 50 bar. For example, the amount of 1-C_4 increased from 28 % within the C_4 fraction (98.6 %) to 37 % (within 99.7 % C_4) at 10 and 50 bar respectively with the **57**/$EtAlCl_2$ catalyst system (Table 3.9, entries 4 and 6). The reason for the increase in the selectivity of 1-C_4 at high ethylene pressures is believed to be due to the competition between

chain transfer and chain isomerization [8b]. Thus at high ethylene concentrations formation of 1-C_4 could be favoured due to rapid chain transfer versus chain isomerization.

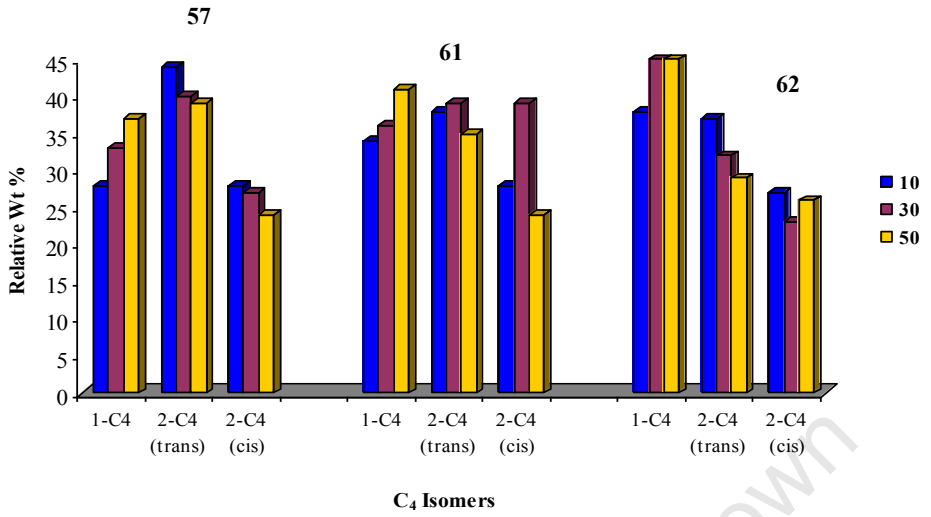

Figure 3.21 *Graphical representation of the effect of ethylene pressure on the C_4 isomer distribution of catalysts **57**, **61**, and **62**/$EtAlCl_2$*

3.2.4 Catalytic Oligomerization of 1-Hexene

In the preliminary investigations of 1-hexene (1-C_6) oligomerization, an intriguing observation was the high catalytic activities displayed by the iminophosphine palladium catalysts systems **56** – **59**/$EtAlCl_2$ in contrast to the poor catalytic activities observed in the oligomerization ethylene. The catalytic reactions were carried out in a Schlenk tube. The iminophosphine catalyst precursors (**56** – **59**) were suspended in the solvent (toluene or methylcyclohexane, *ca.* 5 ml), and this was followed by addition of the co-catalyst ($EtAlCl_2$, Al/Pd = 8, 16, 20). Upon addition of the co-catalyst, the yellow suspension due to the catalyst precursor went into solution, presumably due to formation of the active catalyst. To this mixture was immediately added 1-C_6 (5 ml) resulting in a slight exotherm.

The investigation of the effect of varying the co-catalyst molar ratio on the catalytic activity was carried out with catalysts **56** – **59**/$EtAlCl_2$ for 5 min at room temperature. The catalyst lifetime was probed by adding 5 ml of 1-C_6 at different time intervals. The first addition of 1-C_6 (5 ml) was introduced immediately after the addition of the co-catalyst and was stirred for 5 min (cycle 1). A sample was then collected and a further 5 ml 1-C_6 was added. The reaction mixture was stirred for another 3 min (cycle 2), i.e. 8 min total time, at which time

another sample was collected. This was followed by a third addition of 1-C_6 and stirring for a further 3 min, i.e. 11 min total (cycle 3). Only 76, 89, 82, and 93 % of the 1-C_6 added in the third cycle was converted for catalysts **56** – **59**/$EtAlCl_2$. Thus a fourth cycle was not investigated. The catalytic reaction carried out in toluene and methylcyclohexane (MeCy) yielded comparable catalytic activities. Thus, all subsequent 1-C_6 catalytic investigations were carried out in toluene. For example, catalytic activities of 2.2 and 1.9 x 10^6 $g.mol^{-1}Pd.h^{-1}$ were observed in toluene and methylcyclohexane respectively with catalyst **56**/$EtAlCl_2$ (Table 3.10, entries 3 and 4). Relatively low co-catalyst molar ratios were required (Al/Pd = 8 – 20, Figure 3.22), compared to those employed in ethylene oligomerization (Al/Pd = 50).

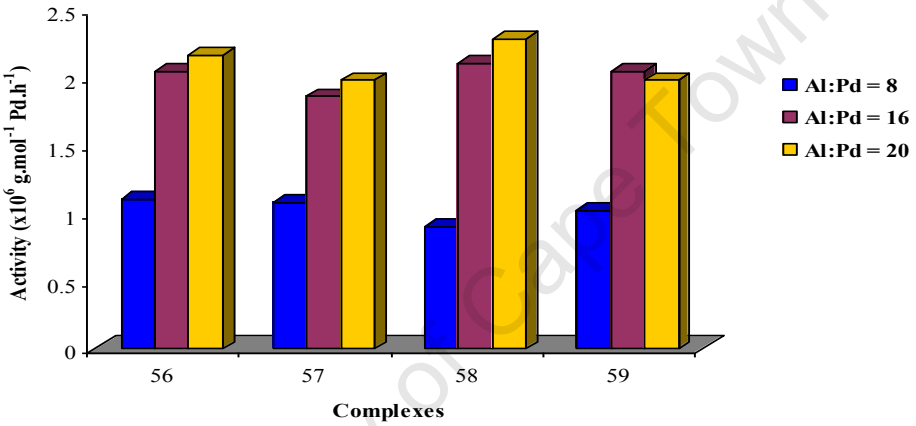

Figure 3.22 *Effect of co-catalyst concentration on catalytic activity with* ***56*** *–* ***59****/$EtAlCl_2$ catalysts for 1-hexene oligomerization*

A lower catalytic activity of 1.1 x 10^6 $g.mol^{-1}Pd.h^{-1}$ (**56**/$EtAlCl_2$, Table 3.10, entry 1) was observed when a lower co-catalyst molar ratio (Al/Pd = 8) was employed, while Al/Pd molar ratios of 16 and 20 gave comparable catalytic activities (2.0 and 2.2 x 10^6 $g.mol^{-1}Pd.h^{-1}$ Table 3.10, entries 2 and 3), suggesting that the molar ratio Al/Pd ≈ 16 was sufficient to achieve optimum activation of the catalyst precursor. Only 1-C_6 dimerization and trimerization products were observed from the GC analyses. The lower catalytic activities observed at lower molar ratios (e.g. Al/Pd = 8) could be due to incomplete or slow activation of the catalyst precursors.

Table 3.10 1-Hexene oligomerization with catalyst systems **56** – **59**/$EtAlCl_2$[a]

Entry	Complex	Al/Pd	Solvent	Time (min)	Cycles[b]	Conversion (wt %)	Yield (g)	Activity[c]
1	**56**	8	Toluene	5	1	54	1.8	1.1
2		16	Toluene	5	1	100	3.4	2.0
3		20	Toluene	5	1	100	3.6	2.2
4		20	MeCy	5	1	100	3.2	1.9
5		20	Toluene	8	2	100	7.2	2.7
6		20	Toluene	11	3	76	8.5	2.1
7	**57**	8	Toluene	5	1	34	1.80	1.1
8		16	Toluene	5	1	100	3.1	1.9
9		20	Toluene	5	1	100	3.3	1.9
10		20	MeCy	5	1	100	3.5	2.1
11		20	Toluene	8	2	100	6.5	2.0
12		20	Toluene	11	3	89	8.9	2.2
13	**58**	8	Toluene	5	1	44	1.5	0.9
14		16	Toluene	5	1	100	3.5	2.1
15		20	Toluene	5	1	100	3.8	2.2
16		20	MeCy	5	1	100	3.6	2.2
17		20	Toluene	8	2	100	6.9	2.1
18		20	Toluene	11	3	82	9.5	2.4
19	**59**	8	Toluene	5	1	51	1.7	1.0
20		16	Toluene	5	1	100	3.4	2.0
21		20	Toluene	5	1	100	3.3	2.0
22		20	MeCy	5	1	100	3.6	2.2
23		20	Toluene	8	2	100	7.1	2.1
24		20	Toluene	11	3	93	8.8	2.2

[a]General Conditions: Temp = 40 – 50 °C; 20 μmol catalyst precursor; 5 ml Toluene, error estimate = ± 0.1. [b]each cycle = 5 ml. [c]Activity = $x10^6$ g(product).mol^{-1}Pd.h^{-1}.

3.2.5 Catalytic Ethylene Oligomerization with Cationic Palladium Complexes

A number of cationic iminophosphine palladium complexes (**64** – **74**, Figure 3.23) were investigated as catalysts in ethylene oligomerization. Owing to their cationic nature, these complexes were used as catalysts in ethylene oligomerization without activation by a co-catalyst. Reaction conditions, such as the reaction temperature, reaction time and ethylene

pressure were varied and their effect on the catalysis was studied. The catalysts employed in the investigations are shown in Figure 3.23.

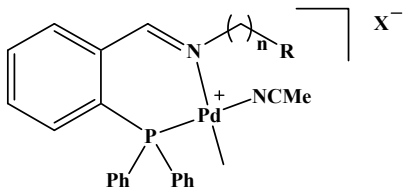

	X	n	R
64	BF_4	1	2-furyl
65	PF_6	1	2-furyl
66	BAr^F_4	1	2-furyl
67	BF_4	1	2-thiophenyl
68	PF_6	1	2-thiophenyl
69	BAr^F_4	2	2-thiophenyl
70	BF_4	2	2-thiophenyl
71	PF_6	2	2-thiophenyl
72	BF_4	2	Ph
73	PF_6	2	Ph
74	BAr^F_4	2	Ph

Figure 3.23 *Palladium single component catalysts*

The cationic complexes above have the vacant site stabilized by a fairly weakly coordinating acetonitrile (NCMe) ligand and a counterion. Complexes bearing different counterions (BF_4^-, PF_6^-, $BAr^F_4^-$, Ar^F = 3,5-$C_6H_3(CF_3)_2$) were prepared in order to explore the effect of the counterion under different reaction conditions. In general, the cationic palladium complexes displayed very low catalytic activities and a wider product distribution compared to the neutral palladium catalysts after activation with co-catalysts.

3.2.5.1 The Influence of Temperature

The effect of temperature on ethylene oligomerization was explored with catalysts **64** – **74**. The details of this study are presented in Table 3.11 and represented graphically in Figure 3.23. As before reaction temperatures of 0 – 10, 40 – 50, and 70 – 80 °C were investigated. The cationic palladium complexes gave even lower catalytic activities than did the neutral palladium catalysts (up to 31.3 $g.mol^{-1}Pd.h^{-1}$ with **65**, Table 3.11 entry 5).

As with the nickel catalysts and the neutral palladium catalysts discussed earlier (section 3.2.2 and section 3.2.3 respectively), increasing the reaction temperature from 0 – 10 to 40 – 50 °C resulted in an improvement in the catalytic activity, while further increase in temperature to 70 – 80 °C resulted in a decline in the catalytic activity. For example, catalyst **69** showed an increase in catalytic activity from 11.4 to 57.2 $g.mol^{-1}Pd.h^{-1}$ at 0 – 10 and 40 – 50 °C respectively (Table 3.11, entries 16 and 17) and a decline to 21.9 $g.mol^{-1}Pd.h^{-1}$ at 70 – 80 °C (Table 3.11, entry 18). This trend was followed by all catalysts investigated (Figure 3.24).

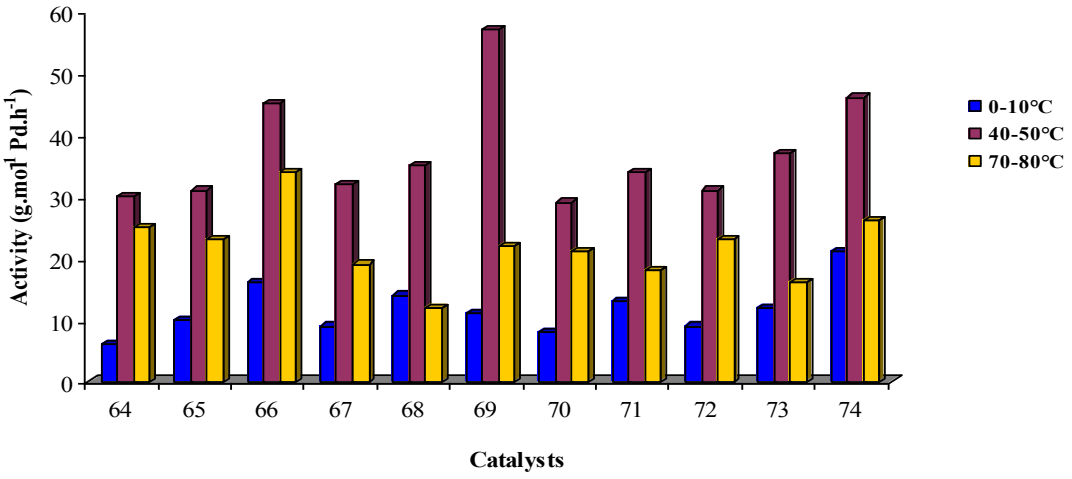

Figure 3.24 *Influence of temperature on catalytic activity with complexes* ***64*** *–* ***74***

In general, a slight influence of the counterion was observed. To a large extent the BF_4^- and PF_6^- counter ions did not have an appreciable influence on the catalytic activity, while a significant improvement in the catalytic activity was observed with $BAr^F{}_4^-$. For instance, at 40 – 50 °C catalytic activities of 39.3, 35.0, 57.2 g.mol^{-1}Pd.h^{-1} (Table 3.11, entries 11, 14, and 17 respectively) were observed with catalysts **67**, **68**, **69** bearing BF_4^-, PF_6^- and $BAr^F{}_4^-$ respectively. This could be due the better stabilization of the catalyst active center by the bulky $BAr^F{}_4^-$ relative to BF_4^- and PF_6^-.

Table 3.11 Influence of temperature on ethylene oligomerization with complexes **64** – **74**[a]

Entry	Complexes	Temp. (°C)	Activity[b]	Oligomerization (wt %)				
				C_4	C_5	C_6	C_7	1-C_4
1	**64**	0 - 10	6.7	66.3	8.2	22.9	2.6	81
2		40 -50	30.3	87.2	-	12.8	-	53
3		70 - 80	25.0	72.6	-	27.4	-	32
4	**65**	0 - 10	10.5	72.3	9.6	14.5	3.6	86
5		40 -50	31.3	89.5	-	10.5	-	46
6		70 - 80	23.8	91.4	-	8.6	-	41
7	**66**	0 - 10	16.5	88.6	-	11.4	-	74
8		40 -50	45.4	95.1	-	4.9	-	43
9		70 - 80	34.9	93.7	-	6.3	-	42
10	**67**	0 - 10	9.8	58.3	12.1	26.2	3.4	84
11		40 -50	35.1	85.5	-	14.5	-	40
12		70 - 80	19.4	73.5	-	22.9	-	38
13	**68**	0 - 10	14.7	77.1	4.3	17.7	0.9	87
14		40 -50	36.4	93.3	-	6.7	-	45
15		70 - 80	12.2	81.5	0.5	17.2	0.8	47
16	**69**	0 - 10	11.4	67.2	12.5	18.1	5.2	88
17		40 -50	29.3	96.6	-	3.4	-	43
18		70 - 80	21.9	85.6	-	14.4	-	41
19	**70**	0 - 10	8.7	63.3	13.1	17.3	6.3	92
20		40 -50	31.1	87.2	-	12.8	-	63
21		70 - 80	21.5	76.4	-	23.6	-	44
22	**71**	0 - 10	13.3	53.6	8.8	35.3	2.3	63
23		40 -50	52.2	78.5	-	21.5	-	47
24		70 - 80	18.4	77.2	-	22.8	-	45
25	**72**	0 - 10	9.0	45.7	19.5	29.5	5.3	96
26		40 -50	31.2	83.9	-	16.1	-	38
27		70 - 80	23.4	71.5	-	28.5	-	36
28	**73**	0 - 10	12.1	56.3	10.7	30.8	2.2	89
28		40 -50	37.4	85.8	-	14.2	-	44
29		70 – 80	16.2	70.2	-	29.8	-	45
30	**74**	0 - 10	21.1	72.7	-	27.3	-	65
31		40 -50	46.0	84.3	-	15.7	-	41
32		70 - 80	26.3	80.6	-	19.4	-	38

[a]General Conditions: 20 μmol catalyst; 50 ml toluene; Pressure = 30 bar; Time = 15min, error estimate = ± 0.1, 1-C_4 component is the proportion within the C_4 fraction. [b]Activity = g.mol^{-1}Pd. h^{-1}.

Compared to the neutral nickel and palladium catalysts discussed before, the cationic palladium catalysts gave low selectivities for the C_4 fraction, as low as 63 % with catalyst **71** (Table 3.11, entry 22). The lower catalytic activities observed for the cationic palladium catalysts could imply that the co-catalyst employed in the case of the neutral counterparts may have played an important role in stabilizing the catalyst. In addition, the low catalytic activities could be due to the stronger interaction between acetonitrile and palladium, which in turn would reduce the rate of acetonitrile displacement by ethylene. In order to probe this, the ether (-Et_2O) coordinated analogue of the cationic palladium catalyst **64** was prepared *in situ* and used for comparison. This complex was obtained from a reaction of the palladium methylchloride complex (**53**) in DCM and $AgBF_4$ in Et_2O at 0 °C for 30 min, followed by filtration of AgCl. The resulting solution was then added to 45 mL DCM in the autoclave. The autoclave was filled with an appropriate amount of ethylene and the stirring was continued for the required time. However, no appreciable improvement in the catalytic activity was observed with this catalyst system. A plausible reason for the lower catalytic activities observed with the cationic complexes could be the competition for coordination by the weakly coordinating ligands (Et_2O and acetonitrile) and ethylene. A similar observation was noted by Brookhart *et al.* with the α-diimine catalyst system [13a]. In addition, Brookhart *et al.* and others have shown that palladium catalysts have higher insertion barriers, which could explain the low catalytic activities observed relative to the nickel counterparts which have lower insertion barriers [13].

Odd-numbered carbon oligomers (C_5 and C_7) were detected, possibly due to the very low catalytic activities (6.7 – 14.7 $g.mol^{-1}Pd.h^{-1}$) displayed by these catalysts. This assumption is supported by the detection of more odd-numbered carbon oligomers with catalysts that displayed the least catalytic activity. For instance, at 0 – 10 °C catalyst **70** gave a catalytic activity of 8.7 $g.mol^{-1}Pd.\ h^{-1}$ with C_5 and C_7 selectivities of 13 and 6.3 % respectively (Table 3.11, entry 19). These odd-numbered carbon oligomers originate from the insertion of two or three molecules of ethylene into the Pd-C bond of the starting Pd-Me complex [1c].

The selectivity for 1-C_4 within the C_4 fraction was observed to be higher at lower temperatures, which may imply that double bond isomerization is favoured at high temperatures. For instance, catalyst **64** gave selectivities of 81, 53, and 32 % at 0 – 10, 40 – 50, and 70 – 80 °C respectively (Table 3.11, entries 1 – 3). In contrast to the neutral

palladium catalysts that gave 2-C_4 as a major component within the C_4 fraction in all cases investigated, the single component **64** – **74** gave 1-C_4 as the major component within the C_4 fraction. Figure 3.25 shows the relative weight percentages of the C_4 isomers for the representative catalysts **64** – **69**. The figure illustrates a significant influence of temperature on the selectivity of 1-C_4. It can be seen that high temperatures favour 1-C_4 isomerization. This could be due to increased rates of 1-C_4 reinsertion at high temperatures.

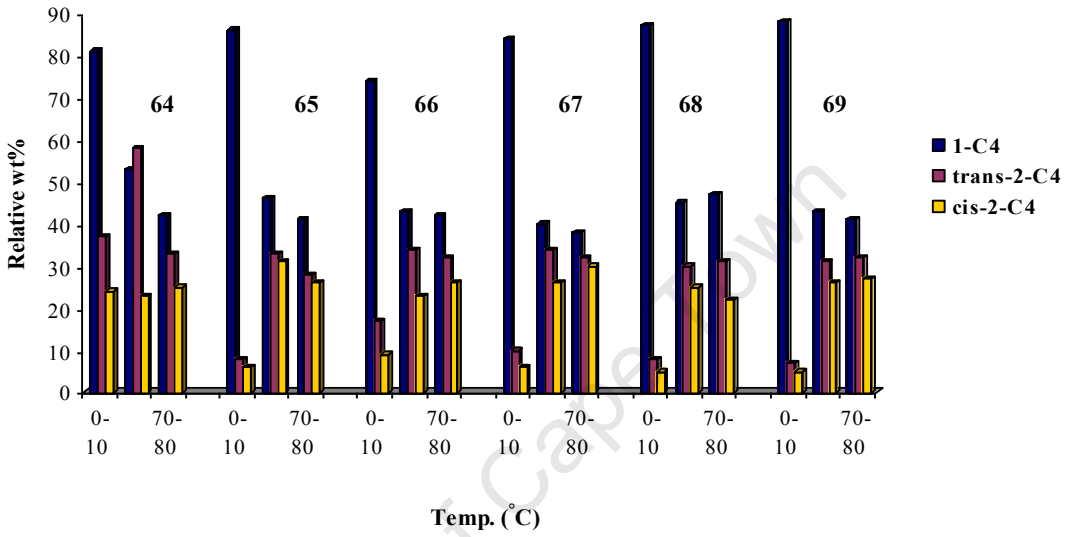

Figure 3.25 *Influence of temperature on the relative wt % of the C_4 fraction with catalysts **64** – **69***

3.2.5.2 The Influence of Reaction Time

The effect of time (1, 5, 15, 30 min) on ethylene oligomerization was explored with catalysts **64** – **71** at 30 bar ethylene and 40 – 50 ºC. The details of this study are presented in Table 3.12 and represented graphically in Figure 3.26.

As was the case with the neutral palladium catalysts, the cationic catalysts (**64** – **71**) proved to have very short lifetimes. The catalytic activities peaked when the catalytic reactions were carried out for 5 min, with the catalytic activity declining when the reaction was carried out at longer reaction times. For example, activities of 9.3, 35.2, 12.4, and 7.2 $g.mol^{-1}Pd.h^{-1}$ were observed when the catalytic reactions were carried out for 1, 5, 15, and 30 min respectively with catalyst **65** (Table 3.12, entries 5 – 8). This trend was also followed by catalysts **64**, **66** – **74** (Figure 3.26).

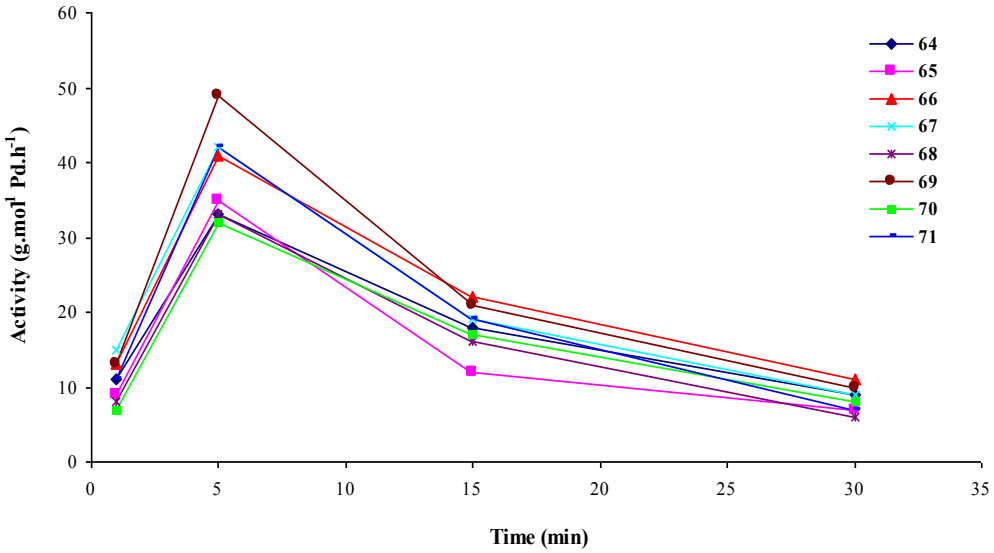

Figure 3.26 *The effect of reaction time on catalytic activity with catalysts* ***64*** *–****71****/EtAlCl$_2$*

In all the cases investigated lower catalytic activities were observed when the catalytic reactions were carried out for 1 min. Sharp increases in the catalytic activities were observed when the reactions were carried out for 5 min. However, increasing the reaction time to 15 and 30 min respectively led to a gradual decline in the catalytic activities (Figure 3.26). Thus, the maximum percentage of the C_4 was observed when the catalytic reactions were carried out for 5 min. For example, selectivities of 47.4, 92.2, 57.8, and 48.3 % for C_4 with catalytic activities of 9.7, 35.2, 12.4, and 7.2 g.mol^{-1}Pd.h^{-1} (Table 3.12, entries 5, 6, 7, 8) were observed for catalyst **65** when the reactions were carried out for 1, 5, 15, and 30 min. The reason for the lower catalytic activities observed at longer reaction times could be that the catalysts were deactivated within the first 5 min of the catalytic reaction. The mode of catalyst deactivation is not yet clear since no palladium black was detected in all cases investigated.

Table 3.12 Influence of time on ethylene oligomerization with complexes **64** – **71**[a]

Entry	Complexes	Time (min)	Activity[b]	Oligomerization (wt %)				
				C_4	C_5	C_6	C_7	1-C_4
1	**64**	1	11.2	53.2	9.6	30.6	6.6	82
2		5	33.4	83.4	-	16.6	-	66
3		15	18.1	77.4	-	22.6	-	56
4		30	9.4	41.8	18.9	30.9	8.4	28
5	**65**	1	9.3	47.4	15.3	29.4	7.9	73
6		5	35.2	92.2	-	7.8	-	52
7		15	12.4	57.8	9.5	28.5	4.2	45
8		30	7.2	48.3	20.5	23.3	7.4	31
9	**66**	1	13.8	59.4	8.4	29.5	2.7	85
10		5	41.3	92.9	-	7.1	-	57
11		15	22.5	87.7	-	12.3	-	38
12		30	11.6	58.2	7.6	31.8	2.4	41
13	**67**	1	15.9	88.3	-	11.7	-	64
14		5	42.4	86.2	-	13.8	-	47
15		15	19.6	83.4	-	16.6	-	42
16		30	9.8	47.6	19.5	23.6	9.3	33
17	**68**	1	8.6	42.7	18.7	30.0	8.6	79
18		5	33.3	90.1	-	9.9	-	69
19		15	16.2	86.6	-	14.4	-	41
20		30	6.5	44.2	17.6	28.7	9.5	37
21	**69**	1	13.4	76.4	-	23.6	-	78
22		5	49.6	97.2	-	2.8	-	57
23		15	21.2	88.7	-	11.3	-	44
24		30	10.8	47.7	11.8	38.1	2.4	41
25	**70**	1	7.5	42.3	19.6	28.7	9.4	84
26		5	32.7	85.8	-	14.2	-	42
27		15	17.3	87.3	-	12.7	-	58
28		30	8.9	47.5	15.9	29.9	6.7	38
28	**71**	1	11.3	52.6	7.4	37.8	2.2	83
29		5	42.2	72.4	-	27.6	-	62
30		15	19.4	83.3	-	16.7	-	48
31		30	7.6	45.6	18.5	30.6	5.3	43

[a]General Conditions: 20 μmol catalyst; 50 ml toluene; Pressure = 30bar; °C; Temp = 40 - 50 C, error estimate = ± 0.1, 1-C_4 component is the proportion within the C_4 fraction. [b]Activity = g(product).mol^{-1}Pd.h^{-1}.

The decline in the amount of C_4 observed with increasing reaction time was accompanied by a gradual decline in the selectivity for 1-C_4 within the C_4 fraction. For example, 1-C_4 selectivities of 73, 52, 45, and 31 % within 47.4, 92.2, 57.8, and 48.3 % C_4 fractions respectively (Table 3.12, entries 5 – 7) were observed with catalyst **65**. In all the cases investigated, 1-C_4 was the major component within the C_4 fraction when the catalytic reactions were carried out for 1 – 15 min. Figure 3.27 describes the trend followed by the representative catalysts **64**, **65**, and **66** bearing BF_4^-, PF_6^-, and $BAr^F{}_4^-$ respectively as counterions. Largely all catalysts displayed a similar C_4 isomer product distribution. The only dissimilarity was observed when the reactions were carried out for 30 min with catalysts **64** and **65** bearing BF_4^- and PF_6^-, where 1-C_4 was not the major component within the C_4 fraction.

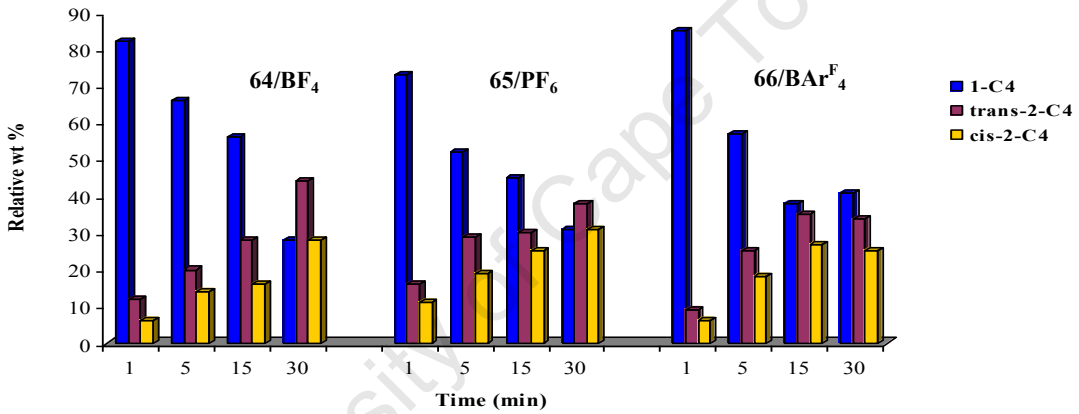

Figure 3.27 *Influence of time on the relative wt % of the C_4 fraction with catalysts **64**, **65**, and **66***

3.2.5.3 The Influence of Pressure

To investigate the effect of ethylene pressure on the catalytic activity and product distribution, catalytic reactions were carried out at 10, 30, or 50 bar. In each case, increasing the ethylene pressure resulted in a gradual increase in both the catalytic activity (Figure 3.28) and selectivity for C_4. For example, a significant increase in the catalytic activity was observed when the catalytic reaction was carried out at 30 bar (43.6 $g.mol^{-1}Pd.h^{-1}$, Table 3.13, entry 8) compared to 10 bar (15.6 $g.mol^{-1}Pd.h^{-1}$, Table 3.13, entry 7) with catalyst **66**. Further increasing the pressure to 50 bar resulted in a slight improvement in the catalytic activity (46.1 $g.mol^{-1}Pd.h^{-1}$, Table 3.13, entry 9). This trend is shown graphically in Figure 3.28 for the catalysts (**64 – 74**) and was observed for all the catalysts investigated.

Table 3.13 Influence of pressure on ethylene oligomerization with complexes **64** – **74**[a]

Entry	Complex	Pressure (bar)	Activity[b]	Oligomerization (wt %)				
				C_4	C_5	C_6	C_7	1-C_4
1	**64**	10	19.8	82.4	-	17.4	-	53.5
2		30	37.2	79.5	-	20.5	-	69.3
3		50	39.7	91.2	-	8.8	-	71.2
4	**65**	10	22.3	81.3	-	18.7	-	53.0
5		30	38.7	88.3	-	11.7	-	54.5
6		50	37.9	90.6	-	9.6	-	56.3
7	**66**	10	15.6	76.9	1.6	20.6	0.89	39.6
8		30	43.6	84.4	-	15.6	-	45.7
9		50	46.1	87.3	-	12.7	-	51.2
10	**67**	10	16.6	72.4	4.7	21.8	1.1	32.4
11		30	34.6	88.8	-	11.2	-	46.1
12		50	37.3	92.6	-	8.4	-	47.5
13	**68**	10	17.3	84.0	-	16.0	-	37.5
14		30	35.4	92.1	-	7.9	-	64.1
15		50	35.6	94.5	-	5.5	-	64.8
16	**69**	10	16.3	82.3	-	17.7	-	42.8
17		30	47.6	87.5	-	9.5	-	55.9
18		50	48.9	91.7	-	8.3	-	58.9
19	**70**	10	18.1	76.6	-	23.4	-	35.6
20		30	34.6	83.1	-	16.9	-	43.7
21		50	34.7	87.1	-	12.9	-	43.9
22	**71**	10	20.2	73.1	-	26.9	-	41.0
23		30	41.5	74.6	-	25.4	-	58.9
24		50	42.1	85.3	-	14.7	-	64.1
25	**72**	10	18.4	80.2	-	19.8	-	32.7
26		30	31.3	81.5	-	18.5	-	54.2
27		50	33.8	87.8	-	15.2	-	58.8
28	**73**	10	17.7	76.4	-	23.6	-	29.0
29		30	38.4	86.7	-	13.3	-	62.6
30		50	37.8	88.3	-	11.7	-	63.4
31	**74**	10	21.3	78.9	-	21.1	-	41.3
32		30	46.2	80.4	-	14.6	-	63.3
33		50	48.3	86.0	-	12.1	-	64.6

[a]General Conditions: 20 µmol catalyst; 50 ml toluene; Time = 5 min; °C; Temp = 40 - 50 C, error estimate = ± 0.1, 1-C_4 component is the proportion within the C_4 fraction. [b]Activity = g(product).mol^{-1}Pd. h^{-1}.

In general, catalysts bearing the $BAr^{F}_{4}^{-}$ counterion (**66**, **69**, and **74**) displayed slightly enhanced catalytic activities compared to those bearing BF_4^- (**64**, **66**, **70**, and **72**) and PF_6^- (**65**, **67**, **70**, and **73**), as shown in Figure 3.28.

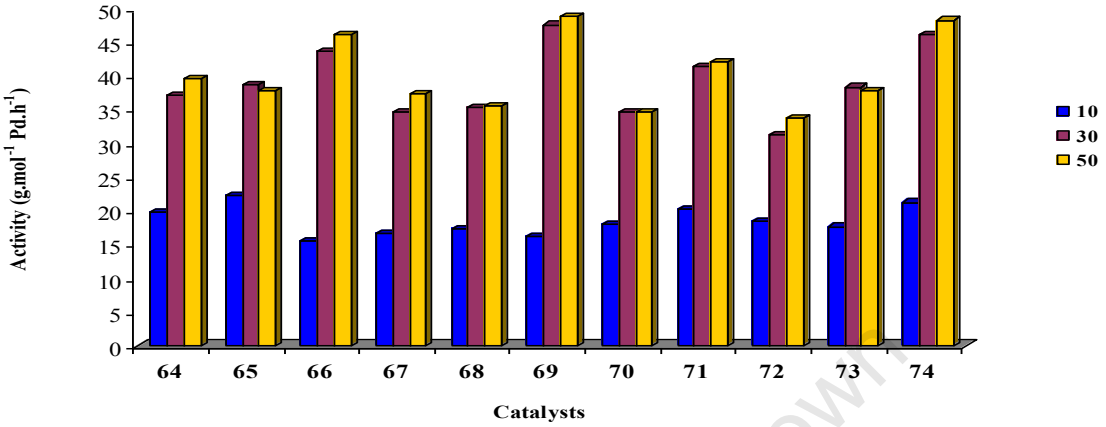

Figure 3.28 *Influence of pressure on the catalytic activity with* ***64 – 74***

The selectivity for 1-C_4 within the C_4 fraction was also observed to increase upon increasing the ethylene pressure. For example, selectivities of 39.6, 45.7, and 51.2 % for 1-C_4 within the C_4 fraction (76.9, 84.4, and 87.3 %) were observed at 10, 30, and 50 bar respectively with catalyst **66 (**Table 3.13, entry 7, 8, 9). The catalytic reactions carried out at 50 bar with catalysts **67**, **68**, and **69** gave C_4 selectivities of 92.6, 94.6, and 91.4 % respectively (Table 3.13, entry 12, 15, 18). Increasing the ethylene pressure also caused significant improvements in the amount of 1-C_4 within the C_4 fraction. For example, selectivities for 1-C_4 of 42.8, 55.9, 58.9 % within 82.3, 87.5, and 91.7 % C_4 fraction respectively were observed for catalyst **69** (Table 3.13, entries 16 – 18). The increase in the amount of 1-C_4 at high ethylene pressures could be due to the high concentrations of ethylene in solution, which in turn retards 1-C_4 reinsertion, and consequently isomerization. This trend is shown graphically in Figure 3.29.

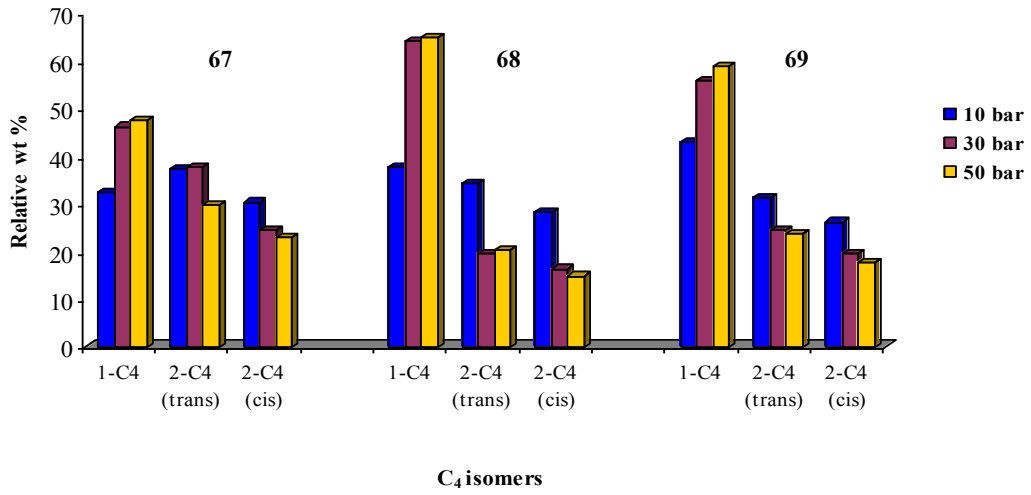

Figure 3.29 *Influence of pressure on the relative wt % of the C_4 components with* ***67*** *–* ***69***

3.2.6 Chromium-Catalyzed Ethylene Oligomerization

A series of neutral iminophosphine (**83** – **87**), and pyridylimine (**88**) chromium catalyst precursor complexes (**83** – **88**, Figure 3.30) were investigated for ethylene oligomerization under various reaction conditions. The effect of changing parameters such as co-catalyst concentration (Al/Cr molar ratio), reaction temperature and ethylene pressure were investigated.

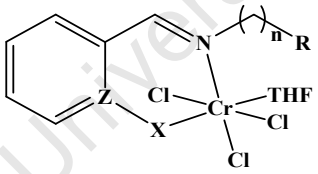

	Z	X	n	R
83	C	PPh_2	1	3-pyridyl
84	C	PPh_2	1	2-furyl
85	C	PPh_2	1	2-thiophenyl
86	C	PPh_2	2	2-thiophenyl
87	C	PPh_2	1	Ph
88	N	.	1	2-furyl

Figure 3.30 *Chromium catalyst precursors employed in the investigations of ethylene oligomerization*

3.2.6.1 The Selection of Co-Catalyst

In this investigation, chromium catalyst precursors **83** – **88** (Figure 3.30) were activated with three co-catalysts (MMAO, $EtAlCl_2$, and $EtAlCl_2$) in an effort of find the most efficient co-catalyst. In this study, the co-catalyst molar ratio (Al/Cr) was varied for each co-catalyst to ascertain the optimum molar ratio (i.e. Al/Cr = 100, 500 and 1000 for MMAO, Al/Cr = 100, 500, for Et_2AlCl, Al/Cr = 50, 100 for $EtAlCl_2$).

In addition, the effect of solvent (toluene or methylcyclohexane (MeCy)) was probed with catalyst precursor **84**. The details of this investigation are given in Table 3.14. The solvent was found to have a marked influence on the catalytic activity, with the reaction in methylcyclohexane (MeCy) yielding better catalytic activities compared to those carried out in toluene. For instance, catalyst **84**/MMAO with Al/Cr = 100 and 500 gave catalytic activities of 3.4 and 3.9 x 10^3 $g.mol^{-1}Cr.h^{-1}$ in toluene (Table 3.14 entries 8 and 9). In methylcyclohexane catalytic activities of 0.9 and 6.2 x 10^3 $g.mol^{-1}Cr.h^{-1}$ were observed (Table 3.14 entries 10 and 11) with the same co-catalyst molar ratios. The increased catalytic activities observed when the catalytic reactions were conducted in methylcyclohexane could be due to the increased solubility of ethylene in methylcyclohexane compared to toluene [14]. The catalytic activity decreased slightly when the co-catalyst molar ratio was increased to 1000 (e.g. 5.1 x 10^3 $g.mol^{-1}Cr.h^{-1}$, for **84**/MMAO, Table 3.14 entry 12). The use of ethylaluminium co-catalysts ($EtAlCl_2$ and Et_2AlCl) largely gave ethylene polymerization catalysts (up to 100 %, Table 3.14 entries 6 and 14). Blum and Sun and co-workers also observed ethylene polymerization or dimerization when ethylaluminium co-catalysts were employed as activators for chromium complexes [15]. The details of these investigations are given in Table 3.14.

Table 3.14 *Influence of co-catalyst and co-catalyst molar ratio on catalytic activity and product distribution for complexes* **83** – **86**[a]

Entry	Complex	Co-catalyst	Al/Cr	Activity[c]	PE (wt %)	Oligomers (wt %)			
						C_4	1-C_4	C_6	1-C_6
1	**83**	MMAO	100	0.2	16.4	7.6	100	76.4	93.1
2		MMAO	500	6.8	49.1	7.8	100	43.1	94.1
3		MMAO	1000	7.2	52.1	7.1	98	40.8	96.4
4		Et_2AlCl	100	0.3	-	100	99	-	-
5		Et_2AlCl	300	1.3	63	37	100	-	-
6		$EtAlCl_2$	50	0.03	100	-	-	-	-
7		$EtAlCl_2$	100	0.5	71.3	28.7	100	-	-
8	**84**	MMAO[b]	100	3.4	46.7	37.3	-	-	-
9		MMAO[b]	500	3.9	57.3	39.3	99.2	3.4	89.6
10		MMAO	100	0.9	58.2	11.8	99.2	30.0	96.2
11		MMAO	500	6.2	63.6	4.9	100	32.3	97.3
12		MMAO	1000	5.1	68.7	8.6	98.4	22.7	97.6
13		Et_2AlCl	100	0.2	35.2	64.8	100	-	-
14		Et_2AlCl	300	0.9	100	-	-	-	-
15		$EtAlCl_2$	50	-	-	-	-	-	-
16		$EtAlCl_2$	100	1.5	88	12	-	-	-
17	**85**	MMAO	100	0.7	14.3	20.1	100	65.6	92.3
18		MMAO	500	8.2	60.8	5.9	100	33.3	97.5
19		MMAO	1000	7.4	62.7	6.1	100	31.2	99.3
20		Et_2AlCl	100	0.09	21.5	78.5	100	-	-
21		Et_2AlCl	300	0.7	73.4	26.6	100	-	-
22		$EtAlCl_2$	50	-	-	-	-	-	-
23		$EtAlCl_2$	100	0.6	86.2	13.8	-	-	-
24	**86**	MMAO	100	3.4	4.3	10.5	100	85.2	98.2
25		MMAO	500	9.1	62.9	6.2	98.3	30.9	98.6
26		MMAO	1000	6.8	100	-	-	-	-
27		Et_2AlCl	100	0.08	100	-	-	-	-
28		Et_2AlCl	300	0.1	100	-	-	-	-
29		$EtAlCl_2$	50	0.03	100	-	-	-	-
30		$EtAlCl_2$	100	0.3	100	-	-	-	-

[a]General conditions: 20 μmol of catalyst precursor; 50 ml methylcyclohexane; [b]toluene; 15 min; 25 °C; 30 bar, error estimate = ± 0.1, 1-C_4 and 1-C_6 components are the proportions within the C_4 and C_6 fractions respectively. [c]Activity = x 10^3 g(product).mol^{-1}Cr.h^{-1}.

For both $EtAlCl_2$ and Et_2AlCl, increasing the co-catalyst concentration resulted in improvements in the catalytic activities. For example, catalytic activities for catalysts

85/Et_2AlCl improved from 0.09 x 10^3 $g.mol^{-1}Cr.h^{-1}$ to 0.7 x 10^3 $g.mol^{-1}Cr.h^{-1}$ at Al/Cr = 100 and 300 respectively (Table 3.14, entries 20 and 21). No catalytic activity was observed when $EtAlCl_2$ molar ratio of Al/Cr = 50 was employed, while Al/Cr = 100 gave 0.6 x 10^3 $g.mol^{-1}Cr.h^{-1}$ with catalyst **85**/$EtAlCl_2$ implying that a molar ratio of Al/Cr = 50 was not sufficient to activate the catalyst precursor (Table 3.14, entries 22 and 23). The results showing the effects of co-catalyst and co-catalyst molar ratio are given in Table 3.14 for catalyst precursors **83** – **86** and are represented graphically in Figure 3.31.

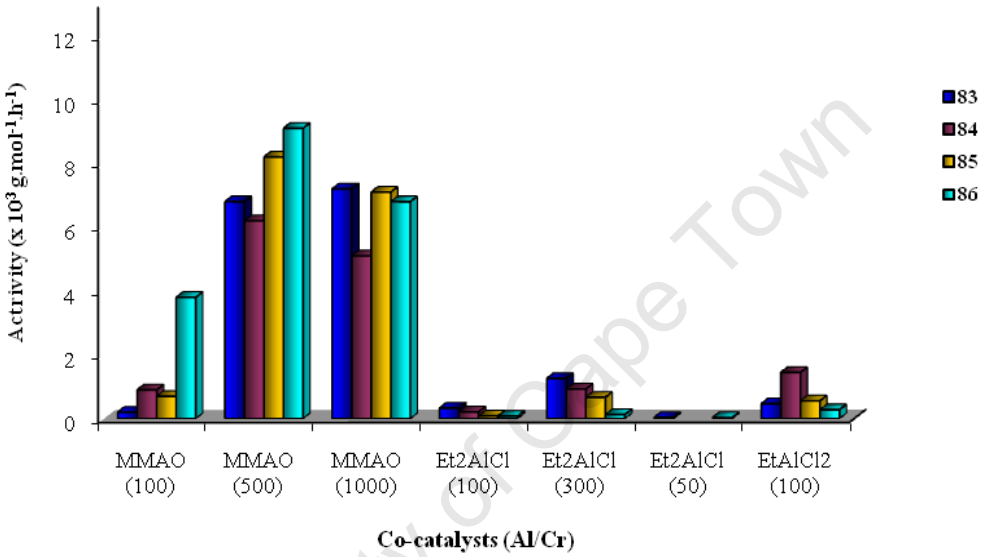

Figure 3.31 *Effect of different co-catalysts on the catalytic activity of complexes* ***83 - 86*** *for ethylene oligomerization*

All the catalysts activated with MMAO gave the best activities (Figure 3.31), thus MMAO was used in subsequent investigations. This is a contrasting result compared to the nickel and palladium catalysts discussed before. However, this behaviour has been noted in the literature [15]. It has been noted in the literature that the catalytic active species for Cr(III) catalyst precursors is the Cr(II) counterpart. Thus, it could be that MMAO was a more efficient reducing agent compared to Et_2AlCl and $EtAlCl_2$ [16].

The reaction product distribution was composed of the oligomer fraction (C_4 and C_6) and polyethylene (Table 3.14). The oligomeric products were mainly α-olefins (92 – 100 %). For example, catalyst **85**/MMAO with Al/Cr = 1000 produced 100 % 1-C_4, and 99.3 % 1-C_6 of the respective fractions. The other products in the case of the C_6 fractions could be cyclic

isomers as discussed in Chapter 1 (section 1.7, pp 37). The high selectivities for α-olefins imply that the reaction proceeds via a metallacyclic pathway [17].

3.2.6.2 Influence of Reaction Temperature

The effect of temperature on ethylene oligomerization was explored with catalysts **83** – **88**/MMAO. The details of this study are presented in Table 3.15 and represented graphically in Figure 3.32. As before, reaction temperature ranges 10 – 20, 40 – 50, and 70 – 80 °C were investigated.

As with the nickel and the neutral palladium catalysts discussed earlier, increasing the reaction temperature ranges from 10 – 20 to 40 – 50 °C led to an improvement in the catalytic activity, whilst a further increase in temperature to 70 – 80 °C resulted in an appreciable decline in the catalytic activity. For example, increasing the reaction temperature from 10 – 20 to 40 – 50 °C with catalyst **83**/MMAO caused a noticeable increase in the catalytic activity (6.6 to 9.2 x 10^3 $g.mol^{-1}Cr.h^{-1}$,Table 3.15 entries 1 and 2). Further increasing the temperature to 70 – 80 °C led to an appreciable decline in the catalytic activity to 6.3 x 10^3 $g.mol^{-1}Cr.h^{-1}$ (Table 3.15, entry 3). The amount of polyethylene produced was observed to increase with increasing reaction temperature. Increases in the amount of polyethylene of 62.0, 67.2, and 86.3 % were observed with catalyst **83**/MMAO at 10 – 20, 40 – 50, and 70 – 80 °C respectively (Table 3.15, entries 1 – 3). This noticeable increase in the amount of polyethylene with increasing reaction temperature was also observed by Blum *et al.* who observed an increase in the amount of polyethylene from 17 to 98 % when the reaction temperature was increased from 24 – 30 to 85 °C [14a]. This observation implies that chain propagation is favoured over chain transfer at higher temperatures. This trend was followed by all catalysts investigated (**83** – **87**), except catalyst **88**/MMAO which showed the best activity at 40 – 50 °C. The details of this investigation are given in Table 3.15 and represented graphically in Figure 3.32.

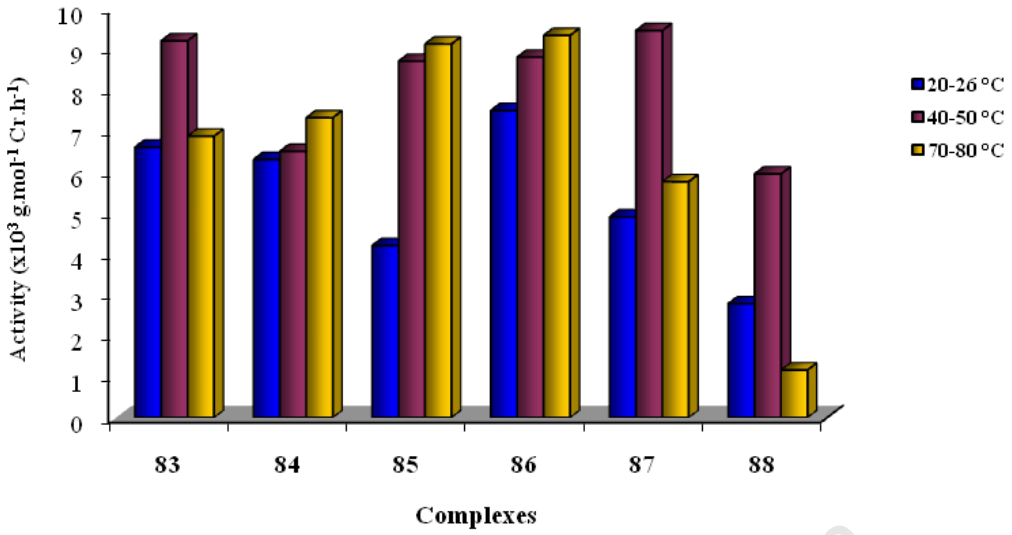

Figure 3.32 *Effect of reaction temperature on catalytic activity with catalysts* ***83*** *–* ***88****/MMAO*

Table 3.15 Influence of temperature on ethylene oligomerization with complexes **83** – **88**/MMAO[a]

Entry	Complex	Temp. (°C)	Activity[b]	PE (wt %)	Oligomers (wt %)			
					C_4	1-C_4	C_6	1-C_6
1	**83**	10 – 20 °C	6.6	62.0	3.1	100	34.9	95
2		40 – 50 °C	9.2	67.2	4.6	97	28.2	96
3		70 – 80°C	6.3	86.3	11.2	98	2.5	98
4	**84**	10 – 20 °C	7.9	54.2	5.3	99	40.5	98
5		40 – 50 °C	7.1	61.2	3.5	99	35.3	97
6		70 – 80°C	7.3	66.2	5.3	98	28.5	97
7	**85**	10 – 20 °C	4.2	61.5	5.9	100	32.6	97
8		40 – 50 °C	8.7	62.6	9.5	98	27.9	98
9		70 – 80°C	9.1	82.4	7.4	100	3.4	98
10	**86**	10 – 20 °C	7.5	69.6	4.5	100	25.9	96
11		40 – 50 °C	8.8	66.8	7.1	99	26.1	97
12		70 – 80°C	9.3	81.6	4.6	100	21.7	98
13	**87**	10 – 20 °C	5.2	62.6	3.7	100	33.6	97
14		40 – 50 °C	9.0	59.0	17.3	100	23.7	98
15		70 – 80°C	5.7	85.2	14.8	100	-	-
16	**88**	10 – 20 °C	2.8	76.6	23.4	98	-	-
17		40 – 50 °C	5.9	75.4	24.6	100	-	-
18		70 – 80°C	1.2	88.3	11.7	100	-	-

General Conditions: [a] 20 µmol catalyst; 50 ml methylcyclohexane; Pressure = 30bar; Time = 15min; Al/Cr = 500, error estimate = ± 0.1, 1-C_4 and 1-C_6 components are the proportions within the C_4 and C_6 fractions respectively. [b]Activity = x 10^3 g(product).mol^{-1}Cr.h^{-1}.

3.2.6.3 Influence of Ethylene Pressure

To investigate the effect of ethylene pressure on the catalytic activity and product distribution, the catalytic reactions were carried out at 10, 30, and 50 bar. In each case, increasing the ethylene pressure resulted in a gradual increase in the catalytic activity. For example, catalytic activities of 5.4, 8.2, and 10.8 x 10^3 g.mol^{-1}Cr.h^{-1} were observed when the ethylene pressure was increased (10, 30, 50 bar respectively) for catalyst **85**/MMAO (Table 3.16 entries 7, 8, and 9). The amount of polyethylene produced in each case was observed to increase with increasing ethylene pressure, suggesting that chain propagation was faster than chain transfer at high ethylene pressures. For example, polyethylene of 62.5, 67.0, and 68.2 % were observed at 10, 30, and 50 bar respectively with **85**/MMAO (Table 3.16, entries 7 – 9). The observed increase in activity and the amount of polyethylene with increasing pressure is in accordance with literature reports [14a, 14b]. All the catalysts investigated followed the above trend. The details of this investigation are shown in Table 3.16 and graphically in Figure 3.33.

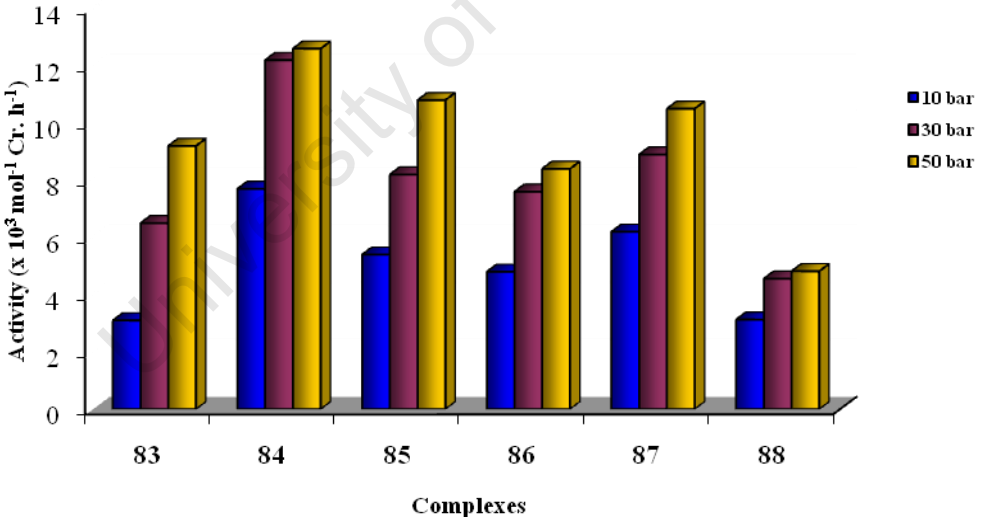

Figure 3.33 *Effect of ethylene pressure on catalytic activity with catalysts* ***83*** *–* ***88****/MMAO*

An oligomeric profile similar to that observed in the preceding temperature investigations was observed in the pressure investigations.

Table 3.16 Influence of pressure on ethylene oligomerization with complexes **64** – **74**[a]

Entry	Complex	Pressure (bar)	Activity[b]	PE (wt %)	Oligomers (wt %)			
					C_4	1-C_4	C_6	1-C_6
1	**83**	10	3.1	54.8	6.1	99	39.1	95
2		30	6.5	62.4	6.4	98	31.2	97
3		50	9.2	66.6	3.9	98	29.5	93
4	**84**	10	7.7	54.9	5.5	99	39.6	96
5		30	12.4	49.5	3.7	99	46.8	98
6		50	11.6	56.7	4.5	98	39.3	98
7	**85**	10	5.4	62.5	6.0	100	31.5	97
8		30	8.2	67.0	10.3	98	22.7	96
9		50	10.8	68.2	7.3	100	24.5	98
10	**86**	10	6.6	64.0	8.6	100	27.5	97
11		30	7.6	66.4	9.8	99	23.8	98
12		50	8.4	71.1	7.7	100	21.2	98
13	**87**	10	6.2	65.0	5.9	98	29.1	97
14		30	8.9	65.7	10.7	98	23.6	98
15		50	10.5	65.0	12.1	98	22.9	97
16	**88**	10	3.1	66.6	31.1	100	2.3	98
17		30	4.6	73.2	26.8	100	-	-
18		50	4.8	75.9	24.1	97	-	-

General Conditions: [a] 20 µmol catalyst; 50 ml methylcyclohexane; Time = 5 min; °C; Temp = 40 - 50 C, error estimate = ± 0.1, 1-C_4 and 1-C_6 components are the proportions within the C_4 and C_6 fractions respectively. [c]Activity = x 10^3 g (product).mol^{-1}Cr.h^{-1}.

3.3 Summary

Upon activation with the co-catalysts, the neutral palladium, nickel, and chromium catalyst precursors of the types Pd(**L**)Cl_2, Ni(**L**)Br_2, and Cr(**L**)Cl_3 were found to be active for ethylene oligomerization. The cationic palladium complexes were used without activation by a co-catalyst. The effects of different reaction parameters (temperature, pressure etc.) on catalytic activity were investigated in order to establish the optimal catalytic reaction conditions. Nickel and palladium systems gave mainly ethylene dimerization and trimerization products. The chromium systems produced ethylene dimerization, trimerization products, as well as polyethylene. The nickel catalysts were found to be the most active. All the palladium catalysts showed much lower activities compared to the nickel and chromium catalysts, with the cationic complexes in particular showing poor activities. Detailed concluding remarks on this chapter are given in the next chapter.

3.4 References

1. a) Guan, Z.; Marshall, W. J. *Organometallics* **2002**, *21*, 3580. b) Daugulis, O; Brookhart, M. *Organometallics* **2002**, *21*, 5926. c) Flapper, J.; Kooijman, H.; Lutz, M.; Spek, A. L.; van Leeuwen,; P. W. N. M.; Elsevier, C. J.; Kamer, P. C. J. *Organometallics*, **2009**, *28*, 1180.
2. Espinet, P.; Soulantica, K. *Coord. Chem. Rev.*, **1999**, *293 – 295*, 499.
3. Clayden, J.; Greeves, N.; Wothers, P. *Organic Chemistry*, Oxford University Press, New York, **2001**, 1159.
4. Willis, D. E. *Chromatographia* **1972**, *5*, 42.
5. a) Tang, X.; Sun, W-H.; Gao, T.; Hou, J. Chen, J.; Chen, W. *J. Organomet. Chem.*, **2005**, *690*, 1570. b) Svejda, S. A.; Brookhart, M. *Organometallics*, **1999**, *18*, 65. c) Hata, G.; Miyake, A. *Bull. Chem. Soc. Jpn.*, **1993**, *41*, 2762. d) Pedeutour, J-N; Radhakrishnan, K.; Cramail, H.; Deffienx, A. *Macromol. Rapid Commun.*, **2001**, *22*, 1095. e) Brown, S. J.; Masters, A. F. *J. Organomet. Chem.* **1989**, *367*, 371. 5f) Meinhard, D.; Wegner, M.; Kipiani, G.; Hearley, A.; Reuter, P.; Fischer, S.; Marti, O.; Rieger, B. *J. Am. Chem. Soc.*, **2007**, 129, 9182.
6. a) Speiser, F.; Braunstein, P.; Saussine, L. *Acc. Chem. Res*. **2005**, *38*, 784. b) Kermagoret, A.; Braunstein, P. *Organometallics* **2008**, *27*, 88. c) Speiser, F.; Braunstein, P.; Saussine, L. *Organometallics* **2004**, *23*, 2633.
7. a) Shen, M.; Hao, P.; Sun, W-H. *J. Organomet. Chem.*, **2008**, *693*. 1683. b) Zhang, S.; Sun, W-H.; Kuang, X.; Vystorop, I.; Yi, J. *J. Organomet. Chem.*, **2007**, *692*. 5307.
8. Kunrath, F. A.; de Souza, R. F.; Casagrande, Jr., O. L.; Brooks, N. R.; Young, Jr., V. G. *Organometallics*, **2003**, *22*, 4739. b) Killian, C. M.; Johnson, L. K.; Brookhart, M. *Organometallics* **1997**, *16*, 2005.
9. Tempel, D. J.; Johnson, L. K.; Huff, R. L.; White, P. S.; Brookhart, M. *J. Am. Chem. Soc.* **2000**, *122*, 6686.
10. a) Yang, P.; Yang, Y.; Zhang, C.; Yang, X-Y.; Hu, H-M.; Gao, Y.; Wu, B. *Inorg. Chim. Acta*. **2009**, *362*, 89. b) Zhang, M.; Gao, R.; Hao, X.; Sun, W-H. *J. Organomet. Chem.*, **2008**, *693*. 3867. c) Tang, X.; Sun, W-H.; Gao, T.; Hou, J.; Chen, J.; Chen, W. *J. Organomet. Chem.*, 2005, *690*. 1570. d) Yang, Y.; Yang, P.; Zhang, C, Li, G.; Yang, X-J.; Wu, B.; Janiak, C. *J. Mol. Catal. A: Chem.*, **2008**, *296*, 9. b)

11. a) Heinicke, J.; Kohler, M.; Peulecke, N.; Kindermann, M. K.; Keim, W.; Kockerling, M. *Organometallics*, **2005**, *24*, 344. b) Chen, H-P.; Liu, Y-H.; Peng, S-M.; Liu, S-T. *Organometallics*, **2003**, *22*, 4893. c) Yang, Q. Z.; Kermagoret, A.; Siri, O.; Braunstein, P. *Organometallics*, **2006**, *25*, 5518.
12. b) Schmid, M.; Eberhardt, R.; Klinga, M.; Leskelae, M.; Rieger, B. *Organometallics*, **2001**, *20*, 2321.
13. a) Svedja, S. A.; Johnson, L. K.; Brookhart, M. *J. Am. Chem. Soc.*, **1999**, 1*21*, 10634. b) Salo, E. V.; Guan, Z. *Organometallics*, **2003**, *22*, 5033.
14. Jabri, A.; Masson, C. B.; Sim, Y.; Gambarotta, S.; Burchell, T. J.; Duchateau, R. *Angew. Chem. Int. Ed.*, **2008**, *120*, 9863.
15. a) Blum, M. E.; Walter, O.; Döring, M. *J. Organomet. Chem.*, **2005**, *690*. 713. b) Zhang, W; Sun, W-H, Tang, X.; Gao, T.; Zhang, S, Hao, P.; Chen, J. *J. Mol.Catal. A: Chem.*, **2007**, *265*, 159. c) Chen, Y.; Zuo, W.; Hao, P.; Zhang, S.; Gao, K.; Sun, W-H. *J. Organomet. Chem.*, **2008**, *693*. 750.
16. Temple, A. J. C.; Crewdson, P.; Gambarotta, S.; Korobkov, I.; Duchateau, *J. Am. Chem. Soc.*, **2006**, *128*, 9238.
17. Overett, M. J.; Blann, K.; Bollmann, A.; Dixon, J. T.; Haasbroek, D.; Killian, E.; Maumela, H.; McGuinness, D. S.; Morgan, D. H. *J. Am. Chem. Soc.*, **2005**, *127***,** 10723.

CHAPTER 4
CONCLUSIONS

4.1 Conclusions

A series of new bidentate iminophosphine, phenoxyimine and iminopyridyl ligands (**L**) have been synthesized in good yield and characterized by spectroscopic and analytical methods. Chromium, nickel and palladium complexes have been prepared from the reaction of the ligands with the appropriate metal precursors i.e. $Cr(THF)_3Cl_3$, $Ni(DME)Br_2$, $Pd(COD)Cl_2$ or Pd(COD)ClMe.

The chromium and nickel complexes were characterized by IR spectroscopy, elemental analysis and mass spectroscopy. Due to the paramagnetic nature of the complexes, NMR results were inconclusive. The molecular structure of the nickel complex **76** was confirmed using X-ray diffraction. The geometry around the metal center was found to be distorted square planar. Although square planar nickel complexes are expected to be diamagnetic, the relatively high degree of distortion in **76** could account for the paramagnetism observed in the nickel complexes. Another plausible reason for the observed paramagnetism could be due to a conformational change (square planar – tetrahedral) in solution.

The palladium dichloride complexes (Pd**L**Cl_2) were isolated in high yields. Due to their extremely low solubility in most organic solvents, ^{13}C NMR data could not be obtained. They were however characterized by IR, ^{1}H and ^{31}P NMR spectroscopy, elemental analysis and mass spectroscopy. The corresponding phosphinoimine methylchloride complexes (Pd**L**MeCl) were more soluble, allowing for full characterization. The structure of complex **53** was unambiguously determined by X-ray diffraction and showed the expected square planar geometry around the palladium center. The *cis* arrangement of the methyl and phosphino groups was also confirmed.

Cationic palladium complexes were prepared by the reaction of halide abstracting agents ($AgBF_4$, $AgPF_6$ and $NaBAr^F{}_4$) with the methylchloride complexes in the presence of a weakly coordinating solvent (acetonitrile). They were characterized by IR, ^{1}H, ^{31}P and ^{13}C

NMR spectroscopy, elemental analysis and mass spectroscopy. The ionic character of the complexes was confirmed using conductance measurements, which also indicated that they were 1:1 electrolytes. The X-ray crystal structure of **71** confirmed the abstraction of the chloride and coordination of an acetonitrile molecule in the formation of the cationic species. The geometry around the palladium center was shown to be square planar.

Neutral nickel (**75** – **82**), palladium (**56** – **63**), and chromium (**83** – **88**) complexes were used as catalyst precursors and were activated with a variety of co-catalysts (MMAO, $EtAlCl_2$, and Et_2AlCl) in an effort to determine an efficient co-catalyst for each catalyst system. $EtAlCl_2$ was found to be an efficient co-catalyst for the neutral nickel and palladium catalyst precursors, while MMAO was found to be an efficient activator for the chromium catalyst precursors. The cationic palladium complexes, however, were used as catalysts without use of a co-catalyst. For each catalyst system, reaction conditions such as temperature, time, and ethylene pressure were investigated in an effort to establish optimum catalytic reaction conditions. These investigations revealed the optimum conditions for nickel/$EtAlCl_2$ and chromium/MMAO catalyst systems to be temperatures of 40 – 50 °C, ethylene pressure of 50 bar and 15 minute reaction times. Both neutral palladium/$EtAlCl_2$ and cationic palladium systems performed best at temperatures of 40 – 50 °C and an ethylene pressure of 50 bar. However the activities of the neutral catalysts peaked at 5 min while those of the cationic complexes peaked at 1 min. In general, palladium catalysts gave poor catalytic activities with the cationic palladium catalysts giving the lowest catalytic activities.

Nickel catalyst precursors activated with only 8 molar equivalents of $EtAlCl_2$ gave high catalytic activities (up to 13.2 x 10^5 $g.mol^{-1}Ni.h^{-1}$). Mainly ethylene dimerization (up to 99.5 %) and trimerization (up to 4.0 %) products were observed with these catalysts. However, very low selectivities of 1-C_4 within the C_4 fraction were observed due to the fact that nickel catalysts are also good double bond isomerization catalysts.

On the other hand, the palladium catalysts gave moderate catalytic activities (up to 7.7 x 10^3 $g.mol^{-1}Pd.h^{-1}$). These catalysts also gave ethylene dimerization (up to 100 %) and trimerization (up to 2.3 %) products with selectivities for 1-C_4 of up to 50 %. In contrast to the moderate catalytic activities observed for ethylene oligomerization, high catalytic activities (up to 2.2 x 10^6 $g.mol^{-1}Pd.h^{-1}$) were observed for 1-C_6 oligomerization. The reasons

for this difference in catalytic performance between ethylene and 1-C_6 are hitherto unclear. Thus, more experiments need to be carried out in order to probe these unexpected findings. The cationic palladium catalyst gave very low catalytic activities (up to 48.3 $g.mol^{-1}Pd.h^{-1}$). These catalysts also gave ethylene dimerization (up to 97.2 %) and trimerization (up to 37.8 %) products. In addition, odd-numbered oligomers (C_5 and C_7 up to 20.5 and 9.4 % respectively) were observed, possibly due to the very low catalytic activities observed.

MMAO was found to be an efficient co-catalyst for the activation of the chromium catalyst precursors. For this catalyst system, the reaction solvent was found to play a significant role, with methylcyclohexane giving better catalytic activities than toluene. These catalysts displayed moderate catalytic activities (up to 13.9 x 10^3 $g.mol^{-1}Cr.h^{-1}$), with the product distribution consisting of ethylene dimers (up to 26.8 %), trimers (up to 46.8 %), and polyethylene (up to 88.3 %). These catalysts gave good selectivity for α-olefins in the liquid fractions (up to 99 %).

The pendent group (R = methyl thiophene, methyl furyl, methyl 3-pyridyl) did not have a significant influene on catalysis. Among this group of substituents, catalysts bearing thiophene gave the best results, while those containing pyridyl gave the least. This could be due to better interaction/stabilization of the active catalyst by the thiophene moiety.

The catalyst system employed in this project proved to be highly stable (catalysts bearing P^N ligands). Even the high exotherms (up to 120 °C) observed with the nickel catalyst system did not deactivate the active catalyst. This suggested that the P^N ligands sufficiently stabilized the active catalyst at high temperatures. Despite low catalytic activities observed with the palladium catalysts, no formation of palladium black was observed implying that the ligand remained bound to the palladium metal centre.

CHAPTER 5
EXPERIMENTAL DETAILS

5.1 General Remarks

All reactions were carried out under a nitrogen or argon atmosphere using a dual vacuum/nitrogen line and standard Schlenk techniques unless stated otherwise. Solvents were dried and purified by heating at reflux under argon in the presence of a suitable drying agent. Hexane, pentane and methylcyclohexane were refluxed and distilled from calcium hydride (CaH_2); tetrahydrofuran (THF), diethyl ether (Et_2O), dimethoxyethane (DME) and toluene were dried over sodium-wire and benzophenone; dichloromethane was dried over P_2O_5 under nitrogen [1]. After the purification procedures, the solvents were transferred under vacuum into a Teflon-valve storage vessel. All reagents were purchased from Aldrich and used without further purification. 2-Diphenylphosphinobenzaldehyde [2], $Pd(COD)Cl_2$ [3], Pd(COD)MeCl [4], $Ni(DME)Br_2$ [5], $Cr(THF)_3Cl_3$ [6], $NaBAr^F{}_4$ (Ar^F = 3,5-$C_6H_3(CF_3)_2$) were prepared by published procedures [7]. Ethylene (99.9%) was purchased from Afrox. Reaction progress and product mixtures were monitored by thin-layer chromatography (TLC) on pre-coated silica-gel F_{254} plates in a suitable solvent system, using the ascending technique; the plates were viewed under a UV light. Column chromatography was carried out with 60 Å silica-gel (70-230 mesh ASTM)

5.2 Instrumentation

Melting points were recorded on a Kofler hotstage microscope (Reichert Thermovar). Elemental analyses were carried out on a Fisons EA 1108 CHNS Elemental Analyzer in the microanalytical laboratory at the University of Cape Town.

^1H, ^{31}P and ^{13}C NMR spectra were recorded on a Varian Mercury-300 MHz (^1H: 300 MHz; ^{13}C: 75.5 MHz; ^{31}P: 121 MHz) or Varian Unity-400 MHz (^1H: 400 MHz; ^{13}C: 100.6 MHz) spectrometer. ^1H NMR spectra were referenced internally using the residual protons in the deuterated solvents ($CDCl_3$: δ 7.27; DMSO: δ 2.50 ppm) and values reported relative to the internal standard tetramethylsilane (δ 0.00). ^{13}C NMR spectra were referenced internally to

the resonance ($CDCl_3$: δ 77.0; DMSO: δ 39.4) and the values reported relative to tetramethylsilane (δ 0.0). All chemical shifts are quoted in δ (ppm) and coupling constants, *J*, in Hertz (Hz).

IR absorptions were measured on a Perkin Elmer Spectrum one FT-IR spectrophotometer. Conductance measurements were performed with a Metrohm 660 conductometer. Measurements were carried out in nitrobenzene on standard solutions with molarities of 5 x 10^{-3} M.

GC analyses were performed using a Varian 3900 gas chromatograph equipped with an FID and a 50 m x 0.20 mm HP-PONA column (0.50 μm film thickness). The carrier gas was helium at 40 psi. The oven was programmed to hold the temperature at 32 °C for 4 min and then to ramp to 200 °C at 10 deg/min and hold for 5 min. The sample in a screw-cap vial and the syringe were cooled in liquid nitrogen before being injected into the GC machine, in an attempt to minimize the loss of the volatile product.

X-ray single crystal intensity data were collected on a Nonius Kappa-CCD diffractometer using graphite monochromated MoKα radiation. Temperature was controlled by an Oxford Cryostream cooling system (Oxford Cryostat). The strategy for the data collections was evaluated using the Bruker Nonius "Collect" program. Data were scaled and reduced using DENZO-SMN software. Absorption corrections were made empirically by utilizing the SADABS program. The structures were solved by direct methods and refined employing full-matrix least-squares with the program SHELXL-97 refining on F^2. Packing diagrams were produced using the program PovRay and graphic interface X-seed. All non-H atoms were refined anisotropically. All hydrogen atoms were fixed geometrically and were refined using a riding model, with C–H = 0.95 – 0.99 Å and U_{iso} = 1.2 or 1.5 x U_{eq}(C). The structure was refined successfully with R = 0.0254. The parameters for crystal data collection and structure refinements are in Table 5.1 (p 166).

5.3 Catalytic Olefin Oligomerization Reactions

A 250 mL thermostable stainless-steel Parr-type autoclave equipped with an overhead magnetic stirrer was heated at 100 °C under vacuum for 1 h and then cooled to room temperature. The autoclave was transferred into the glovebox where anhydrous solvent (toluene or cyclohexane (40 mL), the catalyst precursor complexes (2 – 5 x 10^{-5} mol, nickel, palladium, or chromium) and a co-catalyst ($EtAlCl_2$, Et_2AlCl, or MMAO), in the case of neutral nickel and palladium catalyst precursors, were introduced at room temperature under an inert atmosphere of nitrogen. The autoclave was sealed inside the glovebox before being taken out. However, for the chromium catalyst precursors the co-catalyst was introduced immediately after connection of the autoclave to the ethylene line. The autoclave was then purged three times with ethylene under stirring (300 rpm) before being brought to a working ethylene pressure (10 – 50 bar). The contents of the autoclave were then stirred for the desired time, while maintaining the ethylene pressure throughout the experiment. At the end of the catalytic run the autoclave was cooled to *ca.* -30 °C in a liquid nitrogen cooled acetone bath, at which temperature the excess ethylene was slowly vented. An internal standard (nonane, *ca.* 1 mL) was then added and a sample of the cooled reaction mixture collected in a cooled screw-cap vial for GC analysis.

In cases where solid polyethylene was produced, a cooled liquid sample was collected in a screw-cap vial and the remaining reaction mixture quenched with 2M HCl (30 mL) and stirred vigorously. The polyethylene was then filtered and washed with acetone. After washing with acetone the polyethylene was dried and weighed.

5.4 Ligand Preparation

General procedure (41 – 48):

To DCM solution (15 mL) of 2-diphenylphosphinobenzaldehyde (*ca.* 3 mmol) was added an equimolar amount of the appropriate substituted amine. An excess of magnesium sulphate was also added to the reaction mixture to remove the water by-product. The reaction was left to stir at room temperature for 16 h, after which time the magnesium sulphate was filtered off and the solvent removed *in vacuo* to give a yellow-orange oil. The oily crude products of ligands **41 – 45** were solidified by dissolving the oil in hot hexane, followed by quick hot

filtration of the liquid product. The resultant solution was then cooled at -16°C overnight to give an off-white powder, which was filtered and dried *in vacuo* [8 – 10]. Ligands **46** – **48** were isolated as yellow, orange, or dark brown oils.

Preparation of (2-diphenylphosphino-benzylidene)-pyridin-3-ylmethyl-amine ($C_{25}H_{21}N_2P$) (41)

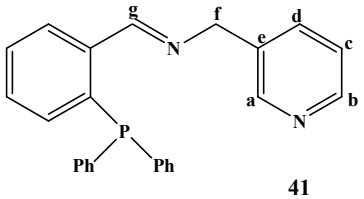

41

This compound was prepared from the reaction of 2-diphenylphosphinobenzaldehyde (1.00 g, 3.50 mmol) and 3-aminomethylpyridine (0.38 g, 3.5 mmol) using the general procedure. The pure product was obtained as an off-white powder (1.13 g, 86 %). M.p. 79 – 81 °C. IR (KBr): 1635 cm^{-1} ($\upsilon_{C=N,\ imine}$). ^1H NMR ($CDCl_3$): δ 9.02 (d, 1H, J_{HP} = 4.9 Hz, H_g), 8.45 (dd, 1H, J_{HH} = 1.7, 4.8 Hz, H_b), 8.42 (d, 1H, J_{HH} = 1.7 Hz, H_a), 8.01 (ddd, 1H, J_{HH} = 1.4, 3.9, 7.6 Hz, ArH), 7.24 – 7.43 (m, 13H, ArH), 7.12 (ddd, 1H, J_{HH} = 0.8, 4.8, 7.8 Hz, ArH), 6.90 (ddd, 1H, J_{HH} = 7.7, 4.7, 1.1 Hz, ArH), 4.67 (s, 2H, H_f). ^{13}C NMR ($CDCl_3$) δ: 161.4 (d, J_{CP} = 21.0 Hz, C_g), 149.4 (C_a), 148.3 (C_b), 137.8 (d, J_{CP} = 19.6 Hz, ArC), 137.1 (d, J_{CP} =17.0 Hz, ArC), 136.4 (d, J_{CP} = 9.4 Hz, ArC), 135.5 (C_d), 134.6 (C_e), 134.1 (d, J_{CP} =20.0 Hz, ArC), 133.4 (ArC), 130.6 (ArC), 129.0 (ArC), 128.7(d, J_{CP} = 7.2 Hz, ArC), 127.9 (d, J_{CP} = 4.1 Hz, ArC), 123.4 (ArC), 122.6 (C_c), 62.34 (C_f). ^{31} P NMR ($CDCl_3$): δ -13.2 (s). EI-MS: *m/z* 379.92 $[M]^+$. Anal. Calc. for $C_{25}H_{21}N_2P$ (380.42): C, 78.93; H, 5.56; N, 7.36. Found: C, 78.91; H, 5.49; N, 7.22.

Preparation of (2-diphenylphosphino)-benzylidene)-furan-2-ylmethyl-amine ($C_{24}H_{20}NOP$) (42)

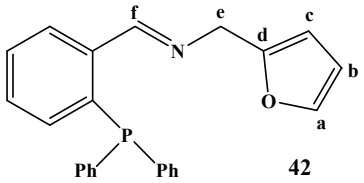

42

This compound was prepared from the reaction of 2-diphenylphosphinobenzaldehyde (1.00 g, 3.44 mmol) and furfurylamine (0.33 g, 3.44 mmol) using the general procedure. The pure product was obtained as an off-white powder (1.03 g, 81 %). M.p. 76 – 77 °C. IR (KBr): 1634 cm^{-1} ($\upsilon_{C=N}$). ^1H NMR ($CDCl_3$): δ 9.01 (d, J_{HH} = 5.1 Hz, H_f), 8.07 (ddd, 1H, J_{HH} = 7.7, 4.0, 1.4 Hz, ArH), 7.25 – 7.42 (m, 13H, ArH), 6.91 (m, 1H, H_a), 6.27 (m, 1H, H_b), 6.05 (dd, 1H, J_{HH} = 3.3, 0.7 Hz, H_c), 4.65 (s, 2H, H_e). ^{13}C NMR ($CDCl_3$) δ: 161.5 (d, J_{CP}= 23.0 Hz, C_f), 152.3 (C_d), 142.0 (C_a), 139.3 (d, J_{CP}= 17.3 Hz, ArC), 137.7 (d, J_{CP}= 19.8 Hz, ArC), 136.4 (d, J_{CP}= 9.7 Hz, ArC), 134.1 (d, J_{CP}= 19.9 Hz, ArC), 133.3 (ArC), 130.5 (ArC), 129.0 (ArC), 128.8 (ArC), 128.6 (d, J_{CP}= 7.1 Hz, ArC), 127.6 (d,

J_{CP}= 4.2 Hz, ArC), 110.3 (C_b), 107.4 (C_c), 57.0 (C_e). ^{31}P NMR ($CDCl_3$): δ -13.9 (s). EI-MS: *m/z* 369.81 $[M+H]^+$. Anal. Calc. for $C_{24}H_{20}NOP$ (369.40): C, 78.03; H, 5.46; N, 3.79. Found: C, 77.79; H, 5.56; N, 3.60.

Preparation of (2-diphenylphosphino)-benzylidene)-thiophen-2-ylmethyl-amine ($C_{24}H_{20}NPS$) (43)

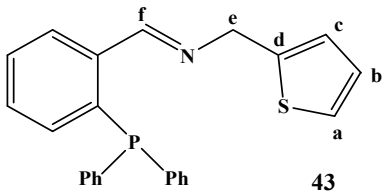

43

This compound was prepared from the reaction of 2-diphenylphosphinobenzaldehyde (1.00 g, 3.44 mmol) and 2-thiophene-methylamine (0.39 g, 3.44 mmol) using the general procedure. The pure product was obtained as an off-white powder (0.97 g, 73 %). M.p. 70 – 72 °C. IR (KBr): 1625 cm^{-1} ($\upsilon_{C=N}$). ^{1}H NMR ($CDCl_3$): δ 9.02 (br d, 1H, J_{HP} = 4.9Hz, H_f), 8.11 (m, 1H, ArH), 7.25 – 7.45 (m, 12H, ArH), 7.20 (dd, 1H, J_{HH} = 5.1, 1.1 Hz, H_a), 6.95 (m, 2H, H_b+ArH), 6.78 (dd, 1H, J_{HH} = 3.1, 1.0 Hz, H_c), 4.86 (s, 2H, H_e). ^{13}C NMR ($CDCl_3$) δ: 160.8 (d, J_{CP} = 23.2 Hz, C_f), 141.8 (C_d), 139.3 (d, J_{CP} = 17.2 Hz, ArC), 137.7 (d, J_{CP} = 19.3 Hz, ArC), 136.3 (d, J_{CP} = 9.7 Hz, ArC), 134.1 (d, J_{CP} = 20.8 Hz, ArC), 133.3 (ArC), 130.6 (ArC), 129.1 (ArC), 128.9 (ArC), 128.7 (d, J_{CP} = 7.1 Hz, ArC), 127.8 (d, J_{CP} = 4.2 Hz, ArC), 126.8 (C_a), 125.1 (C_b), 124.6 (C_c), 59.9 (C_e). ^{31}P NMR ($CDCl_3$): δ -13.99 (s). EI-MS: *m/z* 385.56 $[M]^+$. Anal. Calc. for $C_{24}H_{20}NPS$ (385.46): C, 74.78; H, 5.23; N, 3.63; S, 8.32. Found: C, 74.29; H, 5.29; N, 3.35; S, 8.26.

Preparation of (2-diphenylphosphino-benzylidene)-thiophen-2-ylethyl-amine ($C_{25}H_{22}NPS$) (44)

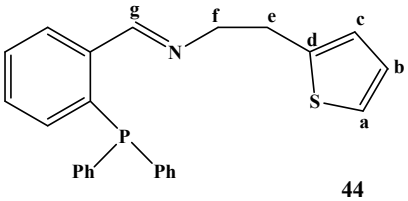

44

This compound was prepared from the reaction of diphenylphosphinobenzaldehyde (2.00 g, 6.89 mmol) and 2-thiopheneethylamine (0.88 g, 6.89 mmol) using the general procedure. The pure product was obtained as an off-white powder (2.54 g, 92 %). M.p. 64 – 65 °C. IR (KBr): 1636 cm^{-1} ($\upsilon_{C=N}$). ^{1}H NMR ($CDCl_3$): δ 8.91 (d, 1H, J_{HP} = 4.9 Hz, C_g), 8.03 (m, 1H, ArH), 7.26 – 7.45 (m, 12H, ArH), 7.08 (dd, 1H, J_{HH} = 5.1, 1.1 Hz, H_a), 6.93 (m, 1H, ArH), 6.88 (m, 1H, H_b), 6.77 (dd, 1H, J_{HH} = 3.3, 0.9 Hz, H_c), 3.78 (t, 2H, J_{HH} = 3.2 Hz, H_f), 3.02 (t, 2H, J_{HH} = 3.2 Hz, H_e),. ^{13}C NMR ($CDCl_3$): δ 160.6 (d, J_{CP} = 21.3 Hz, C_g), 142.4 (C_d), 139.6 (d, J_{CP} = 17.3 Hz, ArC), 137.6 (d, J_{CP} = 19.5 Hz, ArC), 136.7 (d, J_{CP} = 9.6 Hz, ArC), 134.1 (ArC), 134.0 (, J_{CP} = 19.9 Hz, ArC), 133.5 (ArC), 130.3 (ArC), 130.0 (ArC), 128.9 (ArC),

127.8 (d, J_{CP} = 4.3 Hz,ArC), 126.7 (C_a), 125.0 (C_b), 123.5 (C_c), 62.5 (C_f), 31.4 (C_e). ^{31}P NMR ($CDCl_3$): δ -13.55 (s). EI-MS: *m/z* 400.04 $[M]^+$. Anal. Calc. for $C_{25}H_{22}NPS$ (399.49): C, 75.16; H, 5.55; N, 3.51; S, 7.75. Found: C, 75.03; H, 5.64; N, 3.05; S, 8.06.

Preparation of benzyl-(2-diphenylphosphino-benzylidene)-amine ($C_{26}H_{22}NP$) (45)

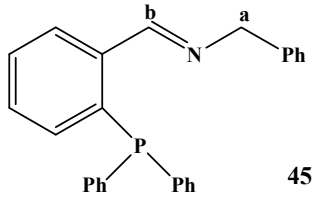

45

This compound was prepared from the reaction of 2-diphenylphosphinobenzaldehyde (1.03 g, 0.35 mmol) and benzylamine (0.38 g, 3.44 mmol) using the general procedure. The pure product was obtained as an off-white powder (0.97 g, 74 %) [9]. M.p. 79 - 81°C. IR (KBr): 1636 cm^{-1} ($\upsilon_{C=N}$). ^{1}H NMR ($CDCl_3$): δ 9.03 (d, 1H, J_{HH} = 5.8 Hz, H_b), 8.10 (m, 1H, ArH), 7.19 – 7.43 (m, 15H, ArH), 7.09 (m, 2H, ArH), 6.94 (ddd, 1H, J_{HH} = 7.7, 4.7, 1.2 Hz, ArH), 4.67 (s, 2H, H_a). ^{13}C NMR ($CDCl_3$): δ 160.5 (d, J_{CP} = 22.4 Hz, C_b), 139.4 (d, J_{CP} = 17.4 Hz, ArC), 138.9 (ArC), 137.5 (d, J_{CP} = 19.5 Hz, ArC), 136.3 (d, J_{CP} = 10.0 Hz, ArC), 134.1 (d, J_{CP} = 20.0 Hz, ArC), 133.2 (ArC), 130.3 (ArC), 128.8 (ArC), 128.6 (d, J_{CP} = 7.3 Hz, ArC), 128.3 (ArC), 127.9 (ArC), 127.7 (d, J_{CP} = 4.2 Hz, ArC), 126.7 (ArC), 65.1 (C_a). ^{31}P NMR ($CDCl_3$): δ -13.6 (s). EI-MS: *m/z* 379.42 $[M]^+$. Anal. Calc. for $C_{26}H_{22}NP$ (379.43): C, 82.30; H, 5.84; N, 3.69. Found: C, 82.56; H, 6.11; N, 3.82.

Preparation of furan-2-methyl-pyridin-2-ylmethylene-amine ($C_{11}H_{10}N_2O$) (46)

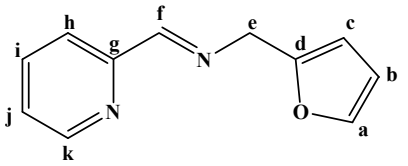

46

This compound was prepared from the reaction of 2-pyridinecarboxaldehyde (3.01 g, 28.01 mmol) and furfurylamine (2.72 g, 28.01 mmol) in 30 mL DCM using the general procedure. The pure product was obtained as a dark brown oil (3.53 g, 67 %).[12] IR (KBr): 1619 cm^{-1} ($\upsilon_{C=N}$). ^{1}H NMR ($CDCl_3$): δ 8.59 (ddd, 1H, J_{HH} = 4.9, 1.7, 1.0 Hz, H_k), 8.43 (m, 1H, H_f), 7.98 (dt, 1H, J_{HH} = 7.9, 1.1 Hz, H_i), 7.66 (m, 1H, H_h), 7.37 (dd, 1H, J_{HH} = 0.9, 1.9 Hz, H_a), 7.28(m, 1H, H_j), 6.30 (m, 1H, H_b), 6.27 (dd, 1H, J_{HH} = 3.2, 0.7 Hz, H_c), 4.83 (s, 2H, H_e). ^{13}C NMR ($CDCl_3$): δ 163.6 (C_f), 154.2 (C_g), 151.6 (C_d), 142.2 (C_h), 142.2 (C_a), 136.3 (C_k), 124.7 (C_j), 121.2 (C_i), 110.2 (C_b), 107.7 (C_c), 56.7 (C_e); EI-MS: *m/z* 186.99 $[M+H]^+$. Anal. Calc. for $C_{11}H_{10}N_2O$ (186.21): C, 70.95; H, 5.41; N, 15.04. Found: C, 71.01; H, 5.33; N, 15.23.

Preparation of (2-bromo-benzylidene)-furan-2-ylmethyl-amine ($C_{12}H_{10}BrNO$) (47)

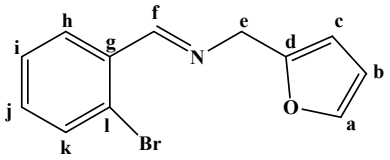

47

This compound was prepared from the reaction of 2-bromobenzaldehyde (5.05 g, 27.29 mmol) and furfurylamine (2.62 g, 27.29 mmol) in 30 mL DCM using the general procedure. The pure product was obtained as an orange oil (6.88 g, 95 %). ^{1}H ($CDCl_3$): δ 8.75 (s, 1H, H_f), 8.07 (dd, 1H, J_{HH} = 1.8, 7.7 Hz, H_h), 7.58 (dd, 1H, J_{HH} = 1.0, 7.9Hz, H_k), 7.42 (dd, 1H, J_{HH} = 0.8, 1.8 Hz, H_a), 7.33 (br t, 1H, J_{HH} = 7.5 Hz, H_i), 7.26 (m, 1H, H_j), 6.38 (m, 1H, H_b), 6.31 (dd, 1H, J_{HH} = 0.7, 3.2 Hz, H_c), 4.84 (s, 2H, H_e),. ^{13}C NMR ($CDCl_3$): δ 162.1 (C_f), 152.2 (C_d), 142.3 (C_a), 134.5 (C_g), 133.0 (C_j), 132.0 (C_k), 129.0 (C_h), 127.7 (C_i), 125.3 (C_l), 110.5 (C_b), 107.6 (C_c), 57.4 (C_e), EI-MS: *m/z* 264.45 $[M]^+$. Anal. Calc. for $C_{12}H_{10}BrNO$ (264.12): C, 54.57; H, 3.82; N, 5.30. Found: C, 54.26; H, 3.77; N, 5.54.

Preparation of 2-[(furan-2ylmethyl)-iminomethyl]-phenol ($C_{12}H_{11}NO_2$) (48)

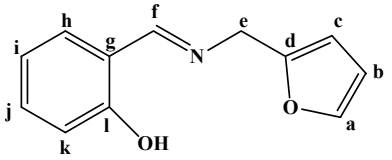

48

This compound was prepared from the reaction of salicylaldehyde (5.01 g, 41.03 mmol) and furfurylamine (3.97 g, 41.03 mmol) in 30 mL DCM using the general procedure. The pure product was obtained as a yellow oil (7.56 g, 91 %) [10]. IR (CH_2Cl_2): 1631 cm^{-1} ($\upsilon_{C=N}$). ^{1}H ($CDCl_3$): δ 13.17 (br s, 1H, OH), 8.39 (s, 1H, H_f), 7.42 (m, 1H, H_h), 7.34 (m, 1H, H_j), 7.28 (dd, 1H, J_{HH} = 1.6, 7.7 Hz, H_a), 7.01 (dd, 1H, J_{HH} = 0.4, 8.3 Hz, H_k), 6.91 (dt, 1H, J_{HH} = 1.1, 7.9 Hz, H_i), 6.33 (m, 1H, H_b), 6.30 (dd, 1H, J_{HH} = 0.7, 3.2 Hz, H_c), 4.77 (s, 2H, H_e). ^{13}C NMR ($CDCl_3$): δ 166.3 (C_f), 161.1 (C_l), 151.3 (C_d), 142.5 (C_a), 132.5 (C_j), 131.6 (C_h), 118.9 (C_g), 118.7 (C_i), 117.1 (C_k), 110.5 (C_b), 108.0 (C_c), 55.2 (C_e). EI-MS: *m/z* 200.34 $[M]^+$. Anal. Calc. for $C_{12}H_{11}NO_2$ (201.22): C, 71.63; H, 5.51; N, 6.96. Found: C, 71.54; H, 5.37; N, 7.06.

General procedure for imine bond reduction of compounds (47 and 48)

To a methanol solution (15 ml) of the appropriate imino-ligand *ca.*10 – 15 mmol (**47** or **48)** was added a slight excess of $NaBH_4$ (2.2 molar equivalents) in three portions, and the mixture was heated under reflux for 1 h. The solvent was then removed under reduced pressure and the unreacted $NaBH_4$ quenched with water (20 mL). The organic product was extracted into diethyl ether, and dried over sodium sulphate. Sodium sulphate was then filtered off and the

solvent removed *in vacuo* to give a yellow oil. The crude product was washed with hexane (2 x 15 mL) to give the pure product as a yellow oil [11].

Preparation of (2-bromo-benzyl)-furan-2-ylmethyl-amine ($C_{12}H_{12}BrNO$) (49)

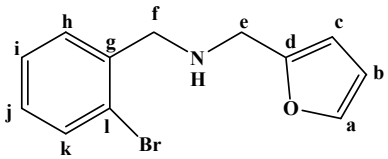

49

This compound was prepared from the reaction of **47** (2.03 g, 10.90 mmol) and $NaBH_4$ (0.91 g, 23.98 mmol) using the general procedure and the pure product obtained as a yellow oil (1.83 g, 63 %). IR (CH_2Cl_2): 3331 cm^{-1} (υ_{N-H}). ^1H ($CDCl_3$): δ 7.56 (d, 1H, J_{HH} = 8.0 Hz, H_h), 7.45 (m, 2H, H_k), 7.38 (m, 1H, H_a), 7.29 (t, 1H, J_{HH} = 7.5 Hz, H_i), 7.13 (dt, 1H, J_{HH} = 1.3, 7.7Hz, H_j), 6.34 (m, 1H, H_b), 6.23 (d, 1H, J_{HH} = 3.1 Hz, H_c), 3.90 (s, 2H, H_f), 3.82 (s, 2H, H_e), 1.90 (s, 1H, NH). ^{13}C NMR ($CDCl_3$): δ 153.7 (C_d), 141.8 (C_a), 138.9 (C_g), 132.8 (C_k), 130.5 (C_h), 128.6 (C_j), 127.4 (C_i), 124.0 (C_l), 110.1 (C_b), 107.0 (C_c), 52.7 (C_e), 45.4 (C_f). EI-MS: *m/z* 266.32 $[M]^+$. Anal. Calc. for $C_{12}H_{12}BrNO$ (266.13): C, 54.16; H, 4.54; N, 5.26. Found: C, 53.96; H, 4.43; N, 5.55.

Preparation of 2-{[(furan-2-ylmethyl)-amino]-methyl-phenol} ($C_{12}H_{13}NO_2$) (50)

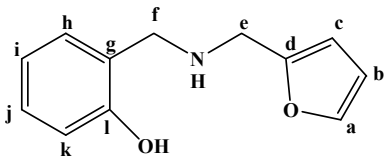

50

This compound was prepared from the reaction of **48** (3.03 g, 15.06 mmol) and $NaBH_4$ (1.24 g, 33.13 mmol) using the general procedure and the pure product obtained as a yellow oil (2.36 g, 77 %). ^1H ($CDCl_3$): δ 7.42 (dd, 1H, J_{HH} = 1.9, 0.8 Hz, H_a), 7.22 (dt, 1H, J_{HH} = 8.1, 1.6 Hz, H_j), 7.01 (br d, 1H, J_{HH} =7.4 Hz, H_h), 6.91 (dd, 1H, J_{HH} = 8.2, 0.8 Hz, H_k), 6.83 (dt, 1H, J_{HH} = 7.4, 1.1 Hz, H_i), 6.55 (br s, 1H, OH), 6.37 (dd, 1H, J_{HH} = 3.2, 1.9 Hz, H_b), 6.24 (dd, 1H, J_{HH} = 3.2, 0.6 Hz, H_c), 3.97 (s, 2H, H_f), 3.83 (s, 2H, H_e). ^{13}C NMR ($CDCl_3$): δ 157.9 (C_l), 151.7 (C_d), 142.4 (C_a), 128.5 (C_h), 128.4 (C_j), 121.9 (C_g), 118.9 (C_i), 116.5 (C_k), 110.4 (C_b), 108,1 (C_c), 51.3 (C_e), 44.3 (C_f). EI-MS: *m/z* 202.86 $[M]^+$. Anal. Calc. for $C_{12}H_{13}NO_2$ (203.20): C, 70.92; H, 6.45; N, 6.89. Found: C, 71.23; H, 6.44; N, 6.58.

5.5 Preparation of the Palladium Complexes (51 – 55)

General procedure

To a DCM solution (10 mL) of the appropriate ligand (*ca.* 0.2 – 0.3 mmol) **41** – **45** was added a DCM solution (10mL) an equimolar amount of Pd(COD)MeCl. The reaction was stirred at room temperature for 6 h. The solvent was then removed *in vacuo*. The crude product was recrystallized from DCM (*ca.* 3 mL) and hexane (15mL). The products were obtained as pale yellow or off-white micro-crystals.

Preparation of [Pd($C_{26}H_{24}N_2P$)Cl] (51)

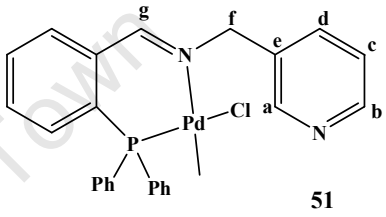

51

This compound was prepared from a reaction of **41** (0.1 g, 0.26 mmol) and Pd(COD)MeCl (0.07 g, 0.26 mmol) using the general procedure. The pure product was obtained as a pale yellow powder (0.12 g, 86 %). M.p. 179 - 181°C. IR (KBr): 1633 cm^{-1} ($\upsilon_{C=N}$, imine). ^{1}H NMR ($CDCl_3$): δ 8.50 (dd, 1H, J_{HH} = 1.6, 4.8 Hz, H_b), 8.33 (s, 1H, H_g), 8.32 (d, 1H, J_{HH} = 2.2, 8.3 Hz, H_a), 7.99 (td, 1H, J_{HH} = 1.8, 7.7 Hz, ArH), 7.63 (m, 1H, ArH), 7.58 (m, 1H, ArH), 7.46 (m, 3H, ArH), 7.39 (m, 4H, ArH), 7.16 (m, 5H, ArH), 7.06 (dd, 1H, J_{HH} = 7.4, 9.7 ArH), 5.48 (s, 2H, H_f), 0.60 (d, 3H, J_{HH} = 3.1 Hz,CH_3);. ^{13}C NMR ($CDCl_3$): δ 163.6 (d, J_{CP} = 4.8 Hz, ArC), 150.4 (C_b), 149.0 (C_a), 137.4 (ArC), 136.1 (d, J_{CP} = 8.7 Hz, ArC), 134.1 (ArC), 133.9 (ArC), 133.8 (ArC), 133.8 (d, J_{CP} = 12.4 Hz, ArC), 132.5 (ArC), 132.3 (d, J_{CP} = 6.7 Hz, ArC), 130.4 (d, J_{CP} = 1.7 Hz, ArC), 131.1 (d, J_{CP} = 2.3 Hz, ArC), 128.7 (d, J_{CP} = 11.2 Hz, ArC), 126.5 (ArC), 123.3 (ArC), 64.4 (C_f), 2.6 (CH_3). ^{31}P NMR ($CDCl_3$): δ 37.3 (s). EI-MS: *m/z* 501.51 $[M\text{-}Cl]^+$. Anal. Calc. for $C_{26}H_{24}ClN_2PPd$ (537.33): C, 58.12; H, 4.50; N, 5.21. Found: C, 58.25; H, 4.66; N, 5.53.

Preparation of [Pd($C_{25}H_{23}NOP$)Cl] (52)

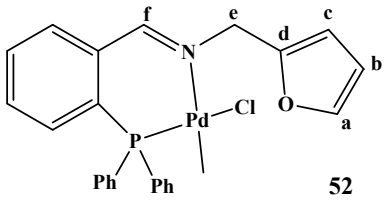

52

This complex was prepared from the reaction of **42** (0.1 g, 0.27 mmol) and Pd(COD)MeCl (0.07 g, 0.27 mmol) using the general procedure. The pure product was obtained as a pale yellow powder (0.092 g, 64 %). M.p. 193 -194°C. IR (KBr): 1637 cm^{-1} ($\upsilon_{C=N}$). ^{1}H NMR ($CDCl_3$): δ 8.21 (s, 1H, H_f), 7.58 (m, 1H, ArH), 7.53 (m, 1H, ArH), 7.44 (m, 3H, ArH), 7.36 (m, 4H, ArH), 7.24 (m, 4H, ArH), 7.10 (m, 1H, ArH), 7.02 (d, 1H, J_{HH} = 2.0 Hz, H_a), 6.68 (d, 1H, J_{HH}= 3.0 Hz, H_b), 6.31 (m, 1H, H_c), 5.43 (s, 2H,

H_e), 0.51 (d, 3H, J_{HH} = 3.2 Hz, CH_3). ^{13}C NMR ($CDCl_3$): δ 163.7 (d, J_{CP} = 5.1 Hz, C_f), 149.5 (C_d), 142.8 (C_a), 136.0 (ArC), 135.9 (d, J_{CP} = 8.7 Hz, ArC), 134.1 (d, J_{CP} = 12.6 Hz, ArC), 133.5 (ArC), 132.2 (d, J_{CP} = 6.8 Hz, ArC), 131.4 (d, J_{CP} = 1.7 Hz, ArC), 130.9 (d, J_{CP} = 2.0 Hz, ArC), 128.7 (d, J_{CP} = 11.2 Hz, ArC), 128.2 (ArC), 126.9 (d, J_{CP} = 57.5 Hz, ArC), 111.3 (C_b), 110.6 (C_c), 59.1 (C_e), 2.9 (CH_3). ^{31}P NMR ($CDCl_3$): δ 37.7 (s). EI-MS: *m/z* 490.42 [M-Cl]$^+$. Anal. Calc. for $C_{25}H_{23}ClNOPPd$ (526.30): C, 57.05; H, 4.40; N, 2.66. Found: C, 56.83; H, 4.25; N, 2.31.

Preparation of [Pd($C_{25}H_{23}$NPS)Cl] (53)

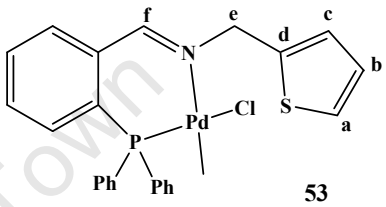

53

This complex was prepared from the reaction of **43** (0.5 g, 1.25 mmol) and Pd(COD)MeCl (0.34 g, 1.25 mmol) using the general procedure. The pure product was obtained as a pale yellow powder (0.48 g, 88 %). M.p. 184 – 189 °C. IR (KBr): 1636 cm^{-1} ($\upsilon_{C=N}$). ^1H NMR ($CDCl_3$): δ 8.23 (s, 1H, H_f), 7.58 (m, 2H, ArH), 7.43 (m, 3H, ArH), 7.34 (m, 4H, ArH), 7.21 (m, 4H, ArH), 7.13 (m, 2H, Ha, ArH), 7.08 (m, 1H, H_b), 6.91 (dd, 1H, J_{HH} =1.1, 3.7 Hz, H_c), 5.60 (s, 2H, H_e), 0.58 (d, 3H, J = 2.9 Hz, CH_3). ^{13}C NMR ($CDCl_3$): δ 162.9 (d, J_{CP} = 4.9 Hz, C_f), 138.8 (C_d), 137.0 (d, J_{CP} = 14.3 Hz, ArC), 136.0 (d, J_{CP} = 8.7 Hz, ArC), 134.0 (d, J_{CP} = 12.5 Hz, ArC), 133.6 (C_a), 132.1 (d, J_{CP} = 6.7 Hz, ArC), 131.3 (d, J_{CP} = 1.5 Hz, ArC), 130.9 (d, J_{CP} = 2.0 Hz, ArC), 128.8 (ArC), 128.9 (d, J_{CP} = 11.1 Hz, ArC), 128.1 (C_a), 127.1 (d, J_{CP} = 42.1 Hz, ArC), 127.0 (C_b), 124.2 (C_c), 60.82 (C_e), 2.3 (CH_3). ^{31}P NMR ($CDCl_3$): δ 37.5 (s). EI-MS: *m/z* 506.92 [M-Cl]$^+$. Anal. Calc. for $C_{25}H_{23}ClNPPdS$ (542.37): C, 55.36; H, 4.27; N, 2.58; S, 5.91. Found: C, 55.37; H, 4.25; N, 2.25; S, 5.99.

Preparation of [Pd($C_{26}H_{25}$NPS)Cl] (54)

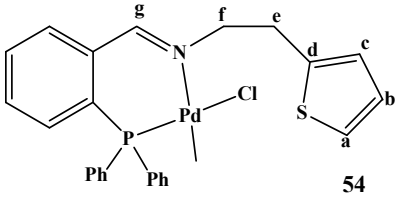

54

This complex was prepared from the reaction of **44** (0.50 g, 1.25 mmol) and Pd(COD)MeCl (0.32 g, 1.25 mmol) using the general procedure. The pure product was obtained as a pale yellow powder (0.44 g, 63 %). M.p. 172 - 175°C. IR (KBr): 1632 cm^{-1} ($\upsilon_{C=N}$). ^1H NMR ($CDCl_3$): δ 7.86 (s, 1H, H_g), 7.34 – 7.43 (m, 13H, ArH), 7. 05 (t, 1H, J_{HH} = 17.6, J = 7.8 Hz, ArH), 6.95 (d, 1H, J_{HH} = 6.8 Hz, H_a), 6.59 – 6.63 (m, 1H, H_b), 6.22 (d, 1H, J_{HH} = 3.9 Hz, H_c), 4.50 (t, 2H, J_{HH} = 13.7, J_{HH} = 6.9 Hz, H_f), 3.31 (t, 2H, J_{HH} = 13.7, J_{HH} = 6.8 Hz, H_e), 0.67 (d, 3H, J_{HH} = 3.3 Hz, CH_3). ^{13}C NMR ($CDCl_3$): δ 163.2 (d, J_{CP} =

5.0 Hz, C_g), 140.8 (C_d), 137.1 (d, J_{CP} = 15.0 Hz, ArC), 136.1 (d, J_{CP} = 9.0 Hz, ArC), 134.5 (ArC), 134.0 (d, J_{CP} = 12.4 Hz, ArC), 132.1 (d, J_{CP} = 6.7 Hz, ArC), 131.3 (d, J_{CP} = 2.2 Hz, ArC), 130.9 (d, J_{CP} = 2.0 Hz, ArC), 128.9 (d, J_{CP} = 11.1 Hz, ArC), 126.8 (C_a), 126.7 (d, J_{CP} = 65.6 Hz, ArC), 125.9 (C_b), 125.9 (d, J_{CP} = 41.7 Hz, ArC), 123.7 (C_c), 66.3 (C_f), 31.2 (C_e), 2.6 (CH_3). ^{31}P NMR ($CDCl_3$): δ 36.6 (s). EI-MS: *m/z* 520.72 $[M\text{-}Cl]^+$. Anal. Calc. for $C_{26}H_{25}ClNPPdS$ (556.40): C, 56.13; H, 4.53; N, 2.52; S, 5.76. Found: C, 56.28; H, 4.51; N, 2.81; S, 5.79.

Preparation of [Pd($C_{27}H_{25}$NOP)Cl] (55)

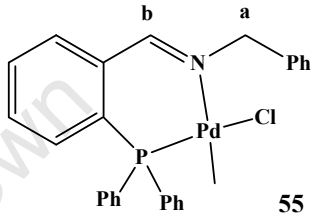

55

This complex was prepared from the reaction of **45** (0.20 g, 0.53 mmol) and Pd(COD)MeCl (0.14 g, 0.53mmol) using the general procedure. The pure product was obtained as a pale yellow powder (0.22 g, 77 %). M.p. 168 - 171°C. IR (KBr): 1636 cm^{-1} ($\upsilon_{C=N}$). ^{1}H NMR ($CDCl_3$): δ 8.81 (s, 1H, H_b), 7.91 (dd, 1H, J_{HH} = 4.3, 6.3 Hz, ArH), 7.83 (br t, 1H, J_{HH} = 7.5 Hz, ArH), 7.69 (br t, 1H, J_{HH} = 7.5 Hz, ArH), 7.56 (m, 2H, ArH), 7.45 (dt, 4H, J_{HH} = 2.3, 7.6 Hz, ArH), 7.29 (m, 1H, ArH), 7.18 (m, 8H, ArH), 7.09 (dd, 1H, J_{HH} = 7.7, 10.5 Hz, ArH), 5.10 (s, 2H, H_a), 0.18 (d, 3H, J_{HH} = 3.2 Hz, CH_3). ^{13}C NMR ($CDCl_3$): δ 164.7 (d, J_{CP} = 4.9 Hz, ArC), 138.4 (d, J_{CP} = 8.2 Hz, ArC), 137.9 (ArC), 137.5 (ArC), 136.0 (d, J_{CP} = 13.6 Hz, ArC), 135.5 (ArH), 134.9 (d, J_{CP} = 12.2 Hz, ArC), 134.2 (ArC), 133.6 (ArC), 132.4 (ArC), 130.2 (d, J_{CP} = 11.7 Hz, ArC), 129.6 (d, J_{CP} = 8.7 Hz, ArC), 127.8 (Arc), 128.0 (ArC), 124.3 (d, J_{CP} = 7.6 Hz, ArC), 124.4 (ArC), 62.3 (C_a), 0.59 (CH_3). ^{31}P NMR ($CDCl_3$): δ 38.5 (s). EI-MS: *m/z* 501.08 $[M\text{-}Cl]^+$. Anal. Calc. for $C_{27}H_{25}ClNOPPd$ (536.34): C, 60.46; H, 4.70; N, 2.61. Found: C, 60.72; H, 4.51; N, 2.81.

General procedure for 56 – 61

To a DCM solution (5 mL) of the appropriate ligand (*ca.*0.2 – 0.3 mmol) **41** – **48** was added a DCM solution (15 mL) of $Pd(COD)Cl_2$. A yellow precipitate formed immediately. The reaction mixture was allowed to stir at room temperature for 6 h and the yellow crude product filtered. The product was then washed three times with 10 mL DCM and dried *in vacuo* to give a yellow powder.

Preparation of [Pd($C_{25}H_{21}NP$)Cl_2] (56)

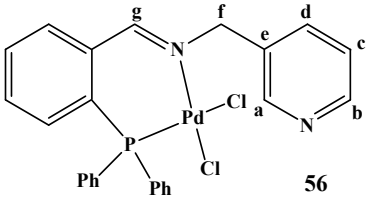

56

This complex was prepared from a reaction of **41** (0.11 g, 0.29 mmol) and Pd(COD)Cl_2 (0.08 g, 0.26 mmol) using the general procedure, to give a pure product as a yellow powder (0.93 g, 64 %). M.p. 210 – 212 °C (decomp.). IR (KBr): 1626 cm^{-1} ($\upsilon_{C=N}$). ^{1}H NMR (DMSO-d_6): δ 8.50 (dd, 1H, J_{HH} = 4.8, 1.8 Hz, H_b), 8.34 (s, 1H, H_g), 8.32 (d, 1H, J_{HH} = 2.2 Hz, H_a), 7.96 (dt, 1H, J_{HH} = 1.8, 7.7Hz,H_c), 7.78 (m, 2H, ArH), 7.56 (m, 4H, ArH), 7.39 (m, 4H, ArH), 7.16 (m, 4H, ArH), 6.99 (m, 1H, ArH), 5.48 (s, 2H, H_f). ^{31}P NMR ($CDCl_3$): δ 37.3 (s). EI-MS: *m/z* 522.11 $[M\text{-}Cl]^+$. Anal. Calc. for $C_{25}H_{21}Cl_2NPPd$ (557.75): C, 53.84; H, 3.80; N, 5.02. Found: C, 53.51; H, 3.99; N, 4.86.

Preparation of [Pd($C_{24}H_{20}NOP$)Cl_2] (57)

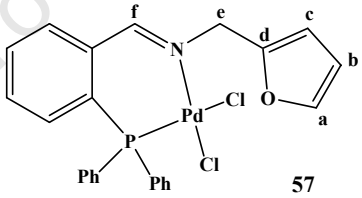

57

This complex was prepared from the reaction of **42** (0.13 g, 0.35 mmol) and Pd(COD)Cl_2 (0.10 g, 0.35 mmol) using the general procedure. The pure product was obtained as a yellow powder (0.15 g, 69 %). M.p. 198 – 199 °C (decomp.). IR (KBr): 1630 cm^{-1} ($\upsilon_{C=N}$). ^{1}H NMR (DMSO-d_6): δ 8.72 (s, 1H, H_f), 8.00 (ddd, 1H, J_{HH} = 1.2, 4.2, 7.6 Hz, ArH), 7.89 (dt, 1H, J_{HH} = 1.5, 7.7 Hz, ArH), 7.75 (tt, 1H, J_{HH} = 1.4, 7.6 Hz, ArH), 7.58 (m, 2H, ArH), 7.45 (td, 4H, J_{HH} = 2.9, 4.8 Hz, ArH), 7.24 (m, 5H, ArH+H_a), 7.05 (dd, 1H, J_{HH} = 7.8, 10.1 Hz, ArH), 6.55 (d, 1H, J_{HH} = 3.2 Hz, H_b), 6.38 (dd, 1H, J_{HH} = 1.9, 3.2 Hz, H_c), 5.56 (s, 2H, H_e). ^{31}P NMR ($CDCl_3$): δ 32.2 (s). EI-MS: *m/z* 511.43 $[M\text{-}Cl]^+$. Anal. Calc. for $C_{24}H_{20}Cl_2NOPPd$ (546.72): C, 52.72; H, 3.69; N, 2.56. Found: C, 52.60; H, 3.58; N, 2.35.

Preparation of [Pd($C_{24}H_{20}NPS$)Cl_2] (58)

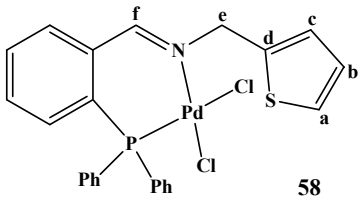

58

This complex was prepared from the reaction of **43** (0.10 g, 0.26 mmol) and Pd(COD)Cl_2 (0.07 g, 0.26 mmol) using the general procedure. The pure product was obtained as a yellow powder (0.97 g, 66 %). M.p. 233 - 234°C (decomp.). IR (KBr): 1629 cm^{-1} ($\upsilon_{C=N}$). ^{1}H NMR (DMSO-d_6): δ 8.81 (s, 1H, H_f), 7.98 (m, 1H, ArH), 7.93 (m, 1H, ArH), 7.74 (m, 1H, ArH), 7.55 (m, 2H, ArH), 7.41 (dt, 5H, J_{HH} = 2.9, 4.9 Hz, ArH), 7.91 (dd, 4H, J_{HH} = 7.8, 4.9 Hz, ArH), 7.18 (m, 2H, H_a, H_b), 6.90 (dd, 1H, J_{HH} = 2.9, 2.0 Hz, H_c), 5.66 (s, 2H, H_e),. ^{31}P NMR ($CDCl_3$): δ 31.8 (s). EI-MS: *m/z* 526.77 $[M\text{-}Cl]^+$. Anal. Calc. for

$C_{24}H_{20}Cl_2NPPdS$ (562.79): C, 51.22; H, 3.58; N, 2.49; S, 5.70. Found: C, 51.48; H, 3.44; N, 2.70; S, 5.97.

Preparation of [Pd($C_{25}H_{22}NPS$)Cl_2] (59)

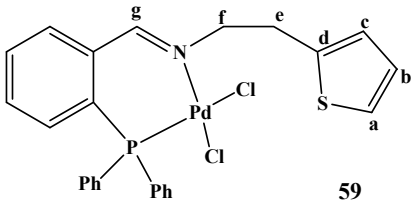

59

This complex was prepared from the reaction of **44** (0.21 g, 0.50 mmol) and Pd(COD)Cl_2 (0.14 g, 0.50 mmol) using the general procedure. The pure product was obtained as a yellow powder (0.23 g, 71 %). M.p. 203 – 205 °C (decomp.). IR (KBr): 1629 cm^{-1} ($\upsilon_{C=N}$). ^1H NMR (DMSO-d_6): δ 8.52 (s, 1H, H_g), 7.93 (dd, 1H, J_{HH} = 1.3, 7.6 Hz, ArH), 7.87 (m, 1H, ArH), 7.73 (tt, 1H, J_{HH} = 1.4, 7.5 Hz, ArH), 7.65 (m, 2H, ArH) 7.56 (dt, 4H, J_{HH} = 3.0, 7.6 Hz, ArH), 7.46 (m, 5H, ArH), 7.23 (dd, 1H, J_{HH} = 1.2, 5.1 Hz, H_a), 6.91 (dd. 1H, J_{HH} = 5.6, 7.7 Hz, ArH), 6.80 (dd, 1H, J_{HH} = 3.4, 5.1 Hz, H_b), 6.57 (dd, 1H, J_{HH} = 0.7, 3.4 Hz, H_c), 4.55 (t, 2H, J_{HH} = 7.7 Hz, H_f), 3.07 (t, 2H, J_{HH} = 7.7 Hz, H_c). ^{31}P NMR ($CDCl_3$): δ 32.3 (s). EI-MS: *m/z* 541.33 $[M\text{-}Cl]^+$. Anal. Calc. for $C_{25}H_{22}Cl_2NPPdS$ (576.81): C, 52.06; H, 3.84; N, 2.43; S, 5.56. Found: C, 52.22; H, 3.63; N, 2.70; S, 5.49.

Preparation of [Pd($C_{26}H_{22}NP$)Cl_2] (60)

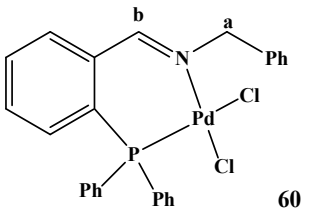

60

This complex was prepared from the reaction of **45** (0.21 g, 0.50 mmol) and Pd(COD)Cl_2 (0.14 g, 0.50 mmol) using the general procedure. The pure product was obtained as a yellow powder (0.23 g, 79 %). M.p. 199 - 201°C (decomp.). IR (KBr): 1627 cm^{-1} ($\upsilon_{C=N}$). ^1H NMR (DMSO-d_6): δ 8.83 (s, 1H, H_b), 8.02 (m, 1H, ArH), 7.91 (m, 1H, ArH), 7.75 (m, 1H, ArH), 7.56 (m, 2H, ArH), 7.38 (dt, 4H, J_{HH} = 2.7, 7.7 Hz, ArH), 7.25 (dd, 4H, J_{HH} = 1.8, 7.9 Hz, ArH), 7.13 (m, 5H, ArH), 6.98 (m, 1H, ArH), 5.50 (s, 2H, H_a). EI-MS: *m/z* 521.02 $[M\text{-}Cl]^+$. Anal. Calc. for $C_{26}H_{22}Cl_2NPPd$ (556.76): C, 56.09; H, 3.98; N, 2.54. Found: C, 55.86; H, 3.76; N, 2.48.

Preparation of [Pd($C_{11}H_{10}N_2O$)]Cl_2 (61)

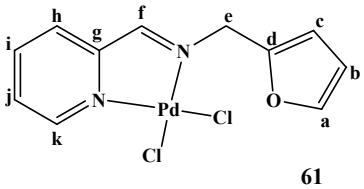

61

This complex was prepared from the reaction of **46** (2.07 g, 11.11 mmol) and Pd(COD)Cl_2 (3.17 g, 11.11 mmol) in DCM (20 mL) using the general procedure. The pure product was obtained as a yellow powder (3.36 g, 83 %). M.p. 221 – 225 °C

(decomp.). IR (KBr): 1625 cm^{-1} ($\upsilon_{C=N}$). ^1H NMR (DMSO-d_6): δ 8.96 (dd, 1H, J_{HH} = 0.8, 5.6 Hz, H_h), 8.58 (s, 1H, H_f), 8.32 (dt, 1H, J_{HH} = 1.5, 7.7 Hz, H_i), 8.19 (dd, 1H, J_{HH} = 1.1, 7.7 Hz, H_k), 7.83 -7.89 (m, 1H, H_j), 7.68 (dd, 1H, J_{HH} = 0.8, 1.8 Hz, H_a), 6.58 – 6.61 (m, 1H, H_b), 6.50 (dd, 1H, J_{HH} = 1.9, 3.2 Hz, H_c), 5.06 (s, 2H, H_e). ^{13}C NMR ($CDCl_3$): δ 172.0 (C_f), 155.5 (C_g), 150.0 (C_h), 147.6 (C_d), 143.6 (C_a), 141.1 (C_k), 128.7 ($C_{i,+}C_j$), 111.2 (C_b), 110.9 (C_c), 53.2 (C_e). EI-MS: *m/z* 328.12 $[M\text{-}Cl]^+$. Anal. Calc. for $C_{11}H_{10}Cl_2N_2OPd$ (363.54): C, 36.34; H, 2.77; N, 7.71. Found: C, 36.04; H, 3.02; N, 7.55.

Preparation of [Pd($C_{20}H_{30}$NOP)Cl_2] (62)

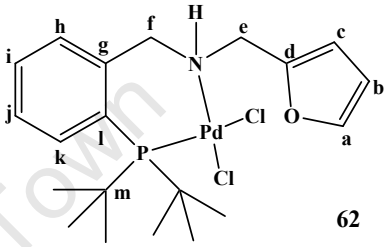

62

To a THF solution of **49** (0.5 g, 1.89 mmol) was added Mg (0.069 g, 2.85 mmol) and a crystal of I_2. The reaction mixture was refluxed for 4 h. The Grignard reagent was then cooled to -78° C, at which temperature $ClP(^tBu)_2$ (0.34 g, 1.89 mmol) was added dropwise to give a yellow solution. The reaction was allowed to warm up to room temperature and left to stir for 16 h. The resulting solution of the ligand was slowly added to a THF solution (20 mL) solution of $Pd(COD)Cl_2$ (0.53g, 1.89 mmol) to give a dark red reaction mixture. The reaction mixture was then allowed to stir at room temperature for 16 h. After removal of the solvent *in vacuo*, the resulting red solid was washed with hexane (3 x 10mL) to yield an dark red powder The resultant powder was recrystallized from DCM and hexane to give a pure product as a dark orange powder (0.64 g, 66 %). M.p. 185 – 189 °C. ^1H NMR ($CDCl_3$): δ 7.86 (dd, 1H, J_{HH} = 1.7, 7.5 Hz, H_h), 7.56 (dd, 1H, J_{HH} = 1.2, 7.9 Hz, H_k), 7.44 (dd, 1H, J_{HH} = 0.8, 1.8 Hz, H_a), 7.32 (dt, 1H, J_{HH} = 1.2, 7.5 Hz, H_i), 7.19 (dt, 1H, J_{HH} = 1.8, 7.7 Hz, H_j), 6.53 (br d, 1H, J_{HH} = 3.2 Hz, H_b), 6.36 (dd, 1H, J_{HH} = 1.9, 3.2 Hz, H_c), 4.53 (s, 1H, NH), 4.21 – 4.44 (m, 2H, H_f), 3.75 (m, 2H, H_e), 1.40 (dd, 18H, J_{HP} = 14.9, 16.7 Hz, CH_3). ^{13}C NMR ($CDCl_3$): δ 28.9 (t, J_{CP} = 5.2 Hz, CH_3), 43.3 (d, J_{CP} = 4.6 Hz, C_m), 47.3 (d, J_{CP} = 3.1 Hz, C_f), 54.1 (d, J_{CP} = 2.7 Hz, C_e), 110.4 (C_c), 110.7 (C_b), 125.2 (C_d), 127.6 (C_j), 130.0 (C_i), 133.0 (C_h), 133.9 (C_k), 135.1 (C_g), 143.0 (C_a). 149.2 (d, J_{CP} = 1.6 Hz, C_l). ^{31}P NMR ($CDCl_3$): δ 158.6 (s). EI-MS: *m/z* 473.51 $[M\text{-}Cl]^+$. Anal. Calc. for $C_{20}H_{30}Cl_2NOPPd$ (508.76): C, 47.22; H, 5.94; N, 2.75. Found: C, 47.13; H, 6.12; N, 2.86.

Preparation of [Pd($C_{30}H_{25}NO_2P$)Cl] (63)

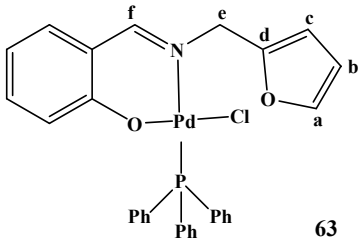

63

To a THF solution of **48** (0.21 g, 1.04 mmol) was added Et_3N (0.16 g, 1.57 mmol). The reaction mixture was allowed to stir at room temperature for 30 min. This mixture was slowly added to a THF solution (10 mL) of $Pd(COD)Cl_2$ (0.30 g, 1.04 mmol) at room temperature. PPh_3 (0.27 g, 1.04 mmol) was then added to give a dark orange solution which was left to stir for 16 h. The reaction mixture was then filtered through Celite, and solvent was removed *in vacuo* to give an orange solid. The crude product was recrystallized from DCM and hexane giving an orange crystalline solid (0.52 g, 82 %), M.p. 193 – 195 °C. IR (KBr): 1625 cm^{-1} ($\upsilon_{C=N}$). ^1H NMR ($CDCl_3$): δ 7.93 (d, 1H, J_{HH} = 16.8 Hz, H_f), 7.76 – 7.84 (m, 6H, ArH), 7.50 – 7.56 (m, 3H, ArH), 7.39 – 7.48 (m, 7H, ArH), 7.17 (dd, 1H, J_{HH} = 7.8, 1.6 Hz, H_a), 7.05 – 7.10 (m, 1H, ArH), 6.58 (d, 1H, J_{HH} = 3.2 Hz, ArH), 6.54 (dt, 1H, J_{HH} = 7.4, 0.9 Hz, ArH), 6.41 (dd, 1H, J_{HH} = 3.1, 1.8 Hz, H_b), 6.10 (d, 1H, J_{HH} = 8.3,Hz, H_c), 5.27 (d, 2H, J_{HP} = 2.4 Hz, H_e). ^{13}C NMR ($CDCl_3$): δ 163. 3 (C_f), 163.9 (ArC), 151.5 (C_d), 142. 6 (C_a), 135.1 (d, J_{CP} = 10.5 Hz, ArC), 134.9 (d, J_{CP} = 10.3 Hz, ArC), 134.6 (d, J_{CP} = 9.5 Hz, ArC), 130.9 (d, J_{CP} = 2.6 Hz, ArC), 128.7 (ArC), 128.1 (d, J_{CP} = 11.0 Hz, ArC), 120.6 (d, J_{CP} = 3.3 Hz, ArC), 120.4 (ArC), 115.3 (ArC), 110.6 (C_b), 110.0 (C_c), 55.0 (C_e). ^{31}P NMR ($CDCl_3$): δ 23.1 (s). EI-MS: *m/z* 357.03 $[M\text{-}Cl\text{-}PPh_3]^+$. Anal. Calc. for $C_{30}H_{25}ClNO_2PPd$ (604.37): C, 63.33; H, 4.43; N, 2.46. Found: C, 63.61; H, 4.38; N, 2.62.

5.6 Preparation of the Cationic Palladium Complexes (64 – 74)

General procedure

To a DCM solution (10 mL) of palladium methylchloride complex (*ca.* 0.3 – 0.4 mmol) **52 - 55** was added an equimolar amount of a halide abstracting reagent ($AgBF_4$, $AgPF_6$, or $NaBAr^F{}_4$) in acetonitrile (2 mL). A white precipitate of AgCl or NaCl formed immediately. The reaction was allowed to stir at room temperature for 1 h. The reaction mixture was filtered through Celite, leaving behind a white precipitate of AgCl or NaCl. The solvent was removed *in vacuo,* to give a crude yellow solid/oil. The crude product was then re-dissolved in DCM (5 mL) and filtered through Celite (where necessary). The crude product was recrystallized from a solution of DCM (*ca.* 3 mL) on addition of pentane (10 mL). The

mixture was then vigorously stirred for 10 min, during which time a yellow precipitate formed. The solid product was filtered and dried *in vacuo* to give a yellow powder.

Preparation of [Pd($C_{27}H_{26}N_2OP$)]BF_4 (64)

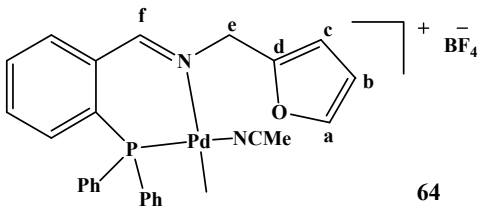

This complex was prepared from the reaction of **52** (0.20 g, 0.38 mmol) and $AgBF_4$ (0.07 g, 0.38 mmol) using the general procedure. The pure product was obtained as an off-white powder (0.19 g, 80 %). M.p. 252 – 255 °C. IR (KBr): 1637 ($\upsilon_{C=N}$), 2289, 2318 cm^{-1} ($\upsilon_{C\equiv N}$). Λ_M = 141 $\Omega^{-1}.cm^2.mol^{-1}$ (in 5 x 10^{-3} M nitrobenzene). ^1H NMR ($CDCl_3$): δ 8.47 (s, 1H, H_f), 7.79 – 7.84 (m, 1H, ArH), 7.70 (br t, 1H, J_{HH} =7.6 Hz, ArH), 7.49 – 7.55 (m, 2H, ArH), 7.41 (dt, 4H, J_{HH} = 7.6, 2.2 Hz, ArH), 7.13 – 7.21 (m, 5H, ArH+H_a), 7.07 (dd, 1H, J_{HH} = 10.4, 7.8 Hz, ArH), 6.36 (d, 1H, J_{HH} = 3.0 Hz, H_b), 6.33 (dd, 1H, J_{HH} = 3.1, 1.8 Hz, H_c), 2.46 (s, 3H, NCC$\underline{H}_3$), 0.32 (d, 3H, J_{HP} = 2.1 Hz, C$\underline{H}_3$). ^{13}C NMR ($CDCl_3$): δ 166.0 (d, J_{CP} = 5.1 Hz, C_f), 148.9 (C_d), 143.0 (C_a), 137.3 (d, J_{CP} = 8.9 Hz, ArC), 136.5 (d, J_{CP} = 14.0 Hz, ArC), 133.8 (d, J_{CP} = 12.3 Hz, C_n), 132.9 (d, J_{CP} = 7.6 Hz, ArC), 132.5 (d, J_{CP} = 2.3 Hz, ArC), 131.7 (d, J_{CP} = 2.6 Hz, ArC), 129.0 (d, J_{CP} = 11.7 Hz, ArC), 126.8 (d, J_{CP} = 57.8 Hz, ArC), 124.1 (d, J_{CP} = 47.5 Hz, ArC), 120.6 (N$\underline{C}CH_3$), 110.7 (C_b), 110.4 (C_c), 60.4 (C_e), 2.74 NC$\underline{C}H_3$), 2.5 (CH_3). ^{31}P NMR ($CDCl_3$): δ 39.3 (s). ESI-MS: *m/z* 577.72 $[M\text{-}NCCH_3]^+$. Anal. Calc. for $C_{27}H_{26}BF_4N_2OPPd$ (618.71): C, 52.41; H, 4.24; N, 4.53. Found: C, 52.22; H, 4.11; N, 4.72.

Preparation of [Pd($C_{27}H_{26}N_2OP$)]PF_6 (65)

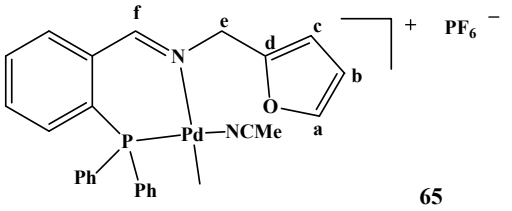

This complex was prepared from the reaction of **52** (0.21 g, 0.39 mmol) and $AgPF_6$ (0.09 g, 0.39 mmol) using the general procedure. The pure product was obtained as a pale yellow powder (0.22 g, 83 %). M.p. 233 – 236 °C. IR (KBr): 1637 cm^{-1} ($\upsilon_{C=N}$), 2284, 2318 cm^{-1} ($\upsilon_{C\equiv N}$). Λ_M = 132 $\Omega^{-1}.cm^2.mol^{-1}$ (in 5 x 10^{-3} M nitrobenzene). ^1H NMR ($CDCl_3$): δ 8.29 (s, 1H, H_f), 7.86 – 7.91 (m, 1H, ArH), 7.81 (t, 1H, J_{HH} = 7.6 Hz, ArH), 7.70 (t, 1H, J_{HH} = 7.6 Hz, ArH), 7.54 – 7.61 (m, 2H, ArH), 7.43 – 7.52 (m, 6H, ArH), 7.19 – 7.27 (m, 5H, ArH), 7.11 – 7.18 (m, 1H, ArH), 6.45 (br s, 1H, H_b), 6.38 (br s, 1H, H_c), 5.06 (s, 2H, H_e), 2.05 (s, 3H, $NCCH_3$), 0.14 (d,

3H, J_{HP} = 2.0 Hz, CH_3). ^{13}C NMR ($CDCl_3$): δ 167.0 (d, J_{CP} = 4.8 Hz, C_f), 150.2 (C_d), 144.2 (C_a), 137.8 (d, J_{CP} = 8.9 Hz, ArC), 136.6 (d, J_{CP} = 13.7 Hz, ArC), 134.7 (d, J_{CP} = 12.2 Hz, ArC), 134.2 (ArC), 133.2 (ArC), 132.4 (ArC), 129.8 (d, J_{CP} = 11.4 Hz, ArC), 127.29 (d, J_{CP} = 57.9 Hz, ArC), 124.8 (d, J_{CP} = 47.4 Hz, ArC), 118.0 ($N\underline{C}CH_3$), 111.3 (C_b), 110.5 (C_c), 57.0 (C_e), 5.1 ($NC\underline{C}H_3$), 1.8 (CH_3). ^{31}P NMR ($CDCl_3$): δ -143.9 (sept, PF_6^-), 40.9 (s). ESI-MS: *m/z* 490.97 $[M\text{-}NCCH_3\text{-}PF_6]^+$. Anal. Calc. for $C_{27}H_{26}F_6N_2OP_2Pd$ (676.9): C, 47.91; H, 3.87; N, 4.14. Found: C, 48.22; H, 3.93; N, 3.92.

Preparation of $[Pd(C_{59}H_{38}N_2OP)]BAr^F_4$ (66)

This complex was prepared from the reaction of **52** (0.23 g, 0.43 mmol) and $NaBAr^F_4$ (0.38 g, 0.43 mmol) using the general procedure. The pure product was obtained as an off-white powder (0.39 g, 65 %). M.p. 202 – 206 °C. IR (KBr): 1640 ($\upsilon_{C=N}$), 2286, 2317 cm^{-1} ($\upsilon_{C\equiv N}$). Λ_M = 131 $\Omega^{-1}.cm^2.mol^{-1}$ (in 5 x 10^{-3} M nitrobenzene). ^1H NMR ($CDCl_3$): δ 8.23 (s, 1H, H_f), 7.72 – 7.76 (m, 8H, ArH), 7.61 – 7.66 (m, 1H, ArH), 7.51 – 7.58 (m, 8H, ArH), 7.43 (dt, 4H, J_{HH} = 7.6, 2.4 Hz, ArH), 7.43 – 7.24 (m, 6H, ArH), 7.11- 7.24 (m, 6H, ArH), 6.32 (dd, 1H, J_{HP} = 3.1, 1.9 Hz, H_b), 6.14 (d, 1H, J_{HH} = 3.3 Hz, H_c), 4.87 (s, 2H, H_e), 2.27 ($NCCH_3$), 0.41 (d, 3H, J_{HP} = 2.1 Hz, CH_3). ^{13}C NMR ($CDCl_3$): δ 166.0 (d, J_{CP} = 5.0 Hz, C_f), 161.7 (dd, (q, J_{CP} = 50.0 Hz, Ar^FC), 147.7 (C_d), 143.6 (C_a), 136.8 (d, J_{CP} = 8.9 Hz, ArC), 135.7 (d, J_{CP} = 13.8 Hz, ArC), 134.8 (br s, Ar^FC), 134.4 (d, J_{CP} = 2.4 Hz, ArC), 133.8 (d, J_{CP} = 12.4 Hz, ArC), 133.6 (ArC), 132.5 (d, J_{CP} = 1.9 Hz, ArC), 132.1 (d, J_{CP} = 2.2 Hz, ArC), 129.3 (d, J_{CP} = 11.8 Hz, ArC), 129.1 (Ar^FC), 128.6 (m, Ar^FC), 126.5 (d, J_{CP} = 59.4 Hz, ArC), 124.4 (d, J_{CP} = 47.1 Hz, ArC), 123.2 (ArC), 120.5 ($N\underline{C}CH_3$), 117.5 (Ar^FC), 110.9 (C_b), 110.3 (C_c), 60.6 (C_e), 3.0 ($NC\underline{C}H_3$), 2.4 ($\underline{C}H_3$). ^{31}P NMR ($CDCl_3$): δ 39.0 (s). ESI-MS: *m/z* 490.88 $[M\text{-}NCCH_3]^+$. Anal. Calc. for $C_{59}H_{38}BF_{24}N_2OPPd$ (1395.11): C, 50.79; H, 2.75; N, 2.01. Found: C, 51.04; H, 2.86; N, 2.13.

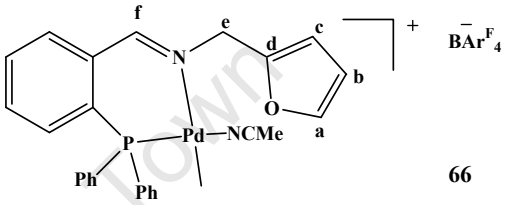

66

Preparation of $[Pd(C_{27}H_{26}N_2PS)]BF_4$ (67)

This complex was prepared from the reaction of **53** (0.20 g, 0.37 mmol) and $AgBF_4$ (0.07 g, 0.37 mmol) using the general procedure. The pure product was obtained as a pale yellow powder (0.18 g, 76 %). M.p.

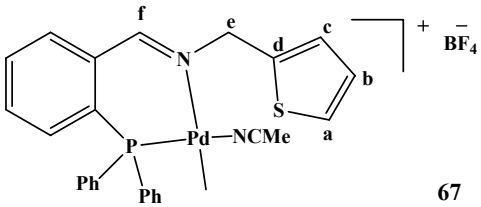

67

227 – 229 °C. IR (KBr): 1639 ($\upsilon_{C=N}$), 2283, 2318 cm^{-1} ($\upsilon_{C\equiv N}$). Λ_M = 131 $\Omega^{-1}.cm^2.mol^{-1}$ (in 5 x 10^{-3} M nitrobenzene). ^{1}H NMR ($CDCl_3$): δ 8.82 (s, 1H, H_f), 7.85 – 7.92 (m, 1H, ArH), 7.81 (t, 1H, J_{HH} = 7.3 Hz, ArH), 7.69 (t, 1H, J_{HH} = 7.7 Hz, ArH), 7.52 – 7.59 (m, 2H, ArH), 7.40 - 7.51 (m, 6H, ArH **)**, 7.08 – 7.25 (m, 7H, ArH +H_a), 6.91 – 6.99 (m, 2H, H_{a+b}), 5.20 (s, 2H, H_e), 2.05 (NCC$\underline{H}_3$), 0.19 (d, 3H, J_{HP} = 2.0 Hz, C$\underline{H}_3$),. ^{13}C NMR ($CDCl_3$): δ 166.2 (d, J_{CP} = 5.2 Hz, C_f), 139.4 (C_d), 137.8 (d, J_{CP} = 8.9 Hz, C_d), 136.7 (d, J_{CP} = 14.1 Hz, ArC), 134.3 (d, 2.0 Hz, ArC), 134.1 (d, J_{CP} = 12.2 Hz, ArC), 133.2 (d, J_{CP} = 1.7 Hz, ArC), 132.3 (d, J_{CP} = 2.3 Hz, ArC), 129.8 (d, J_{CP} = 11.5 Hz, ArC), 128.4 (C_a), 128.0 (d, J_{CP} = 57.6 Hz, ArC), 127.9 (C_b), 127.5 (C_c), 124.7 (d, J_{CP} = 47.4 Hz, ArC), 118.7 (N$\underline{C}$CH$_3$), 50.9 (C_e), 5.1 (NC$\underline{C}$H$_3$), 0.45 (d, J_{HP} = 2.1 Hz,CH_3). ^{31}P NMR ($CDCl_3$): δ 40.3 (s). ESI-MS: *m/z* 593.54 $[M\text{-}NCCH_3]^+$. Anal. Calc. for $C_{27}H_{26}BF_4N_2PPdS$ (634.77): C, 51.09; H, 4.13; N, 4.41; S, 5.05. Found: C, 51.02; H, 4.31; N, 3.88; S, 4.49.

Preparation of [Pd($C_{27}H_{26}N_2PS$)]PF_6 (68)

This complex was prepared from the reaction of **53** (0.20 g, 0.37 mmol) and $AgPF_6$ (0.09 g, 0.37 mmol) using the general procedure. The pure product was obtained as a pale yellow powder (0.21 g, 81 %). M.p. 245 – 257 °C. IR (KBr): 1637 ($\upsilon_{C=N}$), 2289, 2318 cm^{-1} ($\upsilon_{C\equiv N}$). Λ_M = 140 $\Omega^{-1}.cm^2.mol^{-1}$ (in 5 x 10^{-3} M nitrobenzene). ^{1}H NMR ($CDCl_3$): δ 8.47 (s, 1H, H_f), 7.79 – 7.84 (m, 1H, H_i), 7.70 (br t, 1H, J_{HH} = 7.6 Hz, H_j), 7.49 – 7.55 (m, 2H, H_p), 7.41 (dt, 4H, J_{HH} = 7.6, 2.2 Hz, H_o), 7.13 – 7.21 (m, 5H, H_n, H_a), 7.07 (dd, 1H, J_{HH} = 10.4, 7.8 Hz, H_k), 6.36 (d, 1H, J_{HH} = 3.0 Hz, H_b), 6.87 (d, 1H, J_{HH} = 2.8 Hz, H_c), 5.25 (s, 2H, H_e), 2.39 (s, 3H, NCC$\underline{H}_3$), 0.42 (d, 3H, J_{HP} = 1.8 Hz, C$\underline{H}_3$). ^{13}C NMR ($CDCl_3$): δ 165.2 (d, J_{CP} = 5.0 Hz, C_f), 138.2 (C_d), 137.4 (d, J_{CP} = 8.9 Hz, Ar), 136.4 (d, J_{CP} = 14.2 Hz, Ar), 134.0 (d, J_{CP} = 2.0, Ar), 133.7 (d, J_{CP} = 12.3, Ar), 133.0 (d, J_{CP} = 7.6 Hz, Ar), 132.6 (d, J_{CP} = 1.7 Hz, ArC), 131.7 (d, J_{CP} = 2.3 Hz, ArC), 129.1 (d, J_{CP} = 11.7 Hz, Ar), 128.1 (C_a), 128.0 (C_b), 126.9 (d, J_{CP} = 57.4 Hz, ArC),126.2 (C_c), 124.0 (d, J_{CP} = 47.1 Hz, ArC), 120.5 (N$\underline{C}$CH$_3$), 61.9 (C_e), 2.6 (NC$\underline{C}$H$_3$), 2.5 ($\underline{C}$H$_3$). ^{31}P NMR ($CDCl_3$): δ 143.9 (sept), 38.5 (s). ESI-MS: *m/z* 652.01 $[M\text{-}NCCH_3]^+$. Anal. Calc. for $C_{27}H_{26}F_6N_2P_2PdS$ (692.93): C, 46.80; H, 3.78; N, 4.40; S, 4.63. Found: C, 46.98; H, 3.65; N, 3.49; S, 4.58.

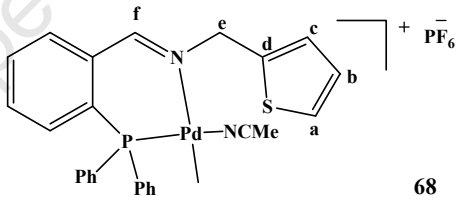

68

Preparation of [Pd($C_{59}H_{38}N_2PS$)] BAr^F_4 (69)

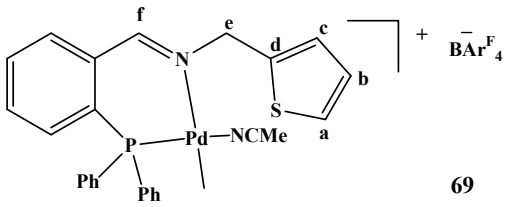

69

This complex was prepared from the reaction of **53** (0.11 g, 0.19 mmol) and $NaBAr^F_4$ (0.17 g, 0.19 mmol) using the general procedure. The pure product was obtained as a off-white powder (0.23 g, 85 %). M.p. 219 – 223 °C. IR (KBr): 1643 ($\upsilon_{C=N}$), 2290, 2318 cm^{-1} ($\upsilon_{C\equiv N}$). Λ_M = 135 $\Omega^{-1}.cm^2.mol^{-1}$ (in 5 x 10^{-3} M nitrobenzene). ^1H NMR ($CDCl_3$): δ 8.23 (s, 1H, H_f), 7.70 – 7.77 (m, 8H, ArH), 7.46 – 7.65 (m, 9H, ArH), 7.39 (dt, 4H, J_{HH} = 7.5, 2.7 Hz, ArH), 7.27 (dd, 1H, J_{HH} = 5.1, 1.0 Hz, H_a), 7.06 – 7.20 (m, 6H, ArH), 6.92 (dd, 1H, J_{HH} = 5.2, 3.5Hz, H_b), 6.70 (dd, 1H, J_{HH} = 3.4, 0.9 Hz, H_c), 5.05 (s, 2H, H_e), 2.23 (s, 3H, $NCCH_3$), 0.45 (d, 2H, J_{HP} = 2.1Hz, CH_3). ^{13}C NMR ($CDCl_3$): δ 165.2 (d, J_{CP} = 4.9 Hz, C_f), 161.7 (q, J_{CP} = 49.9 Hz, Ar^FC), 137.0 (d, J_{CP} = 8.6 Hz, ArC), 135.7 (d, J_{CP} = 13.7 Hz, ArC), 134.8 (br s, Ar^FC), 134.7 (d, J_{CP} = 2.2 Hz, ArC), 133.7 (d, J_{CP} = 12.3 Hz, ArC), 132.6 (d, J_{CP} = 1.7 Hz, ArC), 132.2 (d, J_{CP} = 2.3 Hz, ArC), 129.3 (d, J_{CP} = 11.8 Hz, ArC), 129.1 (m, Ar^FC), 128.8 (m, Ar^FC), 128.4 (ArC), 127.7 (C_a), 128.4 (C_b), 126.3 (d, J_{CP} = 58.4 Hz, ArC), 125.9 (C_c) 124.3 (d, J_{CP} = 47.1 Hz, ArC), 123.2 (ArC), 120.5 (C_c), 119.7 ($N\underline{C}CH_3$), 117.5 (m, Ar^FC), 62.2 (C_e), 2.9 ($NC\underline{C}H_3$), 2.4 ($\underline{C}H_3$). ^{31}P NMR ($CDCl_3$): δ 38.3 (s). ESI-MS: *m/z* 506.89 $[M\text{-}NCCH_3\text{-}BAr^F_4]^+$. Anal. Calc. for $C_{59}H_{38}BF_{24}N_2PPdS$ (1411.18): C, 50.22; H, 2.71; N, 1.99; S, 2.27. Found: C, 50.51; H, 2.99; N, 1.73; S, 2.50.

Preparation of [Pd($C_{28}H_{28}N_2PS$)] BF_4 (70)

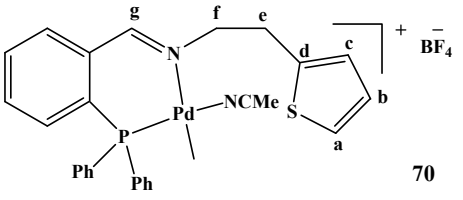

70

This complex was prepared from the reaction of **54** (0.21 g, 0.38 mmol) and $AgBF_4$ (0.07 g, 0.38 mmol) using the general procedure. The pure product was obtained as a pale yellow powder (0.18 g, 73 %). M.p. 232 – 236 °C. IR (KBr): 1634 ($\upsilon_{C=N}$), 2278, 2313 cm^{-1} ($\upsilon_{C\equiv N}$). Λ_M = 133 $\Omega^{-1}.cm^2.mol^{-1}$ (in 5 x 10^{-3} M nitrobenzene). ^1H NMR ($CDCl_3$): δ 8.28 (s, 1H, H_g), 7.66 – 7.74 (m, 2H, ArH), 7.50 – 7.59 (m, 3H, ArH), 7.46 (dt, 4H, J_{HH} = 7.6, 2.5 Hz, ArH), 7.25 – 7.33 (m, 4H, ArH), 7.11 (d, 1H, J_{HH} = 5.1 Hz, H_a), 7.02 – 7.08 (m, 1H, ArH), 6.79 (dd, 1H, J_{HH} = 5.1, 3.5 Hz, H_b), 6.58 (d, 1H, J_{HH} = 3.2 Hz, H_c), 4.30 (t, 2H, J_{HH} = 6.6 Hz, H_f), 3.25 (t, 2H, J_{HH} = 6.6 Hz, H_e), 2.27 (s, 3H, $NCCH_3$), 0.37 (d, 3H, J_{HP} = 2.1 Hz, CH_3). ^{13}C NMR ($CDCl_3$): δ 165.7 (d, J_{CP} = 5.0

Hz, C_g), 140.0 (C_d), 137.7 (d, J_{CP} = 9.1 Hz, ArC), 136.6 (d, J_{CP} =14.5 Hz, ArC), 134.5 (d, J_{CP} = 1.6 Hz, ArC), 133.8 (d, J_{CP} = 12.2 Hz, ArC), 133.0 (d, J_{CP} = 7.5 Hz, ArC), 132.8 (ArC), 132.0 (d, J_{CP} = 1.7 Hz, ArC), 129.3 (d, J_{CP} = 11.6 Hz, ArC), 128.2 (C_a), 127.5 (d, J_{CP} = 57.1 Hz, ArC), 125.0 (C_b), 124.9 (C_c), 124.2 (d, J_{CP} = 46.8 Hz, ArC), 119.1, N$\underline{C}CH_3$), 65.5 (C_f), 31.0 (C_e), 5.1 (NC$\underline{C}H_3$), 2.4 ($\underline{C}H_3$). ^{31}P NMR ($CDCl_3$): δ 40.32 (s). ESI-MS: *m/z* 607.91 [M-$NCCH_3$]$^+$. Anal. Calc. for $C_{28}H_{28}BF_4N_2PPdS$ (648.80): C, 51.83; H, 4.35; N, 4.32; S, 4.99. Found: C, 52.00; H, 4.03; N, 4.31; S, 5.21.

Preparation of [Pd($C_{28}H_{28}N_2PS$)] PF_6 (71)

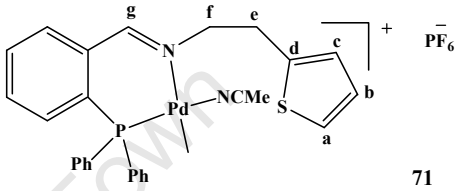

71

This complex was prepared from the reaction of **54** (0.22 g, 0.39 mmol) and $AgPF_6$ (0.08g, 0.39 mmol) using the general procedure. The pure product was obtained as a pale yellow powder (0.25 g, 90 %). M.p. 243 – 245 °C. IR (KBr): 1637 ($\upsilon_{C=N}$), 2278, 2306 cm^{-1} ($\upsilon_{C\equiv N}$). Λ_M = 144 Ω^{-1}.cm^2.mol^{-1} (in 5 x 10^{-3} M nitrobenzene). ^{1}H NMR ($CDCl_3$): δ 8.45 (s, 1H, H_g), 7.78 – 7.82 (m, 2H, ArC), 7.53 – 7.72 (m, 7H, ArC), 7.36 – 7.45 (m, 4H, ArC), 7.23 (dd, 1H, J_{HH} = 5.1, 1.2 Hz, H_a), 7.08 (dd, 1H, J_{HH} = 10.4, 7.9 Hz, ArC), 6.73 (dd, 1H, J_{HH} = 4.9, 3.6 Hz, H_b), 6.48 (d, 1H, J_{HH} = H_c), 4.09 (t, 2H, J_{HH} = 7.0 Hz, H_f), 3.15 (t, 2H, J_{HH} = 7.0 Hz, H_e), 2.05 (s, 3H, $NCCH_3$), 0.35 (d, 3H, J_{HP} = 1.7.1 Hz, CH_3). ^{13}C NMR ($CDCl_3$): δ 165.6 (d, J_{CP} = 5.2 Hz, C_g), 139.8 (C_d), 137.0 (d, J_{CP} = 9.1 Hz, ArC), 136.0 (d, J_{CP} = 14.4 Hz, ArC), 134.0 (d, J_{CP} = 1.9 Hz, ArC), 133.3 (d, J_{CP} = 12.2 Hz, ArC), 133.1 (ArC), 132.5 (d, J_{CP} = 1.9 Hz, ArC), 131.7 (d, J_{CP} = 2.2 Hz, ArC), 129.1 (d, J_{CP} = 11.5 Hz, ArC), 127.6 (d, J_{CP} = 58.2 Hz, ArC), 126.7 (C_a), 125.5 (C_b), 124.2 (C_c), 122.8 (d, J_{CP} = 47.4 Hz, ArC), 120.2 (N$\underline{C}CH_3$), 62.1 (C_f), 30.4 (C_e), 4.8 (NC$\underline{C}H_3$), 0.89 ($\underline{C}H_3$). ^{31}P NMR ($CDCl_3$): δ 143.0 (sept), 40.6 (s). ESI-MS: *m/z* 665.63 [M-$NCCH_3$]$^+$. Anal. Calc. for $C_{28}H_{28}F_6N_2P_2PdS$ (706.96): C, 47.57; H, 3.99; N, 3.96; S, 4.54. Found: C, 47.78; H, 4.12; N, 3.56; S, 4.76.

Preparation of [Pd($C_{29}H_{28}N_2P$)] BF_4 (72)

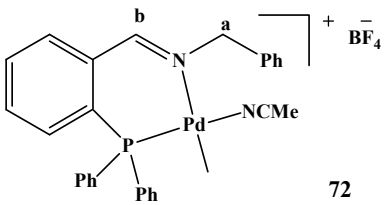

72

This complex was prepared from the reaction of **55** (0.20 g, 0.37 mmol) and $AgBF_4$ (0.07 g, 0.37 mmol) using the general procedure. The pure product was obtained as a pale yellow powder (0.20 g, 86 %). M.p. 223 – 225 °C. IR (KBr): 1634 ($\upsilon_{C=N}$), 2278, 2312 cm^{-1} ($\upsilon_{C\equiv N}$). Λ_M = 134 Ω^{-1}.cm^2.mol^{-1} (in 5 x 10^{-3} M nitrobenzene). ^{1}H NMR

($CDCl_3$): δ 8.53 (s, 1H, H_b), 7.86 (dd, J_{HH} = 6.5, 4.5 Hz, ArH), 7.72 (br t, 1H, J_{HH} = 7.6 Hz, ArH), 7.53 (br t, 3H, J_{HH} = 8.0 Hz, ArH), 7.40 (br t, 4H, J_{HH} = 6.6 Hz, ArH), 7.12 – 7.28 (m, 1H, ArH), 7.10 – 7.19 (m, 6H, ArH), 6.97 – 7.06 (m, 3H, ArH), 5.14 (s, 2H, H_a), 2.39 (s, 3H, $NCCH_3$), 0.30 (d, 3H, J_{HP} = 2.0 Hz, CH_3),. ^{13}C NMR ($CDCl_3$): δ 165.9 (C_b), 137.5 (d, J_{CP} = 9.0 Hz, Ar), 136.7 (d, J_{CP} = 14.3 Hz, Ar), 136.0 (ArC), 134.1 (d, J_{CP} = 2.0 Hz, ArC), 133.7 (d, J_{CP} = 12.3 Hz, ArC), 132.9 (d, J_{CP} = 6.1 Hz, ArC), 132.7 (d, J_{CP} = 1.9 Hz, ArC), 131.7 (d, J_{CP} = 2.2 Hz, ArC), 129.1 (d, J_{CP} = 11.6 Hz, ArC), 128.8 (ArC), 128.1 (ArC), 127.7 (ArC), 127.0 (d, J_{CP} = 57.5 Hz, ArC), 123.4 (d, J_{CP} = 47.7 Hz, ArC), 120.4 ($N\underline{C}CH_3$), 68.2 (C_a), 4.7 ($NC\underline{C}H_3$), 2.5 ($\underline{C}H_3$). ^{31}P NMR ($CDCl_3$): δ 38.6 (s). ESI-MS: *m/z* 587.83 $[M\text{-}NCCH_3]^+$. Anal. Calc. for $C_{29}H_{28}BF_4N_2PPd$ (628.74): C, 55.40; H, 4.49; N, 4.46; S, 4.54. Found: C, 55.54; H, 4.67; N, 4.23; S, 4.00.

Preparation of [Pd($C_{29}H_{28}N_2P$)] PF_6 (73)

This complex was prepared from the reaction of **55** (0.21 g, 0.39 mmol) and $AgPF_6$ (0.10 g, 0.39 mmol) using the general procedure. The pure product was obtained as a pale yellow powder (0.18 g, 67 %), M.p. 212 – 216 °C. IR (KBr): 1638 ($\upsilon_{C=N}$), 2287, 2317 cm^{-1} ($\upsilon_{C\equiv N}$). Λ_M = 130 $\Omega^{-1}.cm^2.mol^{-1}$ (in 5 x 10^{-3} M nitrobenzene). ^{1}H NMR ($CDCl_3$): δ 8.82 (s, 1H, H_b), 7.88 (m, 1H, ArH), 7.83 (br t, 1H, J_{HH} = 7.1 Hz, ArH), 7.69 (br t, 1H, J_{HH} = 7.5 Hz, ArH), 7.53 – 7.60 (m, 2H, ArH), 7.45 (dt, 4H, J_{HH} = 7.6, 2.3 Hz, ArH), 7.25 – 7.32 (m, 1H, ArH), 7.14 – 7.24 (m, 8H, ArH), 7.09 (dd, 1H, J_{HH} = 10.5, 7.7 Hz, ArH), 5.00 (s, 2H, H_a), 2.05 (s, 3H, $NCCH_3$), 0.18 (d, 3H, J_{HP} = 1.3Hz, CH_3). ^{13}C NMR ($CDCl_3$): δ 166.7 (d, J_{CP} = 4.8 Hz, ArC), 138.0 (d, J_{CP} = 8.9 Hz, ArC), 137.6 (ArC), 136.9 (d, J_{CP} = 14.2 Hz, ArC), 134.5 (ArC), 134.1 (d, J_{CP} = 12.3 Hz, ArC), 134.0 (ArC), 133.3 (ArC), 132.4 (ArC), 129.8 (d, J_{CP} = 11.5 Hz, ArC), 129.2 (ArC), 128.9 (ArC), 128.3 (d, J_{CP} = 57.7 Hz, ArC), 123.3 (ArC), 124.2 (d, J_{CP} = 47.7 Hz, ArC), 120.8 ($N\underline{C}CH_3$), 64.5 (C_a), 5.3 ($NC\underline{C}H_3$), 1.79 ($\underline{C}H_3$). ^{31}P NMR ($CDCl_3$): δ – 142.1 (sept, PF_6^-), 41.0 (s). ESI-MS: *m/z* 646.03 $[M\text{-}NCCH_3]^+$. Anal. Calc. for $C_{29}H_{28}F_6N_2P_2Pd$ (686.90): C, 50.71; H, 4.11; N, 4.08. Found: C, 50.59; H, 4.08; N, 4.31.

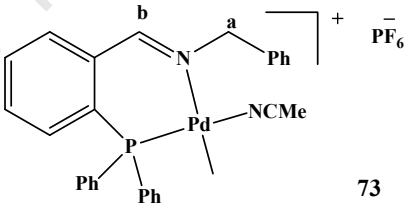

73

Preparation of [Pd($C_{61}H_{40}N_2P$)] BAr^F_4 (74)

This complex was prepared from the reaction of **55** (0.20 g, 0.37 mmol) and $NaBAr^F_4$ (0.33 g, 0.37 mmol) using the

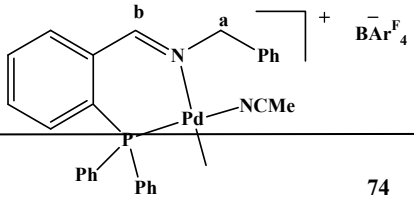

74

general procedure. The pure product was obtained as a pale yellow powder (0.36 g, 68 %). M.p. 224 – 225 °C. IR (KBr): 1640 ($\upsilon_{C=N}$), 2289, 2318 ($\upsilon_{C\equiv N}$) cm^{-1}. Λ_M = 142 $\Omega^{-1}.cm^2.mol^{-1}$ (in 5 x 10^{-3} M nitrobenzene). ^1H NMR ($CDCl_3$): δ 8.27 (s, 1H, H_b), 7.71 – 7.77 (m, 8H, ArH), 7.61 – 7.68 (m, 1H, ArH), 7.50 – 7.58 (m, 8H, ArH), 7.37 – 7.45 (m, 4H, ArH), 7.27 – 7.34 (m, 1H, ArH), 7.07 – 7.24 (m, 7H, ArH), 6.94 (d, 2H, J_{HH} = 6.2 Hz, ArH), 4.99 (s, 2H, H_a), 2.16 (s, 3H, $NCCH_3$), 0.40 (s, 3H, CH_3). ^{13}C NMR ($CDCl_3$): δ 165.7 (C_b), 161.7 (dd, J_{CF} = 99.6, 49.7 Hz, ArC), 136.8 (d, J_{CP} = 8.3 Hz, ArC), 135.8 (ArC), 135.0 (ArC), 134.8 (br s, Ar^FC), 133.6 (d, J_{CP} = 12.3 Hz, ArC), 132.6 (br s, ArC), 132.1 (br s, ArC), 130.0 (ArC), 129.6 (ArC), 129.3 (d, J_{CP} = 11.9 Hz, ArC), 129.2 (ArC), 128.7 (dd, J_{CF} = 5.5, 2.7 Hz, Ar^FC), 128.4 (ArC), 127.6 (m, Ar^FC), 126.5 (d, J_{CP} = 55.6 Hz, ArC), 126.3 (ArC), 122.7 ($N\underline{C}CH_3$), 119.4 (d, J_{CP} = 43.1 Hz, ArC), 117.5 (Ar^FC), 68.3 (C_a), 3.3 ($NC\underline{C}H_3$), 2.3 ($\underline{C}H_3$). ^{31}P NMR ($CDCl_3$): δ 38.52 (s). ESI-MS: *m/z* 1364.43 $[M\text{-}NCCH_3]^+$. Anal. Calc. for $C_{61}H_{40}BF_{24}N_2PPd$ (1405.15): C, 52.14; H, 2.87; N, 1.99, . Found: C, 52.39; H, 2.96; N, 1.73.

5.7 Preparation of Nickel Complexes

General procedure

To a stirred suspension of $Ni(DME)Br_2$ (*ca.*0.26 mmol) in DCM (10 mL) was slowly added an equimolar amount of the appropriate ligand (**41** – **47**) in DCM (10 mL) at room temperature. The reaction mixture was allowed to stir for 18 h. In cases where the product precipitated out of solution, a small amount of diethyl ether was added to complete precipitation. The solid product was then filtered and washed with ice-cooled DCM (3 x 20 mL). Where a homogeneous solution was obtained, the solvent was removed and the resultant solid product recrystallized from DCM and diethyl ether to give the product as a green, dark purple, or pale brown powder.

Preparation of $Ni(C_{25}H_{21}N_2P)Br_2$ (75)

This complex was prepared from a reaction of **41** (0.11 g, 0.29 mmol) in 10 ml DCM and $Ni(DME)Br_2$ (0.09 g, 0.29 mmol) in 5 ml DCM. The pure product was isolated as a pale brown powder (0.12 g, 69 %). M.p. 176 – 178 °C. IR (KBr): 1625 cm^{-1} ($\upsilon_{C=N}$). EI-MS: *m/z* 518.88 $[M\text{-}Br]^+$. Anal. Calc. for $C_{25}H_{21}Br_2N_2NiP$ (598.92): C, 50.13; H, 3.53; N, 4.68. Found: C, 49.87; H, 3.55; N, 4.66.

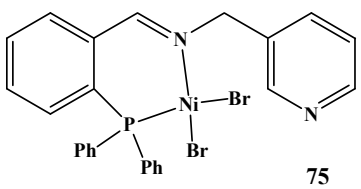

75

Preparations of Ni($C_{24}H_{20}$NOP)Br_2 (76)

This compound was prepared from a reaction of **42** (0.10 g, 0.26 mmol) and Ni(DME)Br_2 (0.08 g, 0.26 mmol). The pure product was obtained as a dark purple powder (0.14 g, 91 %). M.p. 169 – 171 °C. IR (KBr): 1628 cm^{-1} ($\upsilon_{C=N}$). EI-MS: *m/z* 508.36 $[M-Br]^+$. Anal. Calc. for $C_{24}H_{20}Br_2NNiOP$ (587.90): C, 49.03; H, 3.43; N, 2.38. Found: C, 49.17; H, 3.49; N, 2.12.

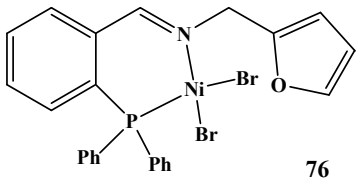

76

Preparations of Ni($C_{24}H_{20}$NPS)Br_2 (77)

This complex was prepared from the reaction of **43** (0.13 g, 0.26 mmol) and Ni(DME)Br_2 (0.08 g, 0.26 mmol). The pure product was obtained as a dark purple solid (0.13 g, 82 %). M.p. 179 – 182 °C. IR (KBr): 1626 cm^{-1} ($\upsilon_{C=N}$). EI-MS: *m/z* 524.19 $[M-Br]^+$. Anal. Calc. for $C_{24}H_{20}Br_2NNiPS$ (603.96): C, 47.73; H, 3.34; N, 2.32; S, 5.31. Found:C, 47.43; H, 3.45; N, 2.23; S, 5.13.

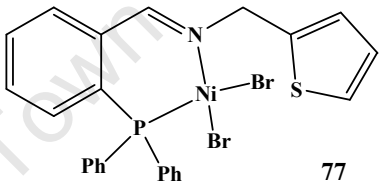

77

Preparations of Ni($C_{25}H_{22}$NPS)Br_2 (78)

This complex was prepared from the reaction of **44** (0.10 g, 0.25 mmol) and Ni(DME)Br_2 (0.08 g, 0.25 mmol). The pure product was obtained as a pale brown powder (0.12 g, 77 %). M.p. 183 – 186 °C. IR (KBr): 1625 cm^{-1} ($\upsilon_{C=N}$). EI-MS: *m/z* 538.24 $[M-Br]^+$. Anal. Calc. for $C_{25}H_{22}Br_2NNiPS$ (617.99): C, 48.59; H, 3.59; N, 2.27; S, 5.19. Found: C, 48.36; H, 3.65; N, 2.04; S, 5.24.

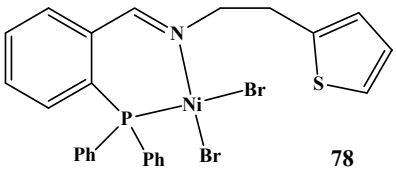

78

Preparation of Ni($C_{26}H_{22}$NP)Br_2 (79)

This complex was prepared from the reaction of **45** (0.12 g, 0.26 mmol) and Ni(DME)Br_2 (0.08 g, 0.26 mmol). The pure product was obtained as a pale brown powder (0.14 g, 90 %). M.p. 172 – 173 °C. IR (KBr): 1618 cm^{-1} ($\upsilon_{C=N}$). EI-MS: *m/z* 517.79 $[M-Br]^+$. Anal. Calc. for $C_{26}H_{22}Br_2NNiP$ (597.93): C, 52.23; H, 3.71; N, 2.34. Found: C, 52.11; H, 3.73; N, 2.52.

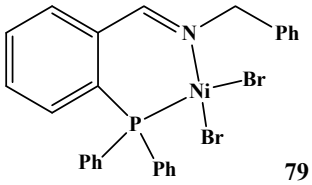

79

Preparation of $Ni(C_{11}H_{10}N_2O)Br_2$ (80)

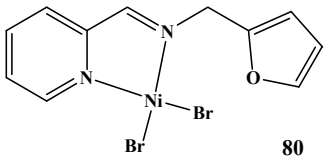

80

This complex was prepared from the reaction of **46** (0.11 g, mmol) and $Ni(DME)Br_2$ (g, 0.26 mmol). The pure product was obtained as a green powder (0.19 g, 79.4 %). M.p. 177 – 180 °C. IR (KBr): 1622 ($\upsilon_{C=N}$). EI-MS: *m/z* 324.85 $[M\text{-}Br]^+$. Anal. Calc. for $C_{11}H_{10}Br_2N_2NiO$ (404.71): C, 32.64; H, 2.43; N, 6.92. Found: C, 32.36; H, 2.33; N, 7.11 .

Preparation of $Ni(C_{20}H_{30}NOP)Br_2$ (81)

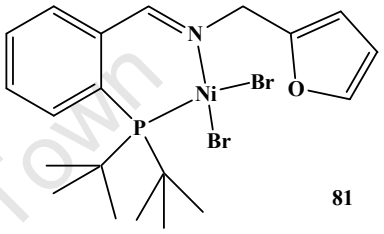

81

To a THF solution of ligand **49** (0.5 g, 1.89 mmol) was added Mg (0.069 g, 2.85 mmol) and a crystal of I_2. The reaction mixture was refluxed for 4 h. The mixture was then cooled to-78° C, at which temperature $ClP(^tBu)_2$ (0.34 g, 1.89 mmol) was added dropwise. The reaction mixture was allowed to warm up to room temperature and left to stir for 16 h. The resulting solution of the ligand was then slowly added to a 10 mL THF suspension of $Ni(DME)Br_2$ (0.58g, 1.89 mmol), immediately forming a brown precipitate. The reaction mixture was stirred at room temperature for 17 h. A small amount of THF (5 mL) was added to the reaction mixture to complete product precipitation. The supernatant liquid was then syringed off and the precipitate washed with diethyl ether (3 x 10ml) to give a pale brown powder (0.77 g, 74 %). The solid product was recrystallized from DCM and diethyl ether.to give the pure product as a pale brown powder. M.p. 192 – 194 °C. IR (KBr): 1622 cm^{-1} ($\upsilon_{C=N}$). EI-MS: *m/z* 468.33 $[M\text{-}Br]^+$. Anal. Calc. for $C_{20}H_{30}Br_2NNiOP$ (547.93): C, 43.68; H, 5.50; N, 2.55. Found: C, 43.82; H, 5.29; N, 2.84.

Preparation of $[Pd(C_{30}H_{25}NO_2P)Cl]$ (82)

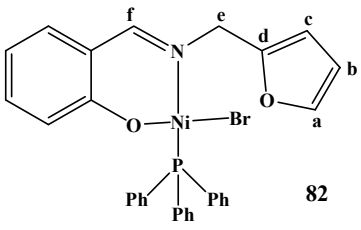

82

To a THF solution of **48** (0.23 g, 1.14 mmol) was added Et_3N (0.17 g, 1.71 mmol). The reaction mixture was allowed to stir at room temperature for 30 min. This mixture was then slowly added to a THF solution (10 mL) of $Ni(DME)Br_2$ (0.35 g, 1.14 mmol) at room temperature. PPh_3 (0.30 g, 1.14 mmol) was then added to give a green solution which was left to stir for 16 h. diethyl ether (5ml) was then added to complete precipitation and the supernatant liquid syringed off and the resultant solid

dried *in vacuo* to give a green powder. The crude product was recrystallized from DCM and diethyl ether giving green powder (0.44 g, 65 %), M.p. 162 – 166 °C. EI-MS: *m/z* 338.59 [M-PPh_3]$^+$. Anal. Calc. for $C_{30}H_{25}BrNNiO_2P$ (601.10): C, 59.94; H, 4.19; N, 2.33. Found: C, 60.37; H, 4.42; N, 2.68.

5.8 Preparation of Chromium Complexes

General procedure

To a suspension of $Cr(THF)_3Cl_3$ *ca.* 0.5 – 1.3 mmol in THF (10 mL) was added a THF (10 mL) solution of an equimolar amount of the appropriate ligand (**41** – **46)** at room temperature and the reaction mixture was stirred for 18 h. In general, a green precipitate formed, in which case a small amount of diethyl ether was added to complete precipitation of the product. The solid product was then filtered and washed with ice-cooled THF and dried to give the pure product as a green powder. In cases where a homogeneous solution was obtained the solvent was removed *in vacuo* and the resultant crude product recrystallized from THF and diethyl ether to give the product as a green powder.

Preparation of [Cr($C_{25}H_{21}N_2P$)Cl_3].THF (83)

This complex was prepared from a reaction of **41** (0.5 g, 1.31 mmol) and $Cr(THF)_3Cl_3$ (0.49 , 1.31 mmol) using the general procedure, to give the pure product as a green powder. (0.56 g, 79 %). M.p. 229 – 231 °C. IR (KBr): 1628 cm^{-1} ($\upsilon_{C=N}$). ESI-MS: *m/z* 611.08 [M]$^+$. Anal. Calc. for $C_{29}H_{29}Cl_3CrN_2OP$ (610.88): C, 57.02; H, 4.78; N, 4.59. Found: C, 56.74; H, 4.81; N, 4.91.

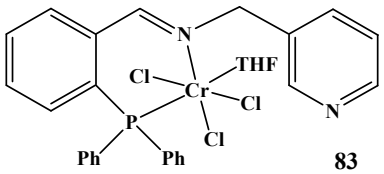

83

Preparation of [Cr($C_{24}H_{20}$NOP)Cl_3] (84)

This complex was prepared from the reaction of **42** (0.2 g, 0.54 mmol) and $Cr(THF)_3Cl_3$ (0.20 g, 0.54 mmol) using the general procedure, to give the pure product as a bright green powder (0.18 g, 63 %). M.p. 220 – 223 °C. IR (KBr): 1627 cm^{-1} ($\upsilon_{C=N}$). ESI-MS: *m/z* 527.66 [M-THF]$^+$.Anal. Calc. for $C_{24}H_{20}Cl_3CrNOP$ (527.75): C, 54.62; H, 3.82; N, 2.65. Found: C, 54.52; H, 3.82; N, 2.94.

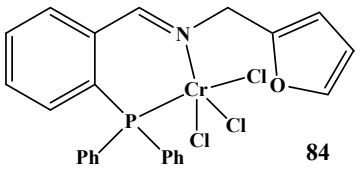

84

Preparation of [($C_{24}H_{20}Cl_3CrNPS$)].THF (85)

This complex was prepared from the reaction of **43** (0.5 g, 1.30 mmol) and $Cr(THF)_3Cl_3$ (0.49 g, 1.30 mmol) using the general procedure, to give the pure product as a bright green powder (0.53 g, 75 %). M.p. 216 – 219 °C. IR (KBr): 1628 cm^{-1} ($\upsilon_{C=N}$). ESI-MS: *m/z* 543.66 $[M\text{-}THF]^+$. Anal. Calc. for $C_{28}H_{28}Cl_3CrNOPS$ (615.92): C, 54.60; H, 4.58; N, 2.27; S, 5.21. Found: C, 54.92; H, 4.51; N, 2.46; S, 5.33.

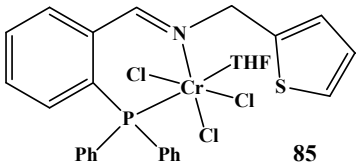

85

Preparation of [$Cr(C_{25}H_{22}NPS)Cl_3$].THF (86)

This complex was prepared from the reaction of **44** (0.4 g, 1.00 mmol) and $Cr(THF)_3Cl_3$ (0.375 g, 1.00 mmol) using the general procedure, to give the pure product as a bright green powder (0.34 g, 62 %). M.p. 221 – 224 °C. IR (KBr): 1627 cm^{-1} ($\upsilon_{C=N}$). ESI-MS: *m/z* 557.75 $[M\text{-}THF]^+$. Anal. Calc. for $C_{29}H_{30}Cl_3CrNOPS$ (629.95): C, 55.29; H, 4.80; N, 2.22; S, 5.09. Found:C, 55.58; H, 4.86; N, 2.51; S, 5.24.

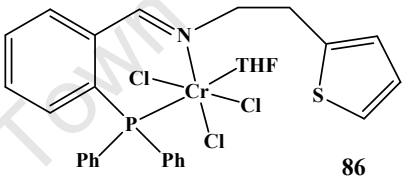

86

Preparation of [$Cr(C_{26}H_{22}NNP)Cl_3$] (87)

This complex was prepared from a reaction of **45** (0.21 g, 0.55 mmol) and $Cr(THF)_3Cl_3$ (0.21 g, 0.55 mmol) using the general procedure, to give the pure product as a green powder. (0.26 g, 87 %). M.p. 230 – 233 °C. IR (KBr): 1629 cm^{-1} ($\upsilon_{C=N}$). ESI-MS: *m/z* 537.93 $[M\text{-}THF]^+$. Anal. Calc. for $C_{26}H_{22}Cl_3NCrNP$ (609.89): C, 59.08; H, 4.96; N, 2.30. Found: C, 58.61; H, 4.72; N, 2.72.

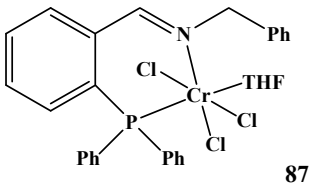

87

Preparation of [$Cr(C_{11}H_{10}N_2O)Cl_3$] (88)

This complex was prepared from a reaction of **L6** (0.20 g, 1.07 mmol) and $Cr(THF)_3Cl_3$ (0.42 g, 1.07 mmol) using the general procedure, to give the pure product as a green powder. (0.29 g, 78 %). M.p. 232 – 235 °C. IR (KBr): 1622 cm^{-1} ($\upsilon_{C=N}$). ESI-MS: *m/z* 344.74 $[M\text{-}THF]^+$. Anal. Calc. for $C_{15}H_{18}Cl_3CrN_2O_2$ (416.67): C, 43.24; H, 4.35; N, 6.72. Found: C, 43.55; H, 4.69; N, 6.28.

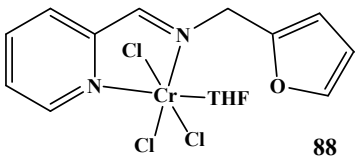

88

5.9 X-ray Crystallography

Summaries of crystal data and collection parameters of crystal structures of complexes **53**, **71**, and **76** are given in Table 5.1.

Table 5.1 X-ray crystallographic data collection parameters for complexes **53**, **71**, and **76**

	53	**71**	**76**
Empirical formula	$C_{25}H_{23}ClNPPdS$	$C_{28}H_{28}F_6N_2P_2PdS$	$C_{24}H_{20}Br_2NNiOP$
Formula weight	542.32	706.92	587.91
T/K	113(2)	173(2)	173(2)
λ/Å	0.71073	0.71073	0.71073
space group	Monoclinic, $P2_1/n$	Monoclinic, $P2_1/c$	Monoclinic, $P2_1/n$
a	9.83260(10)	10.2709 (8)	10.3807(3)
b	21.7925(2)	14.3137 (10)	19.8162(4)
c	10.65960(10)	19.4373 (14)	11.0644(3)
α(deg)	90.0000	90.0000	90.0000
β(deg)	95.6400	90.9150 (10)	95.3140(10)
γ(deg)	90.0000	90.0000	90.0000
V(Å^3)	2273.03(4)	2871.9 (4)	2266.23(10)
Z	4	4	4
$Density_{calc}$ (mg/mL)	1.585	1.635	1.723
Absorption coefficient (mm^{-1})	1.109	0.891	4.469
F(000)	1096	1424	1168
Crystal Size (mm)	0.11 x 0.08 x 0.07	0.13 x 0.12 x 0.09	0.15 x 0.14 x 0.13
Theta Range for Data Collection (deg)	2.28 – 25.68	2.09 – 28.30	2.06 – 25.69
Limiting Indices	-11<=h<=11,-26<=k<=26, -12<=l<=12	-13<=h<=13,-<=k<=19, -26<=l<=26	-12<=h<=12,-4<=k<=24, -13<=l<=13
Reflections Collected / Unique	68820/4283 [R(int) = 0.0581]	25122/7134 [R(int) = 0.0225]	73482/4306 [R(int) = 0.0596]
Completeness to theta	25.68 (99.4%)	28.30 (99.9%)	25.69 (99.8%)
max. and min. transmission	0.9264 and 0.8877	0.9241 and 0.8409	0.5942 and 0.5537
Refinement Method	Full-matrix least squares on F^2	Full-matrix least squares on F^2	Full-matrix least squares on F^2
Data / Restraints / Parameters	4423 / 0 / 273	7134 / 0 / 363	4306 / 0 / 269
Goodness-of-fit on F^2	1.066	1.037	1.082

5.9 References

1. Perrin, D. D.; Araregó, W. L. F.; *Purification of Laboratory Chemicals*, **1988**, Pergamon Press, Oxford.
2. Hoots, J. E.; Rauchfuss, T. B.; Wrobleski, D. A. *Inorg. Chem*., **1982**, *175*.
3. Bailey, C. T.; Linsesky, G. C. *J. Chem. Educ.*, **1985**, *62*,896.
4. Rülke, R. E.; Ernsting, J. M.; Spek, A. L.; Elsevier, C. J.; van Leeuwen, P. W. N. M.; Vrieze, K. *Inorg. Chem.*, **1993**, *32*, 5769.
5. Ward, L. G. L. *Inorg. Synth.*, **1973**, *13*, 154.
6. Herwig, W.; Zeiss, H. H. *J. Org. Chem.*, **1958**, *23*, 1404.
7. Brookhart, M.; Grant, B.; Volpe Jr., A. F. *Organometallics*, **1992**, *11*, 3920.
8. a) Del Zotto, A.; Baratta, W.; Ballico M.; Herdtweck, E.; Rigo, P. *Organometallics*, **2007**, *26*, 5636. b) Masson, J. P.; Bahsoun, A. A.; Youinou, M.; Osborn, J. A. C. R. *Chemie*, 2002, *5*, 305.
9. Liek, C.; Machnitzki, P.; Mickel, T.; Schenk, S.; Tepper, M.; Stelzer, O.; *Zeit. Natur.B*: *Chem. Sci.* **1999**, *54*, 1532.
10. Bhagwart, U. A.; Mukhedkar, V. A.; Mukhedkar, A. J. *J. Chem. Soc. Dalton Trans*., **1980**, 2319.
11. Murali, R.; Surya, P. H.; Scheeren, H. W. *Tetrahedron*, **2001**, *57*, 3165.; Murali, R. Scheeren, H. W. *Tetrahedron. Lett*., **1999**, *40*, 3029.
12. Song, Y.; Xu, Z.; Sun, Q.; Su, B.; Gao, Q,; Liu, H.; Zhao, J. *J. Coord. Chem.*, **2007**, *60*, 2351.

APPENDIX

Supporting Information: X-ray diffraction data for complexes **53**, **71**, and **76** including tables of all bond lengths and angles (CIF files) (refer to attached disk).

Supporting Information:

Compound 53

Table 1. Atomic coordinates (x 10^4) and equivalent isotropic displacement parameters (A^2 x 10^3) **53**. U(eq) is defined as one third of the trace of the orthogonalized Uij tensor.

	x	y	z	U(eq)
Pd(1)	8552(1)	1957(1)	4707(1)	17(1)
Cl(1)	9888(1)	2876(1)	4666(1)	28(1)
S(1)	10985(1)	2119(1)	8107(1)	41(1)
P(1)	7251(1)	1142(1)	4679(1)	15(1)
N(1)	7530(2)	2252(1)	6305(2)	20(1)
C(1)	9544(2)	1611(1)	3269(2)	22(1)
C(2)	8394(3)	2589(1)	7301(2)	25(1)
C(3)	9249(3)	2157(1)	8134(2)	25(1)
C(4)	8802(3)	1756(1)	9062(2)	24(1)
C(5)	9933(3)	1456(1)	9714(3)	39(1)
C(6)	11153(3)	1605(2)	9303(3)	42(1)
C(7)	6299(2)	2158(1)	6552(2)	21(1)
C(8)	5244(2)	1816(1)	5772(2)	19(1)
C(9)	3900(3)	1937(1)	5997(2)	22(1)
C(10)	2806(2)	1648(1)	5323(2)	23(1)
C(11)	3059(2)	1221(1)	4418(2)	21(1)
C(12)	4394(2)	1081(1)	4203(2)	19(1)
C(13)	5498(2)	1371(1)	4869(2)	17(1)
C(21)	7692(2)	653(1)	6047(2)	17(1)
C(22)	6699(2)	423(1)	6764(2)	19(1)
C(23)	7064(2)	78(1)	7833(2)	23(1)
C(24)	8428(3)	-46(1)	8201(2)	25(1)
C(25)	9423(3)	176(1)	7490(3)	27(1)
C(26)	9066(2)	528(1)	6426(2)	24(1)
C(31)	7047(2)	636(1)	3317(2)	17(1)
C(32)	7109(2)	1(1)	3434(2)	19(1)
C(33)	6877(2)	-370(1)	2374(2)	22(1)
C(34)	6585(2)	-108(1)	1199(2)	24(1)
C(35)	6521(2)	526(1)	1070(2)	25(1)
C(36)	6750(2)	899(1)	2120(2)	21(1)

Table 2. Bond lengths [A] and angles [deg] for **53**.

Pd(1)-C(1)	2.040(2)
Pd(1)-N(1)	2.160(2)
Pd(1)-P(1)	2.1874(6)
Pd(1)-Cl(1)	2.3980(6)
S(1)-C(6)	1.695(3)
S(1)-C(3)	1.712(3)
P(1)-C(31)	1.818(2)
P(1)-C(21)	1.824(2)
P(1)-C(13)	1.825(2)
N(1)-C(7)	1.281(3)
N(1)-C(2)	1.487(3)
C(1)-H(1A)	0.9800
C(1)-H(1B)	0.9800
C(1)-H(1C)	0.9800
C(2)-C(3)	1.494(4)
C(2)-H(2A)	0.9900
C(2)-H(2B)	0.9900
C(3)-C(4)	1.422(4)
C(4)-C(5)	1.413(4)
C(4)-H(4)	0.9500
C(5)-C(6)	1.356(4)
C(5)-H(5)	0.9500
C(6)-H(6)	0.9500
C(7)-C(8)	1.468(3)
C(7)-H(7)	0.9500
C(8)-C(9)	1.391(3)
C(8)-C(13)	1.406(3)
C(9)-C(10)	1.385(4)
C(9)-H(9)	0.9500
C(10)-C(11)	1.380(4)
C(10)-H(10)	0.9500
C(11)-C(12)	1.389(3)
C(11)-H(11)	0.9500
C(12)-C(13)	1.389(3)
C(12)-H(12)	0.9500
C(21)-C(22)	1.391(3)
C(21)-C(26)	1.398(3)
C(22)-C(23)	1.383(3)
C(22)-H(22)	0.9500
C(23)-C(24)	1.386(3)
C(23)-H(23)	0.9500
C(24)-C(25)	1.382(4)

C(24)-H(24)	0.9500
C(25)-C(26)	1.385(4)
C(25)-H(25)	0.9500
C(26)-H(26)	0.9500
C(31)-C(32)	1.391(3)
C(31)-C(36)	1.402(3)
C(32)-C(33)	1.390(3)
C(32)-H(32)	0.9500
C(33)-C(34)	1.380(4)
C(33)-H(33)	0.9500
C(34)-C(35)	1.391(4)
C(34)-H(34)	0.9500
C(35)-C(36)	1.383(3)
C(35)-H(35)	0.9500
C(36)-H(36)	0.9500

C(1)-Pd(1)-N(1)	175.31(9)
C(1)-Pd(1)-P(1)	90.67(7)
N(1)-Pd(1)-P(1)	86.28(5)
C(1)-Pd(1)-Cl(1)	89.55(7)
N(1)-Pd(1)-Cl(1)	93.68(5)
P(1)-Pd(1)-Cl(1)	177.03(2)
C(6)-S(1)-C(3)	92.43(14)
C(31)-P(1)-C(21)	106.45(11)
C(31)-P(1)-C(13)	102.85(10)
C(21)-P(1)-C(13)	102.93(10)
C(31)-P(1)-Pd(1)	121.42(8)
C(21)-P(1)-Pd(1)	111.79(8)
C(13)-P(1)-Pd(1)	109.55(8)
C(7)-N(1)-C(2)	114.7(2)
C(7)-N(1)-Pd(1)	129.62(17)
C(2)-N(1)-Pd(1)	115.65(15)
Pd(1)-C(1)-H(1A)	109.5
Pd(1)-C(1)-H(1B)	109.5
H(1A)-C(1)-H(1B)	109.5
Pd(1)-C(1)-H(1C)	109.5
H(1A)-C(1)-H(1C)	109.5
H(1B)-C(1)-H(1C)	109.5
N(1)-C(2)-C(3)	111.2(2)
N(1)-C(2)-H(2A)	109.4
C(3)-C(2)-H(2A)	109.4
N(1)-C(2)-H(2B)	109.4
C(3)-C(2)-H(2B)	109.4
H(2A)-C(2)-H(2B)	108.0
C(4)-C(3)-C(2)	127.3(2)
C(4)-C(3)-S(1)	111.03(19)

C(2)-C(3)-S(1)	121.6(2)
C(5)-C(4)-C(3)	110.2(2)
C(5)-C(4)-H(4)	124.9
C(3)-C(4)-H(4)	124.9
C(6)-C(5)-C(4)	114.1(3)
C(6)-C(5)-H(5)	122.9
C(4)-C(5)-H(5)	122.9
C(5)-C(6)-S(1)	112.2(2)
C(5)-C(6)-H(6)	123.9
S(1)-C(6)-H(6)	123.9
N(1)-C(7)-C(8)	126.5(2)
N(1)-C(7)-H(7)	116.8
C(8)-C(7)-H(7)	116.8
C(9)-C(8)-C(13)	119.0(2)
C(9)-C(8)-C(7)	115.9(2)
C(13)-C(8)-C(7)	125.1(2)
C(10)-C(9)-C(8)	121.8(2)
C(10)-C(9)-H(9)	119.1
C(8)-C(9)-H(9)	119.1
C(11)-C(10)-C(9)	119.0(2)
C(11)-C(10)-H(10)	120.5
C(9)-C(10)-H(10)	120.5
C(10)-C(11)-C(12)	120.1(2)
C(10)-C(11)-H(11)	119.9
C(12)-C(11)-H(11)	119.9
C(11)-C(12)-C(13)	121.3(2)
C(11)-C(12)-H(12)	119.4
C(13)-C(12)-H(12)	119.4
C(12)-C(13)-C(8)	118.8(2)
C(12)-C(13)-P(1)	121.23(18)
C(8)-C(13)-P(1)	119.83(18)
C(22)-C(21)-C(26)	118.8(2)
C(22)-C(21)-P(1)	121.66(18)
C(26)-C(21)-P(1)	119.48(18)
C(23)-C(22)-C(21)	120.6(2)
C(23)-C(22)-H(22)	119.7
C(21)-C(22)-H(22)	119.7
C(22)-C(23)-C(24)	120.3(2)
C(22)-C(23)-H(23)	119.9
C(24)-C(23)-H(23)	119.9
C(25)-C(24)-C(23)	119.6(2)
C(25)-C(24)-H(24)	120.2
C(23)-C(24)-H(24)	120.2
C(24)-C(25)-C(26)	120.4(2)
C(24)-C(25)-H(25)	119.8
C(26)-C(25)-H(25)	119.8

C(25)-C(26)-C(21)	120.3(2)
C(25)-C(26)-H(26)	119.9
C(21)-C(26)-H(26)	119.9
C(32)-C(31)-C(36)	119.4(2)
C(32)-C(31)-P(1)	122.11(18)
C(36)-C(31)-P(1)	118.43(18)
C(33)-C(32)-C(31)	120.3(2)
C(33)-C(32)-H(32)	119.8
C(31)-C(32)-H(32)	119.8
C(34)-C(33)-C(32)	120.0(2)
C(34)-C(33)-H(33)	120.0
C(32)-C(33)-H(33)	120.0
C(33)-C(34)-C(35)	120.3(2)
C(33)-C(34)-H(34)	119.9
C(35)-C(34)-H(34)	119.9
C(36)-C(35)-C(34)	120.1(2)
C(36)-C(35)-H(35)	120.0
C(34)-C(35)-H(35)	120.0
C(35)-C(36)-C(31)	120.0(2)
C(35)-C(36)-H(36)	120.0
C(31)-C(36)-H(36)	120.0

Table 3. Anisotropic displacement parameters (A^2 x 10^3) for **53**. The anisotropic displacement factor exponent takes the form: -2 pi^2 [h^2 a*^2 U11 + ... + 2 h k a* b* U12]

	U11	U22	U33	U23	U13	U12
Pd(1)	16(1)	17(1)	18(1)	-1(1)	5(1)	-3(1)
Cl(1)	30(1)	26(1)	32(1)	-5(1)	12(1)	-12(1)
S(1)	26(1)	56(1)	41(1)	-15(1)	8(1)	-3(1)
P(1)	15(1)	16(1)	16(1)	0(1)	4(1)	-1(1)
N(1)	24(1)	16(1)	21(1)	-2(1)	5(1)	-3(1)
C(1)	18(1)	24(1)	23(1)	1(1)	8(1)	-1(1)
C(2)	29(1)	23(1)	24(1)	-8(1)	6(1)	-7(1)
C(3)	23(1)	30(1)	21(1)	-11(1)	5(1)	-3(1)
C(4)	21(1)	32(2)	20(1)	-9(1)	2(1)	4(1)
C(5)	48(2)	39(2)	31(2)	-8(1)	4(1)	1(1)
C(6)	37(2)	49(2)	38(2)	-18(2)	-8(1)	13(1)
C(7)	25(1)	19(1)	20(1)	-2(1)	6(1)	1(1)
C(8)	21(1)	18(1)	19(1)	4(1)	5(1)	-1(1)
C(9)	28(1)	17(1)	19(1)	1(1)	5(1)	4(1)
C(10)	18(1)	27(1)	26(1)	6(1)	7(1)	6(1)
C(11)	17(1)	22(1)	24(1)	7(1)	1(1)	-1(1)
C(12)	21(1)	16(1)	20(1)	3(1)	4(1)	0(1)

C(13)	17(1)	16(1)	17(1)	4(1)	5(1)	0(1)
C(21)	18(1)	17(1)	16(1)	-3(1)	2(1)	-2(1)
C(22)	16(1)	22(1)	19(1)	-1(1)	1(1)	-1(1)
C(23)	24(1)	29(1)	18(1)	1(1)	6(1)	-7(1)
C(24)	28(1)	29(1)	18(1)	5(1)	-1(1)	2(1)
C(25)	17(1)	34(2)	30(2)	5(1)	-1(1)	5(1)
C(26)	18(1)	29(1)	27(2)	2(1)	7(1)	0(1)
C(31)	14(1)	20(1)	17(1)	0(1)	5(1)	-1(1)
C(32)	17(1)	23(1)	18(1)	2(1)	6(1)	1(1)
C(33)	22(1)	20(1)	24(1)	-3(1)	8(1)	-1(1)
C(34)	21(1)	30(2)	21(1)	-7(1)	5(1)	-2(1)
C(35)	25(1)	32(2)	17(1)	2(1)	1(1)	-2(1)
C(36)	20(1)	21(1)	21(1)	3(1)	3(1)	0(1)

Table 4. Hydrogen coordinates (x 10^4) and isotropic displacement parameters (A^2 x 10^3) for **53**

	x	y	z	U(eq)
H(1A)	10471	1780	3316	32
H(1B)	9045	1723	2460	32
H(1C)	9592	1163	3340	32
H(2A)	7801	2830	7816	30
H(2B)	8996	2879	6902	30
H(4)	7877	1698	9220	29
H(5)	9847	1174	10382	47
H(6)	12003	1440	9647	50
H(7)	6043	2326	7317	25
H(9)	3728	2226	6630	26
H(10)	1895	1742	5481	28
H(11)	2319	1022	3942	25
H(12)	4556	781	3588	23
H(22)	5761	504	6516	23
H(23)	6377	-74	8318	28
H(24)	8677	-281	8937	30
H(25)	10357	86	7733	33
H(26)	9758	684	5952	29
H(32)	7311	-180	4241	23
H(33)	6919	-804	2458	26
H(34)	6428	-363	476	29
H(35)	6321	704	259	29
H(36)	6705	1332	2031	25

Table 5. Torsion angles [deg] for **53**.

C(1)-Pd(1)-P(1)-C(31)	-19.02(11)
N(1)-Pd(1)-P(1)-C(31)	164.55(10)
Cl(1)-Pd(1)-P(1)-C(31)	75.3(5)
C(1)-Pd(1)-P(1)-C(21)	107.96(11)
N(1)-Pd(1)-P(1)-C(21)	-68.47(10)
Cl(1)-Pd(1)-P(1)-C(21)	-157.7(4)
C(1)-Pd(1)-P(1)-C(13)	-138.60(11)
N(1)-Pd(1)-P(1)-C(13)	44.97(10)
Cl(1)-Pd(1)-P(1)-C(13)	-44.3(5)
C(1)-Pd(1)-N(1)-C(7)	-81.9(11)
P(1)-Pd(1)-N(1)-C(7)	-32.3(2)
Cl(1)-Pd(1)-N(1)-C(7)	144.7(2)
C(1)-Pd(1)-N(1)-C(2)	94.8(10)
P(1)-Pd(1)-N(1)-C(2)	144.32(16)
Cl(1)-Pd(1)-N(1)-C(2)	-38.65(16)
C(7)-N(1)-C(2)-C(3)	97.7(3)
Pd(1)-N(1)-C(2)-C(3)	-79.5(2)
N(1)-C(2)-C(3)-C(4)	-72.7(3)
N(1)-C(2)-C(3)-S(1)	110.2(2)
C(6)-S(1)-C(3)-C(4)	-1.4(2)
C(6)-S(1)-C(3)-C(2)	176.2(2)
C(2)-C(3)-C(4)-C(5)	-175.7(2)
S(1)-C(3)-C(4)-C(5)	1.7(3)
C(3)-C(4)-C(5)-C(6)	-1.2(3)
C(4)-C(5)-C(6)-S(1)	0.2(3)
C(3)-S(1)-C(6)-C(5)	0.7(2)
C(2)-N(1)-C(7)-C(8)	-177.1(2)
Pd(1)-N(1)-C(7)-C(8)	-0.4(4)
N(1)-C(7)-C(8)-C(9)	-159.7(2)
N(1)-C(7)-C(8)-C(13)	22.6(4)
C(13)-C(8)-C(9)-C(10)	-2.4(4)
C(7)-C(8)-C(9)-C(10)	179.7(2)
C(8)-C(9)-C(10)-C(11)	1.1(4)
C(9)-C(10)-C(11)-C(12)	0.7(4)
C(10)-C(11)-C(12)-C(13)	-1.0(4)
C(11)-C(12)-C(13)-C(8)	-0.3(3)
C(11)-C(12)-C(13)-P(1)	174.87(18)
C(9)-C(8)-C(13)-C(12)	2.0(3)
C(7)-C(8)-C(13)-C(12)	179.7(2)
C(9)-C(8)-C(13)-P(1)	-173.25(18)
C(7)-C(8)-C(13)-P(1)	4.4(3)
C(31)-P(1)-C(13)-C(12)	10.9(2)
C(21)-P(1)-C(13)-C(12)	-99.6(2)

Pd(1)-P(1)-C(13)-C(12)	141.31(18)
C(31)-P(1)-C(13)-C(8)	-173.95(18)
C(21)-P(1)-C(13)-C(8)	75.5(2)
Pd(1)-P(1)-C(13)-C(8)	-43.5(2)
C(31)-P(1)-C(21)-C(22)	-93.1(2)
C(13)-P(1)-C(21)-C(22)	14.7(2)
Pd(1)-P(1)-C(21)-C(22)	132.24(18)
C(31)-P(1)-C(21)-C(26)	90.1(2)
C(13)-P(1)-C(21)-C(26)	-162.1(2)
Pd(1)-P(1)-C(21)-C(26)	-44.6(2)
C(26)-C(21)-C(22)-C(23)	0.2(4)
P(1)-C(21)-C(22)-C(23)	-176.75(19)
C(21)-C(22)-C(23)-C(24)	-0.4(4)
C(22)-C(23)-C(24)-C(25)	-0.2(4)
C(23)-C(24)-C(25)-C(26)	0.9(4)
C(24)-C(25)-C(26)-C(21)	-1.2(4)
C(22)-C(21)-C(26)-C(25)	0.6(4)
P(1)-C(21)-C(26)-C(25)	177.6(2)
C(21)-P(1)-C(31)-C(32)	5.5(2)
C(13)-P(1)-C(31)-C(32)	-102.4(2)
Pd(1)-P(1)-C(31)-C(32)	134.80(17)
C(21)-P(1)-C(31)-C(36)	-177.76(17)
C(13)-P(1)-C(31)-C(36)	74.37(19)
Pd(1)-P(1)-C(31)-C(36)	-48.4(2)
C(36)-C(31)-C(32)-C(33)	-0.1(3)
P(1)-C(31)-C(32)-C(33)	176.65(17)
C(31)-C(32)-C(33)-C(34)	0.1(3)
C(32)-C(33)-C(34)-C(35)	0.0(4)
C(33)-C(34)-C(35)-C(36)	0.0(4)
C(34)-C(35)-C(36)-C(31)	0.0(4)
C(32)-C(31)-C(36)-C(35)	0.0(3)
P(1)-C(31)-C(36)-C(35)	-176.84(18)

Compound 71

Table 6. Atomic coordinates (x 10^4) and equivalent isotropic displacement parameters (A^2 x 10^3) for **71**. U(eq) is defined as one third of the trace of the orthogonalized Uij tensor.

	x	y	z	U(eq)
Pd(1)	1048(1)	429(1)	8742(1)	20(1)
S(1)	-3852(1)	1272(1)	9003(1)	37(1)
P(1)	1814(1)	-897(1)	8339(1)	19(1)
P(2)	2248(1)	4306(1)	9190(1)	26(1)
F(1)	891(1)	4058(1)	8816(1)	40(1)
F(2)	3606(2)	4544(1)	9557(1)	50(1)
F(3)	2791(2)	3318(1)	8985(1)	87(1)
F(4)	1706(2)	5293(1)	9391(2)	90(1)
F(5)	2771(2)	4729(2)	8506(1)	82(1)
F(6)	1720(2)	3879(2)	9880(1)	84(1)
N(1)	99(2)	598(1)	7756(1)	22(1)
N(2)	181(2)	1643(1)	9127(1)	29(1)
C(1)	1874(2)	226(2)	9687(1)	35(1)
C(2)	-1227(2)	983(1)	7773(1)	25(1)
C(3)	-2128(2)	315(1)	8154(1)	29(1)
C(4)	-3450(2)	741(1)	8244(1)	26(1)
C(5)	-4455(2)	806(2)	7780(1)	35(1)
C(6)	-5548(2)	1284(2)	8048(1)	41(1)
C(7)	-5356(2)	1583(2)	8698(1)	40(1)
C(8)	551(2)	402(1)	7168(1)	23(1)
C(9)	1784(2)	-77(1)	7026(1)	22(1)
C(10)	2298(2)	72(2)	6376(1)	29(1)
C(11)	3436(2)	-366(2)	6178(1)	33(1)
C(12)	4035(2)	-999(2)	6614(1)	33(1)
C(13)	3521(2)	-1177(2)	7257(1)	28(1)
C(14)	2411(2)	-709(1)	7476(1)	22(1)
C(15)	-388(2)	2258(1)	9334(1)	27(1)
C(16)	-1161(2)	3022(2)	9593(1)	39(1)
C(21)	384(2)	-1639(1)	8265(1)	20(1)
C(22)	-203(2)	-1862(1)	7641(1)	23(1)
C(23)	-1422(2)	-2291(1)	7624(1)	28(1)
C(24)	-2042(2)	-2508(1)	8229(1)	30(1)
C(25)	-1444(2)	-2307(2)	8854(1)	29(1)
C(26)	-248(2)	-1860(1)	8872(1)	26(1)
C(31)	3085(2)	-1563(1)	8766(1)	21(1)
C(32)	4212(2)	-1088(1)	8978(1)	28(1)
C(33)	5224(2)	-1576(2)	9292(1)	33(1)

C(34)	5124(2)	-2528(2)	9402(1)	34(1)
C(35)	4016(2)	-3004(2)	9188(1)	34(1)
C(36)	2995(2)	-2524(1)	8868(1)	27(1)

Table 7. Bond lengths [A] and angles [deg] for **71**.

Pd(1)-C(1)	2.040(2)
Pd(1)-N(2)	2.0977(17)
Pd(1)-N(1)	2.1588(16)
Pd(1)-P(1)	2.2054(5)
S(1)-C(7)	1.706(3)
S(1)-C(4)	1.721(2)
P(1)-C(31)	1.8088(19)
P(1)-C(21)	1.8157(19)
P(1)-C(14)	1.8222(19)
P(2)-F(4)	1.5705(18)
P(2)-F(5)	1.5707(18)
P(2)-F(3)	1.5740(18)
P(2)-F(6)	1.5823(17)
P(2)-F(2)	1.5949(16)
P(2)-F(1)	1.6031(14)
N(1)-C(8)	1.277(3)
N(1)-C(2)	1.470(2)
N(2)-C(15)	1.134(3)
C(1)-H(1A)	0.9800
C(1)-H(1B)	0.9800
C(1)-H(1C)	0.9800
C(2)-C(3)	1.531(3)
C(2)-H(2A)	0.9900
C(2)-H(2B)	0.9900
C(3)-C(4)	1.501(3)
C(3)-H(3A)	0.9900
C(3)-H(3B)	0.9900
C(4)-C(5)	1.366(3)
C(5)-C(6)	1.421(3)
C(5)-H(5)	0.9500
C(6)-C(7)	1.350(4)
C(6)-H(6)	0.9500
C(7)-H(7)	0.9500
C(8)-C(9)	1.470(3)
C(8)-H(8)	0.9500
C(9)-C(10)	1.399(3)
C(9)-C(14)	1.410(3)
C(10)-C(11)	1.387(3)

C(10)-H(10)	0.9500
C(11)-C(12)	1.381(3)
C(11)-H(11)	0.9500
C(12)-C(13)	1.394(3)
C(12)-H(12)	0.9500
C(13)-C(14)	1.395(3)
C(13)-H(13)	0.9500
C(15)-C(16)	1.448(3)
C(16)-H(16A)	0.9800
C(16)-H(16B)	0.9800
C(16)-H(16C)	0.9800
C(21)-C(22)	1.389(3)
C(21)-C(26)	1.397(3)
C(22)-C(23)	1.394(3)
C(22)-H(22)	0.9500
C(23)-C(24)	1.386(3)
C(23)-H(23)	0.9500
C(24)-C(25)	1.388(3)
C(24)-H(24)	0.9500
C(25)-C(26)	1.385(3)
C(25)-H(25)	0.9500
C(26)-H(26)	0.9500
C(31)-C(36)	1.393(3)
C(31)-C(32)	1.400(3)
C(32)-C(33)	1.387(3)
C(32)-H(32)	0.9500
C(33)-C(34)	1.384(3)
C(33)-H(33)	0.9500
C(34)-C(35)	1.385(3)
C(34)-H(34)	0.9500
C(35)-C(36)	1.394(3)
C(35)-H(35)	0.9500
C(36)-H(36)	0.9500

C(1)-Pd(1)-N(2)	88.09(8)
C(1)-Pd(1)-N(1)	177.21(8)
N(2)-Pd(1)-N(1)	92.21(6)
C(1)-Pd(1)-P(1)	93.18(7)
N(2)-Pd(1)-P(1)	175.68(5)
N(1)-Pd(1)-P(1)	86.32(4)
C(7)-S(1)-C(4)	92.46(12)
C(31)-P(1)-C(21)	107.78(9)
C(31)-P(1)-C(14)	104.71(9)
C(21)-P(1)-C(14)	107.25(9)
C(31)-P(1)-Pd(1)	123.18(6)
C(21)-P(1)-Pd(1)	103.80(6)

C(14)-P(1)-Pd(1)	109.31(6)
F(4)-P(2)-F(5)	89.62(15)
F(4)-P(2)-F(3)	179.67(15)
F(5)-P(2)-F(3)	90.09(15)
F(4)-P(2)-F(6)	90.41(15)
F(5)-P(2)-F(6)	179.97(15)
F(3)-P(2)-F(6)	89.89(15)
F(4)-P(2)-F(2)	90.37(11)
F(5)-P(2)-F(2)	89.51(10)
F(3)-P(2)-F(2)	89.76(10)
F(6)-P(2)-F(2)	90.51(9)
F(4)-P(2)-F(1)	90.22(10)
F(5)-P(2)-F(1)	90.20(10)
F(3)-P(2)-F(1)	89.65(10)
F(6)-P(2)-F(1)	89.78(9)
F(2)-P(2)-F(1)	179.34(10)
C(8)-N(1)-C(2)	116.87(17)
C(8)-N(1)-Pd(1)	127.78(14)
C(2)-N(1)-Pd(1)	115.35(12)
C(15)-N(2)-Pd(1)	174.03(18)
Pd(1)-C(1)-H(1A)	109.5
Pd(1)-C(1)-H(1B)	109.5
H(1A)-C(1)-H(1B)	109.5
Pd(1)-C(1)-H(1C)	109.5
H(1A)-C(1)-H(1C)	109.5
H(1B)-C(1)-H(1C)	109.5
N(1)-C(2)-C(3)	110.10(15)
N(1)-C(2)-H(2A)	109.6
C(3)-C(2)-H(2A)	109.6
N(1)-C(2)-H(2B)	109.6
C(3)-C(2)-H(2B)	109.6
H(2A)-C(2)-H(2B)	108.2
C(4)-C(3)-C(2)	111.03(16)
C(4)-C(3)-H(3A)	109.4
C(2)-C(3)-H(3A)	109.4
C(4)-C(3)-H(3B)	109.4
C(2)-C(3)-H(3B)	109.4
H(3A)-C(3)-H(3B)	108.0
C(5)-C(4)-C(3)	128.7(2)
C(5)-C(4)-S(1)	110.58(16)
C(3)-C(4)-S(1)	120.72(16)
C(4)-C(5)-C(6)	112.4(2)
C(4)-C(5)-H(5)	123.8
C(6)-C(5)-H(5)	123.8
C(7)-C(6)-C(5)	113.2(2)
C(7)-C(6)-H(6)	123.4

C(5)-C(6)-H(6)	123.4
C(6)-C(7)-S(1)	111.32(18)
C(6)-C(7)-H(7)	124.3
S(1)-C(7)-H(7)	124.3
N(1)-C(8)-C(9)	126.78(18)
N(1)-C(8)-H(8)	116.6
C(9)-C(8)-H(8)	116.6
C(10)-C(9)-C(14)	119.22(18)
C(10)-C(9)-C(8)	116.09(18)
C(14)-C(9)-C(8)	124.54(17)
C(11)-C(10)-C(9)	121.1(2)
C(11)-C(10)-H(10)	119.4
C(9)-C(10)-H(10)	119.4
C(12)-C(11)-C(10)	119.57(19)
C(12)-C(11)-H(11)	120.2
C(10)-C(11)-H(11)	120.2
C(11)-C(12)-C(13)	120.3(2)
C(11)-C(12)-H(12)	119.9
C(13)-C(12)-H(12)	119.9
C(12)-C(13)-C(14)	120.8(2)
C(12)-C(13)-H(13)	119.6
C(14)-C(13)-H(13)	119.6
C(13)-C(14)-C(9)	118.93(17)
C(13)-C(14)-P(1)	120.07(15)
C(9)-C(14)-P(1)	120.98(14)
N(2)-C(15)-C(16)	177.7(2)
C(15)-C(16)-H(16A)	109.5
C(15)-C(16)-H(16B)	109.5
H(16A)-C(16)-H(16B)	109.5
C(15)-C(16)-H(16C)	109.5
H(16A)-C(16)-H(16C)	109.5
H(16B)-C(16)-H(16C)	109.5
C(22)-C(21)-C(26)	119.41(17)
C(22)-C(21)-P(1)	122.92(14)
C(26)-C(21)-P(1)	116.87(14)
C(21)-C(22)-C(23)	119.95(18)
C(21)-C(22)-H(22)	120.0
C(23)-C(22)-H(22)	120.0
C(24)-C(23)-C(22)	120.22(19)
C(24)-C(23)-H(23)	119.9
C(22)-C(23)-H(23)	119.9
C(23)-C(24)-C(25)	120.01(19)
C(23)-C(24)-H(24)	120.0
C(25)-C(24)-H(24)	120.0
C(26)-C(25)-C(24)	119.88(19)
C(26)-C(25)-H(25)	120.1

C(24)-C(25)-H(25)	120.1
C(25)-C(26)-C(21)	120.48(19)
C(25)-C(26)-H(26)	119.8
C(21)-C(26)-H(26)	119.8
C(36)-C(31)-C(32)	119.58(18)
C(36)-C(31)-P(1)	122.50(15)
C(32)-C(31)-P(1)	117.89(15)
C(33)-C(32)-C(31)	119.77(19)
C(33)-C(32)-H(32)	120.1
C(31)-C(32)-H(32)	120.1
C(34)-C(33)-C(32)	120.6(2)
C(34)-C(33)-H(33)	119.7
C(32)-C(33)-H(33)	119.7
C(33)-C(34)-C(35)	120.0(2)
C(33)-C(34)-H(34)	120.0
C(35)-C(34)-H(34)	120.0
C(34)-C(35)-C(36)	120.1(2)
C(34)-C(35)-H(35)	119.9
C(36)-C(35)-H(35)	119.9
C(31)-C(36)-C(35)	120.01(19)
C(31)-C(36)-H(36)	120.0
C(35)-C(36)-H(36)	120.0

Table 8. Anisotropic displacement parameters (A^2 x 10^3) for **71**. The anisotropic displacement factor exponent takes the form: -2 pi^2 [h^2 a*^2 U11 + ... + 2 h k a* b* U12]

	U11	U22	U33	U23	U13	U12
Pd(1)	20(1)	21(1)	19(1)	-2(1)	-1(1)	1(1)
S(1)	33(1)	41(1)	38(1)	-7(1)	0(1)	3(1)
P(1)	18(1)	20(1)	18(1)	0(1)	0(1)	1(1)
P(2)	29(1)	27(1)	23(1)	0(1)	0(1)	1(1)
F(1)	35(1)	50(1)	36(1)	3(1)	-8(1)	-3(1)
F(2)	38(1)	66(1)	47(1)	-3(1)	-10(1)	-12(1)
F(3)	69(1)	48(1)	143(2)	-38(1)	-30(1)	26(1)
F(4)	61(1)	46(1)	163(2)	-45(1)	2(1)	10(1)
F(5)	61(1)	140(2)	46(1)	37(1)	3(1)	-25(1)
F(6)	74(1)	144(2)	34(1)	25(1)	-8(1)	-53(1)
N(1)	23(1)	19(1)	24(1)	2(1)	-1(1)	0(1)
N(2)	34(1)	27(1)	25(1)	-3(1)	0(1)	2(1)
C(1)	38(1)	46(1)	22(1)	-6(1)	-6(1)	7(1)
C(2)	25(1)	25(1)	26(1)	3(1)	-2(1)	4(1)
C(3)	24(1)	25(1)	37(1)	4(1)	-1(1)	2(1)
C(4)	24(1)	24(1)	31(1)	1(1)	1(1)	0(1)

C(5)	29(1)	39(1)	37(1)	0(1)	-4(1)	1(1)
C(6)	25(1)	44(1)	55(2)	12(1)	-6(1)	5(1)
C(7)	29(1)	30(1)	62(2)	4(1)	8(1)	6(1)
C(8)	27(1)	21(1)	22(1)	3(1)	-2(1)	-3(1)
C(9)	25(1)	21(1)	21(1)	-1(1)	1(1)	-4(1)
C(10)	39(1)	27(1)	21(1)	1(1)	2(1)	-6(1)
C(11)	37(1)	37(1)	25(1)	-3(1)	11(1)	-9(1)
C(12)	27(1)	40(1)	31(1)	-7(1)	9(1)	-4(1)
C(13)	26(1)	32(1)	28(1)	-2(1)	3(1)	0(1)
C(14)	22(1)	22(1)	21(1)	-1(1)	2(1)	-3(1)
C(15)	30(1)	26(1)	26(1)	1(1)	1(1)	1(1)
C(16)	39(1)	31(1)	46(1)	-2(1)	12(1)	9(1)
C(21)	18(1)	19(1)	24(1)	2(1)	0(1)	1(1)
C(22)	27(1)	20(1)	23(1)	0(1)	0(1)	0(1)
C(23)	29(1)	24(1)	31(1)	-2(1)	-6(1)	-4(1)
C(24)	24(1)	25(1)	40(1)	1(1)	0(1)	-4(1)
C(25)	27(1)	31(1)	30(1)	4(1)	6(1)	-2(1)
C(26)	25(1)	31(1)	21(1)	4(1)	1(1)	0(1)
C(31)	19(1)	24(1)	21(1)	0(1)	1(1)	3(1)
C(32)	24(1)	26(1)	33(1)	0(1)	-3(1)	0(1)
C(33)	22(1)	38(1)	39(1)	-1(1)	-6(1)	0(1)
C(34)	24(1)	40(1)	39(1)	7(1)	-2(1)	10(1)
C(35)	29(1)	27(1)	45(1)	8(1)	2(1)	7(1)
C(36)	23(1)	25(1)	33(1)	1(1)	0(1)	0(1)

Table 9. Hydrogen coordinates (x 10^4) and isotropic displacement parameters (A^2 x 10^3) for **71**.

	x	y	z	U(eq)
H(1A)	2706	560	9717	53
H(1B)	2025	-443	9760	53
H(1C)	1289	463	10038	53
H(2A)	-1560	1076	7299	30
H(2B)	-1213	1597	8005	30
H(3A)	-2215	-275	7893	34
H(3B)	-1741	166	8608	34
H(5)	-4427	560	7329	42
H(6)	-6334	1384	7795	50
H(7)	-5979	1922	8952	48
H(8)	36	583	6782	28
H(10)	1860	479	6065	35
H(11)	3801	-232	5745	39
H(12)	4800	-1315	6475	39

H(13)	3932	-1622	7550	34
H(16A)	-1415	3436	9215	58
H(16B)	-648	3374	9933	58
H(16C)	-1944	2772	9808	58
H(22)	225	-1723	7226	28
H(23)	-1828	-2435	7197	34
H(24)	-2877	-2794	8215	35
H(25)	-1855	-2475	9268	35
H(26)	145	-1703	9300	31
H(32)	4283	-433	8908	33
H(33)	5991	-1254	9432	39
H(34)	5816	-2856	9624	41
H(35)	3952	-3659	9259	40
H(36)	2237	-2852	8719	32

Table 10. Torsion angles [deg] for **71**.

C(1)-Pd(1)-P(1)-C(31)	-14.43(10)
N(2)-Pd(1)-P(1)-C(31)	-121.5(7)
N(1)-Pd(1)-P(1)-C(31)	168.33(9)
C(1)-Pd(1)-P(1)-C(21)	107.99(10)
N(2)-Pd(1)-P(1)-C(21)	0.9(7)
N(1)-Pd(1)-P(1)-C(21)	-69.25(7)
C(1)-Pd(1)-P(1)-C(14)	-137.83(10)
N(2)-Pd(1)-P(1)-C(14)	115.1(7)
N(1)-Pd(1)-P(1)-C(14)	44.92(8)
C(1)-Pd(1)-N(1)-C(8)	-119.5(16)
N(2)-Pd(1)-N(1)-C(8)	144.53(16)
P(1)-Pd(1)-N(1)-C(8)	-39.53(16)
C(1)-Pd(1)-N(1)-C(2)	60.4(16)
N(2)-Pd(1)-N(1)-C(2)	-35.63(13)
P(1)-Pd(1)-N(1)-C(2)	140.31(12)
C(1)-Pd(1)-N(2)-C(15)	-107.1(17)
N(1)-Pd(1)-N(2)-C(15)	70.1(17)
P(1)-Pd(1)-N(2)-C(15)	0(2)
C(8)-N(1)-C(2)-C(3)	116.66(19)
Pd(1)-N(1)-C(2)-C(3)	-63.20(19)
N(1)-C(2)-C(3)-C(4)	173.75(17)
C(2)-C(3)-C(4)-C(5)	79.5(3)
C(2)-C(3)-C(4)-S(1)	-98.2(2)
C(7)-S(1)-C(4)-C(5)	-0.17(18)
C(7)-S(1)-C(4)-C(3)	177.89(18)
C(3)-C(4)-C(5)-C(6)	-178.2(2)

S(1)-C(4)-C(5)-C(6)	-0.3(3)
C(4)-C(5)-C(6)-C(7)	0.8(3)
C(5)-C(6)-C(7)-S(1)	-1.0(3)
C(4)-S(1)-C(7)-C(6)	0.7(2)
C(2)-N(1)-C(8)-C(9)	-173.19(17)
Pd(1)-N(1)-C(8)-C(9)	6.6(3)
N(1)-C(8)-C(9)-C(10)	-158.16(19)
N(1)-C(8)-C(9)-C(14)	26.5(3)
C(14)-C(9)-C(10)-C(11)	-2.4(3)
C(8)-C(9)-C(10)-C(11)	-178.00(19)
C(9)-C(10)-C(11)-C(12)	3.6(3)
C(10)-C(11)-C(12)-C(13)	-1.9(3)
C(11)-C(12)-C(13)-C(14)	-1.1(3)
C(12)-C(13)-C(14)-C(9)	2.3(3)
C(12)-C(13)-C(14)-P(1)	-176.13(16)
C(10)-C(9)-C(14)-C(13)	-0.6(3)
C(8)-C(9)-C(14)-C(13)	174.63(18)
C(10)-C(9)-C(14)-P(1)	177.86(15)
C(8)-C(9)-C(14)-P(1)	-6.9(3)
C(31)-P(1)-C(14)-C(13)	9.54(18)
C(21)-P(1)-C(14)-C(13)	-104.79(17)
Pd(1)-P(1)-C(14)-C(13)	143.29(15)
C(31)-P(1)-C(14)-C(9)	-168.86(15)
C(21)-P(1)-C(14)-C(9)	76.81(17)
Pd(1)-P(1)-C(14)-C(9)	-35.12(17)
Pd(1)-N(2)-C(15)-C(16)	-5(7)
C(31)-P(1)-C(21)-C(22)	-121.51(16)
C(14)-P(1)-C(21)-C(22)	-9.25(18)
Pd(1)-P(1)-C(21)-C(22)	106.39(15)
C(31)-P(1)-C(21)-C(26)	68.80(16)
C(14)-P(1)-C(21)-C(26)	-178.95(15)
Pd(1)-P(1)-C(21)-C(26)	-63.30(15)
C(26)-C(21)-C(22)-C(23)	0.9(3)
P(1)-C(21)-C(22)-C(23)	-168.51(15)
C(21)-C(22)-C(23)-C(24)	-0.9(3)
C(22)-C(23)-C(24)-C(25)	-0.7(3)
C(23)-C(24)-C(25)-C(26)	2.2(3)
C(24)-C(25)-C(26)-C(21)	-2.2(3)
C(22)-C(21)-C(26)-C(25)	0.6(3)
P(1)-C(21)-C(26)-C(25)	170.70(16)
C(21)-P(1)-C(31)-C(36)	12.24(19)
C(14)-P(1)-C(31)-C(36)	-101.72(17)
Pd(1)-P(1)-C(31)-C(36)	132.82(15)
C(21)-P(1)-C(31)-C(32)	-169.92(15)
C(14)-P(1)-C(31)-C(32)	76.12(17)
Pd(1)-P(1)-C(31)-C(32)	-49.34(18)

C(36)-C(31)-C(32)-C(33)	-0.4(3)
P(1)-C(31)-C(32)-C(33)	-178.34(16)
C(31)-C(32)-C(33)-C(34)	-0.6(3)
C(32)-C(33)-C(34)-C(35)	1.1(4)
C(33)-C(34)-C(35)-C(36)	-0.7(4)
C(32)-C(31)-C(36)-C(35)	0.9(3)
P(1)-C(31)-C(36)-C(35)	178.67(16)
C(34)-C(35)-C(36)-C(31)	-0.3(3)

Compound 76

Table 11. Atomic coordinates (x 10^4) and equivalent isotropic displacement parameters (A^2 x 10^3) for **76**. U(eq) is defined as one third of the trace of the orthogonalized Uij tensor.

	x	y	z	U(eq)
Br(1)	4770(1)	3006(1)	-120(1)	35(1)
Br(2)	5177(1)	1319(1)	459(1)	26(1)
Ni(1)	3683(1)	1974(1)	-675(1)	19(1)
P(1)	2288(1)	1176(1)	-613(1)	20(1)
O(1)	5503(2)	2250(1)	-3535(2)	36(1)
N(1)	2676(2)	2384(1)	-1986(2)	23(1)
C(1)	1446(2)	2432(1)	-2234(2)	28(1)
C(2)	457(2)	2117(1)	-1571(2)	26(1)
C(3)	677(2)	1543(1)	-845(2)	23(1)
C(4)	-358(2)	1243(1)	-341(2)	28(1)
C(5)	-1592(2)	1515(1)	-547(2)	34(1)
C(6)	-1809(2)	2084(2)	-1242(3)	37(1)
C(7)	-797(2)	2381(1)	-1774(2)	35(1)
C(8)	3472(3)	2673(1)	-2912(2)	30(1)
C(9)	4212(2)	2129(1)	-3470(2)	28(1)
C(10)	3891(3)	1530(1)	-3986(2)	37(1)
C(11)	5039(3)	1259(2)	-4402(3)	42(1)
C(12)	5978(3)	1708(2)	-4116(3)	41(1)
C(21)	2310(2)	783(1)	871(2)	21(1)
C(22)	1986(2)	1175(1)	1846(2)	28(1)
C(23)	2084(3)	906(1)	3007(2)	36(1)
C(24)	2495(3)	246(2)	3199(2)	37(1)
C(25)	2814(3)	-143(1)	2237(2)	36(1)
C(26)	2724(2)	125(1)	1074(2)	28(1)
C(31)	2330(2)	505(1)	-1729(2)	24(1)
C(32)	3514(2)	242(1)	-1980(2)	30(1)

C(33)	3568(2)	-282(1)	-2804(2)	33(1)
C(34)	2461(3)	-540(1)	-3389(3)	40(1)
C(35)	1282(3)	-278(2)	-3156(3)	58(1)
C(36)	1207(3)	243(2)	-2328(3)	44(1)

Table 12. Bond lengths [A] and angles [deg] for **76**.

Br(1)-Ni(1)	2.3875(4)
Br(2)-Ni(1)	2.3031(4)
Ni(1)-N(1)	1.8912(19)
Ni(1)-P(1)	2.1497(6)
P(1)-C(21)	1.816(2)
P(1)-C(31)	1.818(2)
P(1)-C(3)	1.820(2)
O(1)-C(12)	1.367(3)
O(1)-C(9)	1.370(3)
N(1)-C(1)	1.284(3)
N(1)-C(8)	1.488(3)
C(1)-C(2)	1.456(4)
C(1)-H(1)	0.9500
C(2)-C(3)	1.400(3)
C(2)-C(7)	1.401(3)
C(3)-C(4)	1.388(3)
C(4)-C(5)	1.390(3)
C(4)-H(4)	0.9500
C(5)-C(6)	1.373(4)
C(5)-H(5)	0.9500
C(6)-C(7)	1.381(4)
C(6)-H(6)	0.9500
C(7)-H(7)	0.9500
C(8)-C(9)	1.490(4)
C(8)-H(8A)	0.9900
C(8)-H(8B)	0.9900
C(9)-C(10)	1.346(4)
C(10)-C(11)	1.422(4)
C(10)-H(10)	0.9500
C(11)-C(12)	1.335(4)
C(11)-H(11)	0.9500
C(12)-H(12)	0.9500
C(21)-C(26)	1.384(3)
C(21)-C(22)	1.396(3)
C(22)-C(23)	1.386(4)
C(22)-H(22)	0.9500
C(23)-C(24)	1.385(4)

C(23)-H(23)	0.9500
C(24)-C(25)	1.380(4)
C(24)-H(24)	0.9500
C(25)-C(26)	1.387(4)
C(25)-H(25)	0.9500
C(26)-H(26)	0.9500
C(31)-C(32)	1.386(3)
C(31)-C(36)	1.388(3)
C(32)-C(33)	1.3871
C(32)-H(32)	0.9500
C(33)-C(34)	1.365(3)
C(33)-H(33)	0.9500
C(34)-C(35)	1.376(4)
C(34)-H(34)	0.9500
C(35)-C(36)	1.388(4)
C(35)-H(35)	0.9500
C(36)-H(36)	0.9500

N(1)-Ni(1)-P(1)	90.82(6)
N(1)-Ni(1)-Br(2)	163.05(6)
P(1)-Ni(1)-Br(2)	89.38(2)
N(1)-Ni(1)-Br(1)	92.51(6)
P(1)-Ni(1)-Br(1)	157.72(2)
Br(2)-Ni(1)-Br(1)	93.708(13)
C(21)-P(1)-C(31)	107.48(11)
C(21)-P(1)-C(3)	103.48(11)
C(31)-P(1)-C(3)	106.02(11)
C(21)-P(1)-Ni(1)	113.15(8)
C(31)-P(1)-Ni(1)	117.25(8)
C(3)-P(1)-Ni(1)	108.35(8)
C(12)-O(1)-C(9)	106.5(2)
C(1)-N(1)-C(8)	115.4(2)
C(1)-N(1)-Ni(1)	131.55(17)
C(8)-N(1)-Ni(1)	112.96(15)
N(1)-C(1)-C(2)	126.5(2)
N(1)-C(1)-H(1)	116.8
C(2)-C(1)-H(1)	116.8
C(3)-C(2)-C(7)	119.6(2)
C(3)-C(2)-C(1)	123.5(2)
C(7)-C(2)-C(1)	116.6(2)
C(4)-C(3)-C(2)	119.2(2)
C(4)-C(3)-P(1)	120.50(19)
C(2)-C(3)-P(1)	120.28(18)
C(3)-C(4)-C(5)	120.3(3)
C(3)-C(4)-H(4)	119.9
C(5)-C(4)-H(4)	119.9

C(6)-C(5)-C(4)	120.7(3)
C(6)-C(5)-H(5)	119.6
C(4)-C(5)-H(5)	119.6
C(5)-C(6)-C(7)	119.8(2)
C(5)-C(6)-H(6)	120.1
C(7)-C(6)-H(6)	120.1
C(6)-C(7)-C(2)	120.4(3)
C(6)-C(7)-H(7)	119.8
C(2)-C(7)-H(7)	119.8
N(1)-C(8)-C(9)	110.3(2)
N(1)-C(8)-H(8A)	109.6
C(9)-C(8)-H(8A)	109.6
N(1)-C(8)-H(8B)	109.6
C(9)-C(8)-H(8B)	109.6
H(8A)-C(8)-H(8B)	108.1
C(10)-C(9)-O(1)	109.7(2)
C(10)-C(9)-C(8)	134.2(2)
O(1)-C(9)-C(8)	116.1(2)
C(9)-C(10)-C(11)	106.8(3)
C(9)-C(10)-H(10)	126.6
C(11)-C(10)-H(10)	126.6
C(12)-C(11)-C(10)	106.7(3)
C(12)-C(11)-H(11)	126.7
C(10)-C(11)-H(11)	126.7
C(11)-C(12)-O(1)	110.4(3)
C(11)-C(12)-H(12)	124.8
O(1)-C(12)-H(12)	124.8
C(26)-C(21)-C(22)	119.5(2)
C(26)-C(21)-P(1)	121.94(19)
C(22)-C(21)-P(1)	118.42(18)
C(23)-C(22)-C(21)	120.0(2)
C(23)-C(22)-H(22)	120.0
C(21)-C(22)-H(22)	120.0
C(24)-C(23)-C(22)	120.0(3)
C(24)-C(23)-H(23)	120.0
C(22)-C(23)-H(23)	120.0
C(25)-C(24)-C(23)	120.2(3)
C(25)-C(24)-H(24)	119.9
C(23)-C(24)-H(24)	119.9
C(24)-C(25)-C(26)	120.0(3)
C(24)-C(25)-H(25)	120.0
C(26)-C(25)-H(25)	120.0
C(21)-C(26)-C(25)	120.3(2)
C(21)-C(26)-H(26)	119.8
C(25)-C(26)-H(26)	119.8
C(32)-C(31)-C(36)	119.0(2)

C(32)-C(31)-P(1)	119.23(17)
C(36)-C(31)-P(1)	121.74(19)
C(31)-C(32)-C(33)	120.25(12)
C(31)-C(32)-H(32)	119.9
C(33)-C(32)-H(32)	119.9
C(34)-C(33)-C(32)	120.57(14)
C(34)-C(33)-H(33)	119.7
C(32)-C(33)-H(33)	119.7
C(33)-C(34)-C(35)	119.7(2)
C(33)-C(34)-H(34)	120.2
C(35)-C(34)-H(34)	120.2
C(34)-C(35)-C(36)	120.6(3)
C(34)-C(35)-H(35)	119.7
C(36)-C(35)-H(35)	119.7
C(31)-C(36)-C(35)	119.9(3)
C(31)-C(36)-H(36)	120.1
C(35)-C(36)-H(36)	120.1

Table 13. Anisotropic displacement parameters (A^2 x 10^3) for **76**. The anisotropic displacement factor exponent takes the form: -2 pi^2 [h^2 a*^2 U11 + ... + 2 h k a* b* U12]

	U11	U22	U33	U23	U13	U12
Br(1)	38(1)	25(1)	39(1)	6(1)	-7(1)	-11(1)
Br(2)	18(1)	25(1)	33(1)	3(1)	-3(1)	1(1)
Ni(1)	17(1)	20(1)	21(1)	3(1)	0(1)	-1(1)
P(1)	17(1)	20(1)	22(1)	-1(1)	2(1)	-1(1)
O(1)	30(1)	37(1)	42(1)	-2(1)	7(1)	-3(1)
N(1)	25(1)	24(1)	22(1)	3(1)	3(1)	2(1)
C(1)	32(1)	30(1)	21(1)	2(1)	-2(1)	6(1)
C(2)	23(1)	31(1)	21(1)	-8(1)	-4(1)	4(1)
C(3)	17(1)	27(1)	25(1)	-9(1)	0(1)	-1(1)
C(4)	21(1)	29(1)	33(1)	-9(1)	3(1)	-3(1)
C(5)	20(1)	46(2)	39(2)	-21(1)	6(1)	-6(1)
C(6)	19(1)	52(2)	40(2)	-18(1)	-4(1)	9(1)
C(7)	29(2)	42(2)	33(2)	-4(1)	-6(1)	11(1)
C(8)	36(2)	30(1)	24(1)	9(1)	7(1)	3(1)
C(9)	29(1)	34(1)	20(1)	7(1)	3(1)	-2(1)
C(10)	40(2)	41(2)	31(2)	-2(1)	4(1)	-7(1)
C(11)	57(2)	35(2)	35(2)	1(1)	11(1)	4(1)
C(12)	39(2)	44(2)	43(2)	4(2)	13(1)	12(1)
C(21)	15(1)	24(1)	25(1)	1(1)	2(1)	-5(1)
C(22)	25(1)	30(1)	29(1)	-1(1)	3(1)	2(1)
C(23)	33(2)	49(2)	25(1)	-4(1)	6(1)	-1(1)

C(24)	38(2)	47(2)	26(1)	9(1)	0(1)	-4(1)
C(25)	43(2)	29(1)	37(2)	8(1)	0(1)	-1(1)
C(26)	31(1)	25(1)	30(1)	-1(1)	4(1)	-1(1)
C(31)	24(1)	23(1)	25(1)	-1(1)	5(1)	-3(1)
C(32)	27(1)	34(2)	27(1)	-4(1)	0(1)	5(1)
C(33)	37(2)	34(2)	30(1)	-3(1)	5(1)	10(1)
C(34)	50(2)	33(2)	37(2)	-14(1)	11(1)	-6(1)
C(35)	37(2)	70(2)	66(2)	-41(2)	7(2)	-19(2)
C(36)	27(2)	55(2)	50(2)	-28(2)	9(1)	-6(1)

Table 14. Hydrogen coordinates (x 10^4) and isotropic displacement parameters (A^2 x 10^3) for **76**.

	x	y	z	U(eq)
H(1)	1153	2698	-2919	33
H(4)	-221	850	145	33
H(5)	-2295	1304	-202	41
H(6)	-2652	2274	-1357	45
H(7)	-953	2765	-2279	42
H(8A)	4080	3011	-2525	35
H(8B)	2902	2904	-3550	35
H(10)	3058	1327	-4058	45
H(11)	5122	840	-4805	50
H(12)	6851	1657	-4291	49
H(22)	1699	1626	1714	34
H(23)	1870	1174	3671	43
H(24)	2557	62	3994	44
H(25)	3096	-595	2371	44
H(26)	2948	-144	414	34
H(32)	4291	422	-1586	35
H(33)	4383	-464	-2962	40
H(34)	2505	-898	-3954	47
H(35)	511	-456	-3566	69
H(36)	388	420	-2172	52

Table 15. Torsion angles [deg] for **76**.

N(1)-Ni(1)-P(1)-C(21)	-154.81(10)
Br(2)-Ni(1)-P(1)-C(21)	42.14(8)
Br(1)-Ni(1)-P(1)-C(21)	-56.14(11)
N(1)-Ni(1)-P(1)-C(31)	79.18(11)
Br(2)-Ni(1)-P(1)-C(31)	-83.86(9)
Br(1)-Ni(1)-P(1)-C(31)	177.86(9)
N(1)-Ni(1)-P(1)-C(3)	-40.68(10)
Br(2)-Ni(1)-P(1)-C(3)	156.27(8)
Br(1)-Ni(1)-P(1)-C(3)	58.00(10)
P(1)-Ni(1)-N(1)-C(1)	35.6(2)
Br(2)-Ni(1)-N(1)-C(1)	126.1(2)
Br(1)-Ni(1)-N(1)-C(1)	-122.4(2)
P(1)-Ni(1)-N(1)-C(8)	-141.21(15)
Br(2)-Ni(1)-N(1)-C(8)	-50.6(3)
Br(1)-Ni(1)-N(1)-C(8)	60.82(15)
C(8)-N(1)-C(1)-C(2)	171.5(2)
Ni(1)-N(1)-C(1)-C(2)	-5.2(4)
N(1)-C(1)-C(2)-C(3)	-23.2(4)
N(1)-C(1)-C(2)-C(7)	162.4(2)
C(7)-C(2)-C(3)-C(4)	0.3(3)
C(1)-C(2)-C(3)-C(4)	-173.9(2)
C(7)-C(2)-C(3)-P(1)	177.92(18)
C(1)-C(2)-C(3)-P(1)	3.7(3)
C(21)-P(1)-C(3)-C(4)	-30.8(2)
C(31)-P(1)-C(3)-C(4)	82.1(2)
Ni(1)-P(1)-C(3)-C(4)	-151.18(18)
C(21)-P(1)-C(3)-C(2)	151.61(19)
C(31)-P(1)-C(3)-C(2)	-95.4(2)
Ni(1)-P(1)-C(3)-C(2)	31.3(2)
C(2)-C(3)-C(4)-C(5)	-0.8(4)
P(1)-C(3)-C(4)-C(5)	-178.35(18)
C(3)-C(4)-C(5)-C(6)	-0.3(4)
C(4)-C(5)-C(6)-C(7)	1.9(4)
C(5)-C(6)-C(7)-C(2)	-2.3(4)
C(3)-C(2)-C(7)-C(6)	1.2(4)
C(1)-C(2)-C(7)-C(6)	175.8(2)
C(1)-N(1)-C(8)-C(9)	-114.8(2)
Ni(1)-N(1)-C(8)-C(9)	62.6(2)
C(12)-O(1)-C(9)-C(10)	0.4(3)
C(12)-O(1)-C(9)-C(8)	-177.5(2)
N(1)-C(8)-C(9)-C(10)	51.2(4)
N(1)-C(8)-C(9)-O(1)	-131.5(2)

O(1)-C(9)-C(10)-C(11)	-0.2(3)
C(8)-C(9)-C(10)-C(11)	177.2(3)
C(9)-C(10)-C(11)-C(12)	0.0(3)
C(10)-C(11)-C(12)-O(1)	0.3(3)
C(9)-O(1)-C(12)-C(11)	-0.4(3)
C(31)-P(1)-C(21)-C(26)	19.3(2)
C(3)-P(1)-C(21)-C(26)	131.2(2)
Ni(1)-P(1)-C(21)-C(26)	-111.78(19)
C(31)-P(1)-C(21)-C(22)	-165.47(18)
C(3)-P(1)-C(21)-C(22)	-53.6(2)
Ni(1)-P(1)-C(21)-C(22)	63.47(19)
C(26)-C(21)-C(22)-C(23)	0.1(4)
P(1)-C(21)-C(22)-C(23)	-175.24(19)
C(21)-C(22)-C(23)-C(24)	-0.4(4)
C(22)-C(23)-C(24)-C(25)	0.4(4)
C(23)-C(24)-C(25)-C(26)	0.0(4)
C(22)-C(21)-C(26)-C(25)	0.2(4)
P(1)-C(21)-C(26)-C(25)	175.40(19)
C(24)-C(25)-C(26)-C(21)	-0.2(4)
C(21)-P(1)-C(31)-C(32)	-85.61(19)
C(3)-P(1)-C(31)-C(32)	164.24(18)
Ni(1)-P(1)-C(31)-C(32)	43.1(2)
C(21)-P(1)-C(31)-C(36)	93.7(2)
C(3)-P(1)-C(31)-C(36)	-16.4(3)
Ni(1)-P(1)-C(31)-C(36)	-137.5(2)
C(36)-C(31)-C(32)-C(33)	-1.1(3)
P(1)-C(31)-C(32)-C(33)	178.27(9)
C(31)-C(32)-C(33)-C(34)	0.89(18)
C(32)-C(33)-C(34)-C(35)	-0.2(4)
C(33)-C(34)-C(35)-C(36)	-0.3(5)
C(32)-C(31)-C(36)-C(35)	0.6(4)
P(1)-C(31)-C(36)-C(35)	-178.7(3)
C(34)-C(35)-C(36)-C(31)	0.1(5)